THE MECHANISM OF PRNA-MEDIATED RELEASE OF RNA POLYMERASE FROM *BACILLUS SUBTILIS* 6S-1 RNA

Dissertation
zur
Erlangung des Doktorgrades
der Naturwissenschaften
(Dr. rer. nat.)

dem

Fachbereich Pharmazie
der Philipps-Universität Marburg
vorgelegt von

BENEDIKT M BECKMANN
AUS RATINGEN

Marburg (Lahn) November 2010

Vom Fachbereich Pharmazie
der Philipps-Universität Marburg
als Dissertation am 14.12.2010 angenommen.

Erstgutachter: Prof. Dr. Roland K Hartmann

Zweitgutachter: Prof. Dr. Albrecht Bindereif

Tag der mündlichen Prüfung am 15.12.2010

ABSTRACT

Adaptation of the transcriptome to nutrient limitation and resupply is a fundamental process in bacteria, particularly in natural habitats. Bacterial 6S RNA, an ubiquitous and growth phase-dependent regulator of transcription, binds to RNA polymerase (RNAP) and inhibits transcription during stationary growth. Upon nutrient resupply, RNAP acts as an RNA-dependent RNA polymerase by transcribing large amounts of short RNAs (pRNAs) from 6S RNA as template, leading to dissociation of 6S RNA-RNAP complexes. Whereas the majority of bacteria express a single 6S RNA species, *Bacillus subtilis* encodes two 6S RNAs (6S-1 and 6S-2) of similar secondary structure, but with different expression profiles.

In this work, we investigated the two 6S RNAs of *B. subtilis*, focusing on pRNA synthesis and its role for the function of 6S RNA. Concurrently, we identified pRNA transcription from 6S-1 RNA *in vivo* using high-troughput sequencing techniques and we developed a novel Northern hybridization protocol for detection of pRNAs in bacterial total cellular extracts.

Our results show that the release of RNAP from 6S-1 RNA, the functional homolog of the well investigated *E. coli* 6S RNA, is regulated by stable pRNA binding. Additionally, we found structural changes of 6S-1 RNA, induced by differences in pRNA length in different growth phases. This specific structural change of 6S RNA seems to be conserved among bacteria. Furthermore, we are able to show that the two processes of RNAP release and 6S-1 RNA degradation are coupled *in vivo*. Taken together, our results expand the current understanding of 6S RNA function and provide insight into the mechanism of RNAP release from 6S RNA in bacteria.

ZUSAMMENFASSUNG

Die Anpassung des Transkriptoms an veränderte Nahrungsbedingungen ist ein grundlegender Prozess in Bakterien, ganz besonders in natürlichen Lebensräumen. Die bakterielle 6S RNA, ein universeller und wachstumsphasenabhängiger Transkriptionsregulator, bindet an die RNA Polymerase (RNAP) und verhindert die Transkription im stationären Wachstum. Nach erneuter Verfügbarkeit von Nährstoffen, fungiert die RNAP als RNA-abhängige RNA polymerase und transkribiert große Mengen einer kurzen RNA (pRNA), wobei sie die 6S RNA als Templat benutzt. Dieser Vorgang führt zur Dissoziation des 6S RNA-RNAP Komplexes. Während in der Mehrheit der Bakterien nur eine einzelne 6S RNA exprimiert wird, gibt es zwei 6S RNAs in *Bacillus subtilis* (6S-1 und 6S-2), die zwar die gleiche Sekundärstruktur einnehmen, aber unterschiedliche Expressionsprofile haben.

Im Rahmen dieser Arbeit haben wir die beiden 6S RNAs aus *B. subtilis* untersucht, wobei ein Fokus auf der Synthese der pRNA und deren Funktion lag. Wir begannen unsere Untersuchungen mit zwei Ansätzen: Wir identifizierten zunächst Transkription von pRNA mit 6S-1 RNA als Templat *in vivo* durch Hochdurchsatz-Sequenzierung und entwickelten außerdem ein neues Northern-Hybridisierungsprotokoll, das es uns erlaubte, pRNAs in bakteriellen Extrakten zu detektieren.

Unsere Ergebnisse zeigen, dass die Dissoziation der RNAP und 6S-1 RNA, dem funktionellen Homolog der gut untersuchten 6S RNA aus *E. coli*, durch stabile Bindung der pRNA reguliert wird. Wir fanden zusätzlich heraus, dass dieser Vorgang zu strukturellen Veränderungen in der 6S-1 RNA führt; ausgelöst durch Unterschiede in der Länge der pRNA in den verschiedenen Wachstumsphasen. Diese spezifische strukturelle Änderung der 6S RNA scheint außerdem ein Merkmal der 6S RNA in Bakterien generell zu sein. Darüber hinaus konnten wir zeigen, dass die Dissoziation der RNAP und der Abbau der 6S-1 RNA *in vivo* verknüpft sind. Zusammenfassend erweitern unsere Ergebnisse das momentane Verständnis der Funktion der 6S RNA und geben Einsicht in den Mechanismus der Dissoziation der RNAP von 6S RNA in Bakterien.

PUBLICATIONS

This thesis is based on the following publications, which in the text will be referred to by their Roman numerals:

I Beckmann BM, Grünweller A, Weber MHW and Hartmann RK: Northern blot detection of endogenous small RNAs (~ 14 nucleotides) in bacterial total RNA extracts.
Nucleic Acids Res 2010; 38(14): e147

II Beckmann BM, Grünweller A, Hartmann RK. "Northern Blot Detection of Small RNAs". In: Handbook of RNA Biochemistry 2nd Edition (eds. R. K. Hartmann, A. Bindereif, A. Schön, E. Westhof), WILEY-VCH, Weinheim, Germany
(accepted; year of publication: 2011)

III Beckmann BM, Burenina OY, Hoch PG, Sharma CM, Kubareva EA and Hartmann RK: *In vivo* and *in vitro* analysis of 6S RNA-templated short transcripts in *Bacillus subtilis*.
In revision: 2010RNABIOL0153

IV Beckmann BM, Hoch PG, Marz M, Salas M and Hartmann RK: The release mechanism of RNA polymerase from *Bacillus subtilis* 6S-1 RNA.
Manuscript in preparation

There are more things in heaven and earth, Horatio,
Than are dreamt of in your philosophy.

— Hamlet, Act I scene 5

ACKNOWLEDGMENTS

PhD is a murky time with some few exceptional bright moments. Neither should be experienced alone. I would like to thank...

Prof. Dr. Roland Hartmann for the possibility to do my PhD in his laboratory, the great supervision during this time and the liberty to perform research off the beaten track.

Prof. Dr. Albrecht Bindereif for reviewing my PhD work and for mentorship.

Prof. Dr. Carsten Culmsee for participating in my examination commission.

Dr. Dagmar Willkomm for guidance, discussion, encouragment, the 6S RNA project and for participating in my examination commission.

the graduate school and that they allowed me to travel the world ("Death of a salesman").

our numerous collaborators.

Uwe Mamat for hosting and teaching. Too sad it didn't work.

Kerstin and Arnold for friendship and toothbrushes, fun and great discussions about science.

Philipp for the 'freakin monkey lab'. I know the project is in good hands.

Mike, Markus, Dan, Dominik, Katja, Andreas, Gabi, Astrid, Maren, Karen, Mila, Olga, Manja, Marcus and Steffie for the great time in the lab, the fun and your help.

my family for their support and help.

and finally Kinga for infinite patience, even in the hard times. Thank you for your love and always believing in me.

CONTENTS

LIST OF FIGURES

LIST OF TABLES

LISTINGS

ACRONYMS

A Adenosine

Amp Ampicillin

APS Alkaline phosphatase

Bp Base pair(s)

PBP Bromophenol blue

C Cytosine

Cam Chloramphenicol

cpm Counts per minute

DNA Deoxyribonucleic acid

DNase Deoxyriboonuclease

dNTP(s) Deoxynucleoside triphosphate(s)

DTT Dithiothreitol

E Extinction

EDTA Ethylenediamine tetraacedic acid

Fig. Figure

g Gram

G Guanosine

h Hour(s)

HEPES N-2-Hydroxyethylpiperazin-N′-2-ethane sulfonic acid

kan Kanamycin

kb Kilo bases

l Liter

LB Luria-Bertani

M Molar [mol/l]

mA Milliampere

min Minutes

nt(s) Nucleotide(s)

NTP Ribonucleosidtriphosphate

OD_{578} Optical density at 578 nm

p.a. pro analysis

PAA Polyacrylamide

PAGE Polyacrylamide gel electrophoresis

PCR Polymerase chain reaction

pRNA product RNA (derived from 6S RNA)

RACE Rapid amplification of cDNA ends

RNase Ribonuclease

RNAP RNA polymerase

rpm Revolutions per minute

RT Reverse transcriptase

s Second

SDS Sodiumdodecyl sulfate

SSC Standard salt citrate buffer

T Thymine

TBE Tris-Borat-EDTA buffer

TE Tris-EDTA buffer

Tm Melting temperature

Tris Tris-hydrosymethylaminomethane

U Unit(s) (for enzyme activity)

U Uracil

wt Wild-type

XCB Xylene cyanol blue

Part I

INTRODUCTION

1 INTRODUCTION

'To Start Press Any Key'.
Where's the ANY key?

— Homer Simpson

1.1 NON-CODING RNA IN BACTERIA

'Small' and 'regulatory' ncRNA are often used synonymously.

Regulatory non-coding RNAs (ncRNAs) are a heterogenous group of short RNAs that act by diverse mechanisms to regulate the bacterial cell physiology. The majority of ncRNAs enable the cell to adjust to environmental changes by affecting transcription initiation, post-transcriptional regulation, translation initiation, membrane modulation and a variety of other functions (Waters and Storz, 2009; Repoila and Darfeuille, 2009). Recently, a group of RNA regulators, known as CRISPR RNAs, have been shown to form a basic adaptive immune system of bacterial cells by interfering with plasmid and phage infections (Karginov and Hannon, 2010). Some ncRNAs form chimeras with protein-coding sequences like riboswitches or RNA thermometers, while others act in *cis* as antisense transcripts of their target RNA. Many ncRNAs are described from independent genes and therefore work in *trans* when binding to target transcripts. Finally, some few ncRNAs directly bind to proteins which they regulate.

CRISPR = clustered regularly interspaced short palindromic repeats

The first chromosomally encoded small RNA regulator MicF was identified in E. coli in 1984.

In E. coli alone, ~80 ncRNAs have been found.

Although the sequences of many ncRNAs have been known for decades (Brownlee, 1971; Mizuno et al., 1984), their contributions to cellular responses to environmental changes were not appreciated until the beginning of the millenium (Wassarman et al., 1999). Beginning from the year 2001, diverse groups reported the identification of RNAs originating from intergenic regions in *E. coli* (Livny and Waldor, 2007) and started to investigate their function. Nowadays, more than 140 ncRNAs have been identified using diverse approaches (Vogel and Wagner, 2007) such as computational predictions (Livny et al., 2008), deep sequencing (Sittka et al., 2008; Sharma et al., 2010) and tiling arrays (Landt et al., 2008).

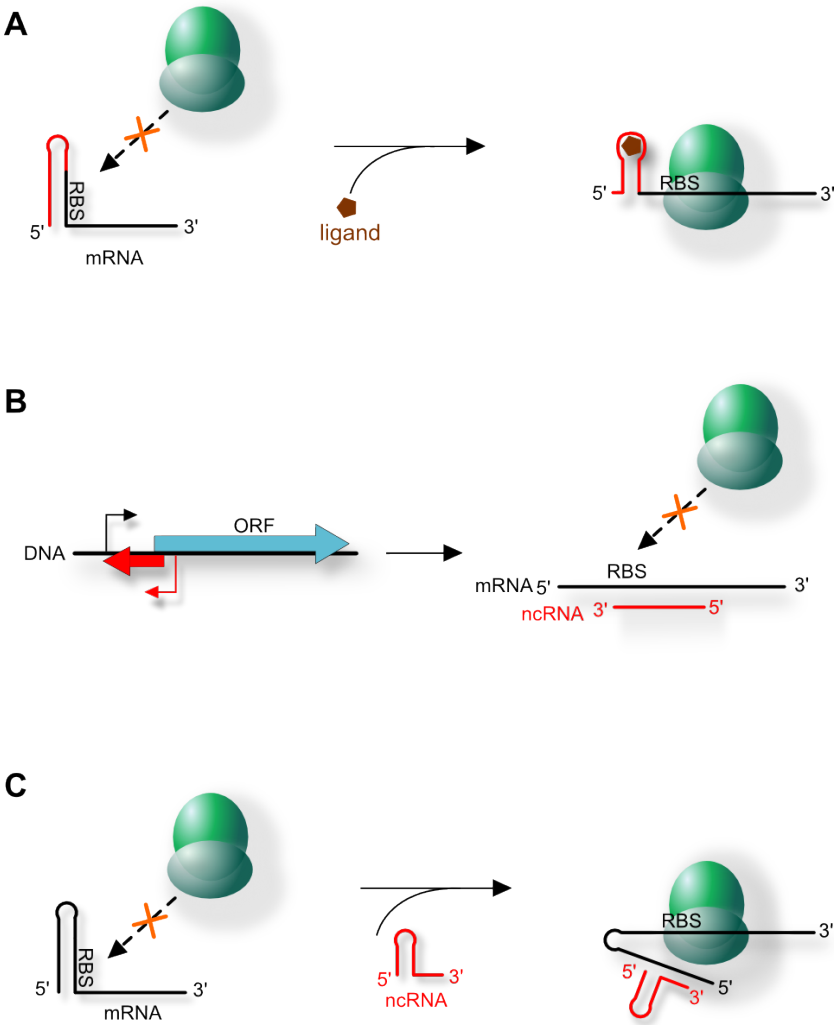

Figure 1: Functionality of diverse types of ncRNAs. (A) Example of a riboswitch: a masked ribosomal binding site (RBS) becomes accessible to the ribosome after binding of a ligand to the riboswitch aptamer. (B) Example of a *cis*-encoded ncRNA. Binding of the fully complementary ncRNA prevents binding of the ribosome and blocks initiation of translation. (C) Example of a *trans*-encoded ncRNA. A masked RBS becomes accessible after binding of the ncRNA, resulting in increased translation efficiency.

1.1.1 *Riboswitches & RNA thermometers*

2% of B. subtilis genes are regulated by riboswitches.

Riboswitches and RNA thermometers are simplified regulatory modules located at the 5′-end of mRNAs. Riboswitches are leader sequences consisting of two parts: the aptamer region which binds a ligand with usually high specificity and the expression platform which regulates the expression of the downstream gene (Mandal and Breaker, 2004). The respective mRNA is usually directly involved in the metabolism or intracellular control of the

(ligand-) metabolite.
Thermometers are complex RNA structures usually located in the 5′-UTR of protein encoding genes that change their conformation in response to temperature. This mechanism regulates transcription of genes involved in heat- or cold-shock as well as expression of virulence factors upon successful intrusion in host organisms (Narberhaus et al., 2006).

1.1.2 *Base pairing ncRNAs*

The majority of characterized ncRNAs regulate gene expression by base pairing with mRNAs. *Cis*-encoded ncRNAs are encoded on the antisense strand of their target RNA and therefore have extensive potential for base pairing. Many of these ncRNAs originate from bacteriophages, plasmids and transposons and play a role in maintaining the number of these mobile elements (Brantl, 2007). *Cis*-encoded ncRNAs expressed from chromosomes often control mRNAs that are toxic at high levels (Gerdes and Wagner, 2007).
The other ncRNAs acting by base pairing are *trans*-encoded, which means that they are synthesized as discrete transcripts with dedicated promoter and terminator sequences (Aiba, 2007; Gottesman, 2005). In many cases, ncRNAs bind to the 5′-UTR, especially the RBS, and thereby block translation initiation (Bouvier et al., 2008). These interactions are often facilitated by the Hfq protein, at least in Gram-negative bacteria. A single ncRNA can bind to multiple mRNA targets. On the other hand, one protein coding transcript can be regulated by diverse ncRNAs. Both can be found in the regulation of proteins of the outer membrane in Gram-negative bacteria (Guillier et al., 2006; Vogel and Papenfort, 2006). One of the most versatile ncRNAs is RNAIII in *Staphylococcus aureus* (Huntzinger et al., 2005; Novick and Geisinger, 2008). It binds to a variety of mRNAs, thereby regulating virulence of this important human pathogen, and it also encodes for a small protein.

Regulation of most of the trans-encoded ncRNAs is negative.

RBS = ribosomal binding site

Hfq = Sm-like RNA chaperone

1.1.3 *NcRNAs modulating protein activity*

To date, three ncRNAs are known that directly bind to proteins and regulate their function: CsrB, GlmY and 6S RNA. They all act by mimicking other nucleic acids. In *E. coli*, CsrB and CsrC regulate the RNA-binding protein CsrA which is important for carbon usage and motility (Babitzke and Romeo, 2007).
Sugar metabolism of *E. coli* is under control of GlmY, a ncRNA that sequesters GlmS. GlmY mimics another RNA, GlmZ, which normally binds to GlmS (Görke and Vogel, 2008).
Finally, 6S RNA has been shown to bind to the housekeeping

csr = carbin storage regulator

GlmS = glucosamine-6-phosphate synthase

RNA polymerase (RNAP) in *E. coli*, thus inhibiting transcription from certain promoters upon entry into stationary phase (Willkomm and Hartmann, 2005; Wassarman, 2007).

1.2 6S RNA IN BACTERIA

As many other ncRNAs, 6S RNA had been found decades before its function was revealed. The first description of 6S RNA as a distinct cellular RNA was reported in the late 1960's (Hindley, 1967) in *E. coli*; the RNA's sequence was revealed 4 years later (Brownlee, 1971). However, the role of 6S RNA remained completely nebulous for the following 30 years. One of the reasons for this might be the fact that cells lacking 6S RNA did not show a notable phenotype (Lee et al., 1985).

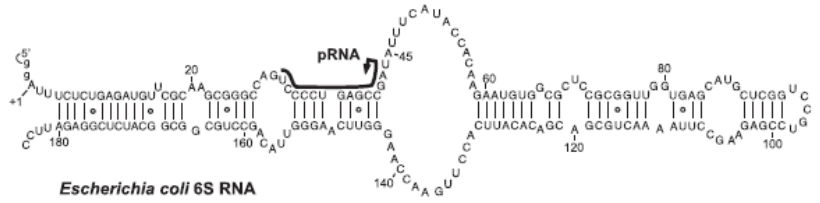

Figure 2: The secondary structure of *E.coli* 6S RNA. The typical 6S RNA features are a mainly rod-shaped, double stranded structure with a large central bulge. 6S RNA also serves as template for transcription of 10 – 20 nt pRNAs, initiating from U 44.

1.2.1 *6S RNA in E. coli*

RNAP core consists of β, β′ and 2 α subunits.

In 2000, Wassarman and Storz (2000) revealed the function of 6S RNA in *E. coli*. They found that 6S RNA coimmunoprecipitated with the σ^{70} RNA polymerase holoenzyme (Gruber and Gross, 2003), forming the hitherto unidentified 11S RNA-protein complex. However, 6S RNA bound to the σ^{70}-holoenzyme but not to the RNAP core or to the σ^{70} factor alone. Also, RNA polymerase holoenzymes containing the σ^{32} factor (a factor involved in diverse stress responses) were not subject to 6S RNA binding (Wassarman and Storz, 2000; Trotochaud and Wassarman, 2005), whereas binding to σ^{S}-holoenzymes (σ^{S} = cofactor for transcription of stationary phase-specific genes) was detectable, but much weaker than to the σ^{70}-holoenzyme (Gildehaus et al., 2007).

The structure of 6S RNA (Fig. 2) is highly conserved among bacteria and was hypothesized to be the key for RNAP binding as it resembles a DNA open promoter (Trotochaud and Wassarman, 2005; Barrick et al., 2005). 6S RNA is a rod-shaped RNA with a

large unstructured central bulge. Promoter regions of DNA adopt a similar shape after melting and forming the open promoter structure (Fig. 3).

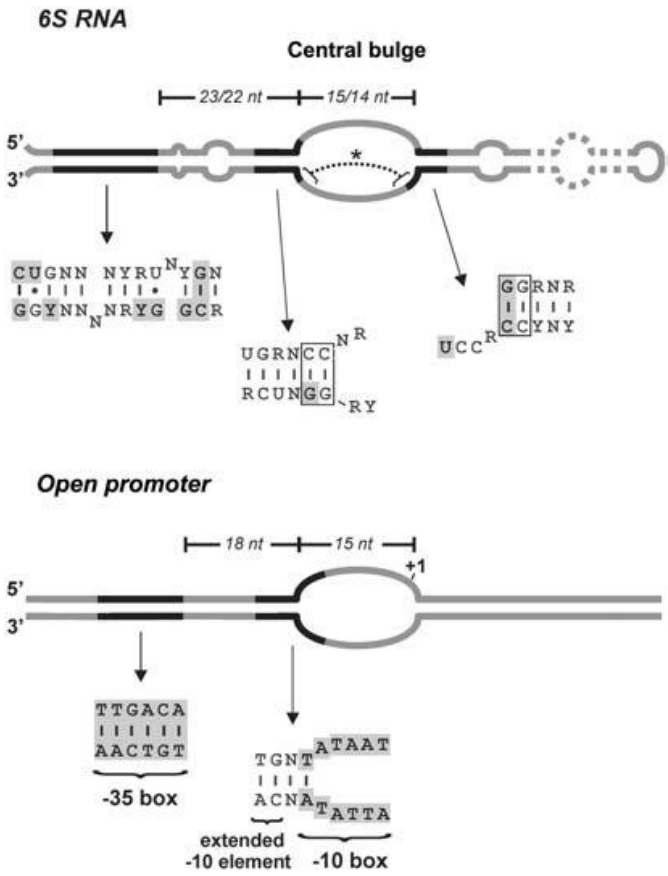

Figure 3: Comparison of the bacterial 6S RNA consensus with an open promoter. Black: regions of sequence conservation; the central bulge of 6S RNA is 'clamped' by GC base pairs (adapted from Willkomm and Hartmann (2005).

This promoter mimic hypothesis was further endorsed by studies on *E. coli* promoters, showing that region 4.2 of the σ^{70} cofactor binds to 6S RNA as well as to promoter DNA. Using microarray experiments, expression of hundreds of genes has been identified to be altered in a 6S RNA-dependent manner (Cavanagh et al., 2008). However, only a subset of σ^{70}-dependent promoters was affected; the strength of the -10 and -35 elements obviously determines if a promoter is regulated by 6S RNA-mediated inhibition of RNAP in stationary growth phase (Cavanagh et al., 2008). In a subsequent study using a series of σ^{70} mutants Klocko and Wassarman (2009) showed that the binding sites of 6S RNA and the -35 element of promoter DNA do not coincide in the 4.2 region (Fig. 4) but are overlapping. They therefore concluded that competition between 6S RNA and the -35 region of promoter DNA is the mechanism underlying 6S RNA-mediated inhibition

of transcription.

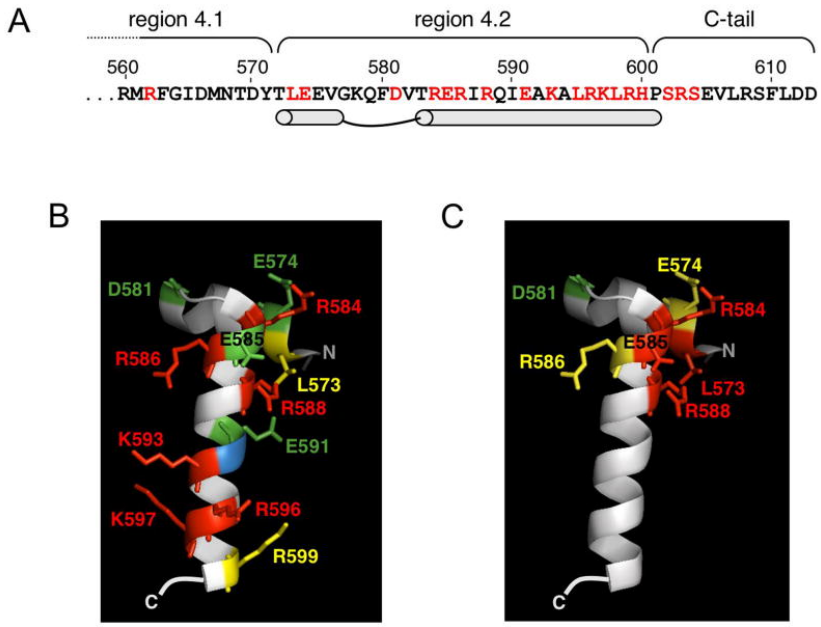

Figure 4: Differences in binding of 6S RNA and DNA to the C-terminal region of σ^{70}. (A) The amino acid sequence of regions 4.1, 4.2 and the C-tail; alanine substitutions are shown in red. The relative effects on 6S RNA binding (B) or DNA binding (C) for alanine substitutions are indicated by color: Red, strong defect in binding; yellow moderate defect in binding and green increased binding (adapted from Klocko and Wassarman (2009)).

Another breakthrough in understanding the mechanism of 6S RNA came in 2006 when it became clear that 6S RNA can bind at the active site of RNAP and may serve as a template for the synthesis of *de novo* RNA products (pRNAs) (Wassarman and Saecker, 2006; Gildehaus et al., 2007). Similar to transcription from promoter DNA, pRNA synthesis starts at a defined nucleotide within the central bubble, demonstrated by ATP being the only nucleotide able to initiate pRNA transcription (Fig. 5). Synthesis of these short transcripts was found mainly in outgrowth from stationary phase. Analysis of cellular extracts and gel retardation experiments revealed that pRNAs form hybrids with their templating 6S RNA. Furthermore, addition of rifampicin prevented pRNA synthesis as well as hybrid formation (Wassarman and Saecker, 2006; Wurm et al., 2010).

ATP = adenosine-triphosphate

Rifampicin = antibiotic blocking transcription initiation by RNAP.

Upon synthesis of pRNA, RNAP is released from the complex, an event that can also be prevented by addition of rifampicin or by deprivation of NTPs (Wurm et al., 2010). Measuring the half-life of 6S RNA resulted in the conclusion that pRNA synthesis

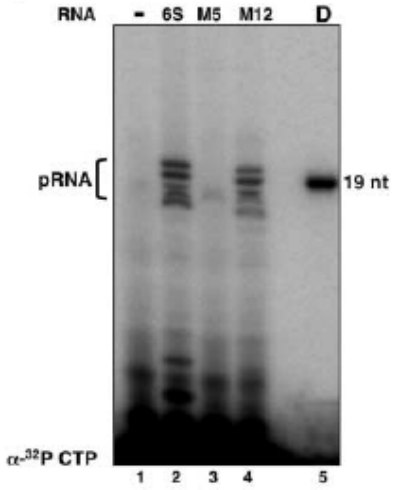

Figure 5: Synthesis of pRNA in *E. coli*. 6S RNA templates transcription by σ^{70}-RNAP *in vitro* in the presence of NTPs and α-^{32}P CTP. An inactive 6S RNA mutant (M5), lacking the central bulge, was no template for pRNA transcription (adapted from Wassarman and Saecker (2006)).

and hybrid formation trigger the degradation of 6S RNA during outgrowth (Wassarman and Saecker, 2006; Wurm et al., 2010).

1.2.2 *6S RNA in other bacteria*

In 2005, homologs of *E. coli* 6S RNA were identified in more than 100 bacteria. First, Trotochaud and Wassarman (2005) found 6S RNA homologs in β-proteobacteria by biochemical means and identified two 6S RNAs in *Bacillus subtilis* by co-immunoprecipitation with RNAP. In *Aquifex aeolicus*, 6S RNA was found to be one of the most abundant small RNAs (Willkomm et al., 2005). Finally, Barrick et al. (2005) used computer searches based on trained covariance models to predict 6S RNA homologs among bacteria (Fig. 6). All 6S RNAs identified so far share a highly conserved secondary structure: a largely double-stranded rod with a central bulge. However, despite some few conserved nucleotides near the central bulge (Fig. 3), the sequence conservation is very low (Willkomm and Hartmann, 2005).

The predicted 6S RNA homologs can be found at the rfam database (Griffiths-Jones et al., 2003).

Next to mere bioinformatic prediction, identification and verification of 6S RNA homologs by biochemical and genetic means have been performed in a variety of bacterial organisms. *Synechococcus sp.* 6S RNA, although found very early by (Watanabe et al., 1997), was initially not recognized for what it was. 6S RNA of *Salmonella typhimurium* (Sittka et al., 2008), *Sinorhizobium meliloti* (Schlüter et al., 2010), *Staphylococcus aureus* (P. Romby, per-

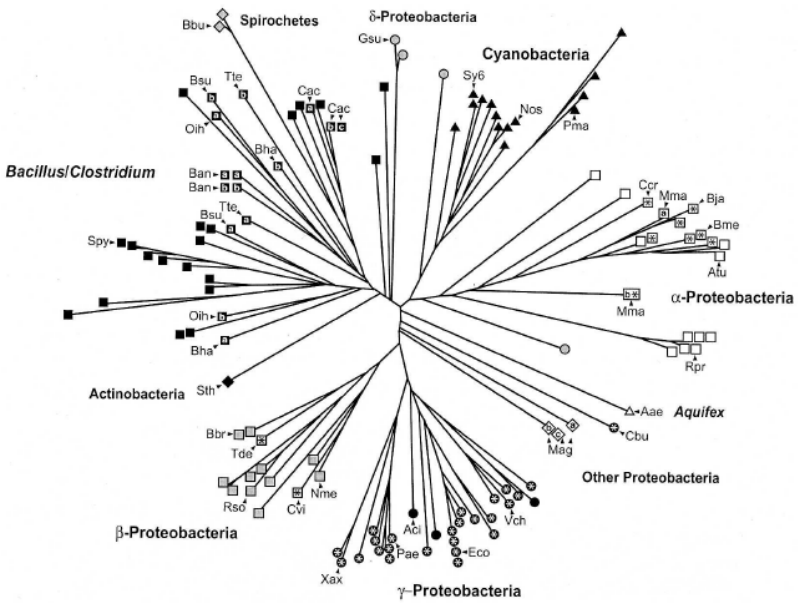

Figure 6: The phylogenetic tree of 6S RNA homologs shows the presence in all branches of the bacterial kingdom. The symbols represent the taxonomic classification of the genomes containing each a 6S RNA sequence (adapted from Barrick et al. (2005)).

sonal communication) and *Helicobacter pylori* (Sharma et al., 2010) were analyzed in the course of deep sequencing approaches. *H. pylori* 6S RNA was shown to serve as template for two different pRNA species; transcription of the two pRNAs is initiated at one side of the central bulge, ~ 70 nt apart. Microarray experiments in *Legionella pneumophila* revealed that 6S RNA is important for virulence as knockout strains were impaired in intracellular multiplication in both protists and mammalian cells (Faucher et al., 2010).

Generally, there is one copy of 6S RNA per microbial genome. In low-GC Gram-positive bacteria, however, two different 6S RNAs are present (Barrick et al., 2005). Moreover, two distinct types of 6S RNA have been reported in *Prochlorococcus* (Axmann et al., 2007).

1.3 THE TWO 6S RNA SPECIES OF BACILLUS SUBTILIS

Ando et al. (2002) and Suzuma et al. (2002) identified two abundant RNAs in *B. subtilis*, one 190 nt (with a 201 nt precursor) and the second 203 nt in length, respectively. They were recognized as 6S RNAs by Trotochaud and Wassarman (2005) in co-immunoprecipitation experiments with RNAP. Interestingly, a

third RNA was co-purified, but its sequence could not be determined. The two RNAs were renamed to 6S-1 RNA (201/190 nt) and 6S-2 RNA (203 nt). Secondary structure prediction of both RNAs and structure probing experiments of 6S-1 RNA (Trotochaud and Wassarman, 2005; Barrick et al., 2005) indicated that both have the typical 6S RNA 'shape' (Fig. 7). Intriguingly, the

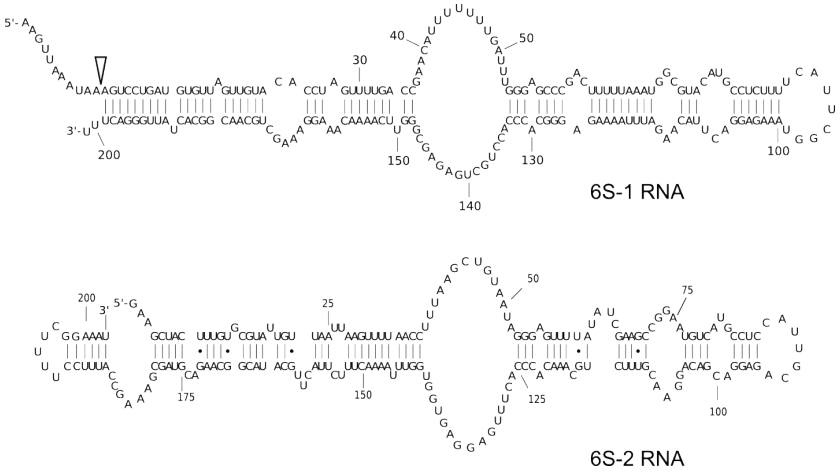

Figure 7: Secondary structure of the two 6S RNAs of *B. subtilis*, 6S-1 RNA and 6S-2 RNA. The triangle denotes the cleavage site of the 201 nt 6S-1 RNA precursor resulting in the mature 190 nt 6S-1 RNA.

expression patterns of both RNAs diverge. 6S-1 RNA levels peak, as for *E. coli* 6S RNA, in stationary phase, whereas 6S-2 RNA is most abundant during exponential growth and its levels drop upon entry into stationary phase (Barrick et al., 2005), which suggested that 6S-1 RNA is the ortholog of *E. coli* 6S RNA.

1.4 OPEN QUESTIONS IN THE CURRENT VIEW OF 6S RNA

Mainly based on investigations in *E. coli*, the current model of 6S RNA function in bacteria is as follows (Fig. 8): 6S RNA binds to the sigma factor of housekeeping RNAP by mimicking a DNA open promoter structure in a growth phase dependent manner. The housekeeping RNAP, constituting the main RNAP species in bacterial cells, is responsible for transcription of the majority of genes, especially during exponential growth. If nutrient scarcity triggers entry into stationary phase, 6S RNA levels increase and sequester mainly the housekeeping RNAP, but not polymerases with other σ factors. Thus, transcriptional regulation is altered towards expression from genes with promoters that are not affected by 6S RNA-mediated inhibition. Upon nutrient resupply and increase in transcriptional activity (outgrowth), RNAP is released

from 6S RNA. A prerequisite for this release is transcription of pRNAs from 6S RNA as a template.

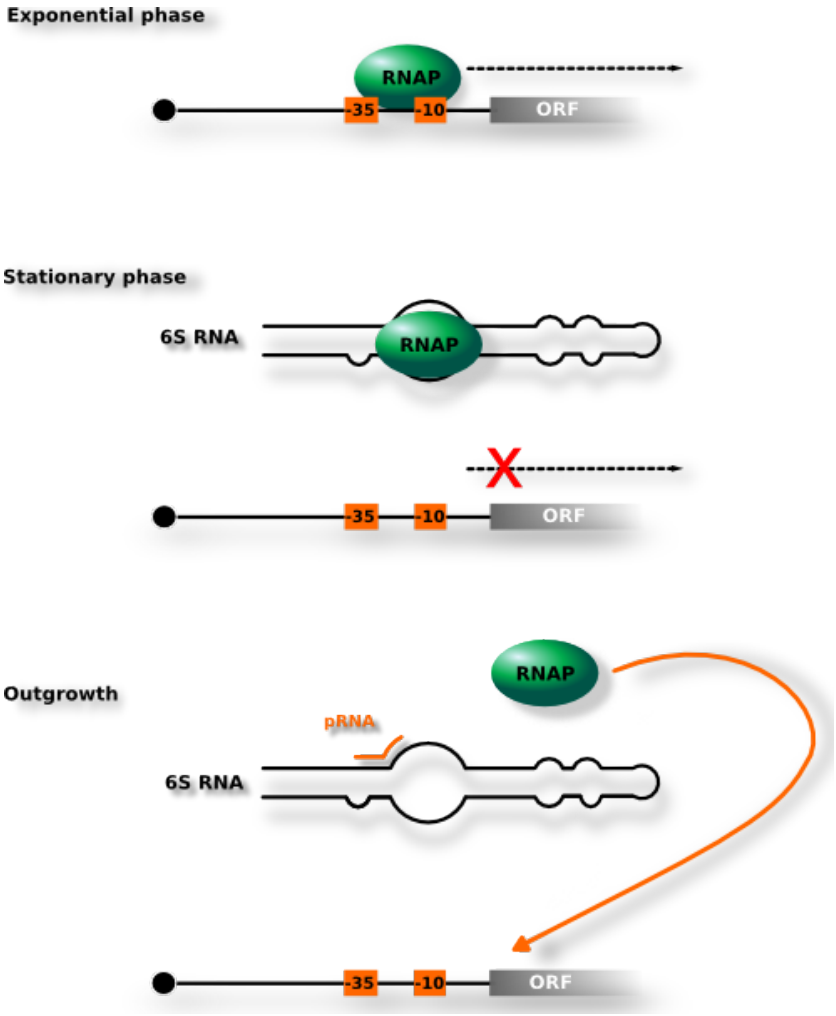

Figure 8: Current model of 6S RNA function. Transcription of 6S RNA-dependent genes by the housekeeping RNAP (exponential phase) is inhibited by large amounts of 6S RNA under nutrient limitation (stationary phase). Upon resupply with nutrients (outgrowth), RNAP is released by synthesis of short transcripts (pRNA).

This current model raises several questions: First, the promoter mimicry hypothesis is mainly based on secondary structure determination of 6S RNA. So far, the interactions between 6S RNA and RNAP have been investigated by mutational analyses, *in vivo* crosslinking, gel shift assays and RNA cleavage assays only. As yet, no tertiary structure information is available; neither from 6S RNA alone nor from 6S RNA-RNAP complexes. Therefore, this model awaits further proof.
Second, maturation of 6S RNA and its degradation are still unclear. *E. coli* 6S RNA, for example, is cotranscribed with the down-

stream *ygfA* gene and rapidly excised by an unknown mechanism (Hsu et al., 1985). Also, maturation of *B. subtilis* 6S-1 RNA from the 201 nt precursor to the 190 nt mature form (Fig. 7) is carried out by a yet unidentified nuclease. Even more important, the proposed degradation of 6S RNA during outgrowth and after pRNA-mediated release of RNAP has not been characterized so far.

Finally, release of RNAP by pRNA synthesis constitutes a unique mechanism, considering that a DNA-dependent RNA polymerase accepts RNA as template for transcription. As levels of pRNA massively increase after induction of outgrowth (Wassarman and Saecker, 2006), the question was raised whether pRNAs themselves might play a role in transcriptional regulation (Wurm et al., 2010). PRNAs were observed mainly as a by-product of RNAP release. The question how they trigger the dissociation of the RNAP-6S RNA complex has not been addressed yet. Also, the trigger of pRNA synthesis itself remaines unknown. It has been speculated that increasing NTP levels during outgrowth (Murray et al., 2003) provide the signal for pRNA transcription (Wassarman and Saecker, 2006).

1.5 GOAL OF THE PROJECT

Although identified in several organisms, 6S RNA function has been investigated nearly exclusively in *E. coli*. To broaden our understanding of this ubiquitous riboregulator, we initiated our investigations on 6S RNAs in *B. subtilis*. This organism was of particular interest as it i) is one of the best investigated Gram-positive model organisms and therefore a counterpart to Gram-negative *E. coli*, ii) is closely related to several pathogenic organisms (e.g. *B. anthracis*) and many ncRNAs are important for regulation of virulence (see above); discoveries in *B. subtilis* might be testable and also applicable in these pathogens and iii) the presence of two 6S RNA species was intriguing as, once the ortholog of the canonical 6S RNA is found, the role of the second 6S RNA species might give further insights into the function of this global regulator of transcription.

One focus of the project was to identify pRNAs in *B. subtilis* and, given they could be found, investigate if they are also a prerequesite for the release of RNAP, as in the case of 6S RNA in *E. coli*. After proving this, we wanted to understand the role of these short transcripts in the mechanism of release of RNAP from 6S RNA in general.

Part II

MATERIALS AND METHODS

2 MATERIALS AND METHODS

Chew, if only you could see
what I've seen with your eyes!

— Roy Batty

Manufacturers of chemicals, enzymes and kits as well as the phenotypes of bacterial strains and plasmids are listed in the appendix.

2.1 STANDARD BUFFERS AND SOLUTIONS

Some buffers and solutions were used throughout the complete work.

5 x TBE	445 mM Tris, 445 mM borate, 10 mM EDTA
20 x SSC	3M NaCl, 300 mM Na-citrate pH 7.0
10 x MOPS	200 mM MOPS, 50 mM NaOAc pH 7.0, 20 mM EDTA
10 x TE	100 mM Tris-HCl pH 8.0, 10 mM EDTA
Tris buffers	1 M Tris stock buffers, adjusted with HCl at room temperature to pH values from 6.8 to 8.0
Phosphate buffers	1 M Na_2HPO_4 and 1 M NaH_2PO_4 were mixed in a defined ratio (Sambrook and Russel, 2001) and filled up with water to obtain 100 mM Na-phosphate buffers with pH values from 5.8 to 8.0
HEPES	1 M Tris stock buffers, adjusted with NaOH at room temperature to pH 7.5

Table 1: Standard buffers and solutions.

2.2 BACTERIAL CELL CULTURE

Media were usually autoclaved in culture flasks directly and stored until needed.

All media, buffer, flasks and pipets used in bacterial cell culture were autoclaved for 20 min at 121°C and 1 bar pressure. As an alternative, heat unstable solutions were sterile filtrated before usage.

Peptone	10 g/l
Yeast extract	5 g/l
NaCl	10 g/l
demin. H_2O	ad 1 litre

Table 2: LB medium for bacterial cell culture.

ANTIBIOTIC	STOCK	E. COLI	B. SUBTILIS
Ampicillin	100 mg/ml (in ddH_2O)	100 µg/ml	-
Kanamycin	50 mg/ml (in ddH_2O)	50 µg/ml	10 µg/ml
Chloramphenicol	25 mg/ml (in EtOH)	25 µg/ml	-
Spectinomycin	25 mg/ml (in EtOH)	100 µg/ml	-
Rifampicin	25 mg/ml (in MetOH)	-	100 µg/ml

Table 3: Antibiotics used in bacterial cell culture. The final concentration used for cell culture of *E. coli* and *B. subtilis* are indicated.

2.2.1 *Bacterial cell culture in liquid medium*

Large culture volumes were usually grown in baffled flasks for increased growth speed.

E. coli and *B. subtilis* cells were grown at 37°C in LB medium. Antibiotics were added in concentrations summarized in Table 3. For long time storage, *E. coli* and *B. subtilis* cultures were diluted in 1 volume of glycerol, frozen in liquid nitrogen and stored at -80°C. LB-medium was prepared as described in Table 2 and adjusted to pH 7.5 with NaOH before autoclaving.

2.2.1.1 *Antibiotics used in bacterial cell culture*

Antibiotics were prepared as stock solutions and added to autoclaved liquid media directly before use.

2.2.1.2 *Growth curve experiments*

For growth curve experiments, culture flasks without baffles were used.

DETERMINATION OF OPTICAL DENSITY To estimate doubling time and speed of growth of bacteria, 100 µl aliquots of liquid cultures were diluted in a 1:10 ratio with fresh medium and optical density (OD) at 576 nm was measured in a 1 cm cuvette. The respective medium was used for baseline correction. If $OD_{576\ nm}$ exceeded a value of 0.7, the sample was again diluted in a 1:10

X-Gal	0.2 mg/ml (in dimethylformamide)
IPTG	500 µM

Table 4: Supplements for blue/white selection in cloning experiments.

ratio. To start growth curve experiments, culture medium was inoculated with a starting density of $OD_{576\,nm}$ 0.05.

B. SUBTILIS GROWTH STAGES *B. subtilis* was analyzed in different growth stages, which were defined as follows:

For an example growth curve see Fig. 23.

- EXPONENTIAL PHASE Cells in exponential growth phase were harvested at $OD_{576\,nm}$ 1.0.
- LATE STATIONARY PHASE Cells in late stationary phase were harvested at $OD_{576\,nm}$ 3.0. This stadium was usually reached 24 hrs after inoculation.
- OUTGROWTH Outgrowth was induced by diluting cells in late stationary phase in a 1:5 ratio in fresh, prewarmed medium. If not stated otherwise, cells were harvested 3 minutes after dilution.

2.2.2 *Bacterial growth on agar plates*

To grow bacterial cells on agar plates, LB medium was supplemented with 12 g/l agar-agar. Antibiotics (3) were added after autoclaving and cooling down to 55°C. For experiments using blue/white selection of strains harboring the *lacZ* gene, plates were additionally supplemented with X-Gal and IPTG (Table 4).

Blue/white selection was optimized by incubating grown cells on plate for 2 h at 4°C.

2.2.3 *Preparation of bacterial cell extracts*

Bacterial cell pellets from liquid cultures of 25 $OD_{576\,nm}$ were resuspended in 1 ml CE lysis buffer (Table 5) by rigorous vortexing. The solution was added to 200 µl autoclaved glass beads. Cell disruption was performed utilizing a cell homogenizer with intervalls of 45 s at 5 m/s and 15 s on ice (6 repetitions). Cell lysates were separated from the beads by centrifugation (10 min at 11,000 x g and 4°C) and distributed into 200 µl aliquots. Each aliquot was again diluted with 1 volume of CE lysis buffer.

Bacterial cell lysates were always prepared directly before experiments.

2.2.4 *Preparation of chemically competent E. coli cells*

To prepare chemically competent *E. coli* cells for uptake of foreign DNA, we applied the $CaCl_2$ method. 100 ml LB medium were inoculated with 3 ml overnight culture and incubated at 37°C

Chemically competent E. coli DH5α cells were used for all cloning purposes.

Tris (HCl) pH 8.0	20 mM
KCl	150 mM
$MgCl_2$	1 mM
Lysozyme	0.5 mg/ml

Table 5: Cell lysis buffer for preparation of bacterial cell extracts.

$CaCl_2$	75 mM
Glycerol	25% (v/v)

Table 6: CCB solution for preparation of chemically competent *E. coli* cells.

and 220 rpm until $OD_{576\ nm}$ reached 0.5 - 0.7. Cells were cooled on ice for 5 min and then centrifuged for 5 min at 2,500 x g and 4°C. The cell pellet was resuspended in 30 ml cold 100 mM $CaCl_2$, incubated on ice for 5 min and centrifuged again. After discarding the supernatant, cells were resuspended in 3 ml CCB solution (Table 6) and aliquots of 100 µl were taken. Competent cells were frozen in liquid nitrogen and stored at -80°C.

2.2.5 *Preparation of naturally competent B. subtilis cells*

This method was applied to generate genomic mutant strains of B. subtilis.

Although naturally competent cells can be stored, freshly prepared cells had a higher competence in DNA uptake.

For an efficient uptake of PCR products into *B. subtilis* cells, we used the SpC/SpII medium method to obtain natural competent cells. 3 ml SpC medium (Table 7) were inoculated with a single colony from an agar plate and incubated over night at 37°C and 180 rpm. The culture was then transfered to 20 ml of fresh, prewarmed SpC medium and incubated at 37°C and 180 rpm until $OD_{576\ nm}$ remained unchanged for 20 min. 5 ml were diluted in 45 ml of SpII medium (Table 8) and grown for another 90 min at 37°C and 180 rpm. Cells were centrifuged for 5 min at room temperature and 2,500 x g and subsequently resuspended in a mixture of 4.5 ml supernatant and 0.5 ml 99% glycerol. Aliquots of 100 µl were frozen in liquid nitrogen and stored at -80°C.

T-base	20 ml
50% Glucose (w/v)	0.2 ml
1.2% $MgSO_4 \cdot 7\ H_2O$ (w/v)	0.3 ml
1% Peptone (w/v)	0.5 ml
10% Yeast extract (w/v)	0.4 ml

Table 7: SpC medium for preparation of naturally competent *B. subtilis* cells.

T-base	200 ml
50% Glucose (w/v)	2 ml
1.2% $MgSO_4 \cdot 7\ H_2O$ (w/v)	14 ml
1% Peptone (w/v)	2 ml
10% Yeast extract (w/v)	2 ml
0.1 M $CaCl_2$	1 ml

Table 8: SpII medium for preparation of naturally competent *B. subtilis* cells.

$(NH_4)_2SO_4$	2 g
$K_2HPO_4 \cdot H_2O$	18.3 g
KH_2PO_4	6 g
$Na_3Citrat \cdot 2H_2O$	1 g
ddH_2O	ad 1000 ml

Table 9: T-base for SpC- and SpII media.

2.2.6 *Transformation of chemically competent E. coli cells*

50 µl of chemically competent *E. coli* cells (2.2.4) were thawed on ice and 5 µl of a ligation mixture or 20 ng plasmid preparation were added. Cells were incubated on ice for 20 min and then heat-shocked for 30 s at 42°C. After incubating on ice for another 2 min, 600 µl of LB medium was added and cells were incubated for 1 h at 37°C while shaking. 100 µl of the suspension were then plated onto an agar plate containing antibiotics for selection of transformed cells (2.2.1.1) and incubated at 37°C overnight.

2.2.7 *Transformation of naturally competent B. subtilis cells*

To transform natural competent *B. subtilis* cells (2.2.5), 5 µg of a PCR product was mixed with 100 µl of competent cells and incubated for 2 h at 37°C while shaking. The complete mixture was plated on an agar plate containing antibiotics for selection of transformed cells (2.2.1.1) and incubated at 37°C overnight.

2.3 GENERAL NUCLEIC ACID TECHNIQUES

DNA/RNA samples were kept at -20°C for long time storage and cooled on ice when experiments were performed. In general, nucleic acids were dissolved in double distilled water if not stated otherwise. DNA and RNA sequences are always given in 5′ to 3′ direction.

Ethanol abs.	2.5 volume
Isopropanol abs.	1 volume

Table 10: Alcohols used for precipitation of nucleic acids

2.3.1 *Precipitation of nucleic acids*

Precipitation of nucleic acids using alcohol is a widely used method. It is employed to concentrate DNA/RNA and to remove salts. Nucleic acids precipitate in the presence of monovalent cations and are recovered by centrifugation and redissolving in water. The majority of salts remains in the alcohol supernatant.

We regularly precipitated RNA before shipping by post-services.

For precipitation, $^1/_{10}$ volume of 3 M NaOAc pH 5.0 was added to one volume of DNA/RNA solution, followed by mixing with the appropriate amount of absolute alcohol as shown in Table 10. Samples were cooled at -20°C for 20 min and subsequently centrifuged for at least 30 min at 11,000 x g and 4°C. If isopropanol was used for precipitation, an additional washing step with 70% (v/v) ethanol was performed. After removing the supernatant, the DNA/RNA pellet was dried at room temperature for 5 min and dissolved in an appropriate amount of double-distilled water.

Care was taken to not overdo drying as this may lead to insolubility of nucleic acids.

2.3.2 *Phenol/chloroform extraction of nucleic acids*

Phenol/chloroform extraction is a widely used technique to purify nucleic acids from proteins in *in vitro* experiments or from total cell extracts. In this two-step procedure, proteins are first denatured by addition of phenol. In a second step, residual phenol is finally extracted by chloroform.

In another variant of this technique, phenol, chloroform and isoamylalcohol were pre-mixed in a 24:24:1 ratio.

One volume of TE-saturated (10 mM Tris-HCl, 1 mM EDTA, pH 7.5 - 8.0) phenol is added to a DNA/RNA sample and vigorously vortexed. If cellular RNA was prepared from bacteria, acid (saturated with 300 mM NaOAc pH 4.9) phenol was used to improve separation from cellular DNA (Mülhardt, 2002). After centrifugation for 5 min at 11,000 x g and room temperature in a table-top centrifuge, the upper aqueous phase was removed and transferred into a new tube. Care was taken to avoid the interface containing proteins (and DNA in the case of cellular RNA preparation). The aqueous phase was extracted again using 1 volume of chloroform. Finally, the DNA/RNA in the aqueous layer was precipitated as described (2.3.1).

% AGAROSE (W/V)	DNA FRAGMENT SIZE (KBP)
0.5	1.0 – 30
0.7	0.8 – 12
1.0	0.5 – 7
1.2	0.4 – 6
1.5	0.2 – 3
2.0	0.1 – 2

Table 11: Separation range of DNA fragments in agarose gels.

Bromophenol blue	0.25% (w/v)
Xylene cyanol blue	0.25% (w/v)
Glycerol	25% (v/v)
5 x TBE buffer	fill up volume

Table 12: 5 x DNA loading buffer for agarose gels.

2.3.3 *Nucleic acid gel electrophoresis*

Analysis of nucleic acids usually includes length separation by gel electrophoresis. Negatively charged nucleic acids separate in an electric field according to their size, whereas short molecules migrate faster in the gel matrix. Electrophoretic mobility is proportional to the field strength and net charge of the molecule.

2.3.3.1 *Agarose gel electrophoresis*

For analysis of DNA, agarose gels were used. Agarose is a polysaccharide composed of galactose and its derivatives. To prepare agarose gels, agarose was dissolved in 1 x TBE buffer by heating in a microwave oven. When the gel solution was cooled down to 55°C, ethidium bromide was added to a final concentration of 400 ng/ml and the solution was poured into a gel tray with a comb. Concentration of agarose depended on the size of expected fragments (see Table 11). 1 x TBE was also used as running buffer. DNA samples were dissolved 1:5 in 5 x DNA loading buffer (Table 12) before loading. Gels were run at 7.5 mA/cm width of the gel.

2.3.3.2 *Polyacrylamide gel electrophoresis (PAGE)*

Short DNA fragments as well as RNA of a size up to 300 nt were analyzed on polyacrylamide (PAA) gels. Acrylamide and bisacrylamide are able to form cross-links upon polymerization. The length of the polymer chains and the pore size is defined

	20% DENATURING	20% NATIVE
5x TBE buffer	200 ml	200 ml
Acrylamide (48%): Bisacrylamide (2%)	400 ml	400 ml
Urea	8 M	–
H_2O	ad 1000 ml	ad 1000 ml

Table 13: PAA gel stock solutions for denaturing and native gels.

	2X DENATURING	2X NATIVE
Bromophenol blue	0.02% (w/v)	0.02% (w/v)
Xylene cyanol blue	0.02% (w/v)	0.02% (w/v)
Glycerol	–	30% (v/v)
Urea	2.6 M	–
Formamide	66% (v/v)	–
5x TBE buffer	ad 1000 µl	–
H_2O	–	ad 1000 µl

Table 14: PAA gel sample loading buffers.

by acrylamide concentration (5 - 20%) and the ratio of acrylamide:bisacrylamide (48:2).
Polymerization of PAA is a radicalic reaction, initiated by addition of APS (Ammonium persulfate) and TEMED (N,N,N′,N′,-tetramethylethylendiamin). We used native and denaturing PAGE (Table 13) to analyze RNA. For denaturing gels, we added urea which forms stacking interactions as well as hydrogen bonds to bases of nucleic acids. This leads to destabilization of RNA secondary structures (Priyakumar et al., 2009).

Analysis of 6S RNA was usually performed on 10% PAA gels whereas pRNA analysis was conducted on 15% - 20% PAA gels.

For preparation of PAA gels, PAA gel solution was prepared as 20% stock and diluted with 5 x TBE urea to the desired percentage (5 - 20%). For denaturing PAA gels, the stock solution and 5 x TBE was supplemented with 8 M urea. Table 15 indicates the fragment size of single stranded DNA comigrating with either the BPB or XCB dyes of the loading buffer.

The polymerization reaction was induced by addition of 10% APS (0.01 volume) and TEMED (0.001 volume). The gel solution was poured between two glass plates separated by plastic spacers (1 mm) and a comb was placed on the top. Care was taken that no air bubbles formed between the plates. The gel was left until the PAA solution had completely polymerized (~30 min) which was controlled by a small aliquot of the solution left to polymerize in

% POLYACRYLAMIDE	BPB [NT]	XCB [NT]
5	35	130
6	26	106
8	19	70-80
10	12	55
20	8	25

Table 15: Size of DNA fragments comigrating with the dyes of the loading buffer in denaturing polyacrylamide gels; BPB = bromophenol blue; XCB = Xylene cyanol blue.

a beaker. After removal of the comb, gel pockets were immediately rinsed with 1 x TBE using a syringe to remove urea which tends to diffuse into the pockets of denaturing gels as well as to prevent further polymerization of remaining polyacrylamide solution within the pockets.
The gel was placed in a suited gel chamber with 1 x TBE filling the two separated buffer reservoirs. Prior to loading, nucleic acid samples were mixed with 1 volume 2 x denaturing loading buffer or 1 volume 2 x native loading buffer (Table 14), respectively. In the case of RNA (but not in gel retardation assays), samples were heated to 95°C for 5 min to destroy RNA secondary structures and placed on ice immediately. The samples were loaded into the pockets using a thin pipet tip and electrophoresis was performed using 0.1 mA/cm².

2.3.3.3 *Detection of nucleic acids in gel electrophoresis*

ETHIDIUM BROMIDE STAINING In polyacrylamide and agarose gel electrophoresis, nucleic acids were most frequently visualized by ethidium bromide staining. Ethidum bromide intercalates between stacked bases of nucleic acids and emits fluorescent light at 590 nm (orange) when excited by UV light (254 - 366 nm). To stain polyacrylamide gels, glass plates were carefully removed after electrophoresis was finished and the gel was incubated in 1 x TBE containing 300 ng/ml ethidium bromide for 10 min at room temperature with gentle shaking. Afterwards, the gel was placed on a UV-transilluminator and nucleic acids were visualized and documented using a digital camera system.
In the case of agarose gels, ethidium bromide was already added during gel preparation (2.3.3.1).

As an alternative, SYBR Gold staining provides even higher detection sensitivity, especially for short nucleic acids.

For preparative agarose gels, crystal violet stained gels were used instead of the mutagenic ethidium bromide staining, which was sometimes advantageous for cloning of PCR fragments purified by agarose gel extraction.

CRYSTAL VIOLET STAINING OF DNA Agarose gels containing DNA for preparation were stained with crystal violet. Although being less sensitive than ethidium bromide, crystal violet binds to DNA via static interactions; an interaction that is strong as long as an electric field is applied. Therefore, DNA bands should be excised immediately after finishing the electrophoresis. Agarose was dissolved in 1 x TBE (2.3.3.1) and crystal voilet was added afterwards to a final concentration of 10 µg/ml to the gel solution and to the running buffer. After electrophoresis, the gel was placed on a glass plate and bands were excised using a sterile scalpel.

UV SHADOWING In the case of preparative polyacrylamide gels, nucleic acids were visualized by UV shadowing without staining. After electrophoresis and careful removal of the glass plates, the gel was wrapped in transparent foil, placed on a fluorescent chromatography plate and illuminated by UV light (256 nm). As DNA and RNA absorb light of this wavelength, bands appeared as dark shadows. Bands of interest were marked with a pen and excised with a sterile scalpel.

AUTORADIOGRAPHY ^{32}P labeled nucleic acids were visualized using a phosphoimaging analyzer. After electrophoresis, the glass plates were removed, the gel was wrapped in transparent foil and an imaging plate was exposed to it. Exposure time varied from 1 min to overnight depending on the amount of radioactive material. The image plate was scanned using a BIO-imaging analyzer BAS 1000 and the PC-BAS software. Evaluation was performed using the imaging software AIDA.

2.3.3.4 *Gel elution of nucleic acids*

Elution of nucleic acids was performed by either using a gel extraction kit for agarose gels (DNA preparation) or by diffusion from polyacrylamide gels (RNA preparation).

EXTRACTION OF DNA FROM AGAROSE GELS For extraction of DNA from agarose gels, the Wizard®SV Gel and PCR Clean-Up System kit was used according to the manufacturer's instructions.

Vortex vigorously for 1 min before precipitation.

EXTRACTION OF RNA FROM POLYACRYLAMIDE GELS RNA was extracted from polyacrylamide gels by diffusion. After gel electrophoresis and UV shadowing or autoradiography (see above), the gel slice containing the RNA was placed in a 1.5 ml reaction tube and incubated overnight in 5 volume of 1 M NaOAc pH 5.0 at 4°C and rigid shaking. The next day, the eluate was removed and RNA was concentrated by ethanol precipitation (2.3.1).

2.3.4 *Photometric concentration determination of nucleic acids*

The concentration of nucleic acids in solution was determined by UV spectroscopy. According to the law of Lambert-Beer, the concentration can be calculated by determining the absorbance at 260 nm (A_{260}):

$$E = \epsilon \cdot c \cdot d \tag{2.1}$$

with ϵ = molar extinction coefficient $[1/(M \cdot cm)]$, c = molar concentration [M] and d = path length of the cuvette [cm].

1 µl of DNA or RNA was diluted in 199 µl water and the absorbance (A_{260}) was measured in an UV-spectrophotometer relative to water. The nucleic acid concentration was calculated using the known values c(1 A_{260}) that represent the concentration corresponding to one absorbance unit at 260 nm (1 A_{260}):

- 1 A_{260} double-stranded DNA corresponds to a c(1 A_{260}) of ~50 µg/ml
- 1 A_{260} single-stranded DNA corresponds to a c(1 A_{260}) of ~33 µg/ml
- 1 A_{260} RNA corresponds to a c(1 A_{260}) of ~40 µg/ml

This results in a general formula for DNA/RNA concentration calculation:

$$c[\mu g/\mu l] = \frac{A_{260} \cdot c(1A_{260}) \cdot D_f}{1000} \tag{2.2}$$

(c is concentration in µg/µl, D_f is the dilution factor)

2.4 DNA TECHNIQUES

2.4.1 *Preparation of bacterial chromosomal DNA*

Genomic DNA of bacteria was prepared using a robust and fast protocol that makes use of Na-perchlorate (Sambrook and Russel, 2001). An overnight culture (3 ml volume) was centrifuged for 10 min at 7,000 rpm and room temperature to pellet bacteria. The pellet was washed two times in TE buffer and finally ressolved in 300 µl TE buffer. To increase efficiency of cell lysis, 30 µl lysozyme solution (20 mg/ml in TE buffer) was added and incubated for 10 min at room temperature. Next, 100 µl 10% SDS solution, 100 µl 5 M Na-perchlorate and 500 µl chloroform/isoamylalcohol (24:1) solution were added and mixed by shaking the tube for 30 s by hand. The mixture was then centrifuged for 5 min at 11,000 x g and room temperature. The upper aqueous phase (~400 µl) was transfered to a new tube and precipitated using 800 µl

Solution I	50 mM glucose, 25 mM Tris(HCl) pH 8.0, 10 mM EDTA
Solution II	0.2 N NaOH, 1% (w/v) SDS
Solution III	3 M K-acetate pH 5.2

Table 16: Solutions for plasmid minipreparation.

cold ethanol. The clearly detectable DNA was carefully wrapped around a sterile pipet tip and transfered to a new tube containing 200 µl 70% ethanol. After centrifugation for 2 min at 11,000 x g and room temperature, ethanol was removed. The DNA pellet was air-dried for 5 min and dissolved in 300 µl double distilled water.

2.4.2 *Preparation of plasmid DNA*

Preparation of plasmid DNA from bacteria was performed either by an alkaline extraction procedure (Birnboim and Doly, 1979) or using plasmid purification kits. Both methods rely on the same principle, whereas the final purification of DNA relies on either precipitation or the usage of spin columns (kit variant).
For alkaline extraction, an overnight culture (3 ml volume) was centrifuged for 5 min at 11,000 x g in an eppendorf tube and the medium supernatant was discarded. The pellet was resuspended in 150 µl cold solution I by rigorous vortexing. 5 µl RNaseA (10 mg/ml) were added and incubated for 5 min. Next, 150 µl freshly prepared solution II was added, mixed by inverting the tube 5 times and incubated for 3 min. For precipitation of proteins and membranes, 150 µl cold solution III was added and mixed by inverting the tube 5 times which leads to immediate formation of cloudy precipitates. The mixture was centrifuged for 5 min at 11,000 x g and room temperature and care was taken to transfer only the clear supernatant to a new tube. The plasmid DNA was then precipitated as described above (2.3.1).
If the GeneJet™Plasmid Miniprep Kit was used, the last step was replaced by adding the DNA solution to silica membranes from the kit, bound and washed before elution with double distilled water. All buffers (solution I - III, wash buffer) were kit-supplied and were used according to the manufacturer's instructions.

Solution I and III were stored at 4°C.

Prepare solution II always fresh from a 10 N NaOH stock.

2.4.3 *Restriction digest of DNA*

For analytical purposes as well as for cloning experiments, cleavage of DNA at specific sites has been conducted using restriction

DNA	up to 5 µg
10 x Reaction buffer	5 µl
Restriction enzyme	up to 40 U
ddH_2O	ad 50 µl

Table 17: Restriction digest mixture.

DNA LIGATION	CONC.	VOLUME
Plasmid DNA	100 ng/µl	1 µl
Insert DNA	100 ng/µl	5 µl
Reaction buffer	10 x	2 µl
T4 DNA Ligase	5 Weiss U/µl	2 µl
ddH_2O		ad 20 µl

Table 18: DNA ligation reaction mixture.

endonucleases. Type II restriction endonucleases usually recognize short (often 6 bp) palindromic sequences and cleave DNA directly in this sequence or in close vicinity. This group can be further subdivided into enzymes producing a 'blunt cut' or enzymes that cut both strands displacedly ('sticky ends'). A list of enzymes used and their recognition sequences is provided in the appendix.

Double digestion reactions with two enzymes at the same time were performed according to the manufacturer's instructions.

All restriction digestion reactions were performed according to the manufacturer's instructions and the provided buffers were used. Usually, up to 5 µg DNA was incubated with 20 - 40 Units of a restriction enzyme for 120 min at 37°C. After this, restriction efficiency was analyzed on a small ethidium bromide stained agarose gel (2.3.3.1) and DNA was purified using spin columns from the QIAquick®PCR Purification Kit.

2.4.4 *Ligation of DNA fragments*

Ligation of DNA was usually necessary to introduce (short) DNA fragments into plasmids. After digestion of two DNA fragments with the same restriction enzyme (see above) producing the same 5'- or 3'- overhangs, T4 DNA Ligase was used to form the phospodiester bond between the complementary sticky ends. The ligation mixture (18) was incubated at room temperature for at least 3 h or over night at 4°C.

ENZYME	ORIGIN	SPEED	ERROR RATE
Taq	*Thermus thermophilus*	~1000 nt/min	$285 \cdot 10^{-6}$
Pfu	*Pyrococcus furiosus*	~500 nt/min	$7.69 \cdot 10^{-7}$
Vent	*Thermococcus litoralis*	~500 nt/min	$57 \cdot 10^{-6}$

Table 19: DNA polymerases used in PCR reactions.

2.4.5 *PCR*

PCR (polymerase chain reaction) is a standard method in molecular biology allowing to multiply DNA in an exponential manner (Mullis et al., 1994) and modify its sequence (mutation), given suitable primers are being used. PCR was employed to identify positive clones in cloning procedures (screen PCR) as well as to prepare inserts for plasmids or genomes.

2.4.5.1 *Standard PCR*

Taq reaction buffer: 10 mM Tris(HCl) pH 8.8, 50 mM KCl, 0.08% (v/v) Non-idet P40

Pfu reaction buffer: 20 mM Tris(HCl) pH 8.8, 10 mM $(NH_4)_2SO_4$, 10 mM KCl, 0.1 mg/ml BSA

Vent reaction buffer: 20 mM Tris(HCl) pH 8.8, 10mM $(NH_4)_2SO_4$, 10 mM KCl, 2 mM $MgSO_4$, 0.1% (v/v) Triton X-100

Standard PCR was performed to generate DNA sequences for insertion into plasmids during cloning processes or for screening of positive clones.using a buffer containing ethanol Different DNA polymerases were used according to their features (e.g. speed, proof-reading). Taq- and Pfu-polymerase were either available as lab stocks or purchased. For self-prepared polymerases, 1 µl was used in PCR reactions routinely.

Usually, 100 ng DNA were used as template for a 50 µl PCR reaction. To screen for positively transformed clones, a bacterial colony was picked from an agar plate, diluted in 30 µl double distilled water, heated for 5 min at 95°C, and 5 µl of this cell debris was used directly as template for PCR. Primer annealing temperature (T_M) was calculated using a web tool[1] which makes use of a nearest-neighbor two-state model (Allawi and SantaLucia, 1997). Mg^{2+}-ion concentration was usually 2.5 mM and was altered from 1.5 mM to 5 mM when initial PCR reactions failed. For standard PCR reactions, 30 PCR cycles were applied. Afterwards, samples were purified using the QIAquick®PCR Purification Kit and an aliquot was analyzed on an ethidium bromide stained agarose gel (2.3.3.1).

2.4.5.2 *Mutagenesis PCR*

In many cases, DNA has to be modified to obtain altered gene products (RNA or proteins). Mutagenesis of DNA involves single nucleotide mutations as well as addition or deletion of larger

1 http://eu.idtdna.com/analyzer/Applications/OligoAnalyzer/Default.aspx

	FINAL CONC.	VOLUME
100 ng/µl DNA template	2 ng/µl	1 µl
10 x reaction buffer	1 x	5 µl
25 mM $MgCl_2$	2.5 mM	5 µl
10 mM dNTP-Mix	0.4 mM	2 µl
100 µM Primer forward	500 nM	0.5 µl
100 µM Primer reverse	500 nM	0.5 µl
5 U/µl Polymerase	0.1 U/µl	1 µl
ddH_2O		ad 50 µl

Table 20: Standard PCR reaction mixture.

	TIME	TEMP.
Initial denaturation	2 min	94°C
Denaturation	2 min	94°C
Annealing	0.5 min	b
Elongation	a	72°C
Final elongation	3 min	72°C

Table 21: PCR cycle program. Standard setup: 30 cycles. a: depending on product length and elongation rate of the polymerase. b: depending on the primer's sequence.

PHOSPHORYLATION	FINAL CONC.	VOLUME
Primer (100 pmol/µl)	20 pmol/µl	10 µl
10 x T4 PNK buffer A (forward)	1 x	5 µl
10 mM ATP	1 mM	5 µl
10 U T4 PNK	0.4 U/µl	2 µl
ddH_2O		ad 50 µl

Table 22: 5′-end phosphorylation of DNA.

parts of a gene. The first was achieved by site directed mutagenesis, the latter by generation of megaprimers or extension overlap PCR.

SITE DIRECTED MUTAGENESIS Site directed mutagenesis is a simple technique to introduce single nucleotide mutations in plasmid DNA. One of the two primers for this PCR contains a mismatch flanked by sequences complementary to the wild-type DNA, whereas the second primer is fully complementary. 5′-ends of both primers are directly adjacent to each other but binding to different strands of the DNA (their 3′-ends are facing in the opposite direction). Using such a primer combination leads to amplification of the complete plasmid with two nicks (see Fig.9). To ligate the ends of the PCR products, we phosphorylated primers with T4 polynucloetide kinase before using them in mutagenesis PCR. The phosphorylation mixture was incubated for 60 min at 37°C followed by a heat-inactivation step at 70°C for 5 min. The phosphorylated primers were then used without further purification (see table 23).

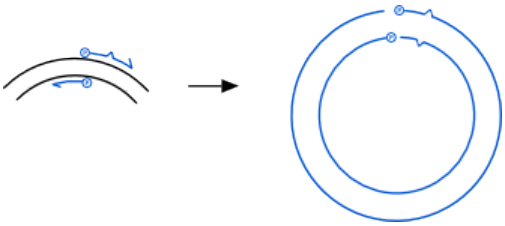

Figure 9: Scheme of site directed mutagenesis. Two adjacent phosphorylated primers allowed amplification of the complete plasmid. The new plasmid (blue) carried a point mutation introduced by one of the two primers.

To differentiate between template plasmid and PCR product, we performed a restriction digest using the DpnI enzyme (2.4.3). As plasmid DNA was prepared from *E. coli* cells encoding the protein Dam methylase, the sequence `GATC` is methylated at the

N^6 position of the adenine (Marinus and Morris, 1973; Geier and Modrich, 1979). DpnI is sensitive to methylated `GATC` only and hence will cleave template DNA but no unmethylated PCR products. After ligation of the PCR product (2.4.4), *E. coli* cells were transformed as described (2.2.4).

MEGAPRIMER PCR Introduction of larger modifications as insertion of additional genes into DNA can be achieved by the megaprimer PCR technique. With this method, a PCR product which contains the desired DNA was generated by a first PCR. This PCR product itself was used in a second PCR as two self-complementary large primers for amplification of plasmid DNA (see Fig. 10). The strategy requires that the short primers in the first step already carry flanking sequences to generate complementarity for the second 'megaprimed' mutagenesis step (see Table 23). As for site directed mutagenesis, DpnI digest was performed to eliminate template plasmid DNA and the remaining mutated DNA was used to transform *E. coli* cells (2.2.4).

We usually introduce a novel restriction site in the megaprimer to easily distinguish template from product plasmid.

No further ligation of the final plasmid is required; nicks will be repaired in vivo after transformation.

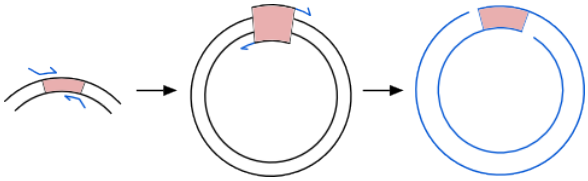

Figure 10: Mutagenesis using a 'megaprimer'. A PCR fragment was generated from an external source (left panel) using primers with complementary sequences to the target plasmid (black, middle panel). The two strands of the PCR product served as megaprimer for insertion of the fragment resulting in a new plasmid (blue).

EXTENSION OVERLAP PCR An alternative to the megaprimer technique was the use of extension overlap PCR to generate mutated DNA. Here, two or more PCR products were generated separately. These DNA fragments were then tethered to each other in a short extension PCR (Table 21 without primers and only 10 cycles) in which each part's end is complementary to the next and was thereby used as primer. In a final PCR with the two external primers, the complete fragment was amplified (see Fig. 11). The final PCR product was digested with two restriction enzymes (2.4.3), ligated with plasmid DNA and used for transformation (2.2.4).

Alternatively, the final product could be used as a megaprimer if restriction digest was unfavorable.

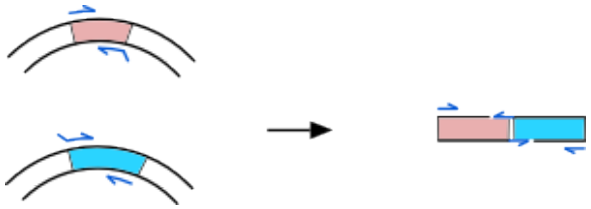

Figure 11: Mutagenesis using extension overlap PCR. First, two different PCR products were generated using primers with complementary sequences to the other PCR product (left panel). Next, both PCR poducts were annealed; their overlapping sequences served as primers. Finally, a standard PCR was performed using the two terminal primers (right panel) to amplify the whole fragment.

	S.D.	MEGA	E.O.
DNA template	10 ng	10 ng	5 µl + 5 µl
Reaction buffer	1 x	1 x	1 x
$MgCl_2$	2.5 mM	2.5 mM	2.5 mM
dNTP-Mix	0.4 mM	0.4 mM	0.4 mM
Primer forward	25 pmol	5 µl	50 pmol
Primer reverse	25 pmol	–	50 pmol
Polymerase	5 U	5 U	5 U
ddH_2O	ad 50 µl	ad 50 µl	ad 50 µl

Table 23: Mutagenesis PCR reaction mixtures. S.D. = site directed mutagenesis, primer were phosphorylated before usage; MEGA = megaprimer PCR, 5 µl megaprimer were used; E.O. = extension overlap PCR, usually 5 µl DNA + 5 µl fragments were used as templates.

2.5 RNA TECHNIQUES

2.5.1 *Preparation of bacterial total RNA*

To prepare total cellular RNA from bacterial cells, two different protocols were used. A fast and reliable way to purify RNA is the single step method (Chomczynski and Sacchi, 1987) in which a chaotropic salt is used to protect RNA from degradation during the extraction process. If high amounts of very clean RNA were needed, we used the hot phenol method (Mattatall and Sanderson, 1996). The latter comes with the (dis-)advantage that RNA duplexes and secondary structures may be destroyed due to the heating step inbetween.

SINGLE STEP METHOD The single step method (Chomczynski and Sacchi, 1987) is the basis for the commercially available Trizol purification kits and relies on guanidinium thiocyanate as chaotropic agent to protect cellular RNA. First, 100 mg of cells were resuspended in 1 ml denaturation solution (4 M guanidinium thiocyanate, 25 mM Na-citrate pH 7.0, 0.5% (w/v) N-lauroylsarcosine, 0.1 M β-mercaptoethanol) by vortexing. 100 µl lysozyme (20 mg/ml in TE buffer) was added and the mixture was incubated for 10 min at room temperature. Next, 100 µl 2 M Na-acetate pH 4.0, 1 ml acid phenol and 200 µl chloroform were added and mixed by vortexing. The suspension was incubated on ice for 15 min and precipitated as described above (2.3.1) using isopropanol. The pellet was again dissolved in 300 µl denaturation solution and precipitation was repeated.

Denaturation solution can be stored for 4 weeks at room temperature.

Acid phenol was prepared by shaking neutral phenol 3 times with 1/10 volume of 300 mM Na-acetate pH 4.8.

HOT PHENOL METHOD To prepare large amounts of cellular RNA for deep sequencing experiments, we used the hot phenol method (Mattatall and Sanderson, 1996). 100 ml bacterial cell cultures were grown to a designated $OD_{567\,nm}$, pelleted by centrifugation and frozen in liquid nitrogen. The pellet was resuspended in 3 ml cold extraction buffer (10 mM Na-acetate pH 4.8, 150 mM sucrose) by vigorous vortexing. 100 µl lysozyme (20 mg/ml in TE buffer) was added and the mixture was incubated at room temperature for 10 min. Next, 333 µl 10% SDS and 3 ml acid phenol (pre-heated to 65°C) were added and mixed by vortexing. The mixture was incubated at 65°C for 5 min followed by incubation on ice for 5 min before it was centrifuged for 20 min at 11,000 x g and 4°C. The upper aqueous phase was transfered into a new tube and subsequently, a phenol/chloroform extraction (2.3.2) was performed.

Extraction buffer was stored at 4°C.

2.5.2 *In vitro RNA transcription*

DNA-dependent phage RNA polymerases have been described to transcribe DNA either single- or double stranded (Milligan and Uhlenbeck, 1989). T7 RNA polymerase recognizes a specific promoter sequence (`TAA TAC GAC TCA CTA TA`) and initiates polymerization immediately downstream. The efficiency of transcription using T7 polymerase increases if the first nucleotide comprises a G-residue (Hartmann et al., 2005). To ensure that 5′-OH ends are generated during *in vitro* transcription, guanosine was added which effectively competes with guanosine 5′ triphosphate (GTP) as starter. Free 5′-OH are required for diverse downstream applications, especially 5′-end labeling with γ^{32}P-ATP. For efficient transcription termination, so called run-off transcription was performed by usage of linear DNA templates

Run-off transcription however does not provide completely homogeneous 3′-ends due to addition of unspecific nucleotides by T7 polymerase.

	FINAL CONC.	50 µL	1000 µL
1 M HEPES pH 8.0	80 mM	4 µl	50 µl
100 mM DTT	15 mM	7,5 µl	150 µl
3 M $MgCl_2$	33 mM	0.55 µl	11 µl
100 mM spermidine	1 mM	0.5 µl	10 µl
20 mg/ml BSA	0.12 mg/ml	0.3 µl	6 µl
100 mM NTP-mix	15 mM	7.5 µl	150 µl
Template DNA		5 µl	50 µl
200 U/µl pyrophosphatase	2 U/ml	0.5 µl	5 µl
20 mM guanosine	9 mM	-	300 µl
T7 RNA polymerase	-	1 µl	30 + 20 µl
ddH_2O		24.46 µl	188 µl

Table 24: T7 *in vitro* transcription reaction.

(generated usually by PCR). The transcription is terminated when the polymerase reaches the DNA template's end.

T7 RUN-OFF TRANSCRIPTION *In vitro* transcription with T7 RNA polymerase was either conducted for analytical purposes (50 µl scale) or for preparative purposes (1 ml scale). Preparative reactions were splitted in two halves during incubation. Guanosine was pre-heated to 75°C prior to addition to the mixture. The reaction mix (Table 24) was incubated using 30 µl T7 RNA polymerase (lab stock) for 2 h at 37°C. Then, a second aliquot of T7 RNA polymerase (20 µl) was added and the mixture was incubated for another 2 h at 37°C. A small aliquot (5 µl) was analyzed by denaturing PAGE (2.3.3.2) to test the transcription efficiency. If the large scale transcription was successful, the RNA was purified by phenol/chloroform extraction (2.3.2) and denaturing PAGE (2.3.3.2) followed by UV shadowing. After elution from the gel by diffusion (2.3.3.4) and precipitation (2.3.1), the RNA was resuspended in double distilled water and concentration was determined (2.3.4).

RNA DEPENDENT TRANSCRIPTION OF PRNAS In *Bacillus subtilis*, the RNA polymerase holoenzyme accepts both 6S RNA species as template for pRNA synthesis. For further investigation of this phenomenon, *in vitro* transcription experiments were conducted using internal labeling of transcripts. *B. subtilis* RNA polymerase was prepared as described by collaborators (Sogo et al., 1979).

For further details, see publication III and IV.

Tris-HCl pH 8.0	200 mM
$MgCl_2$	25 mM
KCl	800 mM
DTT	5 mM

Table 25: 5 x pRNA transcription buffer.

ATP, CTP, GTP	1 mM each
UTP	250 µM

Table 26: 5 x pRNA transcription NTP mixture.

	FINAL CONC.	VOLUME
10 µM Template 6S RNA	1 µM	1 µl
5 x pRNA transcription buffer	1 x	2 µl
5 x pRNA transcription NTP mix	1 x	2 µl
α-^{32}P-UTP	30,000 cpm	<1 µl
8 mg/ml RNA polymerase (holoenzyme)	1 µM	0.53 µl
ddH_2O		ad 10 µl

Table 27: pRNA *in vitro* transcription reaction.

	FINAL CONC.	VOLUME
10 x T4 PNK buffer (forward reaction)	1 x	1.5 µl
25 mM DTT	2.5 mM	1.5 µl
30 pmol RNA	0.66 µM	up to 6 µl
γ-^{32}P-ATP (3000 Ci/mmol)	1.32 µM	3 µl
10 U/µl T4 PNK	0.66 U/µl	1 µl
ddH_2O		ad 15 µl

Table 28: 5′-end labeling of RNA.

Before addition of the NTPs (Table 26) to the reaction mixture (Table 27), the other components were incubated for 30 min at 37°C to allow binding of the RNA polymerase to the RNA template. After addition of the nucleotides, the mixture was incubated for another 30 min to 1 h at 37°C. Next, 10 µl 2 x native or denaturing loading buffer were added and the transcription was analyzed by PAGE (2.3.3.2) and autoradiography (2.3.3.3).

2.5.3 *Radiolabeling of RNA*

5′-END LABELING RNA molecules were 5′-end labeled using T4 polynucleotide kinase (T4 PNK) from *E. coli* phage T4 to transfer the radioactive phosphate group of γ-^{32}P-ATP to the 5′-OH ends of the RNA. The 5′-hydroxyl group was generated by T7 run-off transcription of RNA in presence of guanosine as starter nucleotide (2.5.2). The reaction mix was (Table 28) incubated for 90 min at 37°C. After incubation, 15 µl of 2 x denaturing loading buffer (14) were added and the mix was purified by denaturing PAGE (2.3.3.2) and eluted by diffusion (2.3.3.4). After ethanol precipitation (2.3.1), the pellet was dissolved in 10 µl double distilled water and the overall yield of labeled RNA was measured using a scintillation counter.

3′-END LABELING Labeling of RNA molecules at their 3′-end was achieved by ligation of 5′-^{32}P cytidine-3′,5′-bisphosphate (pCp) to 3′-terminal hydroxyl groups (England and Uhlenbeck, 1978). The ligation reaction is catalyzed by T4 RNA ligase that is able to covalently link the pCp 5′-phosphate group to the 3′-end of another RNA. As only 3′-hydroxyl groups are suitable substrates for the reaction, cyclic phosphates at the 3′-ends have to be removed prior to labeling (Cameron and Uhlenbeck, 1977). The reaction mix (Table 29) was incubated overnight at 8°C. Next, 10 µl of 2 x denaturing loading buffer were added (14) and the

	FINAL CONC.	VOLUME
10 x T4 RNA ligase buffer	1 x	0.6 µl
2 mM ATP	300 µM	0.9 µl
RNA	1 pmol/µl	x µl
(5′-^{32}P)pCp (3000 Ci/mmol)	1.32 µM	4 µl
10 U/µl T4 RNA ligase	1 U/µl	1 µl
ddH_2O		ad 10 µl

Table 29: 3′-end labeling of RNA.

	FINAL CONC.	VOLUME
1 M imidazole (HCl) pH 6.0	100 mM	10 µl
10 mM ATP	100 µM	1 µl
RNA	3 µM	x µl
2 M $MgCl_2$	10 mM	0.5 µl
10% 2-mercaptoethanol	0.07%	0.7 µl
2 mg/ml BSA	20 ng/µl	1 µl
10 U/µl T4 PNK	0.2 U/µl	2 µl
ddH_2O		ad 1000 µl

Table 30: Removal of 2′,3′-cyclic phosphates from RNA.

radiolabeled RNA was purified by denaturing PAGE (2.3.3.2), eluted by diffusion (2.3.3.4), and finally an ethanol precipitation was performed (2.3.1). The RNA was resuspended in 10 µl double-distilled water and the overall activity was measured using a scintillation counter.

REMOVING THE 2′,3′-CYCLIC PHOSPHATE AT 3′-ENDS OF RNA

It is necessary to remove 2′,3′-cyclic phosphates at 3′-ends of RNA (e.g. generated by *cis*-cleavage of a HDV-ribozyme) for efficient 3′-end labeling (see above). A side activity of the T4 PNK, which usually has a 5′-kinase activity, can be used to remove 3′-phosphates of RNA molecules. The reaction mix (Table 30) was incubated at 37°C for 6 h and was subsequently subjected to phenol/chloroform extraction (2.3.2) and ethanol precipitation (2.3.1). Finally, RNA was resuspended in 20 µl double-distilled water and concentration was determined (2.3.4).

2 x NATIVE BUFFER	1.25 x DENATURING BUFFER
100 mM HEPES (NaOH) pH 7.0	25 mM Na-citrate
9 mM $Mg(OAc)_2$	8.75 M urea
200 mM NH_4OAc	1.25 mM EDTA

Table 31: Buffers for enzymatic structure probing with T1 or V1 nuclease.

2.5.4 *Structure determination of RNA*

Interactions between RNA molecules, particularly of non-coding RNAs, is highly dependent on the structure of the regulatory RNA. Enzymatic and chemical probing is a popular approach for mapping the conformation of RNA under defined experimental conditions. To investigate the secondary structure of an RNA molecule, the reactivitiy of each nucleotide is mapped towards enzymes or chemicals with different and complementary specificities.
We routinely used 5'- or 3'-end labeled RNA which was mapped enzymatically using either T1 and V1 nuclease or chemically using lead(II). Unspecific digestion of RNAs to generate a nucleotide ladder was achieved by alkaline hydrolysis. Structure probing was generally performed *in vitro*.

ENZYMATIC PROBING USING RNASE T1 AND V1 RNase T1 from *Aspergillus oryzae* specifically cleaves single-stranded RNA after guanosine residues, producing 3'-phosphorylated ends. RNase T1-specific cleavage was used to map single stranded G-residues under native conditions and also served to generate a guanosine-specific ladder using denaturing conditions. RNase V1 purified from cobra venom cleaves base-paired RNA in a nucleotide-unspecific manner. It was used complementary to RNase T1 to map the secondary structure of 6S-1 RNA. To start RNase T1/V1 digestion, the RNase T1/V1 reaction mixture (Table 32) was incubated at 37°C for 10 min. The reaction was started by addition of 1 µl of 0.8 U/µl RNase T1 or 0.05 U/µl RNase V1. The mixture was incubated at 37°C for 12 - 20 min, depending on the RNA. Next, the reaction was stopped using 15 µl of 2 M NH_4OAc and precipitated (2.3.1). The pellet was then resuspended in 7 µl 2 x denaturing loading buffer and analyzed on a thin (0.5 mm) sequencing PAA gel containing 8 M urea (2.3.3.2).

The 1.25 x denaturing buffer is stable for 1 week at room temperature.

CHEMICAL PROBING USING LEAD(II) IONS Among the di- and trivalent metal ions that have been shown to induce degradation of RNA molecules in a non-oxidative manner, Pb^{2+}-ions are

	FINAL CONC.	NATIVE	DENATURING
5′- or 3′-labeled RNA	20,000 cpm	x µl	x µl
unlabeled RNA (10 µM)	200 nM	1 µl	1 µl
2 x native buffer	1 x	25 µl	-
1.25 x denaturing buffer	1 x	-	40 µl
ddH_2O		ad 50 µl	ad 50 µl

Table 32: RNase T1/V1 reaction mixture.

	FINAL CONC.	VOLUME
5′- or 3′-labeled RNA	20,000 cpm	x µl
unlabeled RNA (10 µM)	200 nM	1 µl
10 x PA buffer	1 x	10 µl
ddH_2O		ad 90 µl

Table 33: Lead(II) reaction mixture. 10 x PA buffer: 500 mM Tris(HCl) pH 7.5, 1M NH_4Cl.

widely used to map RNA secondary structures. Cleavage occurs preferentially in flexible regions like bulges, loops or other single stranded stretches of the RNA, whereas double stranded regions are usually resistant to Pb^{2+}-induced cleavage. The metal ion is suggested to act as a Brønsted base abstracting a proton from the 2′-OH group of the ribose. The activated 2′-O^- attacks the phosphorus atom which results in formation of a penta-coordinated intermediate state. After cleavage of the phosphodiester bond, a 2′,3′-cyclic phosphate and a 5′-OH group are generated (Hartmann et al., 2005). The lead(II) reaction mix was incubated at 37°C for 10 min. Next, 10 µl 2.5 mM $Pb(OAc)_2$ was added and incubated for another 3 min at 37°C. To stop the reaction, 20 µl of 10 mM EDTA were added and the mixture was precipitated (2.3.1), resuspended in 7 µl 2 x denaturing loading buffer and analyzed on a thin sequencing PAA gel containing 8 M urea.

$Pb(OAc)_2$ was always freshly diluted from a 50 mM $Pb(OAc)_2$ stock solution.

UNSPECIFIC ALKALIC HYDROLYSIS OF RNA To generate a RNA ladder, end-labeled RNA was incubated at 100°C for 7 min in 50 mM $NaHCO_3$. The reaction was stopped using 15 µl of 10 mM EDTA and the mixture was precipitated (2.3.1). After dissolving the pellet in 7 µl 2 x denaturing loading buffer, it was

	FINAL CONC.	VOLUME
5′- or 3′-labeled RNA	20,000 cpm	x µl
unlabeled RNA (10 µM)	200 nM	1 µl
$NaHCO_3$ (500 mM)	50 nM	1.5 µl
ddH_2O		ad 15 µl

Table 34: OH-ladder reaction mixture.

	FINAL CONC.	VOLUME
total RNA	up to 250 ng/µl	x µl
reverse DNA primer	100 fmol/µl	x µl
40 mM dNTP mix	2 mM/µl	1 µl
ddH_2O		ad 12 µl

Table 35: RT reaction mixture.

used as a size-marker for enzymatic or chemical probing of RNA molecules.

2.5.5 *Reverse transcription of RNA*

To generate cDNA from RNA, Reverse Transcriptase (RT) was used. We used the Superscript II Kit according to the manufacturer's instructions. To start the reverse transcription, the RT reaction mix was incubated at 65°C for 5 min and immediately placed on ice. Next, 4 µl of 5 x First-Strand buffer and 2 µl of 100 mM DTT were added and the mixture was incubated for 2 min at 42°C. Finally, 1 µl Superscript II RT (200 U/µl) was added and the RT program was started: 10 min at 25°C, 50 min at 42°C and 15 min at 70°C. 2 µl of the resulting cDNA was direcly used as template for a PCR (2.4.5) without further purification.

2.5.6 *Northern hybridization*

Detection and (semi-)quantification of cellular RNA can be achieved by Northern hybridization. After separation by gel electrophoresis, cellular RNA is blotted on a membrane and covalently attached by crosslinking. The membrane is then incubated with a labeled nucleic acid probe complementary to the target RNA. After washing the membranes and blocking of unbound sites of the membrane, detection is achieved by autoradiography or antibodies coupled to enzymes catalyzing a chemoluminescence reaction.

	FINAL CONC.	VOLUME
PCR product	50 ng/µl	x µl
10 x labeling mix	1 x	2 µl
5 x T7 transcription buffer	1 x	4 µl
10 U/µl T7 RNA polymerase	1 U/µl	2 µl
ddH_2O		ad 20 µl

Table 36: Northern hybridization probe transcription.

2.5.6.1 *Standard Northern hybridization protocol*

For detection of cellular RNA, we used non-radioactive Northern hybridization utilizing Digoxygenin (DIG)-labeled RNA probes. For generation and detection of the DIG-labeled probes, we used the Northern Starter Kit (Roche).

PROBE GENERATION To produce DIG-labeled RNA probes, a linear template was generated by PCR (2.4.5). The primers were chosen to add a T7 promoter to the reverse complement strand of the target RNA sequence. After checking the PCR product on an agarose gel (2.3.3.1) and concentration determination (2.3.4), the RNA probe was generated by T7 run-off transcription (Table 36), thereby incorporating digoxigenin-11-UTP which is part of the 10 x labeling mix. The reaction was incubated at 37°C for 1 h and was stopped by addition of 2 µl 200 mM EDTA pH 8.0. Probes were stored at -20°C.

Probes were re-used once and stored at -20°C after the first usage.

RNA PREPARATION: CHOICE OF GELS AND QUALITY CONTROL As only relatively short RNAs (< 250 nt) were subjected to Northern hybridization, we used PAA gels for electrophoretic separation (2.3.3.2). To test the quality of cellular extracts (2.5.1), 3 µg of total cellular RNA were analyzed on a 5% denaturing PAA gel and subsequently ethidium bromide stained. The RNA was assumed to be intact if the two major bands (comprising the 23S and 16S rRNA in bacteria) were discrete without a smear which would indicate degradation of the RNA. After electrophoresis, the gel was washed for 5 min in 0.5 x TBE buffer.

For analysis of 6S RNAs, 10 - 12% denaturing PAA gels were utilized. Normally, 2 - 10 µg of total RNA (2.5.1) were loaded onto each lane.

TRANSFER AND FIXATION OF RNA TO MEMBRANES To immobilize the total RNA, it was transferred to a membrane by semi-dry blotting. A piece of positively charged nylon membrane and two pieces of whatman paper, all in the size of the PAA gel, were soaked in 0.5 x TBE buffer. One piece of whatman paper was placed on the anode of the blotter. The wet membrane was placed exactly upon the whatman paper, followed by the PAA

gel and the second whatman paper. Care was taken to avoid air bubbles forming in between. Finally, the cathode was placed on top and transfer of the RNA was run overnight using 0.27 mA/cm² of the membrane.

Alternatively, UV crosslinking is widely used.

The next day, after removal of the whatman papers and the PAA gel, the membrane was placed on a glass plate and incubated for 30 min at 80°C in an oven to crosslink the RNA to the membrane before storage at 4°C.

HYBRIDIZATION For hybridization to RNA, RNA or DNA probes can be used. For routine Northern hybridization, we used RNA probes generated by T7 run-off transcription from PCR fragments. These RNA probes can either be radiolabeled post-transcriptionally (5'-end labeling with γ^{32}P-ATP) or during transcription by incorporation of modified nucleotides such as α^{32}P-NTPs or DIG-11-UTP. In formaldehyde buffer sytems, the standard hybridization temperature for RNA probes is 68°C (42°C in formamide buffers), whereas lower temperatures are usually applied to hybridization with DNA probes.

7 ml of the DIG Easy Hyb Granules or a self-made hybridization buffer (50 mM Na_2HPO_4/NaH_2PO_4 pH 7.0, 0.02% (w/v) SDS, 4M urea) were pre-heated to 68°C. During this time, the membranes were placed in a hybridization tube or a 50 ml Falcon tube, respectively, ensuring that the 'RNA side' did not touch the glass wall but was directed inward. The pre-heated hybridization solution was added and the tube was placed in an hybridization oven for 2 h at 68°C with slow rotation. After that time, again 7 ml of hybridization solution were pre-heated to 68°C and 10 µl of T7-transcribed probe was added. The pre-hybridization solution was discarded and immediately replaced by the solution containing the RNA probe. Hybridization was performed overnight (or at least for 6 h) at 68°C with slow rotation in the hybridization oven.

The probe was denatured for 3 min at 95°C and immediately put on ice for another 3 min before addition to the solution.

DETECTION OF DIG-LABELED PROBES Visualization of DIG-labeled probes is achieved by immunological detection using an antibody (Anti-Digoxigenin-AP Fab Fragments) specific for the DIG-modified nucleotides. The antibody is coupled to an alkaline phosphatase which dephosphorylates a dioxetane phenyl phosphate (CDP-Star). The resulting chemoluminescent signal is detected by exposing an X-ray film to the membrane.

For detection, all steps were carried out using clean glass/plastic ware. Care was taken that membranes were covered with buffer and that shaking took place at low speed and at room temperature. First, membranes were washed twice in stringent wash buffer 1 (1 x SSC, 0.1% (w/v) SDS) for 5 min and then twice in stringent wash buffer 2 (0.1 x SSC, 0.1% (w/v) SDS) before

Strictly keep to the incubation times until...

rinsing with double-distilled water. Next, the membrane was incubated in blocking solution (0.1 M maleic acid, 0.15 M NaCl pH 7.5, 1 x Blocking solution (Roche)) for 30 min and then in antibody solution (0.1 M maleic acid, 0.15 M NaCl pH 7.5, 1 x Blocking solution (Roche), 1:10,000 diluted Anti-Digoxygenin-AP Fab Fragments (Roche)) for 30 min. The membrane was washed twice in wash buffer (0.1 M maleic acid, 0.15 M NaCl, 0.3%(v/v) Tween-20 pH 7.5) for 15 min before incubation in detection buffer (0.1 M Tris(HCl), 0.1 M NaCl pH 9.5) for 5 min. The membrane was placed on a kitchen wrapping film and some drops of CDP-Star (Roche) were added until the membrane was covered with the solution. After wrapping the membrane completely, it was incubated for 10 min at room temperature to allow development of a robust chemical signal. Finally, a photo film (Kodak BioMax Light Film) of identical size was placed on the membrane and exposed for 5 min to 1 h, depending on the signal intensity. The photo film was then developed accoding to the manufacturer's instructions.

...membranes are in wash buffer where they can be incubated for several hours.

STRIPPING OF PROBES FROM MEMBRANES Membranes can be re-used for hybridization with a second probe. For this purpose, care was taken that the membrane did not run dry during the first detection process. After that, the membrane was washed twice in double-distilled water for 5 min at room temperature and then incubated twice in stripping buffer (50 mM Tris(HCl) pH 7.5, 50% (v/v) formamide, 5% (w/v) SDS) for 60 min at 80°C. Next, the membrane was washed twice in 2 x SSC for 5 min at room temperature before pre-hybridization (see above).

Stripping buffer was always freshly prepared.

2.5.6.2 *Detection of tiny RNAs in bacterial total cellular RNA*

The standard Northern hybridization protocol was used for detection of RNAs of $\geqslant$ 100 nt in length. However, very short RNAs such as miRNA (~22 nt) or pRNA (8 - 22 nt) are hardly detectable using this technique. We developed a novel nNorthern hybridization protocol which is sensitive enough to detect such short RNA species in bacterial total cellular extracts. For this purpose, we combined i) chemical crosslinking of RNA to positively charged nylon membranes using 1-ethyl-3-(3-dimethylaminopropyl)-carbodiimide (EDC), ii) 5'-digoxygenin-endlabeled DNA/LNA mixmer probes for enhanced binding to the short RNAs and iii) native polyacrylamide gels.

The method as well as example applications are described in detail in publication I and II.

2.5.7 *RNA 5'- and 3'-end determination using RACE*

RNA in bacteria is usually subject to maturation by cleavage at specific positions. Mapping of precursor- and mature RNA-ends

	VOLUME
RNA	x µl
10 x DNase buffer	5 µl
2 U/µl Turbo DNase	5 µl
ddH_2O	ad 50 µl

Table 37: DNase digestion reaction.

in vivo was performed by RACE (rapid amplification of cDNA-ends) experiments, which was either directed to find 5′-ends (5′-RACE) or 3′-ends (3′-RACE).

2.5.7.1 *5′-RACE*

For mapping of RNA 5′-ends, DNA contamination was first removed from total cellular RNA using Turbo DNase (Ambion). Next, the RNA was split into two halves. One half was treated with Tobacco Acid Pyrophophatase (TAP, Epicentre) which hydrolyzes the phosphoric acid anhydride bonds in the 5′-triphosphate of precursor RNAs releasing a pyrophospate and generating a 5′-monophosphorylated terminus on the RNA molecule. This half was usually marked as '+' (for inclusion of primary transcripts). Then, an adaptor-oligonucleotide was ligated to the 5′-ends of cellular RNAs in both libraries and cDNA was generated and amplified by reverse transcription (RT-PCR) using a gene-specific reverse primer and a forward primer binding to the adaptor. The resulting PCR-products were analyzed on agarose gels and specific bands were gel-eluted, subcloned by TOPO-TA cloning and the TOPO-vector was then DNA-sequenced. Analyzing several clones (usually 10 or more), 5′-ends were identified by their position directly downstream of the adaptor sequence.

DNA REMOVAL For DNA removal, 20 µg of total RNA (2.5.1) were digested using Turbo DNase twice. The DNase digestion reaction (Table 37) was incubated at 37°C for 30 min. Then, phenol/chloroform extraction (2.3.2) was performed and digestion was repeated. The RNA was finally resuspended in 50 µl double-distilled water.

TAP TREATMENT 50 µl of DNase-digested cellular RNA was filled up with double-distilled water to a volume of 176 µl and 20 µl of 10 x TAP digestion buffer (Epicentre) was added. Then, the solution was split into two eppendorf reaction tubes and 1.5 µl TAP (10 U/µl, Epicentre) was added to one tube (+TAP). The other tube was filled with 1.5 µl double-distilled water and

	VOLUME
RNA/adaptor	25 µl
0.1% (v/v) BSA	4 µl
10 x RNA ligase buffer (Fermentas)	4 µl
10 mM ATP	4 µl
10 U/µl T4 RNA ligase (Fermentas)	3 µl

Table 38: RNA ligation reaction.

	VOLUME
5 x RT buffer (Invitrogen)	4µl
40 mM dNTP mix	1 µl
100 mM DTT	2 µl

Table 39: RACE RT mixture.

served as negative control (TAPctr). Both tubes were incubated at 37°C for 40 min. The reaction was stopped by phenol/chloroform extraction (2.3.2) and RNA was resuspended in 25 µl double-distilled water.

5'-ADAPTOR LIGATION The two samples (+TAP and TAPctr) were subjected to 5'-adaptor ligation. 1 nmol adaptor oligomer (GTC AGC AAT CCC TAA CGA G; DNA = normal letters, RNA underlined) were added to each sample, followed by incubation at 90°C for 1 min and immediate storage on ice. The RNA ligation reaction was incubated at room temperature for 3 h or at 4°C overnight. Next, phenol/chloroform extraction (2.3.2) was performed and the RNA was resuspended in 25 µl double-distilled water.

RT-PCR From each of the two samples, 4.5 µl were transferred into a new tube marked RT. Again, 4.5 µl from each sample were transferred into a new tube; this time marked RTctr. To all four tubes, 2 pmol gene-specific reverse primer and 7 µl double-distilled water was added. The solution was incubated at 65°C for 5 min and immediately put on ice. After addition of the RACE RT mixture (Table 39) to the tube, the mixture was incubated at 42°C for 2 min. 1 µl Superscript II RT (200 U/µl) was added to the two samples that had been marked with RT and 1 µl double-distilled water was added to the control reactions marked with RTctr before running the RACE RT program (Table 40). Afterwards, 0.5 µl RNaseH (5 U/µl) were added to each sample to remove RNA from DNA:RNA hybrids. 2 µl of the cDNA were directly used

TIME	TEMP.
5 min	42°C
20 min	55°C
20 min	60°C
20 min	65°C
5 min	85°C

Table 40: RACE RT program.

for PCR (2.4.5) using Taq DNA polymerase and 35 cycles. Additionally, a final elongation step of 8 min at 72°C was performed to ensure addition of A overhangs by the Taq polymerase. As primers, the gene-specific reverse primer and the 5′-RACE adaptor primer (see appendix) were used. After PCR, the products were loaded onto an ethidium bromide-stained agarose gel and bands were eluted as described (2.3.3.4) fromusing a buffer containing ethanol the samples marked with RT. The other samples served as controls only.

TOPO-TA CLONING To store and multiply PCR products, we performed TOPO-TA cloning. A mixture of a linearized vector carrying 3′-T overhangs and Topisomerase II allow incorporation of the PCR product carrying a 3′-A overhang independent of the sequence of the PCR product. TOPO-TA cloning was performed according to the manufacturer's instructions using either *E. coli* TOP10 cells (kit supplied) or DH5α (lab stock) cells and blue/white screening (2.2.2). TOPO plasmids from several clones were prepared for minipreparation (2.4.2) and sent to DNA sequencing.

2.5.7.2 *3′-RACE*

For mapping of 3′-ends of cellular RNA, we used the 3′-RACE technique. Although being very similar to 5′-RACE, TAP treatment is omitted in 3′-RACE and instead of adaptor ligation, a poly-C stretch is attached to cellular RNAs using Poly(A) polymerase which catalyzes the addition of nucleotides to the 3′-end of RNA in a sequence-independent fashion.

DNA REMOVAL See 2.5.7.1 but resuspend RNA in 25 µl double-distilled water.

C-TAILING For sequence-independent addition of cytosine to cellular RNA, we mixed the C-tailing reaction (Table 41) and incubated first without the enzyme at 37°C for 5 min. Then, 1.5

	VOLUME
RNA	25 µl
25 mM $MgCl_2$	4 µl
25 mM $MnCl_2$	4 µl
10 x C-tailing buffer	5 µl
10 mM CTP	3 µl
ddH_2O	8 µl

Table 41: C-tailing reaction mixture for RNA.

µl Poly(A) polymerase (2.5 U/µl) were added and the mixture was incubated at 37°C for 90 min. Finally, a phenol/chloroform extraction (2.3.2) was performed and the RNA was resuspended in 25 µl double-distilled water.

RT-PCR RT-PCR was performed as described (2.5.7.1) using 10 µl RNA as starting material and 3 reverse anchor primers (see appendix), 33 pmol each.

TOPO-TA CLONING TOPO-TA cloning was performed as described (2.5.7.1).

2.5.8 *Gel retardation experiments*

Complex formation of RNA with proteins or other RNA molecules *in vitro* was analyzed by gel retardation experiments. When part of a complex, RNA migrates slower in low percentage polyacrylamide gels compared to free RNA molecules. To measure the fraction of RNA that is either free or part of a bigger complex, trace amounts of radiolabeled RNA were added to the reaction and analyzed by autoradiography.

2.5.8.1 *RNA-RNA gel shifts*

To study 6S RNA-pRNA interactions, we mixed *B. subtilis* 6S-1 RNA generated by T7 run-off transcription (2.5.2) with RNA oligomers comprising the natural pRNA sequence. As pRNA alone is not able to invade the secondary structure of 6S-1 RNA to form 6S-1 RNA-pRNA hybrids, the mixture (Table 42) was heated to 95°C to destroy secondary structures and cooled down stepwise to 37°C.

If not stated otherwise, 6S-1 RNA was adjusted to 1 µM final concentration. 6S-1 pRNA was usually added in a 10 fold molar excess (10 µM) over 6S-1 RNA although this was varied in some experiments. Radiolabeled RNA was added in trace amounts (up

	FINAL CONC.	VOLUME
10 µM 6S-1 RNA	1 µM	0.6 µl
6S-1 RNA (radiolabeled)	up to 50,000 cpm	x µl
50 µM 6S-1 pRNA	10 µM	1.2 µl
10x TE buffer	1 x	0.6 µl
ddH_2O		ad 6 µl

Table 42: 6S-1 RNA-pRNA hybridization mixture.

	TIME	TEMP.
Initial denaturation	5 min	95°C
Stepwise cooling	5 min	90°C
	5 min	80°C
	5 min	70°C
	5 min	60°C
	5 min	50°C
Final temperature	5 - ∞	37°C

Table 43: 6S RNA-pRNA hybridization program.

to 50,000 cpm) and not considered for concentration determination.
Alternatively, RNA:RNA interactions were also analyzed from total cellular extracts. To avoid denaturation of RNA, we used only the single step method (2.5.1) for RNA preparations that were intended for gel shift experiments.
In either case, RNA samples after hybridization or directly after total RNA extraction were mixed with 1 volume of 2 x native loading buffer and loaded onto a 5 - 10% native PAA gel (2.3.3.2). Care was taken to run the gel at low voltage to avoid heating of the gel and denaturation of the samples. RNA shifts were either detected by autoradiography in the case of labeled samples or the gels were used for Northern hybridization in the case of cellular total RNA samples.

2.6 CLONING EXPERIMENTS

2.6.1 *Cloning of 6S RNA genes*

The two genes for 6S-1 (*bsrA*) and 6S-2 (*bsrB*) RNA were cloned in the pUC18 vector for storage and mutation purposes. Additionally, the T7 promoter directly upstream of the 6S RNA genes

allowed efficient *in vitro* transcription by T7 RNA polymerase (2.5.2).

PBB1 (PUC18-T7-BSRA-190) The coding sequence of the mature (190 nt) 6S-1 RNA was amplified by PCR (2.4.5) using primers 142a and 143 and genomic DNA from *B. subtilis* 168 as template. The PCR product was analyzed by agarose gel electrophoresis (2.3.3.1) before a restriction digestion (2.4.3) with EcoRI and HindIII was performed to cleave both ends of the PCR product. The pUC18 vector was also digested using EcoRI and HindIII, resulting in a linearized plasmid. Linearization was tested by agarose gel electrophoresis. Next, plasmid and PCR-product DNA were ligated (2.4.4) and *E. coli* DH5α cells were transformed with the ligation reaction (2.2.4) and selected on ampicillin plates. The next day, 5 single bacterial colonies were picked, 3 ml LB-medium cultures were inoculated and grown overnight (2.2.1). Then, 500 µl from each culture were mixed with 1 volume of glycerol and were snap-frozen in liquid nitrogen for long-time storage. The remaining 2.5 ml were used for plasmid minipreparation (2.4.2). Finally, plasmids (Fig. 12) were sent for DNA sequencing using primers 6 and 7.

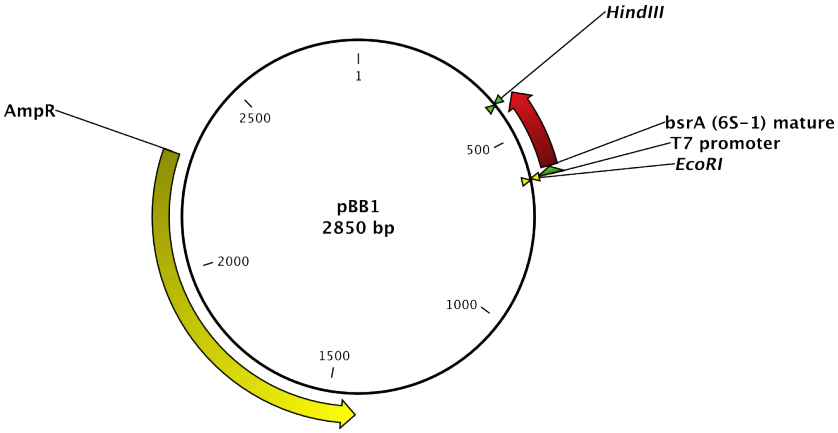

Figure 12: pBB1: pUC18-T7-bsrA-190, a pUC18-derived plasmid containing the *B. subtilis* mature 6S-1 RNA coding sequence under control of a T7 promoter.

PBB2 (PUC18-T7-BSRA-201) The coding sequence of the 6S-1 RNA precursor (201) nt was amplified by PCR (2.4.5) using primers 142b and 143 and genomic DNA from *B. subtilis* 168 as template. The PCR product was then analyzed and cloned into the EcoRI/HindIII sites of the pUC18 vector as described above. The resulting plasmid was named pBB2 (Fig. 13) and verified by DNA sequencing.

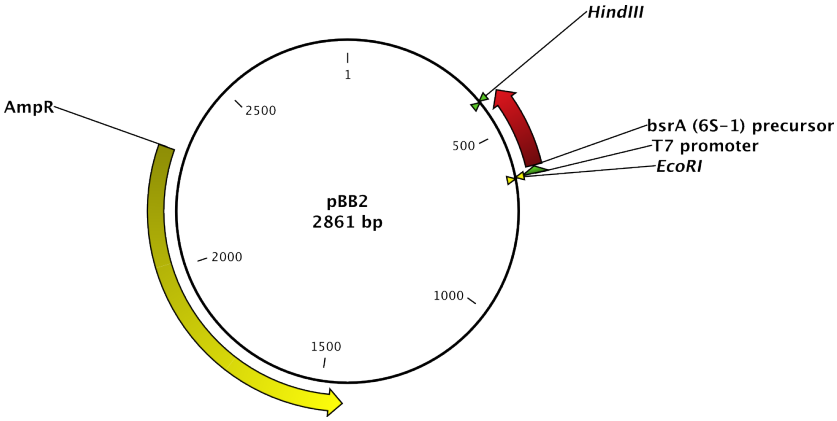

Figure 13: pBB2: pUC18-T7-bsrA-201, a pUC18-derived plasmid containing the *B. subtilis* precursor 6S-1 RNA coding sequence under control of a T7 promoter.

PBB3 (PUC18-T7-BSRB-203) The coding sequence of the 6S-2 RNA (203) nt was amplified by PCR (2.4.5) using primers 144 and 145 and genomic DNA from *B. subtilis* 168 as template. The PCR product was then analyzed and cloned into the EcoRI/HindIII sites of the pUC18 vector as described above. The resulting plasmid was named pBB3 (Fig. 14) and verified by DNA sequencing.

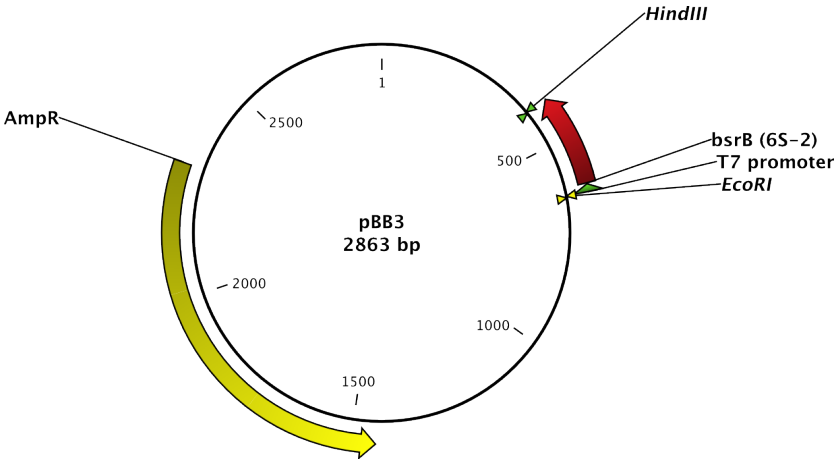

Figure 14: pBB3: pUC18-T7-bsrB-203, a pUC18-derived plasmid containing the *B. subtilis* 6S-2 RNA coding sequence under the control of a T7 promoter.

PBB4 (PUC18-T7-BSRA-190-HDV) To assure 3′-end homogeneity of *in vitro*-transcribed 6S-1 RNA which is important for 3′-end labeling (2.5.3), a HDV ribozyme was added downstream of the *bsrA* gene. The HDV ribozyme cleaves at a defined position at

its 5′-end directly after transcription of the RNA. First, the HDV sequence was amplified by PCR (2.4.5) using primers 146 and 147 from pUC18-HDV (lab stock). The PCR product was used as a megaprimer (2.4.5.2) to mutate pBB1 and insert the HDV sequence directly downstream the *bsrA* sequence. The resulting plasmid was named pBB4 (Fig. 15) and verified by DNA sequencing.

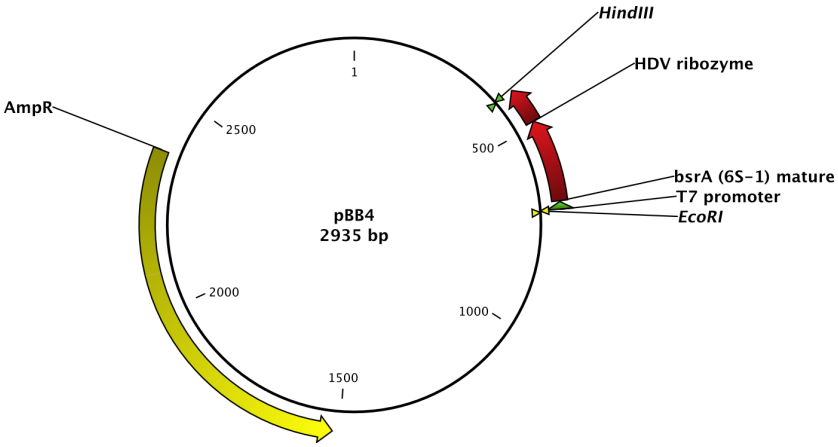

Figure 15: pBB4: pUC18-T7-bsrA-190-HDV, a pBB1-derived plasmid containing an additional HDV sequence downstream of the *B. subtilis* mature 6S-1 RNA sequence.

PBB5 (PUC18-T7-BSRA-190(C40T)) To elucidate the role of the starting nucleotide of the pRNA of 6s-1 RNA, we mutated the complementary residue (C40) to thymin. Synthesis from this 6S RNA template then results in pRNA with an adenin at the +1 position. Using pBB1 as template, we used phosphorylated primers 113 and 114 for site directed mutagenesis PCR (2.4.5.2). The resulting plasmid was named pBB5 (Fig. 16) and verified by DNA sequencing.

PBB6 (PUC18-T7-BSRA-190-CP) Structure probing of 3′-end labeled 6S-1 RNA revealed a stacked region at the bottom region of the central bulge after hybridization with pRNA that was inaccessible to chemical or enzymatic probing (see publication IV). To verify this stacking with 5′-end labeled 6S-1 RNA, we generated a circularly permuted RNA (6S-1 cp) with its 5′-end in the apical loop region (Fig. 17). This strategy allowed structure probing experiments at a higher resolution than 5′-end labeled wildtype 6S-1 RNA. First, the sequence of the mature (190 nt) 6S-1 RNA was amplified by PCR from pBB1 using primers 150 and 143. The PCR product was cloned into the HindIII site of pBB1. The resulting plasmid was named pBB6 (Fig. 18) and its sequence was verified by DNA sequencing. To generate templates

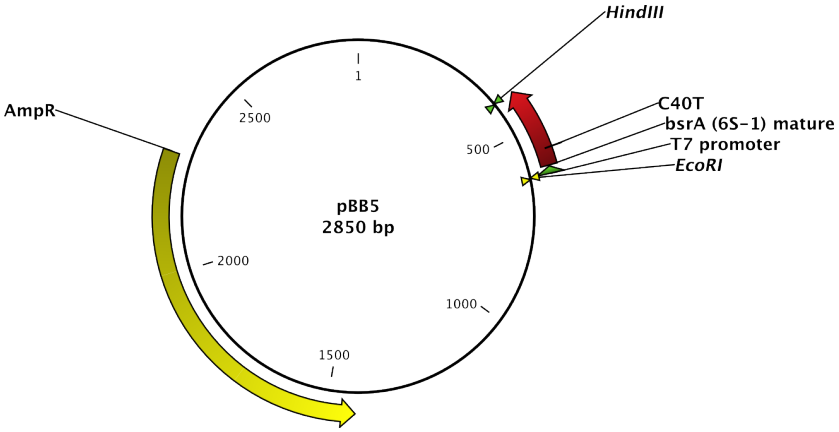

Figure 16: pBB5: pUC18-T7-bsrA-190(C40T), a mutated version of the pBB1 plasmid. The position 40 of the *bsrA* gene was point-mutated from C to T.

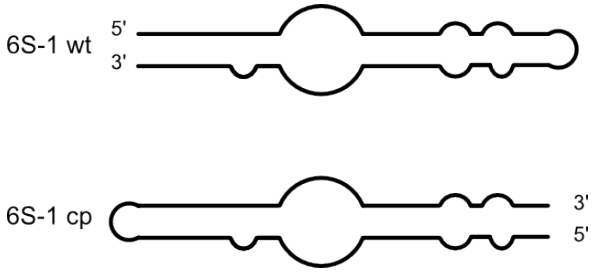

Figure 17: Scheme of circularly permuted 6S-1 RNA. The wildtype situation (top) and the 6S-1 cp mutant which is fully functional (see publication IV).

for *in vitro* transcription, PCR was performed using primers 151 and 152.

2.6.2 *Generation of B. subtilis mutant strains*

GENERATION OF A KANAMYCIN RESISTANCE CASSETTE For generation of mutant *B. subtilis* strains, the *bsrA* locus as well as 500 bp of up- and downstream DNA (Fig. 19) were amplified by PCR using oligonucleotides 108 and 109, digested with EcoRI and HindIII and cloned into pUC18, resulting in vector pBB-6S-1. Next, a kanamycin resistance cassette was amplified from pDG780 (Guérout-Fleury et al., 1995) using primers 111 and 112 resulting in a ~1.5 kbp fragment. As the sequences in primers 111 and 112 were partially complementary to the downstream region of the *bsrA* gene, we used this PCR fragment as primer for megaprimer PCR on pBB- 6S-1 as template (2.4.5.2). The novel plasmid was named pBB6S-1-kan. To introduce the *bsrA* C40T

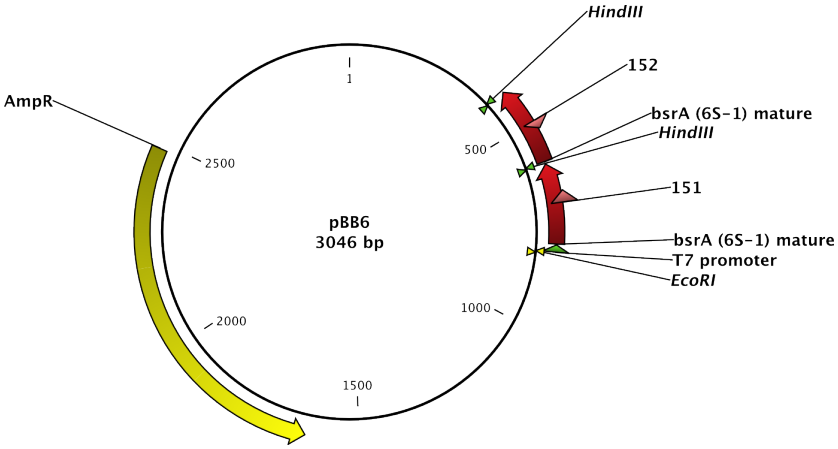

Figure 18: pBB6:pUC18-T7-bsrA-bsrA, a pBB1-derived plasmid. A second *bsrA* gene was inserted downstream of the first one to allow generation of templates for a circularly permuted 6S-1 RNA variant.

point mutation, the pBB6S-1-kan plasmid was amplified with two 5′ phosphorylated primers 113 and 114. The linear fragment was ligated with T4 DNA ligase before cloning in *E. coli* DH5α; the resulting plasmid was named pBB6S-1-mut-kan. Final plasmid constructs were verified by sequencing. For chromosomal insertion, linear PCR products were generated either from pBB6S-1-kan (resulting in strain BB bsrA) or from pBB6S-1-mut-kan (resulting in strain BB bsrA (C40T)) using primers 108 (see above) and 110. Naturally competent *B. subtilis* 168 cells (2.2.5) were transformed with the generated fragments and selected for kanamycin resistance. Finally, several colonies were picked and correct insertion of the bsrA-kanamycin cassette was verified by PCR and sequencing.

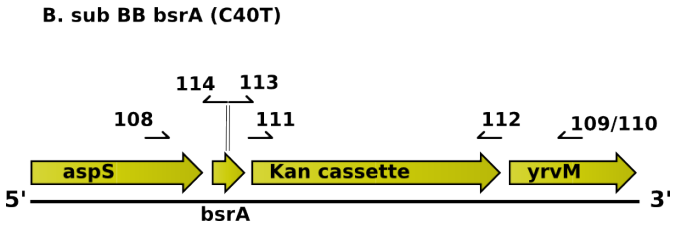

Figure 19: The genomic context of the *bsrA* gene locus in *B. subtilis* BB bsrA (C40T). The direction of surrounding genes is indicated by arrows. The position of primers used for cloning and sequencing and their numbers are indicated.

2.7 BIOINFORMATIC ANALYSES

Bioinformatic analyses were carried out on an i686 personal computer with a Mobile AMD Sempron™Processor 3500+ using the Debian GNU/Linux 5.0.5 operating system. Analysis of deep sequencing experiments, secondary structure prediction and 6S RNA phylogenetic analysis were performed using Perl and awk scripts which are available upon request.

2.7.1 *Analysis of deep sequencing data*

For further details on library construction and dRNA-Seq, see publication III.

Total cellular RNA from *B. subtilis* 168 cells in three different growth phases (exponential, stationary and outgrowth) were used for a differential deep sequencing (dRNA-Seq) approach (Sittka et al., 2008; Sharma et al., 2010). After 454 sequencing (Margulies et al., 2005), six sequencing libraries with a total number of ~ 165,000 sequences were obtained. Data analysis was performed in collaboration as well as in our laboratory.

2.7.1.1 *Annotation of deep sequencing reads*

Sequence reads in fasta format obtained by dRNA-Seq were aligned to the *B. subtilis* 168 genome (NC_000964.2) using `WU-BLAST v.2.0` (Altschul et al., 1990) or `segemehl v.0.0.9.3` (Hoffmann et al., 2009) with the options shown in the listings below.

Listing 2.1: BLAST command-line options

```
$ BLAST -B=1 -V=1 -m=1 -n=-3 -Q=3 -R=3 -gspmax=1 -hspmax=1 -
    mformat=2 -e=0.0001
```

Listing 2.2: segemehl command-line options

```
$ segemehl.x -x NC_NNN.idx -d NC_NNN.fa
$ segemehl.x -i NC_NNN.idx -d NC_NNN.fa -q library -M 500 -H
    2 -A 90 > out.map
```

The resulting alignment informations were parsed and the sequencing reads were graphically displayed using the `Integrated Genome Browser v.4.56` (Nicol et al., 2009).

2.7.1.2 *Identification of 6S pRNA transcripts*

Due to the short length of pRNAs (8 - 14 nt), alignment and identification of these transcripts could not be achieved by `WU-BLAST` or `segemehl`. Therefore, we manually searched for pRNAs using a sliding window approach. Each library was screened for complementary sequences to 8 nt windows of both 6S RNA sequences. Hits were counted and plotted as a function over the

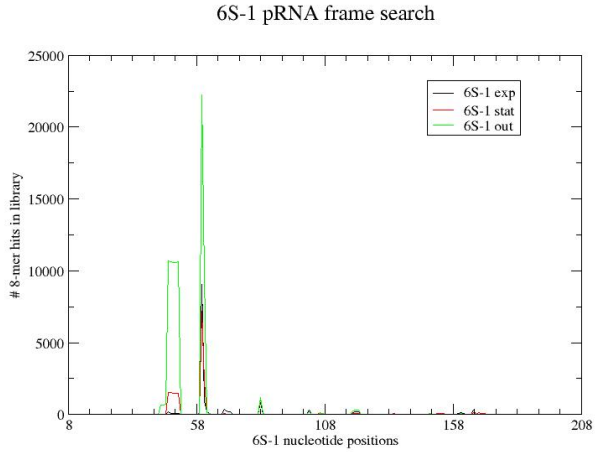

Figure 20: Representative image of the sliding window approach. 6S-1-derived pRNA sequences peak at position 40. Note that the plateau denotes the length of 9 - 14-mers.

sequence of the respective 6S RNA (see Fig.20). The identified pRNA sequences were then investigated manually in more detail.

2.7.2 *RNA secondary structure prediction*

Secondary structure prediction of RNA was performed using `RNAfold` (Hofacker, 2003) with default options from the Vienna package (see listing below) (Gruber et al., 2008). For prediction of *B. subtilis* 6S RNA stability, the -C option (constraint) was used to prevent base pairing of the central bulge nucleotides.

Listing 2.3: RNAfold command-line options

```
$ RNAfold < sequence.fa > structure.out
```

2.7.3 *Prediction of pRNA-induced hairpin formation*

To investigate the possibility that pRNA induces extended hairpin formation (see publication IV) in 6S RNA of other bacteria than *B. subtilis*, we downloaded known 6S RNA sequences and predicted secondary structures from `Rfam v.10.0` (Griffiths-Jones et al., 2003), RF00013_seed.stk. By manually adding Aquificalis sequences the alignment contained 163 sequences (see appendix). We performed three steps:
(1) *Negative control.* To simulate the case of no pRNA and no structural rearrangement, we tested the 3′ internal loop region (alignment positions 184–209, a length of 12–20 nt without gaps)

to form a helix with `RNAfold v.1.6` (Hofacker, 2003). (2) *Positive control.* For a simulation of pRNA:6S RNA hybrid we extended our region of unpaired nucleotides and tested the alignment positions 184–224 (a length of 20–30 nt) with the same method for stable hairpins (see Fig. 21 for a scheme). (3) *Collapse of central bulge.* Whether the conserved hairpins can be even extended by interacting with the 5′ internal loop of 6S RNA, we used `RNAduplex` (Hofacker, 2003) between alignment positions 55–70 and 210–241 (two interacting sequences of length 12–20nt and 17–29). All input and output files can be obtained here: `http://bioinf.pharmazie.uni-marburg.de/supplements/136`. Finally, we used `SplitsTree v.4` (Huson and Bryant, 2006) to create a NJ-Tree and evaluate these finding furthermore. We color-coded the energy values of positive control(2) ranging from -0.40 kcal/mol (blue) to -9.50 kcal/mol (red). The collapse of the central bulge was marked by squares in case of energy values below -1.30 kcal/mol (see publication IV).

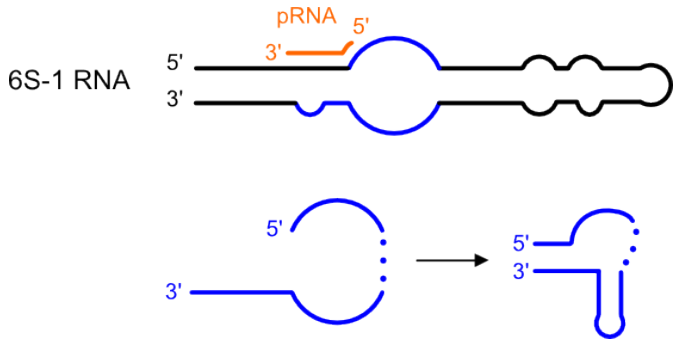

Figure 21: Schematic model of prediction of pRNA-induced extended hairpin formation in 6S RNA sequences.

Part III

RESULTS AND DISCUSSION

3 RESULTS AND DISCUSSION

It's necessary to be slightly underemployed
if you are to do something significant.

— James D Watson

This section is a summary and discussion of the results obtained in publications I - IV. For more detailed information concering the results, see the respective publication in the appendix.

Starting our investigations on the two 6S RNAs of *B. subtilis*, we realized soon that 6S RNA-templated pRNA synthesis could not be investigated *in vivo* by standard techniques such as normal Northern hybridization or RT-PCR due to their short length. We therefore started to set up an improved Northern blot protocol customized for the detection of very short RNAs in total cellular RNA. Concurrently, we started a deep sequencing approach to screen *B. subtilis* cellular RNA for pRNAs in an unbiased manner.

3.1 DETECTION OF PRNA IN VIVO (PUBLICATIONS I & II)

The discovery of pRNA synthesis in *E. coli* and its role in the release of RNA polymerase (Wassarman and Saecker, 2006; Gildehaus et al., 2007) tempted us to investigate this mechanism in more detail. Focusing on *B. subtilis*, which harbors two 6S RNA species (6S-1 and 6S-2) (Ando et al., 2002; Suzuma et al., 2002; Barrick et al., 2005), we started to search for techniques that allowed us to detect RNAs of 10 – 20 nt in length. We initially failed to detect pRNAs using standard techniques such as Northern hybridization, although using DNA/LNA mixmers as probes. LNA residues increase the hybridization efficiency of nucleic acids by arresting the ribose moiety in its C3'-*endo* conformation, which leads to a significant increase in melting temperature (Vester and Wengel, 2004; Grünweller and Hartmann, 2007). In a similar approach, miRNAs, which are ~ 22 nt in length, had been successfully detected using chemical crosslinking by EDC (Kim et al., 2010). We further used native instead of denaturing PAA gels which resulted in improved detection efficacy. We speculate that denaturing agents such as urea interfere with the crosslinking reaction of EDC and thus decrease the immobilization efficiency for RNA.

LNA = Locked Nucleic Acid

EDC = 1-ethyl-3-(3-dimethylaminopropyl)-carbodiimide

During these studies, we realized that the design of the DNA/LNA mixmer probes can be challenging; especially the correct placing of the LNA residues is crucial for a good signal to noise ratio during detection. We postulated several rules for a favorable insertion of LNA residues and compared several probes with respect to their sensitivity and reduction of background, for example when targeting *E. coli* pRNA (Fig. 22). Using this novel protocol, we confirmed pRNA synthesis in *B. subtilis*.

For the rules how to place LNA residues, see publication II.

3.2 ANALYSIS OF B. SUBTILIS 6S RNAS AND PRNAS (PUBLICATION III)

3.2.1 *Expression and maturation of the two 6S RNA species of B. subtilis*

We started our analysis of 6S RNA in *B. subtilis* measuring the RNA levels of 6S-1 RNA and 6S-2 RNA *in vivo* by Northern blotting. Our results confirmed previous analyses (Trotochaud and Wassarman, 2005; Barrick et al., 2005) showing that 6S-1 RNA levels are high during entry into stationary phase, whereas 6S-2 RNA levels peak during exponential phase (Fig. 23). We further detected a fragment of 6S-1 RNA which appeared in late stationary phase only. By 5'- and 3'-end mapping using RACE, we found cleavage of 6S-1 RNA in the apical loop region. We

Both RNAs were identified by binding to the σ^A-containing housekeeping RNAP of B. subtilis.

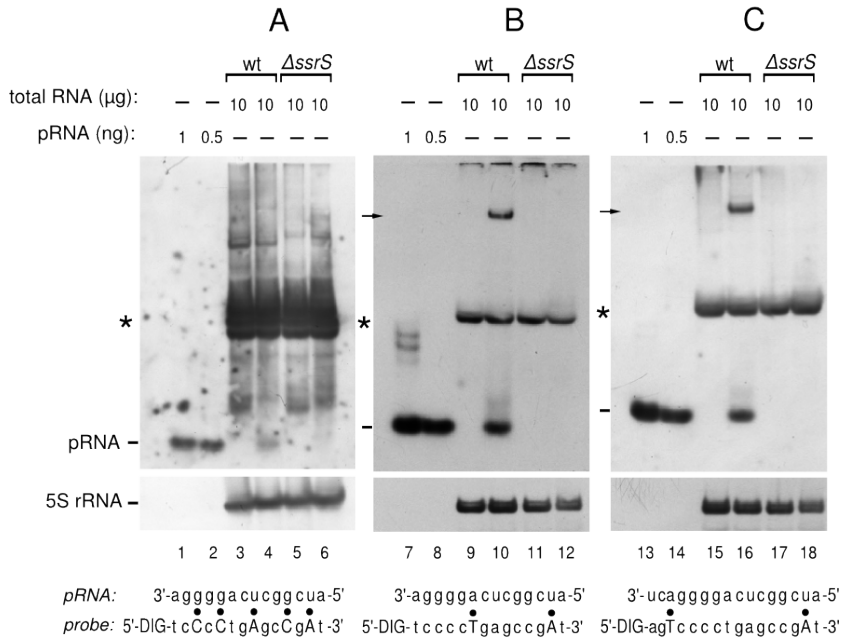

Figure 22: Northern blot of *E. coli* pRNA using three different probes (bottom panel; capital letters denote LNA residues). Endogenous pRNA is detectable during outgrowth in wild-type *E. coli* strains (wt), but not in the 6S-RNA knockout (Δ*ssrS*). Furthermore, 6S RNA-pRNA hybrids could be detected (arrows). Asterisks denote unspecific binding.

speculate that this event marks the first step in the degradation of 6S-1 RNA by a yet unknown nuclease activity. To validate

RACE = Rapid amplification of cDNA ends

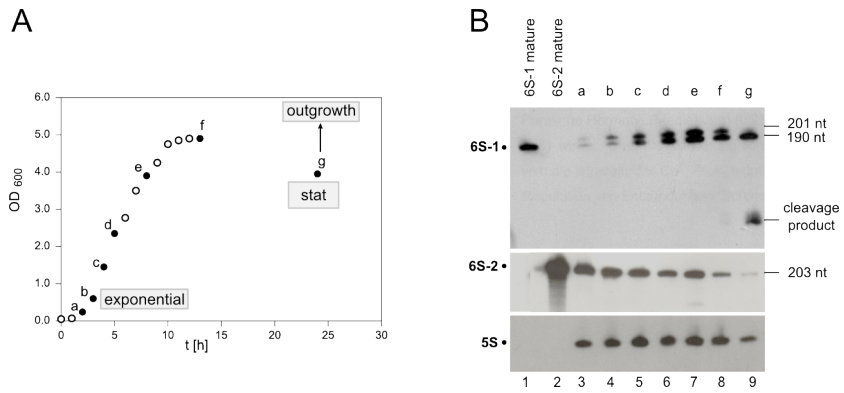

Figure 23: 6S RNA levels in *B. subtilis*. Total cellular RNA from cells in different growth stages (A) was used for Northern hybridization of both 6S RNAs (B). 6S-1 RNA levels are high during stationary phase whereas 6S-2 RNA levels peak during exponential growth.

the proposed secondary structure of 6S-2 RNA (Trotochaud and Wassarman, 2005), we performed structure probing experiments

using enzymatic (Nuclease T1) and chemical (Pb^{2+}) probes. We found that 6S-2 RNA, despite its unusal abundance in exponential growth phase, indeed folds into the typical 6S RNA 'shape' with an unstructured central bulge and flanking helices.

3.2.2 *Analysis of pRNA derived from 6S-1 RNA*

dRNA-Seq = differential RNA sequencing

We initiated a transcriptome-wide, unbiased screen for pRNAs using the dRNA-Seq approach which had been successfully utilized for the detection of a plethora of novel RNAs in *Salmonella typhimurium* (Sittka et al., 2008) and *Helicobacter pylori* (Sharma et al., 2010). A key feature of this technique is the splitting of each RNA sample. One half is enriched for primary transcripts (starting with a 5'-triphosphate), whereas the second half represents the unchanged bacterial transcriptome. Analyzing only short transcripts (< 50 nt), we found pRNAs templated by 6S-1 RNA in three key physiological growth stages, with particularly high numbers in the libraries that were enriched for primary transcripts (Fig. 24). To our surprise, 6S-1 pRNA levels were already

We compared exponential, stationary and outgrowth phase.

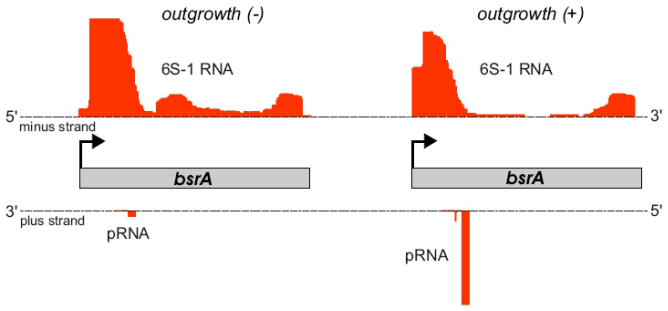

Figure 24: Graphical representation of the expression patterns of fragments of 6S-1 RNA (*bsrA*) and the corresponding pRNA; the latter was mainly found in the libraries after enrichment for primary transcripts (+) and in lower amounts in untreated libraries (-).

The relative amount of 6S-1 pRNA increased from 7.25% to 47% of the deep sequencing libraries enriched for primary trancripts after induction of outgrowth.

The longer 14-mer pRNA accumulated in outgrowing cells.

abundant during stationary phase. According to the proposed model of pRNA-mediated RNAP release (Fig. 8), we expected pRNA synthesis to occur exclusively after induction of outgrowth. The presence of large amounts of 6S-1 pRNA in stationary phase cells points to a much more flexible mechanism of RNAP release than hitherto anticipated. However, during outgrowth, pRNA levels increased drastically. Finally, we also observed that pRNA length was not distributed randomly: 8–12-mers and 14/15-mers were most abundant according to our dRNA-Seq data, and 4/5-mers, 8/9-mers and 14-mers represented the major *in vitro* transcription products; the synthesis of pRNA 14-mers was further confirmed by Northern blotting (Fig. 25).

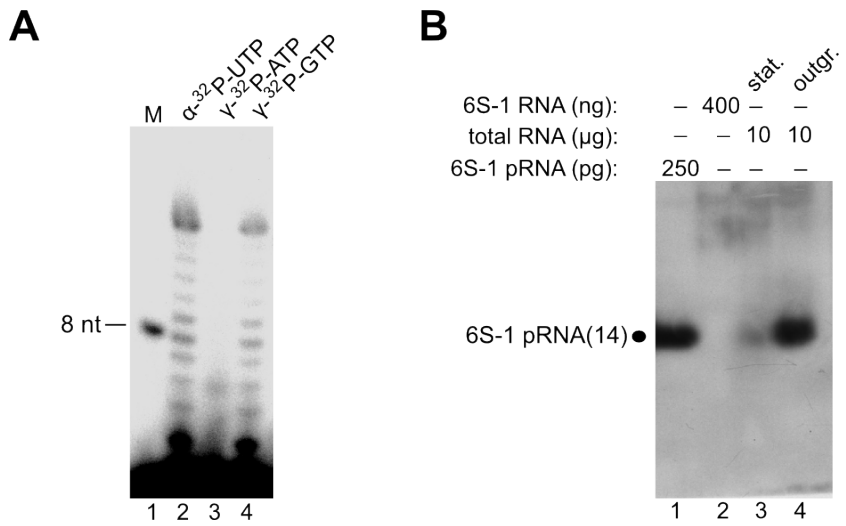

Figure 25: (A) *In vitro* transcription of pRNA using RNAP holoenzyme and 6S-1 RNA as template. Mainly 4-mer, 8/9-mer and 14-mer pRNAs were synthesized. (B) Detection of 6S-1 pRNA in either stationary or outgrowing cell using our Northern blot protocol confirmed the drastical increase in pRNA synthesis directly after induction of outgrowth.

The unique mechanism of release of RNAP via pRNA synthesis when nutrients are resupplied initially led to the assumption that NTP pools might trigger this event (Wassarman and Saecker, 2006). Furthermore, NTP pools in *B. subtilis* play a crucial role for transcription regulation; especially the intracellular GTP pool is a key instrument for the regulation of many genes (Lopez et al., 1979; Krásny and Gourse, 2004). This regulation is linked to the +1 nucleotide identity of the transcript (Krásny et al., 2008). To elucidate if the same regulatory mechanism also affects pRNA synthesis, we generated a *B. subtilis* mutant strain (BB*bsrAC40T*) carrying a point mutation in the *bsrA* gene. Analysis of pRNA from 6S-1 RNA in the mutant strain background revealed decreased levels of pRNA synthesis in general compared to the wild-type situation, but still highest expression levels during outgrowth. This led to the conclusion that pRNA synthesis is evolutionarily optimized for transcription starting with a G residue; however, we did not find convincing evidence that the initiator nucleotide concentration might be a key regulator of pRNA synthesis.

Wild-type pRNA initiates with a G residue; our mutant with an A residue.

3.2.3 *The enigmatic 6S-2 RNA*

Having found high levels of pRNA synthesis from 6S-1 RNA, we were surprised that we did not find pRNAs templated by 6S-2

RNA in our dRNA-Seq. Similar results from a global *B. subtilis* transcriptome analysis were published recently (Irnov et al., 2010). We expected to find pRNAs at least in exponential phase, when 6S-RNA levels were high (Fig. 23). Using an *in vitro* transcription assay, we found efficient transcription of pRNA from 6S-2 RNA by purified RNAP. By incorporation of different radiolabeled nucleotides, we were able to identify the sequence of 6S-2 pRNA. The discrepancy between the *in vivo* and *in vitro* results needs to be addressed in future investigations.
Furthermore, a 6S-2 RNA (*bsrB*) knockout strain did not show any detectable phenotype (Ando et al., 2002), raising the question of the potential role of the second 6S RNA in *B. subtilis*. We speculate that 6S-2 RNA might play a more specialized role compared to prototypical global regulators such as *E. coli* 6S-RNA or *B. subtilis* 6S-1 RNA. Therefore, investigation of diverse stress conditions or sporulation should be carried out to elucidate the role of 6S-2 RNA in transcriptional regulation. However, being able to detect pRNAs also from 6S-2 RNA by our Northern blot technique, one might exploit the appearance of 6S-2 pRNAs *in vivo* as a marker for potential 6S-2 RNA relevance when screening different physiological conditions.

3.3 THE ROLE OF PRNA IN THE RELEASE OF RNA POLYMERASE FROM 6S-1 RNA (PUBLICATION IV)

To scrutinize the role of pRNA synthesis during RNAP release from 6S RNA, we investigated 6S-1 RNA from *B. subtilis* in more detail. First, we performed *in vitro* transcription and gel retardation assays to analyze the formation of 6S-1 RNA-pRNA hybrids (Fig. 26). Using the 6S-1 pRNA sequence properties (`5'-GUU CGG UCA AAA CU`), we performed *in vitro* transcription with the RNAP holoenzyme in the presence of all NTPs (synthesis of 14-mer pRNA possible) or omitting ATP (only 8/9-mer pRNAs possible) thus mimicking the natural situation found in the dRNA-Seq approach (see above). Only the longer 14-mer pRNA can bind stably to 6S-1 RNA, whereas the shorter 8-mer pRNA and 6S-1 RNA do not form hybrids. Subsequent studies showed that, in principle, 13- and 12-mer pRNAs are also able to bind to 6S-1 RNA *in vitro*, but with reduced stability. Comparing free 6S-1 RNA and pre-annealed hybrids for their capability to be complexed by the RNAP holoenzyme, we found that free 6S-1 RNA is subject to RNAP binding, whereas the capacity of 6S-1 RNA-pRNA complexes to bind to RNAP is drastically reduced (Fig. 27). We concluded that the hybrid represents an inactive 'off' state of 6S-1 RNA.

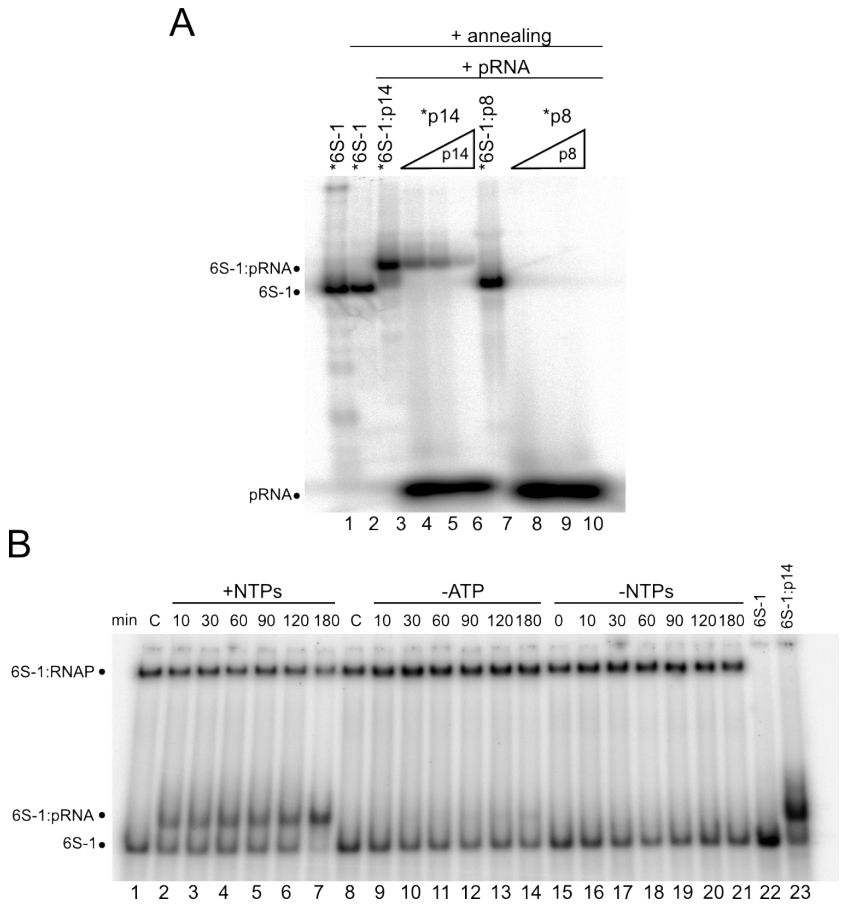

Figure 26: Formation of stable 6S-1 RNA-pRNA hybrids. (A) Formation of hybrids *in vitro* using either radiolabeled 6S-1 RNA or pRNA. Only the 14-mer pRNA binds stably to 6S-1 RNA; the 8-mer does not form stable hybrids. (B) *In vitro* transcription of pRNA analyzed on native PAGE. Stable hybrid formation occurs only in the presence of all NTPs (synthesis of 14-mer pRNA possible; lanes 1–7). Omission of ATP (leads to exclusive formation of 8-mers; lanes 8–14) inhibits formation of the hybrid.

Next, we analyzed how hybridization of pRNA to 6S-1 RNA influences the secondary structure of the templating RNA. We compared free 6S-1 RNA with hybrid 6S-1-pRNA by structure probing experiments, using either specific nucleases (T1 or V1 nuclease) or the divalent metal ion Pb^{2+} to determine structural changes in the radiolabeled 6S-1 RNA. Upon binding of a pRNA of at least 14 nt, the structure of 6S-1 RNA changes drastically (Fig. 28). Binding to the upstream region of the central bulge, pRNA disrupted the closing helix. The nucleotides that become unpaired upon pRNA invasion, are then able to basepair with nucleotides a) in the bottom part of the central bulge, permitting formation of an extended hairpin, or b) in the top part of the

A pRNA length of 14 nt is crucial for efficient stable hybrid formation, see publication IV.

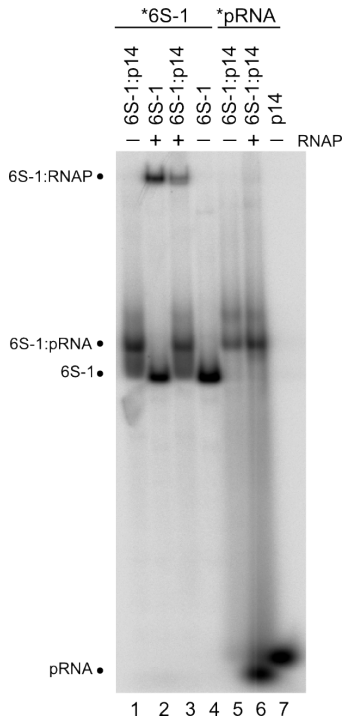

Figure 27: 6S-1 RNA-pRNA hybrids comprise an inactive state of 6S-1 RNA. Gel retardation assays using either free 6S-1 RNA or pre-annealed hybrids show that radiolabeled pRNA is detectable as part of the 6S-1 RNA-pRNA hybrid (lane 5). Hybrid formation, however, drastically reduces complexation with RNAP (cf. lanes 2, 3 and 6)

central bulge, resulting in a collapse of the flexible central bulge. The same effect could be obtained by an all-LNA 8-mer pRNA, indicating that not pRNA length itself but rather the stability of the hybrid is pivotal for induction of the structural rearrangement. It is tempting to speculate that this 'inactive' 6S-1 RNA structure might be preferentially recognized by nucleases and therefore degraded faster than free 6S-1 RNA. However, we have not found evidence for this possibility. Apparently, effective protection of 6S-1 RNA from intracellular degradation is only conferred by complexation with RNAP.

All pRNAs found so far originate from the central bulge region.

Finally, we used bioinformatic methods to predict similar structural changes in 6S RNA in all bacterial phyla. Assuming pRNA synthesis originating roughly at the same position as in 6S-1 RNA, we predicted formation of extended hairpins as well as central bulge collapses in the vast majority of 6S RNAs, despite the fact that 6S RNA sequences are only very weakly conserved. We therefore concluded that pRNA-induced structural changes are conserved among baceria.

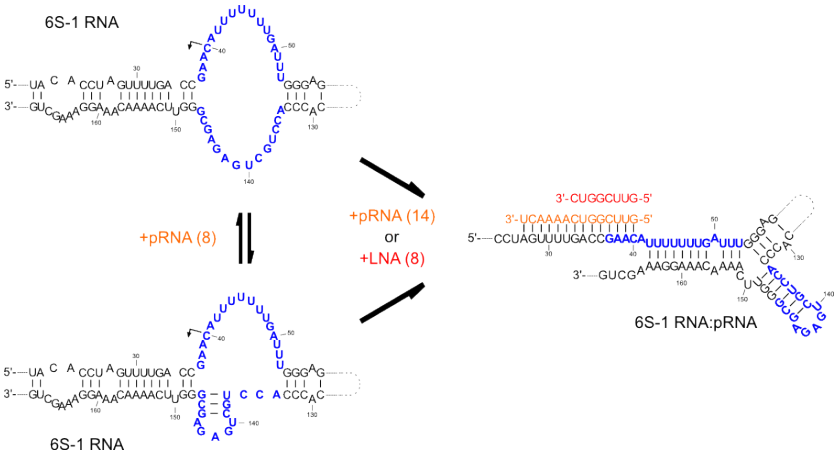

Figure 28: Structural rearrangement in 6S-1 RNA induced by pRNA. Free 6S-1 RNA forms a short hairpin in the central bulge region (nucleotides in blue) only transiently (left panel). Synthesis of 8-mer pRNA is insufficient to change this structural state of the RNA. Upon transcription of 14-mer pRNA (or artificial hybridization with an all LNA 8-mer), a structural rearrangement is induced (right panel), resulting in extended hairpin formation at the bottom of the bulge and collapse of the central bulge.

3.4 SUMMARY OF THE PROJECT

We investigated the role of short pRNA transcripts templated by 6S-1 RNA in *B. subtilis*. A picture emerges according to which 6S RNAs in general bind tightly to the housekeeping RNA polymerase, thereby sequestering it to inhibit transcription from many genes under nutrient deprivation. This global inhibition is resolved during outgrowth from stationary phase when RNAP is released from 6S RNA by synthesis of pRNA. The role of these short transcripts was unclear when we started our investigations.

After basic work to compare the two 6S RNA levels in *B. subtilis* we initiated a dual strategy to investigate pRNAs in this organism. First, we started to develop a novel Northern blot protocol to be able to detect such short RNA species in bacterial cellular extracts. In the meantime, we used the dRNA-Seq approach to screen the *B. subtilis* transcriptome in three key physiological stages for 6S RNA templated pRNA synthesis. As both approaches were successful, our work provides a toolbox for the analysis of pRNAs and other tiny RNAs in bacteria and also eukarya.

Focusing on 6S-1 RNA of *B. subtilis*, we next started to reveal the function of pRNA synthesis during the release of RNAP. Our model (Fig. 29) expands the current view of how RNAP is re-

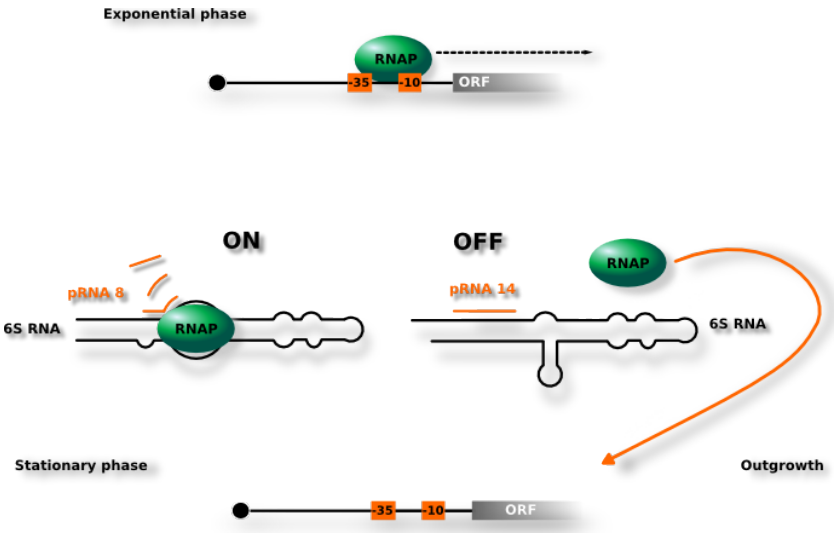

Figure 29: Model of pRNA-length mediated release of RNAP from 6S-1 RNA. Synthesis of pRNA alone is not sufficient for RNAP release (stationary phase) as long as pRNA length is below a certain treshold (< 12 nt in *B. subtilis*), 6S RNA keeps its binding-competent structure (ON state). During outgrowth from stationary phase, synthesis of pRNA of ~ 14 nt in length increases which leads to the inactive (OFF state) form of 6S RNA via induction of a structural rearrangement by hybridized pRNA.

leased from 6S RNA and assigns a mechanistic function to pRNA transcription. According to our results, pRNA is synthesized at all stages of bacterial growth. However, during stationary phase, the fraction of shorter and ineffective pRNAs (< 12-mers) was found to be higher than during outgrowth. The significane of this observation has to be scrutinized in follow-up studies.

We found that only the longer pRNA binds stably to 6S-1 RNA and that this leads to formation of a stable hybrid which is not subject to RNAP binding and therefore represents an inactive state of 6S-1 RNA. Furthermore, structural analyses unraveled the details of this hybrid formation. Only pRNAs of at geq 12 nt in length are able to induce a structural rearrangement of the 6S-1 RNA central bulge, resulting in extended hairpin formation and collapse of the central bulge. We conclude that this event is the trigger of RNAP release and we provide evidence that this mechanism is conserved among all bacteria. Taken together, we elucidated the role of pRNA in the mechanism of RNAP release from 6S-1 RNA and we propose that this function is a fundamentally conserved feature of 6S RNA in bacteria.

3.5 OUTLINE OF FUTURE WORK

Our work opened the door for a variety of follow-up studies. First of all, our proposed mechanism awaits verification in other bacterial species. A major problem here will be to first find the exact pRNA sequence, even if the 6S RNA had been identified in the respective organism. In many cases, already available deep sequencing data might yield this information. However, such short sequences are often at risk to be dropped during automatical alignment. We already have first results indicating that 6S-2 RNA of *B. subtilis* and its pRNA work in a similar fashion as 6S-1 RNA, at least *in vitro*.

A main question of the proposed mechanism remains unanswered however: what triggers synthesis of pRNA of sufficient length to induce a structural change? We observed accumulation of pRNA 14-mers in outgrowing cells, but we were unable to determine the elicitor of this effect yet. Our initial concept that NTP pools might directly affect pRNA synthesis could not be experimentally verified so far. We plan to screen for additional cofactors that may be involved in altering pRNA length.

Attempts to gain detailed knowledge about the structure properties of 6S RNA, for example by cristallographic studies, NMR or cryo-electron microscopy, failed so far. It would be of particular interest to be able to compare RNAP bound to either promoter DNA or 6S RNA to prove the open promoter model.

NMR = nuclear magnetic resonance

A completely neglected field in 6S RNA research is the regulation of the RNA's maturation and degradation. To our knowledge, RNases involved in this process have not been spotted so far in any organism and await identification. We obtained *B. subtilis* mutants with chromosomally deleted RNase genes and will screen them for differences in 6S RNA maturation and turnover.

Finally, the function of 6S-2 RNA has to be elucidated. We speculate that this 6S RNA may be involved in transcriptional regulation during yet unknown stress conditions or specialized physiological states, such as sporulation or biofilm production. In this respect, we will also test the ability of 6S-2 RNA to bind to RNA polymerases with σ-factors other than the housekeeping σ^A, as such more specialized σ-factors are usually involved in stress response regulation circuits.

Part IV

APPENDIX

A

APPENDIX

A.1 EQUIPMENT

DEVICE	MANUFACTURER
Agarose gel chamber	Biorad, Mini Sub Cell
Autoclave	Systec V95
Blotting device	C.B.S. Scientific Company Inc.
Cell homogenizer	MPI FastPrep 24
Centrifuges	Eppendorf 5810R, Heraeus Biofuge Fresco, Sigma 112
Gel documentation	Cybertech CS1
Glass beads 0.1mm	Roth
Hand monitor	Berthold LB 1210 B
Heating block	Biometra TB1
Incubator	Memmert BE400
Imager cassettes	Fuji Film Bas cassette 4043
Magnetic stirrers	Heidolph MR 2002
Power supply	Pharmacia EPS 3500,Biorad 160/1.6
PAA-gel chamber	Custom-made, University of Lübeck
PCR cycler	Biometra TGradient Thermocycler
pH-Meter	WTW pH Level 1
Phosphoimager	Raytest Bio-Imaging Analyser BAS 1000 (Fujifilm) , FLA 3000 (Fujifilm)
Pipets	Eppendorf Research (0.1–2.5 µl, 2–20 µl, 20–200 µl, 100–1000 µl)
Quartz cuvette	Hellma 104-QS, 105.202, 115B-QS, 105
Mixer	Eppendorf Thermomixer 5436
Shaking incubator	GFL 3033
Spectrophotometer	Thermo Spectronic Biomate 3
Scintillation counter	Perkin Elmer Wallac WINSPECTRAL a/b 1414

Table 44: List of devices.

CHEMICAL	MANUFACTUER
1-methylimidazol (99 %)	ACROS ORGANICS
2 log DNA Ladder	NEB
2-mercaptoethanol	Merck
Acrylamid M-Bis	GERBU
Agar Agar	SERVA
Agarose GTQ	Roth
Ammonium acetate	Fluka
Ammoniumpersulfate (APS)	Roth
Ampicillin	Roth
Boric acid (99.8%)	Roth
Bromophenol blue (BPB)	Merck
Chloroform	Merck
CDP-Star	Roche
Crystal violet	Fluka
Deoxynucleosidtriphosphates (dNTPs)	Fermentas
Disodiumhydrogenphosphate	Merck
Dithiothreitol (DTT)	Gerbu
Ethylendiamine-tetraacetate (EDTA)	GERBU
Ethanol p.a. (99.8%)	Roth
Ethidiumbromide	Roth
Formamide	GERBU
Formaldehyde	Roth
Glycerol (99.5%)	GERBU
Hydrochloric acid (HCl)	Roth
Isopropanol	Roth
Magnesium chloride	Fermentas
Maleic acid	Roth
Methanole	Roth
N-(3-Dimethylaminopropyl)-N-ethylcarbodimid Hydrochlorid (EDC)	Sigma-Aldrich
Natriumcitrate-Dihydrate	Roth
Peptone	Roth
Phenol	Roth
Potassiumacetate	Roth
Sodiumacetate	Fluka
Sodium chloride	Roth
Sodiumdihydrogenphosphate	Merck

Spermidine	Roth
SDS ultra pure	Roth
Sucrose	Roth
Tetramethylethylendiamin (TEMED)	Sigma-Aldrich
Tris X	GERBU
Tween20	Sigma-Aldrich
Urea	Gerbu
Xylen cyanol blue	Merck
Yeast extract	Gerbu

Table 45: List of chemicals.

A.2 KITS AND ENZYMES

KIT	PURPOSE	MANUFACTUER
GeneJet™Plasmid Miniprep Kit	Plasmid Miniprep	Fermentas
Wizard®SV Gel and PCR Clean-Up System	Agarose gel extraction	Promega
QIAquick®PCR Purification Kit	PCR purification	Roche
TOPO TA Cloning®Kit	Sub-cloning	Invitrogen
DIG Easy Hyb Northern Starter Kit	Northern blotting	Roche

Table 46: List of kits. Kits were used according to the manufacturer's instructions.

Restriction digest of DNA was performed using the enzymes indicated in the table below. The enzymes cut at the indicated recognitions sequence; the arrow marks the exact cleavage site. Restriction enzymes were used in combination with the supplied buffers.

ENZYME	RECOGNITION SEQUENCE	MANUFACTUER
BamHI	G↓GATCC	Fermentas
HindIII	A↓AGCTT	Fermentas
EcoRI	G↓AATTC	Fermentas
DpnI	Gm6A↓TC	Fermentas

Table 47: List of restriction enzymes.

ENZYME	PURPOSE	ORIGIN
T4 DNA ligase	DNA ligation	Fermentas
T4 RNA ligase	RNA ligation	NEB
T4 polynucleotide kinase	5′-phosporylation	Fermentas
Turbo DNase	DNA digestion	Ambion
RNase A	RNA digestion	Roche
RNase H	RNA digestion	NEB
RNase T1	RNA digestion	Ambion
RNase V1	RNA digestion	Ambion
Alkaline phosphatase	5′-phosphate removal	Fermentas
Tobacco acid phosphatase	5′-pyrophosphate removal	Epicentre
Taq DNA polymerase	DNA polymerization	Fermentas/ lab stock
Pfu DNA polymerase	DNA polymerization	Fermentas/ lab stock
Vent DNA polymerase	DNA polymerization	NEB
T7 RNA polymerase	RNA polymerization	Fermentas/ lab stock
B. subtilis RNA polymerase	RNA transcription	(Sogo et al., 1979)
SuperscriptII RT	Reverse Transcription	Invitrogen

Table 48: List of DNA-/RNA-modifying enzymes.

A.3 BACTERIAL STRAINS AND PLASMIDS

STRAIN	GENOTYPE	REFERENCE
E. coli DH5α	*supE44 hsdR17 recA1 endA1 gryA96 thi-1 relA1*	(Sambrook and Russel, 2001)
E. coli K12 MG1655	F- lambda- *ilvG- rfb-50 rph-1*	(Guyer et al., 1981)
B. subtilis 168	wildtype	Bacillus genetic stock center
B. subtilis BB bsrA (C40T)	*bsrA::bsrA(C40T)-kan*	This work

B. subtilis BB bsrA Kan	*bsrA::bsrA-kan*	This work

Table 49: List of bacteria.

STRAIN	GENOTYPE	REFERENCE
pUC18	pMB1 Amp^r	(Yanisch-Perron et al., 1985)
pDG780	Kan^r	(Guérout-Fleury et al., 1995)
pBB1	ϕ10 *bsrA*(190) Amp^r	This work
pBB2	ϕ10 *bsrA*(201) Amp^r	This work
pBB3	ϕ10 *bsrB*(203) Amp^r	This work
pBB4	ϕ10 *bsrA*(190) *hdv* Amp^r	This work
pBB5	ϕ10 *bsrA(C40T)*(190) Amp^r	This work
pBB6	ϕ10 *bsrA*(190) *bsrA*(190) Amp^r	This work

Table 50: List of plasmids.

A.4 SYNTHETIC SHORT OLIGONUCLEOTIDES

RNA oligonucleotides were purchased at Noxxon or IDT DNA Technologies. DNA/LNA mixmer probes were 5′-DIG labeled and purchased at Exiqon. Underlined nucleotides denote LNA residues.

OLIGO	TYPE	5′→3′ SEQUENCE
Bsub 6S-1 (14)	RNA	GUU CGG UCA AAA CU
Bsub 6S-1 (14-mut)	RNA	GUU CGG UCA CGA CU
Bsub 6S-1 (8)	RNA	GUU CGG UC
Bsub 6S-2 (12)	RNA	AAA GGU UAA AAC
Eco pRNA (14)	RNA	AUC GGC UCA GGG GA
Bsub 1:p14 probe	DNA/LNA	A<u>G</u>T T<u>T</u>T G<u>A</u>C C<u>G</u>A <u>A</u>C
Bsub 1:p14-mut probe	DNA/LNA	A<u>G</u>T CG<u>T</u> G<u>AC</u> CGA <u>A</u>C
Bsub 2:p12 probe	DNA/LNA	G<u>T</u>T T<u>T</u>A A<u>C</u>C T<u>T</u>T
Eco p14 probe 1	DNA/LNA	T<u>C</u>C C<u>C</u>T G<u>A</u>G C<u>G</u>G <u>A</u>T
Eco p14 probe 2	DNA/LNA	TCC CC<u>T</u> GAG CCG <u>A</u>T
Eco p16 probe 3	DNA/LNA	AG<u>T</u> CCC CTG AGC CG<u>A</u> T

Table 51: List of RNA or DNA/LNA oligomers.

A.5 SYNTHETIC DNA OLIGONUCLEOTIDES

DNA oligonucleotides were obtained from Metabion. Underlined sequences indicate either restriction enzyme recognition, bold letters indicate introduced mutations whereas italics denote overlapping regions or the T7 promoter sequence. Lowercase letters indicate RNA residues in mixmer oligonucleotides.

NO.	PURPOSE	5′→3′ SEQUENCE
6	DNA sequencing	GCC ATT CGC CAT TCA GGC
7	DNA sequencing	CAC ACA GGA AAC AGC TAT GAC C
21	5′ RACE rv	TAC GGC GAC CCA TCG C
22	5′ RACE rv	CTG GCT TCT GCT CTG GGA TTA TC
5X	5′ RACE adaptor	GTC AGC AAT CCC TAA Cga g
23	3′ RACE fw	ATG TCA GGA GCC TGA TTT CGT C
3X	3′ RACE first strand	AGG AGC CAT CGT ATG TCG GGG GGG GGG GGG GX; X = A/T/C
108	Kan cassette	GCG C<u>AA GCT T</u>AT GAC CTC GTC
109	Kan cassette	CAG <u>GAA TTC</u> GTT TTA TTT GCA GCA CCC ATGC
110	C40T mutation	GTT TTA TTT GCA GCA CCC ATG C
111	C40T mutation	GTG CGC AGA AAA AAC GGC TGC TCA TGG AT*A TCG ATA AAC CCA GCG AAC C*
112	C40T mutation	CGT ATT CTG GTT TCA TCT ATA AAA TGG CTG *ATC GAT ACA AAT TCC TCG TAG GC*
113	C40T mutation	GTT TTG ACC GAA **T**AT TTT TTT GAT TTG G
114	C40T mutation	TAG GTG TAC AAC TAA CAC ATC AGG ACT TTA TTT AAC

142a	*bsrA* cloning	CAG GAA TTC *TAA TAC GAC TCA CTA TAG G* AGT CCT GAT GTG TTA GTT GTA CAC CTA G
142b	*bsrA* cloning	CAG GAA TTC *TAA TAC GAC TCA CTA TAG* GAA GTT AAA TAA AGT CCT GAT GTG TTA GTT GTA CAC CTA G
143	*bsrA* cloning	CAG AAGCTT AAA GTC CCA ATA GTG CCG TTG
144	*bsrB* cloning	CAG GAA TTC *TAA TAC GAC TCA CTA TAG* GAA GCT ACT TTG TGC GTA TTG TTA ATT AAG
145	*bsrB* cloning	CAG AAG CTT *ATT TCC GAA AAG GAA ATG GCT TTC*
146	HDV cloning	*CAA CGG CAC TAT TGG GAC TTT* GGC CGG CAT GGT CCC AG
147	HDV cloning	*GGC CAG TGC CAA GCT T*GT CCC ATT CGC CAT TAC CGA G
150	cp mutation	CAG AAGCTT AGT CCT GAT GTG TTA GTT GTA CAC CTA G
151	cp mutation	*TAA TAC GAC TCA CTA TA*G GTA AAG AGG ACT TAC AAG ATT TAA AA
152	cp mutation	GAA TGA AAA GAG GCA TGT ACG
N1	Eco 5S probe	TGC CTG GCG GCA GTA GCG
N2	Eco 5S probe	*TAA TAC GAC TCA CTA TAG* GGA TGC CTG GCA GTT CCC TA
N3	Bsub 5S probe	AGA GGT CAC ACC CGT TCC CAT
N4	Bsub 5S probe	*TAA TAC GAC TCA CTA TAG* GGG GCG GCG TCC TAC TCT CA

N5	Eco 6S probe	ATT TCT CTG AGA TGT TCG CAA
N6	Eco 6S probe	*TAA TAC GAC TCA CTA TAG* GGG AAT CTC CGA GAT GCC GC
N7	Bsub 6S-1 probe	AAG GGA AAT AAA GTC CTG ATG TGT TAG TTG
N8	Bsub 6S-1 probe	*TAA TAC GAC TCA CTA TAG* GGA AAG TCC CAA TAG TGC CGT TG
N9	Bsub 6S-2 probe	GAA GCT ACT TTG TGC GTA TTG TTA ATT AAG
N10	Bsub 6S-2 probe	*TAA TAC GAC TCA CTA TAG* GGT TTC CGA AAA GGA AAT GGC TTT

Table 52: List of DNA primers.

B

PUBLICATION I

Northern blot detection of endogenous small RNAs (~ 14 nucleotides) in bacterial total RNA extracts.

Nucleic Acids Res 2010; 38(14): e147

Author contributions:
Research design: 75%
Experimental work: 95%
Data analysis and evaluation: 80%
Manuscript writing: 50%

Nucleic Acids Research Advance Access published May 26, 2010

Nucleic Acids Research, 2010, 1–10
doi:10.1093/nar/gkq437

Northern blot detection of endogenous small RNAs (~14 nt) in bacterial total RNA extracts

Benedikt M. Beckmann, Arnold Grünweller, Michael H. W. Weber and Roland K. Hartmann*

Institut für Pharmazeutische Chemie, Philipps-Universität Marburg, D-35037 Marburg, Germany

Received October 9, 2009; Revised April 16, 2010; Accepted May 7, 2010

ABSTRACT

Here we describe a northern blot procedure that allows the detection of endogenous RNAs as small as ~14 nt in total RNA extracts from bacteria. RNAs that small and as part of total bacterial RNA extracts usually escape detection by northern blotting. The approach combines LNA probes 5′-digoxigenin-endlabeled for non-radioactive probe detection with 1-ethyl-3-(3-dimethylaminopropyl)-carbodiimide-mediated chemical crosslinking of RNAs to nylon membranes, and necessitates the use of native PAGE either with the TBE or MOPS buffer system.

INTRODUCTION

The discovery of small regulatory RNAs in all domains of life and their multi-faceted key roles in cell biology has propelled advances in technologies for their analysis. This includes the use of LNA probes in hybridization approaches to increase sensitivity (1,2), development of the looped-primer RT–PCR technique to quantify mature miRNAs (3), as well as high-throughput methods such as RNomics to generate cellular RNA libraries for deep sequencing (4) or miRNA profiling arrays (5). Despite these advances, the classic northern blot technique has remained irreplaceable, since the approach allows the researcher to visualize and roughly quantify cellular levels of RNAs and their processing intermediates relative to endogenous RNA standards (e.g. 5S rRNA). The northern blot has even gained importance owing to the growing number of small RNA candidates identified by high-throughput and bioinformatic methods, which need to be verified experimentally. Recently, Hamilton and co-workers (6,7) reported the use of 1-ethyl-3-(3-dimethylaminopropyl)-carbodiimide (EDC) to covalently couple small RNAs via their 5′-phosphates to amino groups at the surface of nylon membranes. Relative to the standard UV crosslinking to nylon membranes, this reportedly 5′-end-selective attachment enhanced the detection of RNAs <40 nt 25- to 50-fold. The likely reason is that UV crosslinking to the free amines of nylon membranes occurs via the bases (primarily uracil) which, in contrast to immobilization via the phosphate, sterically blocks accessibility of the immobilized nucleic acid for hybridization, particularly in the case of small RNAs owing to their limited interaction surface. Furthermore, the number and positions of UV-crosslinked bases vary depending on the particular RNA sequence and the applied UV crosslinking conditions (length of irradiation, UV light intensity), making UV crosslinking a process that is hard to control (6,7).

We were faced with the limitations of standard northern blot protocols when trying to detect small so-called product RNAs (pRNAs, ~14 nt in length) in total RNA extracts from *Bacillus subtilis*; pRNAs are short transcripts synthesized by bacterial RNA polymerases in an RNA-dependent RNA polymerization reaction using 6S RNA as template. 6S RNA, ~200 nt in size, has been identified as a growth-phase dependent riboregulator of bacterial transcription (8). In *Escherichia coli*, this RNA acts by complex formation with the σ^{70} housekeeping RNA polymerase (RNAP) holoenzyme ($E\sigma^{70}$) and accumulates during stationary phase. 6S RNA is primarily helical, with a large single-stranded loop in the center. This highly conserved secondary structure is essential for the ability of 6S RNA to form stable complexes with $E\sigma^{70}$ and to serve as a template for the synthesis of pRNAs (9,10). Synthesis of these short transcripts leads to dissociation of 6S RNA–RNAP complexes. In contrast to *E. coli* with only one 6S RNA gene, the *B. subtilis* genome harbors two 6S RNA homologs, termed 6S-1 and 6S-2 (11,12). Both RNAs were co-immunoprecipitated with the σ^{A} housekeeping RNAP holoenzyme using antibodies against σ^{A} or the α subunit (13). Our identification of 8- to 15-mer pRNAs derived from transcription on 6S-1 RNA as template in *B. subtilis* by a deep sequencing approach (unpublished results), but the failure to detect those by northern blotting, prompted us to explore improved northern blot protocols tailored to the detection of cellular RNAs as small as 14 nt.

*To whom correspondence should be addressed. Tel: +49 6421 2825827; Fax: +49 6421 2825854; Email: roland.hartmann@staff.uni-marburg.de

MATERIALS AND METHODS

Strains and growth conditions

Bacillus subtilis 168 and PY79, *E. coli* MG1655, and 6S RNA knockout strains *B. subtilis* PY79 Δ*bsrA* and *E. coli* MG1655 Δ*ssrS* were grown in LB medium at 37°C. In preparation for outgrowth experiments, 50 ml of fresh medium were inoculated with an overnight culture to an OD_{600} of 0.05; cells were then grown to stationary phase for ~24 h. Then 20 ml of stationary culture were diluted with 80 ml fresh pre-warmed LB medium to induce outgrowth at 37°C under shaking; total RNA was extracted 3 min after outgrowth had been started. Construction and phenotype of the 6S-1 RNA knockout strain *B. subtilis* PY79 Δ*bsrA* and the 6S RNA knockout strain *E. coli* MG1655 Δ*ssrS* will be reported elsewhere (manuscript in preparation).

RNA extraction

Cellular total RNA was prepared using the hot phenol method (14). Briefly, *B. subtilis* or *E. coli* cell pellets were resuspended in extraction buffer (10 mM sodium acetate pH 4.8, 150 mM sucrose) and incubated with 0.1 volumes of lysozyme (20 mg/ml, Roth, Karlsruhe, Germany) for 10 min at room temperature. 10% SDS was added to a final concentration of 1% prior to vigorous vortexing. After addition of 1 volume of phenol (preheated to 65°C) and vortexing, the mixture was incubated for 5 min at 65°C and 5 min on ice, followed by centrifugation at 4°C for 30 min (8220*g*). Phenol extraction was repeated, followed by chloroform (1+1) extraction and ethanol precipitation. RNA concentration was determined by UV spectroscopy.

Northern blotting

For northern blotting, 6 or 10 µg of total cellular RNA were loaded per gel lane. Mature *B. subtilis* 6S-1 RNA (190 nt) and *E. coli* 6S RNA (186 nt) included as controls (Figure 1) were synthesized by *in vitro* runoff transcription using T7 RNA polymerase. Chemically synthesized pRNA oligonucleotides 5′-GUU CGG UCA AAA CU-3′ (*B. sub* 6S-1p wt), 5′-GUU CGG UCA CGA CU-3′ (*B. sub* 6S-1p mut) and 5′-AUC GGC UCA GGG GA-3′ (*E. coli* 6Sp wt) were obtained from Noxxon (Berlin, Germany). 14- or 16-mer probes complementary to pRNAs included 5′-digoxigenin-aGt tTt gAc cGa Ac-3′ (probe for *B. subtilis* wt 6S-1 pRNA), 5′-digoxigenin-aGt cgT gAC cga Ac-3′ (probe for *B. subtilis* mutant 6S-1 pRNA), 5′-digoxigenin-tcC cCt gAg cCg At-3′ (*E. coli* 6S pRNA probe 1), 5′-digoxigenin-tcc ccT gag ccg At-3′ (*E. coli* 6S pRNA probe 2) and 5′-digoxigenin-agT ccc ctg agc cgA t-3′ (*E. coli* 6S pRNA probe 3), with uppercase letters indicating LNA and lowercase letters DNA residues (Figures 1 and 7); 5′-digoxigenin-labeled, LNA-containing probes were obtained from Exiqon (Vedbaek, Denmark). For specific detection of *B. subtilis* and *E. coli* 5S rRNA loading controls and for *E. coli* 6S RNA, antisense transcripts covering the respective full-length RNA and internally labeled with digoxigenin-UTP were synthesized from PCR templates by T7 RNA polymerase (according to the DIG RNA Labeling Mix protocol provided by Roche Diagnostics, Mannheim, Germany). For native PAGE, samples were adjusted to 1× native loading buffer by mixing with 6× native loading buffer [0.25% (w/v) bromophenol blue, 0.25% (w/v) xylene cyanol blue, 30% (v/v) glycerol]. For denaturing PAGE, samples were adjusted to 1× denaturing loading buffer [0.01% (w/v) bromophenol blue, 0.01% (w/v) xylene cyanol blue, 1.3 M urea, 33% (v/v) formamide, 1× TBE]. Before gel loading, samples were heated to 95°C for 3 min, followed by immediate cooling on ice. Generally, 10 or 20% polyacrylamide gels were used for RNA separation under native or denaturing conditions. For native PAGE, gel solutions as well as electrophoresis buffers either contained 89 mM Tris, 89 mM borate and 2 mM EDTA (TBE buffer system) or 20 mM MOPS–NaOH, pH 7, (MOPS–NaOH buffer system). For denaturing PAGE, gel solutions as well as electrophoresis buffers either contained 89 mM Tris, 89 mM borate, 2 mM EDTA and 8 M urea (TBE buffer system) or 20 mM MOPS–NaOH, pH 7 and 2% formaldehyde (MOPS–NaOH buffer system). RNA was blotted on positively charged nylon membranes (Roche Diagnostics) overnight using a semi-dry blotter with 3.75 mA/cm^2 and 0.5× TBE as transfer buffer. To add a 5′-phosphate to the chemically synthesized pRNAs, the oligonucleotide was incubated with ATP and T4 polynucleotide kinase (Fermentas, St. Leon-Rot, Germany) according to the manufacturer's instructions. Efficiency of phosphorylation was analyzed on a 20% denaturing polyacrylamide gel (TBE buffer system), with the 5′-phosphorylated oligonucleotide migrating faster than the 5′-OH variant owing to its extra negative charge; pRNAs with 5′-OH and 5′-phosphate were subjected to preparative co-electrophoresis, followed by gel excision and gel elution in 1 M Na(OAc) pH 4.9. Finally, pRNAs were concentrated by ethanol precipitation.

Hybridization and detection

Classical RNA immobilization was performed by incubation of the wet membrane at 80°C for 30 min and storage at 4°C. Alternatively, EDC crosslinking was utilized to detect very small RNAs, exactly as described (7). Briefly, 245 µl of 12.5 M 1-methylimidazole (Sigma Aldrich, Taufkirchen, Germany) were added to 9 ml of double-distilled water and the pH was adjusted to 8.0 using HCl. Directly prior to use, 0.75 g EDC [1-ethyl-3-(3-dimethylaminopropyl)-carbodiimide, Sigma Aldrich] were added and the volume was adjusted to 24 ml with double-distilled water. The wet membrane was placed on a Whatman paper soaked with EDC solution (160 mM EDC, 130 mM 1-methylimidazole pH 8.0), wrapped in plastic foil and incubated for 2 h at 60°C. After careful washing with water, the membrane was stored at 4°C. For pre-hybridization, 7 ml of hybridization solution (termed 'DIG Easy Hyb Granules', Roche Diagnostics) were heated to 50°C (in the case of DIG-LNA/DNA mixmer probes) or 68°C (in the case of T7 transcript probes >100 nt) and added to the membrane in a hybridization tube (avoid sticking of the membrane to the tube wall), followed by slow rotation in an

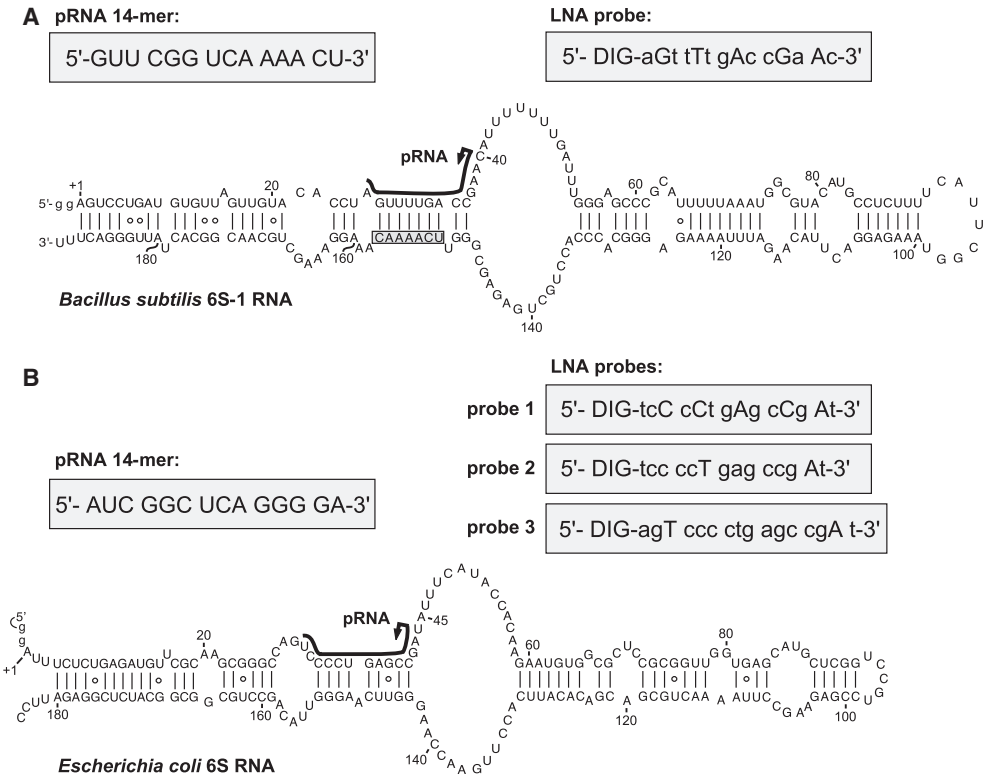

Figure 1. Secondary structure presentation of (**A**) mature *B. subtilis* 6S-1 RNA (190 nt), adapted from (11), and (**B**) of *E. coli* 6S RNA according to (9); both RNAs were transcribed with two artificially added G residues (lowercase letters) for reasons of efficient synthesis by T7 RNA polymerase. In both panels, the black lines along the sequence indicate the region of *B. subtilis* 6S-1 RNA and *E. coli* 6S RNA that serve as a template for the synthesis of small transcripts (product RNAs = pRNAs) by RNA polymerase (this study, 9); arrows mark the starting point of pRNA transcription; the chemically synthesized pRNA mimics are depicted in the grey boxes on the left above the 6S RNA structures. In panel A, 6S-1 RNA nt 151–157 complementary to nt 2–8 of the LNA probe are boxed. LNA probes for pRNA detection are shown in grey boxes on the right above the secondary structures; DIG, digoxigenin attached to the 5′-end via a C6 linker; small letters depict DNA residues, capital letters LNA residues.

hybridization oven for 2 h at 50 or 68°C, respectively. Probes, either 10 µl T7 transcript or 300 pmol DIG-LNA/DNA mixmer, were denatured for 3 min at 95°C, followed by immediate transfer on ice. The probe was then added to 7 ml pre-heated (50 or 68°C) hybridization solution to replace the pre-hybridization solution. Hybridization was conducted for at least 6 h, usually overnight, at 50 or 68°C under slow rotation in a hybridization oven. In some cases (Figure 8A) the (pre-)hybridization temperature for LNA/DNA mixmer probes was increased (depending on the probe's G/C content and extent of LNA modification) in order to suppress non-specific signals. Immunological detection of RNA was performed according to the instructions of the DIG Northern Starter Kit (Roche Diagnostics). X-ray films (Kodak BioMax Light Film, Sigma Aldrich) were exposed to the membrane for chemiluminescence detection (usually 20–45 min). Developed X-ray films were scanned (BioRad GS-800) for documentation.

RESULTS

From a deep sequencing library we knew that pRNA transcripts, predominantly 8–15 nt in length, accumulate in *B. subtilis* cells under conditions of outgrowth from stationary phase (unpublished results, manuscript in preparation). The pRNAs are synthesized by RNA polymerase using 6S-1 RNA as the template (Figure 1A). However, we and others (Jörg Vogel, personal communication) had been unable to detect pRNA transcripts by northern blot analysis. Such an example, where we used 20% PAGE/8 M urea and classical 'baking' of the membrane at 80°C for RNA immobilization, is shown in Figure 2 (comparable results were obtained with UV crosslinking; data not shown). Although we employed an LNA/DNA mixmer probe (Figure 1A) for efficient hybridization, no endogenous pRNA signal could be detected in up to 20 µg of total RNA from *B. subtilis* cells at 3 min of outgrowth from stationary phase (Figure 2, lanes 6–8). Yet, when gels were loaded with 0.5, 1 or 5 ng of a chemically synthesized pRNA 14-mer, signals were obtained (Figure 2, lanes 1–3). Likewise, a signal of similar intensity as in lane 3 (5 ng pRNA) was observed when 5 ng of the pRNA 14-mer were added to 5 µg of total cellular RNA from outgrowth bacteria (lane 4). These findings admitted different explanations: (i) endogenous pRNA levels were below the sensitivity level of the applied northern blot setup; (ii) endogenous pRNAs might be masked in the context of total

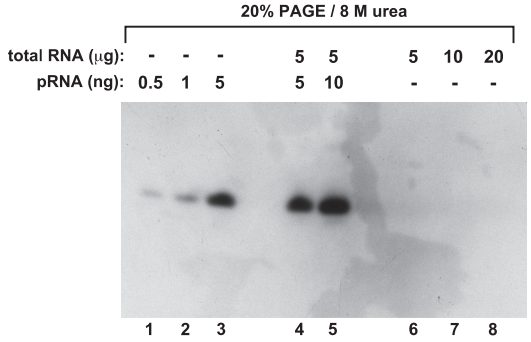

Figure 2. Standard denaturing northern blot using the classical 'baking' of the membrane at 80°C for RNA immobilization. Lanes 1–3: various amounts of the chemically synthesized pRNA 14-mer (with 5′-OH terminus; Figure 1A); lanes 4 and 5: 5 or 10 ng of the chemically synthesized pRNA 14-mer mixed with 5 μg of total RNA from *B. subtilis* before electrophoresis and membrane transfer; lanes 6–8: samples with varying amounts of total RNA from *B. subtilis* for the purpose of endogenous pRNA detection. Total cellular RNA was isolated 3 min after outgrowth from stationary phase using the hot phenol method; the 5′-digoxigenin-labeled LNA–DNA mixmer shown in Figure 1A was used as probe. (for details, see 'Materials and Methods' section).

cellular RNA extracts owing to their association with 6S-1 RNA; non-specific masking could be excluded based on the results shown in Figure 2, lanes 4 and 5.

Native versus denaturing PAA gels combined with EDC crosslinking

Since the oligonucleotide coupling to nylon membranes is thought to occur via primary amino groups (15), we considered the possibility that the amino groups of urea in denaturing PAA/TBE gels might compete with the membrane amines during the coupling step. Moreover, the necessity of denaturing conditions for electrophoretic separation according to size is certainly less mandatory for short RNA oligonucleotides compared with larger and more structured RNAs. To address these points, we performed northern blots with native and denaturing PAA gels, either using the 1× TBE or the MOPS buffer system, and applying EDC crosslinking for RNA coupling to the nylon membrane (Figure 3). In the case of native but not denaturing conditions, we were now able to detect endogenous pRNAs in total RNA extract from outgrowth bacteria (Figure 3A, lane 5; Figure 3B, lane 6). The endogenous pRNA signal co-migrated with the chemically synthesized pRNA 14-mer (Figure 3A and B, lanes 1–3). Assuming that the 5′-end groups (5′-OH for the chemically synthesized pRNA, 5′-triphosphate for the endogenous pRNA) had little effect on gel mobility in native 10% PAA gels, our results suggest that the bulk of endogenous pRNAs transcribed from 6S-1 RNA have sizes of ~14 nt, in line with the prevalence of 8- to 15-mer sequence reads in our deep sequencing library (data not shown). The absence of an endogenous pRNA signal in the presence of 8 M urea (Figure 3A, lane 10 versus 5) or 2% formaldehyde (Figure 3B, lane 12 versus 6) can be explained by urea competing with amino groups at the membrane surface for reaction with EDC and formaldehyde reacting with membrane amino groups which then become unavailable to reaction with the EDC crosslinker.

In Figure 3A, lanes 5 and 10, additional signals of RNAs larger than pRNA were observed; less additional signals were observed in the corresponding lanes 6 and 12 of Figure 3B, but here a another total RNA preparation from outgrowth bacteria was used. Thus, we attribute this difference to variations in the quality of RNA preparations. Yet, to rule out that the observed differences were related to the type of PAA buffer system, we used the same RNA preparation as in Figure 3B for native PAGE blots, either TBE or MOPS buffered (Figure 4). Here, only signals attributable to 6S-1 RNA (owing to the probe's complementarity to seven consecutive nucleotides of 6S-1 RNA; nt 151–157 in Figure 1A) and endogenous pRNA were detected (Figure 4, lanes 6 and 12), indicating that the quality of the total RNA preparation rather than the buffer system determines the extent of non-specific signals.

Role of 5′-end groups of RNA oligonucleotides for EDC crosslinking efficiency

Although our chemically synthesized *B. subtilis* reference pRNA carried a 5′-hydroxyl group, northern blot signals were detected (e.g. Figure 4, lanes 1–3 and 7–9). This implied that EDC crosslinking to membranes had occurred despite the absence of a 5′-terminal phosphate. To further analyze this aspect, we 5′-phosphorylated this pRNA and compared northern blot signal intensity to that of the 5′-hydroxylated pRNA. Signal intensity was largely (~10-fold) increased owing to the presence of the 5′-phosphate (Figure 5, lanes 1–3 versus 5–7). However, the presence of a 5′-phosphate is not essential, indicating that internal phosphodiesters can react as well, although with reduced efficiency.

Verification of pRNA detection specificity

As mentioned before, we observed additional signals beyond that for pRNA in some of our initial gels (e.g. Figure 3A, lane 5). To increase confidence that we indeed detected genuine endogenous 6S-1 pRNAs, we also prepared total RNA from a *B. subtilis* PY79 *ΔbsrA* strain, in which the 6S-1 RNA gene was replaced with a spectinomycin resistance cassette (unpublished results, manuscript in preparation). In contrast to the wild-type PY79 strain, no pRNA signal was observed for total RNA derived from the PY79 *ΔbsrA* strain harvested under outgrowth conditions (Figure 6, lanes 5 versus 7), indicating that the signal in lane 5 indeed represents authentic 6S-1 pRNAs.

Detection of 14-mer sequence variants and influence of intramolecular RNA secondary structure

Our results raised the question if northern blot detection of a 14-mer is sensitive to sequence identity and, since we have employed native gel systems here, if potential intramolecular secondary structures might negatively affect detection sensitivity. Both questions were simultaneously addressed by designing the variant pRNA mut with two

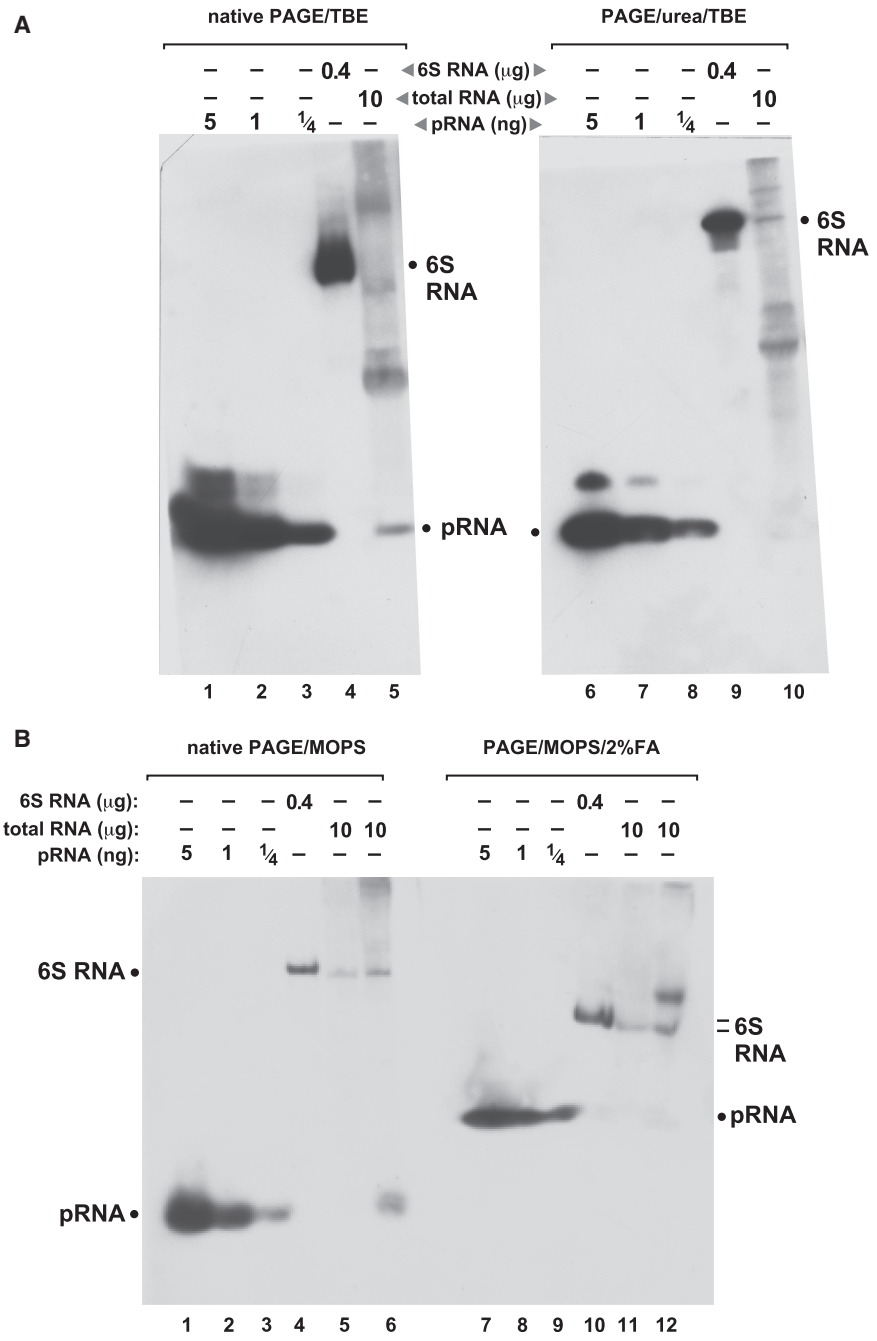

Figure 3. Comparison of northern blots performed in different buffer systems under native and denaturing conditions, using EDC crosslinking for RNA immobilization on nylon membranes. (**A**) Northern blots of RNA separated by native (left) and denaturing (right) PAGE using the TBE buffer system. Lanes 1–3 and 6–8: varying amounts of the chemically synthesized pRNA 14-mer (Figure 1A); lanes 4 and 9: 400 ng of *in vitro* transcribed *B. subtilis* 6S-1 RNA loaded onto the gels; the northern blot signal is attributable to the probe's complementarity to seven consecutive nucleotides of 6S-1 RNA (nts 151–157; Figure 1A), including three LNA/RNA base pairs; lanes 5 and 10: 10 μg of total cellular RNA prepared from *B. subtilis* cells after 3 min of outgrowth from stationary phase ('Materials and Methods' section); the endogenous pRNA yielded a signal under native but not under denaturing conditions (lanes 5 versus 10). Likewise, pRNA signals in lanes 1–3 were more intense than those in lanes 6–8. (**B**) The same samples as in panel A were analyzed by MOPS-buffered PAGE and northern blotting in the absence (lanes 1–6) and presence (lanes 7–12) of 2% formaldehyde as denaturing agent. Additionally, total RNA prepared from stationary phase cells was loaded onto the gels (lanes 5 and 11); endogenous pRNA in the outgrowth RNA fraction was again only detectable under native conditions (compare lanes 6 and 12). Note that PAGE with MOPS and formaldehyde generally resulted in less efficient separation of RNAs according to size. Film exposition times were 20–45 min; the two part figures in panel A originate from the same blot and exposed film; exposition time in panel B slightly differed from that in panel A; criterion for exposition length was good visibility of the pRNA signal (lane 5 in panel A, lane 6 in panel B), thus often two or more films were exposed to the same blot for different periods of time to optimize blot performance.

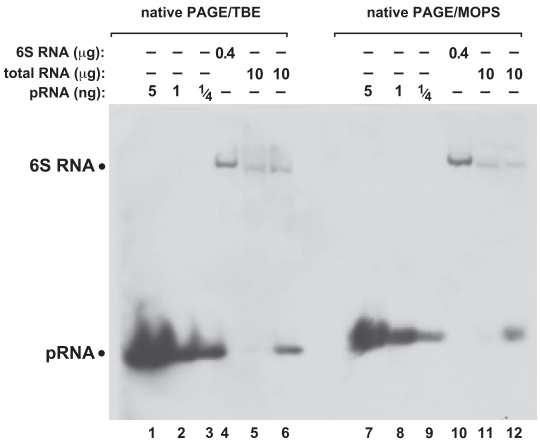

Figure 4. Comparison of native PAGE northern blots using the TBE (lanes 1–6) or MOPS (lanes 7–12) buffer systems. The two different gels were blotted simultaneously onto the same nylon membrane. For further details, see legend to Figure 3B.

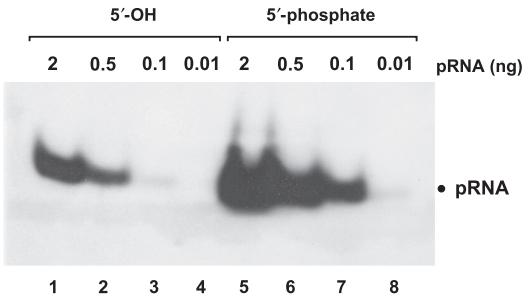

Figure 5. Functional groups at the 5′-terminus have a strong impact on signal strength. pRNA with a 5′-phosphate (lanes 5–8) yielded enhanced signal strength (~10-fold) compared to the same RNA with a 5′-hydroxyl end (lanes 1–4). Gel electrophoresis: 10% native PAGE, 1× TBE; RNAs were coupled to nylon membranes by EDC crosslinking.

consecutive base exchanges relative to the wild-type 6S-1 pRNA; the two point mutations generated the potential of the 14-mer to form a small hairpin structure with a 3-bp stem (Figure 7, top). The two chemically synthesized pRNA variants were separated on a 20% native PAA gel (TBE buffer system), followed by northern blotting using two different 5′-digoxigenin-LNA/DNA mixmer probes, either fully complementary to wild-type pRNA or to pRNA mut. Figure 7 illustrates that, for both pRNA variants, higher detection sensitivity was obtained with the fully complementary probe, although both probes were also able to mutually recognize the corresponding mismatching pRNA variant. Detection sensitivity of the wild-type pRNA probe generally exceeded that of the pRNA mut probe, which is attributed to the different distribution of LNA modifications in the two probes (Figure 7). This illustrates the sensitivity of the method to the design of LNA probes in terms of the number and positioning of LNA residues. Of note, pRNA mut

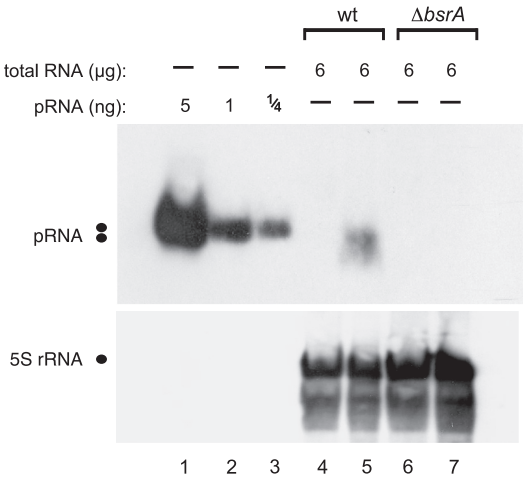

Figure 6. Specificity of pRNA detection demonstrated by using total RNA from the *B. subtilis* wild-type (wt) strain PY79 (lanes 4 and 5) versus a 6S-1 RNA knockout derivative strain, PY79 *ΔbsrA* (lanes 6 and 7); lanes 4 and 6, total RNA from cells harvested in stationary phase; lanes 5 and 7, total RNA from cells harvested during outgrowth (for details, see 'Materials and Methods' section). 5S rRNA was used as an internal loading control in lanes 4–7; since we used native PAGE here, the expanded area of 5S rRNA signals may be due to different 5S rRNA conformers.

migrated somewhat faster than wild-type pRNA in the native 20% PAA gel, suggesting that its hairpin structure indeed formed during electrophoresis, at least transiently. However, the blot in Figure 7 provides no evidence for a substantial influence of hairpin formation on detection sensitivity.

Detection of small RNAs in *E. coli*

To test if our approach is also applicable to organisms other than *B. subtilis*, we isolated total RNA from the *E. coli* wild-type strain MG1655 and a derivative 6S RNA knockout strain (*ΔssrS*). *Escherichia coli* was chosen because the bacterium represents the major model system for studies of 6S RNA, and pRNAs of similar size (14–20 nt) have been described (9). We initially designed probe 1 (14 nt) for the detection of *E. coli* pRNAs, but the specific signal was weak, with a strong background of non-specific signals (Figure 8A). Since two of the five LNA modifications were in the stretch of four C residues, we were concerned that this may have led to non-specific interactions with complementary tetra-G stretches in other RNA molecules. We then designed probes 2 (14 nt) and 3 (16 nt) with only two LNA residues located outside the tetra-C stretch. This largely improved the sensitivity and specificity of the northern blot (Figure 8B and C). *E. coli* pRNAs were only detected under outgrowth conditions in the wild-type strain, but not in the 6S RNA knockout (*ΔssrS*) strain (Figure 8A–C, lanes 4, 10 and 16 versus lanes 6, 12 and 18). This is in line with the results observed for *B. subtilis* (Figure 6), where no pRNA signal could be detected in the 6S-1 RNA deletion strain Δ*bsrA*.

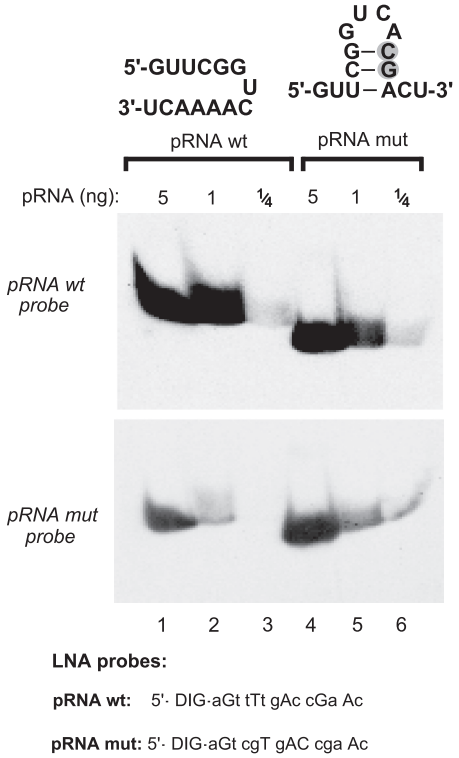

Figure 7. Evaluation of the influence of potential intramolecular RNA secondary structures on detection efficiency. A mutated version of the 6S-1 pRNA (pRNA mut with two consecutive point mutations, grey-shaded; lanes 4–6), designed to have the potential to form a hairpin with a 3-bp stem, migrated somewhat faster than wt pRNA (lanes 4–6 versus 1–3) in a 20% native PAA gel (TBE buffer system), suggesting that the hairpin indeed formed at least transiently during electrophoresis. The two pRNA variants (carrying 5′-OH termini) were mutually detected with LNA probes either complementary to wt pRNA (top panel) or to pRNA mut (bottom panel), with LNA probes specified below the blots (uppercase letters indicate LNA and lowercase letters DNA residues). Films were exposed to the blot for 35 min.

We further observed a hybridization signal suspected to represent pRNA complexed with *E. coli* 6S RNA (Figure 8B and C, arrows). To address this possibility, we ran a native 10% PAA gel, where we loaded identical sample sets onto the left and right half of the gel. After blotting to a nylone membrane, the blot was cut into the two halves with identical sample sets and hybridized either to the *E. coli* pRNA probe 3 or to a digoxigenin-labeled 6S RNA antisense transcript (Figure 8D and E). This experiment revealed (i) that the aforementioned band is indeed a 6S RNA:pRNA hybrid, as the signal was detected with both probes (arrows in panels D and E), (ii) that 6S RNA is present in the *E. coli* MG1655 wild-type, but not in Δ*ssrS* derivative strain, also verifying that signals marked with asterisks in Figure 8A–D are not related to 6S RNA, thus representing a cross-hybridizing RNA of unknown identity. The chemically synthesized *E. coli* pRNA 14-mer tended to form aggregates (Figure 8D, lanes 2 and 3). We therefore added denaturing instead of native loading buffer to this RNA and heated the sample to 95°C for 5 min (Figure 8C, lanes 13 and 14). Shortening of this heating step to 2 min (Figure 8D, lanes 2 and 3) was insufficient to dissolve the RNA multimers. Noteworthy, the presence of low amounts of denaturing agents introduced into the gel via the denaturing loading buffer did not perceivably compromise EDC crosslinking.

DISCUSSION

We have developed a northern blot technique that permits to detect cellular RNAs as small as ~14 nt in a reproducible and highly sensitive manner. This technique is novel in that it combines three elements: (i) 5′-digoxigenin-endlabeled LNA/DNA mixmer probes, (ii) EDC crosslinking of RNAs to nylon membranes, and (iii) native PAGE systems. The method was successfully applied to the detection of 'tiny' pRNAs from two different model systems, *B. subtilis* and *E. coli*, which leads us to conclude that the procedure will be broadly applicable. Parallel analysis of *B. subtilis* and *E. coli* 6S RNA knockout strains unequivocally confirmed specific detection of endogenous pRNAs.

Our detection of *B. subtilis* 6S-1 RNA with the pRNA-specific LNA/DNA mixmer probe (Figure 3A, lanes 4 and 9, Figure 3B and Figure 4), attributed to formation of seven consecutive base pairs (to 151–157 nt of 6S-1 RNA, Figure 1A), suggested that even RNAs smaller than 14 nt will be detectable by the approach. Detection of natural RNA oligonucleotides <10 nt may be interesting for the method's application to the detection of eukaryotic small RNAs, e.g. of RNA 9-mers derived from Ago2 cleavage of siRNA passenger strands. For shorter target RNA interactions, LNA probes with an increased proportion of LNA residues (possibly combined with 2′-OCH_3 instead of DNA residues), or even all-LNA variants, possibly with a single 5′-terminal non-LNA residue carrying the 5′-digoxigenin label, may preserve high detection sensitivity for target RNA oligonucleotides as short as 8-mers (16). 8- to 9-meric LNA probes have indeed been shown to form stable duplexes with their target [(16,17); for review, see (18)]. Thus, even the aforementioned RNA 9-mers derived from Ago2 cleavage of siRNA passenger strands in eukaryotic cells (19) should be detectable with our northern blot protocol, a prediction we are currently testing. Another application may be detection of short abortive transcripts (2–15 nt) synthesized by bacterial and eukaryotic RNA polymerases (20). However, successful application of such very short all-LNA probes in northern blot experiments will depend on how specific signals can be distinguished or separated from non-specific interactions. 5′-digoxigenin LNA probes may also be replaced with 5′-^{32}P-labeled LNA probes, as efficient 5′-end labeling of LNA oligonucleotides by T4 polynucleotide kinase has been reported (21).

As expected, RNA oligonucleotides carrying a 5′-phosphate are efficient substrates for EDC crosslinking to nylon membranes. Nevertheless, RNA variants with a

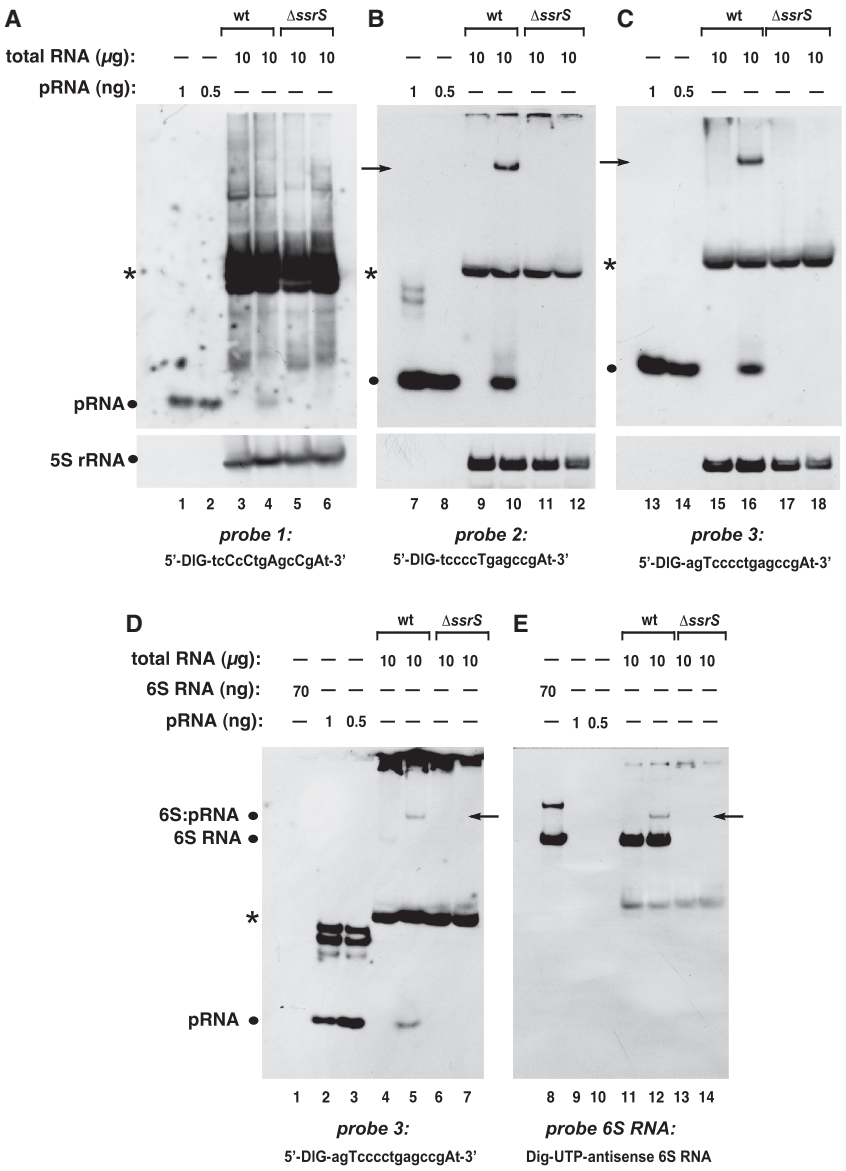

Figure 8. Specificity of different probes for the detection of pRNAs in RNA extracts from *E. coli*. (**A–C**) Detection of pRNAs derived from *E. coli* 6S RNA in total RNA extracts from the wild-type (wt) strain MG1655 (lanes 3, 4, 9, 10, 15 and 16) versus RNA extracts derived from a MG1655 6S RNA knockout (Δ*ssrS*) strain (lanes 5, 6, 11, 12, 17 and 18) using three different probes shown below each panel (uppercase letters indicate LNA and lowercase letters DNA residues). Deviating from our standard procedure ('Materials and Methods' section), RNA samples were heated in denaturing loading buffer for 5 min at 95°C immediately before gel loading. In analogy to *B. subtilis* (Figure 6), RNA harvested from cells in stationary phase (lanes 3, 5, 9, 11, 15 and 17) or during outgrowth (lanes 4, 6, 10, 12, 16 and 18) was analyzed. The chemically synthesized *E. coli* pRNA 14-mer (Figure 1B) was loaded as size control in lanes 1, 2, 7, 8, 13 and 14 (pRNA positions marked by dots at the left margin of each panel). NC filters were stripped after hybridization with pRNA probes and hybridized with a 5S rRNA-specific probe (as loading control) shown at the bottom of each panel. A pRNA signal was seen under outgrowth conditions for wt bacteria (lanes 4, 10 and 16), but not for Δ*ssrS* bacteria (lanes 6, 12, 18). Probe 1 (A) was the least specific and yielded the highest background among the three different probes, which we attribute to the high number of five LNA residues, two of which are in the tetracytidylate stretch that is able to basepair with tetraguanylates. Signals indicated by arrows in lanes 10 and 16 are 6S RNA:pRNA hybrids (see below); asterisks mark a cross-hybridizing RNA of unknown identity. (**D** and **E**) The two panels are halves of the same blot, representing identical sample sets, but hybridized to different probes (probe 3 in D, antisense 6S RNA in E). The signals in lanes 5 and 12, indicated by arrows, are inferred to be 6S RNA:pRNA hybrids, as they migrate at identical position and are detected with both probes. For control, *in vitro* transcribed *E. coli* 6S RNA was loaded (lanes 1 and 8). All samples in D and E were heated for 2 min at 95°C in denaturing loading buffer immediately before gel loading. Deviating from the standard protocol ('Materials and Methods' section), the hybridization temperature was 72°C instead of 50°C for probe 1, and 68°C instead of 50°C for probes 2 and 3.

5′-hydroxyl group can be crosslinked as well, although with substantially reduced efficiency (Figure 5), indicating that internal phosphodiesters are also substrates for EDC crosslinking. Thus, in the case of detection of small RNAs with 5′-OH groups derived from upstream cleavage events, a 5′-phosphorylation step before electrophoresis and membrane transfer should be included to enhance detection sensitivity.

Our results with the chemically synthesized *B. subtilis* pRNA and its mutant derivative (Figure 7) illustrated that intramolecular secondary structures of RNA oligonucleotides appear to have little effect on detection sensitivity. Also, one should take into account that extent and stability of intramolecular structure formation are limited for a 14-mer owing to its limited sequence space. The experiment of Figure 7 provided evidence that the number and positioning of LNA residues in LNA/DNA mixmer probes affects detection sensitivity. The detection of pRNAs in *E. coli* then substantiated this observation, demonstrating that the number and positioning of LNA residues profoundly affects sensitivity as well as specificity (Figure 8). Researchers are advised to restrict the number of LNA residues, for example by incorporating only 2 LNA residues at separate positions into a 14-nt long LNA/DNA mixmer. Formation of oligonucleotide dimers is another issue, but here the routinely conducted heating step before gel loading may mitigate this problem in many cases. Nonetheless, as shown for the chemically synthesized *E. coli* pRNA 14-mer, RNA multimerization can be a problem (Figure 8D, lanes 2 and 3). We solved this problem by adding denaturing instead of native loading buffer to the RNA gel samples and by extending the 95°C heating step to 5 min (Figure 8C, lanes 13 and 14).

Our protocol utilizes non-denaturing electrophoresis conditions. Apparently, denaturing reagents, such as formaldehyde or chaotropic compounds like urea and guanidine hydrochloride, interfere with EDC chemistry involving derivation of amino groups. Since short target RNA oligonucleotides, such as 6S RNA-derived pRNAs, can be released from complexes with complementary RNAs by a heating step, and after release do not form complex intramolecular structures that may lead to aberrant gel migration, the non-denaturing conditions used in our protocol do not entail any significant disadvantage relative to denaturing gel systems. Though we have not observed *B. subtilis* 6S-1 RNA:pRNA hybrids with our native PAGE-based procedure, this was clearly different for the *E. coli* system. Here, a fraction of endogenous 6S RNA:pRNA hybrids survived the hot phenol RNA extraction as well as the heating step (5 min at 95°C) in denaturing loading buffer (Figure 8B and C). This extraordinary stability of *E. coli* 6S RNA:pRNA hybrids, even under denaturing conditions, has also been observed by others (22). Detection of 6S RNA:pRNA complexes with native PAGE also illustrates a potential advantage of native versus denaturing gel systems, i.e. the increased likelihood to identify biologically relevant RNA–RNA interactions under non-denaturing conditions.

FUNDING

Deutsche Forschungsgemeinschaft (HA 1672/16-1, GK 1384). Funding for open access charge: Deutsche Forschungsgemeinschaft (GK 1384).

Conflict of interest statement. None declared.

REFERENCES

1. Válóczi,A., Hornyik,C., Varga,N., Burgyán,J., Kauppinen,S. and Havelda,Z. (2004) Sensitive and specific detection of microRNAs by northern blot analysis using LNA-modified oligonucleotide probes. *Nucleic Acids Res.*, **32**, e175.
2. Várallyay,E., Burgyán,J. and Havelda,Z. (2007) Detection of microRNAs by northern blot analyses using LNA probes. *Methods*, **43**, 140–145.
3. Chen,C., Ridzon,D.A., Broomer,A.J., Zhou,Z., Lee,D.H., Nguyen,J.T., Barbisin,M., Xu,N.L., Mahuvakar,V.R., Andersen,M.R. *et al.* (2005) Real-time quantification of microRNAs by stem-loop RT-PCR. *Nucleic Acids Res.*, **33**, e179.
4. Berezikov,E., Thuemmler,F., van Laake,L.W., Kondova,I., Bontrop,R., Cuppen,E. and Plasterk,R.H.A. (2006) Diversity of microRNAs in human and chimpanzee brain. *Nat. Genet.*, **38**, 1375–1377.
5. Castoldi,M., Schmidt,S., Benes,V., Noerholm,M., Kulozik,A.E., Hentze,M.W. and Muckenthaler,M.U. (2006) A sensitive array for microRNA expression profiling (miChip) based on locked nucleic acids (LNA). *RNA*, **12**, 913–920.
6. Pall,G.S., Codony-Servat,C., Byrne,J., Ritchie,L. and Hamilton,A. (2007) Carbodiimide-mediated cross-linking of RNA to nylon membranes improves the detection of siRNA, miRNA and piRNA by northern blot. *Nucleic Acids Res.*, **35**, e60.
7. Pall,G.S. and Hamilton,A.J. (2008) Improved northern blot methods for enhanced detection of small RNA. *Nat. Protocols*, **3**, 1077–1084.
8. Wassarman,K.M. and Storz,G. (2000) 6S RNA regulates *E. coli* RNA polymerase activity. *Cell*, **101**, 613–623.
9. Wassarman,K.M. and Saecker,R.M. (2006) Synthesis-mediated release of a small RNA inhibitor of RNA polymerase. *Science*, **314**, 1601–1603.
10. Gildehaus,N., Neußer,T., Wurm,R. and Wagner,R. (2007) Studies on the function of the riboregulator 6S RNA from *E. coli:* RNA polymerase binding, inhibition of *in vitro* transcription and synthesis of RNA-directed *de novo* transcripts. *Nucleic Acids Res.*, **35**, 1885–1896.
11. Barrick,J.E., Sudarsan,N., Weinberg,Z., Ruzzo,W.L. and Breaker,R.R. (2005) 6S RNA is a widespread regulator of eubacterial RNA polymerase that resembles an open promoter. *RNA*, **11**, 774–784.
12. Willkomm,D.K. and Hartmann,R.K. (2005) 6S RNA – an ancient regulator of bacterial RNA polymerase rediscovered. *Biol. Chem.*, **386**, 1273–1277.
13. Trotochaud,A.E. and Wassarman,K.M. (2005) A highly conserved 6S RNA structure is required for regulation of transcription. *Nat. Struct. Mol. Biol.*, **12**, 313–319.
14. Mattatal,N.R. and Sanderson,K.E. (1996) *Salmonella typhimurium* LT2 possesses three distinct 23S rRNA intervening sequences. *J. Bacteriol.*, **178**, 2272–2278.
15. Ghosh,S.S. and Musso,G.F. (1987) Covalent attachment of oligonucleotides to solid supports. *Nucleic Acids Res.*, **15**, 5353–5372.
16. Elayadi,A.N., Braasch,D.A. and Corey,D.R. (2002) Implications of high-affinity hybridization by locked nucleic acid oligomers for inhibition of human telomerase. *Biochemistry*, **41**, 9973–9981.
17. Mouritzen,P., Noerholm,M., Nielsen,P.S., Jacobsen,N., Lomholt,C., Pfundheller,H.M. and Tolstrup,N. (2005) ProbeLibrary: a new method for faster design and execution of quantitative real-time PCR. *Nat. Methods*, **2**, 313–316.
18. Grünweller,A. and Hartmann,R.K. (2007) Locked nucleic acid oligonucleotides: the next generation of antisense agents? *BioDrugs*, **21**, 235–243.

19. Matranga,C., Tomari,Y., Shin,C., Bartel,D.P. and Zamore,P.D. (2005) Passenger-strand cleavage facilitates assembly of siRNA into Ago2-containing RNAi enzyme complexes. *Cell*, **123**, 607–620.
20. Goldman,S.R., Ebright,R.H. and Nickels,B.E. (2009) Direct detection of abortive RNA transcripts *in vivo*. *Science*, **324**, 927–928.
21. Wengel,J. and Nielsen,P. (2002) Oligonucleotide analogues, Patent US 2002/0068708 A1.
22. Wurm,R., Neusser,T. and Wagner,R. (2010) 6S RNA-dependent inhibition of RNA polymerase is released by RNA-dependent synthesis of small *de novo* products. *Biol. Chem.*, **391**, 187–196.

C

PUBLICATION II

Northern blot detection of small RNAs.

Handbook of RNA Biochemistry 2nd Edition, *accepted*

Author contributions:
Manuscript writing: 75%

1
Northern Blot Detection of Small RNAs

Benedikt M. Beckmann, Arnold Grünweller & Roland K. Hartmann

1.1
Introduction

During the last years, new classes of small RNAs (sRNA) have been discovered [1, 2], also owing to advances in high-throughput sequencing. Characterization of these short RNA species often requires modifications of established methods, primarily RT-PCR and Northern hybridization, to ensure sensitive and specific detection and quantification. Although quantification of sRNAs can be achieved by qRT-PCR (such as the stem-loop primer technique developed for miRNAs [3]), the Northern blot has remained indispensable, since it permits to visualize and roughly quantify cellular levels of RNAs and their processing intermediates relative to endogenous RNA standards, such as 5S rRNA. Analysis of sRNAs < 30 nt (e.g. miRNAs) using Northern hybridization is challenging due to their limited interaction surface which increases the sensitivity to steric impediments caused by immobilization on hybridization membranes. Different adaptations to overcome these limitations have been described for mature miRNAs [4, 5], ~ 22 nt in length, but were insufficient for the detection of even smaller cellular RNAs in our hands. We have developed an approach combining 1-ethyl-3-(3-dimethylaminopropyl)-carbodiimide (EDC) crosslinking with non-radioactive 5'-digoxygenin (DIG)-endlabeled mixmer probes and native polyacrylamide gels to detect RNAs as short as ~ 14 nt with high sensitivity and specificity [6]. Apart from such very short cellular RNAs, the described Northern blot procedure can be easily adapted to larger sRNAs mainly by using an *in vitro* transcribed RNA probe internally labeled with DIG-11-UTP.

1.1.1
Isolation of RNA

Purified cellular RNA of highest quality is usually the starting point of a Northern hybridization. Different purification methods and protocols have been described and

several commercial kits are available for different purposes and cell types.

Kits Using a kit is a convenient way to obtain RNA extracts from cells. RNA preparation by this route is usually fast. Another advantage are quality-controlled enclosed buffers and solutions. A feature of kit-based procedures can be the exclusion of RNAs falling below or exceeding certain length limits, especially if spin columns are used for nucleic acid purification. As a potential drawback, RNA extracted from kits designed for a special purpose (e.g. extraction of small RNAs) do not fully represent the biological RNA distribution [7]. For this reason, we prefer total RNA extracts even for Northern hybridization of short RNAs.

Do it yourself We routinely use two robust methods to extract total RNA from bacterial cells as well as from eukaryotic cell lines:

- single step method (Trizol)
- hot phenol method

The "single step method" provides in general high quality RNA due to the chaotropic reagent guanidinium isothiocyanate that inactivates cellular nucleases and therefore protects the RNA during the purification process [8, 9].
In our hands, the "hot phenol method" [10] usually results in higher amounts of purified RNA compared to the single step method. It should however be taken into consideration that due to the 65°C heating step, RNA duplexes will be (partially) denatured. Therefore, the hot phenol method is not recommended if the native fold of RNA(s) of interest or intermolecular RNA-RNA interactions are at risk to be irreversibly disrupted at 65°C.

Quality control An important step after purification is the quality control of the cellular RNA. This is usually achieved by analyzing a small amount of RNA on a denaturing gel and subsequent ethidium bromide staining. The abundance of the the two major cellular RNA species (16 – 18S and 23 – 28S ribosomal RNA) is then used as a marker for the overall integrity of the purified RNA. For details, see the troubleshooting section.

1.1.2 Native versus denaturing gels

Electrophoretic separation of RNAs is usually achieved by denaturing gels. For long RNAs (> 200 nt), agarose gels containing glyoxal or formaldehyde [11] may be used. For shorter RNAs, polyacrylamide (PAA) gels containing up to 8 M urea are commonly utilized. As our focus is on short RNAs, only PAA gels will be discussed.
Native PAA gels provide the possibility to detect intermolecular RNA-RNA interactions, to identify conformational differences between RNA molecules of identical length, and to evaluate the conformational homogeneity of single RNA species. We have reported evidence that native compared to denaturing gels increase the detection sensitivity for RNAs shorter than 20 nt in protocols involving EDC crosslinking

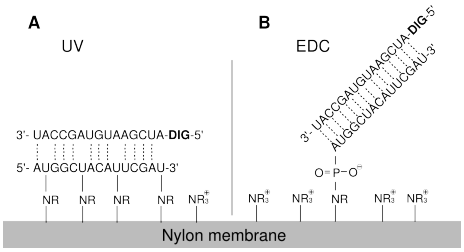

Figure 1.1 Schematic presentation of differences between UV- and EDC crosslinking procedures. (A) Treatment of RNA with UV light leads to covalent attachment of bases to amine groups of the nylon membrane. Probe hybridization to these and likely also neighboring bases is then precluded. (B) EDC crosslinking occurs primarily via 5'-phosphate groups, thus leaving the nucleobases unaffected and consequently accessible to pairing with the probe.

[6]. Apparently, urea interferes with EDC chemistry at the membrane surface, resulting in less efficient RNA immobilization and thus weaker Northern blot signals [6]. Nonetheless, at least for miRNAs, robust Northern blot protocols involving denaturing (8 M urea) PAA gels have been developed [12].

1.1.3
Transfer of RNA and fixation to membranes

To transfer short RNAs from PAA gels to nylon membranes, we use semi-dry blotting in 0.5 x TBE as transfer buffer for at least 6 h.
For subsequent RNA fixation on the membrane, several methods are in use, the most common techniques being UV crosslinking or baking of the membrane at 80 - 120°C. These methods, however, entail the disadvantage that the nitrogenous bases, e.g. uracil, form covalent bonds to free amine groups of the membrane surface [4, 5]. These bases are then no longer available for Watson-Crick base pairing to the complementary probe (Fig. 1.1), leading to a decrease of signal strength. To circumvent this problem, which deteriorates for short RNAs, chemical crosslinking with EDC can be applied [4, 5]. Here, primarily the 5'-phosphate group of RNA is covalently linked to a membrane amine group, leaving the bases accessible to base pairing with the probe. Chemical EDC crosslinking is thus most efficient for 5'-phosphorylated RNA, but also works, with reduced efficiency, for RNAs carrying a 5'-OH end, apparently through reaction of internal phosphodiesters [6].

1.1.4
Hybridization with a complementary probe

For hybridization to RNA, RNA or DNA probes can be used. For routine Northern hybridization, we use RNA probes generated by T7 run-off transcription from PCR fragments or linearized plasmid DNAs. These RNA probes can either be radiolabeled post-transcriptionally (5'-endlabeling with γ^{32}P-ATP) or during transcription by incorporation of modified nucleotides such as α^{32}P-NTPs or DIG-11-UTP.
An effective strategy to improve binding of Northern probes to short RNAs is incorporation of LNA residues into DNA oligonucleotides [13, 14]. Such DNA/LNA mixmers increase duplex stability and thus permit to apply elevated hybridization temperatures [15, 16], such as 72°C. We have used 5'-DIG endlabeled DNA/LNA mixmer probes (custom-synthesized by Exiqon[1)]) in combination with EDC crosslinking of short RNAs (< 20 nt) to nylon membranes. This approach, but using denaturing PAGE, has also been applied to the detection of mature (~ 22 nt) miRNAs [12].

Design of DNA/LNA mixmer probes Design of DNA/LNA mixmers as probes can be challenging, especially for short oligonucleotides. One of the main features of LNA is the fixation of the ribose moiety in its C3'-*endo* conformation leading to a significant increase in melting temperature [15, 16]. A single LNA residue stabilizes not only base pairing with the complementary RNA nucleotide, but also that of immediate DNA neighbors with their complementary RNA bases. Thus, DNA/LNA mixmers confer substantial duplex stabilization, making the use of all-LNA probes unnecessary. In addition, for all-LNA probes, the risk of self-complementarity and dimerization increases. We apply several rules for our design of probes which are usually 12 – 16 nt in length (see also Fig. 1.2):

- Run `mfold`[2)] [17] and/or `RNAfold`[3)] [18] with your probe sequence to check for secondary structures. Nucleotides predicted to form internal duplexes should not be considered for LNA positioning.
- To check for potential dimerization, run `mfold` or `RNAfold` with a tandem repeat of your sequence, the two identical sequence stretches connected by a 'NNNNN' linker; alternatively, use `RNAcofold`[4)] [19] (paste identical sequence in 1 st and 2 nd window). Avoid LNA modifications in regions predicted to be base-paired.
- Use 2 to 5 LNA modifications for a 9 – 16 nt probe.
- Do not position LNA residues within homo-G or -C stretches (e.g. 5'-NNN GGG GNN NNN-3'; Fig. 1.2 C), as this will increase nonspecific binding and will compromise sensitivtiy (see Fig. 1.3).
- Use `BLAST`[5)] to screen for probe complementarity to other regions of the genome.

1) http://www.exiqon.com
2) http://mfold.bioinfo.rpi.edu/cgi-bin/rna-form1.cgi
3) http://rna.tbi.univie.ac.at/cgi-bin/RNAfold.cgi
4) http://rna.tbi.univie.ac.at/cgi-bin/RNAcofold.cgi
5) http://blast.ncbi.nlm.nih.gov/Blast.cgi

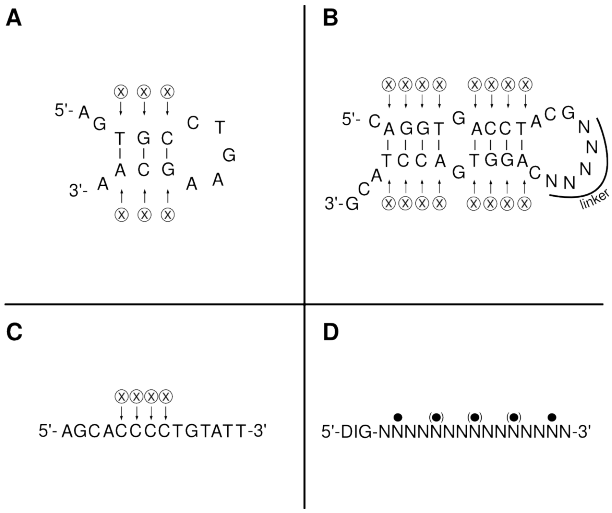

Figure 1.2 Rules for LNA/DNA mixmer design of short (< 20 nt) probes. Use a folding program to detect either (A) self-complementarity or (B) dimerization potential. Avoid LNA residues in such paired regions. (C) LNA modifications in C- or G-stretches increase the danger of interactions with such motifs in other RNAs, e.g. ribosomal RNAs; ⊗ omit LNA modification. (D) General scheme of placing LNA modifications; • place LNA modification, (•) optional LNA modification.

Keep in mind, however, that only expressed RNAs may cause nonspecific signals. If you find hits in annotated genes, place LNAs in positions that lack complementarity to this potentially cross-hybridizing cellular RNA.

- If the probe's length is too short (< 18 nt) for `BLAST`, try other bioinformatic tools such as `RNAbob`[6] or `fragrep` [20].
- If possible, place LNA modifications at the second and the penultimate position of the probe to increase stability (Fig. 1.2 D).
- Keep in mind that LNA favors the C3'-*endo* conformation of its two neighboring DNA residues. Therefore, one LNA modification should be followed by two unmodified DNA nucleotides.
- A useful tool for LNA/DNA mixmer design can also been found at Exiqon's homepage.

6) rnabob (http://selab.janelia.org/software.html) as well as fragrep (http://www.bierinformatik.de/Software/fragrep/) are not available as web based services but have to be installed locally and run as console programs

1.1.5 Detection of DIG-labeled probes

Visualization of DIG-labeled probes is achieved by immunological detection using an antibody (Anti-Digoxigenin-AP Fab Fragments) specific for the DIG-modified nucleotides. The antibody is coupled to an alkaline phosphatase which dephosphorylates a dioxetane phenyl phosphate (CDP-Star). The resulting chemoluminiscent signal is then detected by exposing an X-ray film to the membrane. As DIG technology is owned by Roche [7)], we obtained all reagents and antibodies from this source.

1.1.6 Troubleshooting

Several problems may arise during this multi-step procedure. Consider the following hints:

- Quality of RNA: When total RNA has been prepared, check its integrity before conducting a Northern blot. Prepare a denaturing 1% agarose gel [11] or a denaturing 5% polyacrylamide gel and load 2 – 3 µg total RNA using a denaturing loading buffer (see below). Run the gel until the bromophenol blue is close to the bottom and stain with ethidium bromide. If the RNA is intact, 28S and 18S rRNA species in mammals (23S and 16S rRNA in bacteria, respectively) should constitute the main bands, with the larger rRNA yielding roughly twice the staining intensity of the smaller rRNA. Both bands should be discrete; smearing indicates degradation of the RNA.
- Loading control: Loading the same amounts of total cellular RNA is not sufficient to ensure comparability between different samples. One possibility is to stain the gel with ethidium bromide prior to blotting and check for equal amounts of ribosomal or tRNA species. A commonly used strategy is additional detection of a housekeeping RNA such as 5S rRNA. After detection of the RNA of interest, the membrane is stripped from its first probe (see below) and 5S rRNA levels are determined and compared with a 5S rRNA-specific probe.
- Background signals: there are many reasons for this problem; they also differ depending on membrane material, probe, etc. The reader is referred to [11], section 7.45, for a first troubleshooting. When using EDC crosslinking and/or DIG-labeled probes for short RNA detection, additional problems might arise:
  - Longer exposure of X-ray films to the AP Fab Fragments/CDP-Star solution leads to high background: since the CDP-Star solution is highly concentrated, dilute it 1:20 in detection buffer and increase exposure time by a factor of 2 – 3 [21].
  - Signal speckles may appear all over the membrane, likely caused by aggregation of DIG/LNA probes. Increase hybridization temperature up to 72°C or design a probe with fewer LNA modifications.

7) http://www.roche-applied-science.com

- Shadow-like background signals: centrifuge the Anti-Digoxygenin antibody before usage (5 min, 11,000 x g).
- Weak signal: adjust hybridization temperature. Do not forget to heat the probe to 95°C for 3 min directly before hybridization.
- RNA aggregation: due to the lack of denaturing reagents in the gel, RNA may form multimers. Since low amounts of urea do not substantially disturb EDC crosslinking, the usage of a denaturing gel loading buffer in combination with heating the samples for up to 5 min at 95°C was shown to resolve such multimers [6].

1.1.7 Application example

We applied the described method to detect short RNA species in bacterial cells. In *E. coli*, RNA polymerase synthesizes so-called pRNAs, ~ 10 – 20 nt in length, using the abundant riboregulator 6S RNA as template [22]. Synthesis of pRNAs peaks during outgrowth from stationary phase (see Fig. 1.3).

1.1.8 Limitations of the method

We further explored the performance of our method with respect to the detection of RNAs even shorter than 14 nt. In an example experiment, we spotted an RNA 14-mer, fully complmentary to the 14-meric DNA/LNA probe, and an RNA 8-mer, complementary to the distal 8 nucleotides of the DNA/LNA probe, on a nylon membrane (Fig. 1.4 A). Detection sensitivity was largely decreased for the RNA 8-mer compared to the "full length" 14-mer. However, the sensitivity of detection could be partially restored using an isosequential all-LNA 8-mer.
We then tested different temperatures and buffer conditions in order to improve detection of the RNA 8-mer. While lowering the hybridization temperature from 50 to 25°C tended to slightly improve the lower detection limit, reductions in the concentration of the chaotropic urea did not improve detection sensitivity (Fig. 1.4 B). While the Roche buffer tends to minimize background signals, we see a slightly increased detection sensitivity for our simple phosphate buffer containing 4 M urea [23] in the case of 8-mer detection at both temperatures.
Based on these observations, we advice researchers trying to detect RNAs of such short length (< 14 nt) to decrease the hybridization temperature to 25°C, to use a hybridization buffer containing 4 M urea, and, optionally, to include an LNA-based size marker as reference. However, be aware that such small all-LNA probes tend to have a slower migration velocity in native PAA gels (own observation).

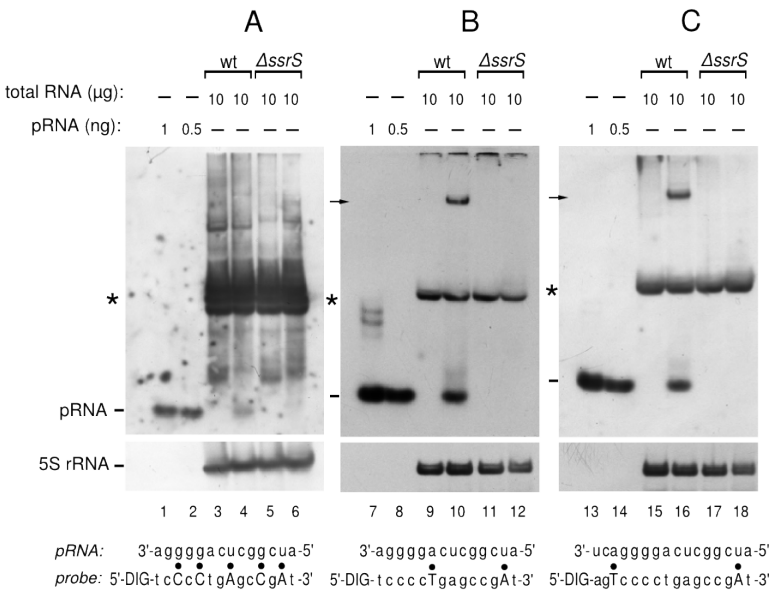

Figure 1.3 Specificity of different probes for the detection of pRNAs in RNA extracts from *E. coli*. (A to C) Detection of pRNAs derived from *E. coli* 6S RNA in total RNA extracts from the wild-type (wt) strain MG1655 (lanes 3, 4, 9, 10, 15 and 16) versus RNA extracts derived from a MG1655 6S RNA knockout (Δ*ssrS*) strain (lanes 5, 6, 11, 12, 17 and 18) using three different probes shown below each panel; upper-case letters indicate LNA and lower-case letters DNA residues, with filled circles indicating to which *E. coli* pRNA residues the LNA residues base pair; the sequence of a chemically synthesized pRNA 14-mer is shown above the probes; in panel C, a 16-mer probe was used to extend base pairing to longer endogenous pRNA by two nucleotides; these two nucleotides (lower size letters) are not present in the chemically synthesized pRNA 14-mer (5'-AUC GGC UCA GGG GA-3'). Deviating from the standard procedure, RNA samples were heated in denaturing loading buffer for 5 min at 95°C immediately before gel loading. Total RNA was extracted from cells in stationary phase (lanes 3, 5, 9, 11, 15 and 17) or during outgrowth (lanes 4, 6, 10, 12, 16 and 18) by the hot phenol method; for definition of stationary phase and outgrowth see [6]. The chemically synthesized *E. coli* pRNA 14-mer was loaded as size control in lanes 1, 2, 7, 8, 13 and 14 (pRNA positions marked by dashes at the left margin of each panel). Membranes were stripped after hybridization with pRNA probes and hybridized with a 5S rRNA-specific probe (as loading control) shown at the bottom of each panel. A pRNA signal was seen under outgrowth conditions for wt bacteria (lanes 4, 10 and 16), but not for Δ*ssrS* bacteria (lanes 6, 12, 18). Probe 1 (panel A) was the least specific and yielded the highest background among the three different probes, which we attribute to the high number of 5 LNA residues, two of which are in the tetracytidylate stretch where they favor base pairing with tetraguanylates in other RNAs. Signals indicated by arrows in lanes 10 and 16 are 6S RNA-pRNA hybrids [6]; asterisks mark a cross-hybridizing RNA of unknown identity. Generally, the hybridization temperature was 72°C instead of 50°C in panel A, and 68°C instead of 50°C in panels B and C. Adapted from [6].

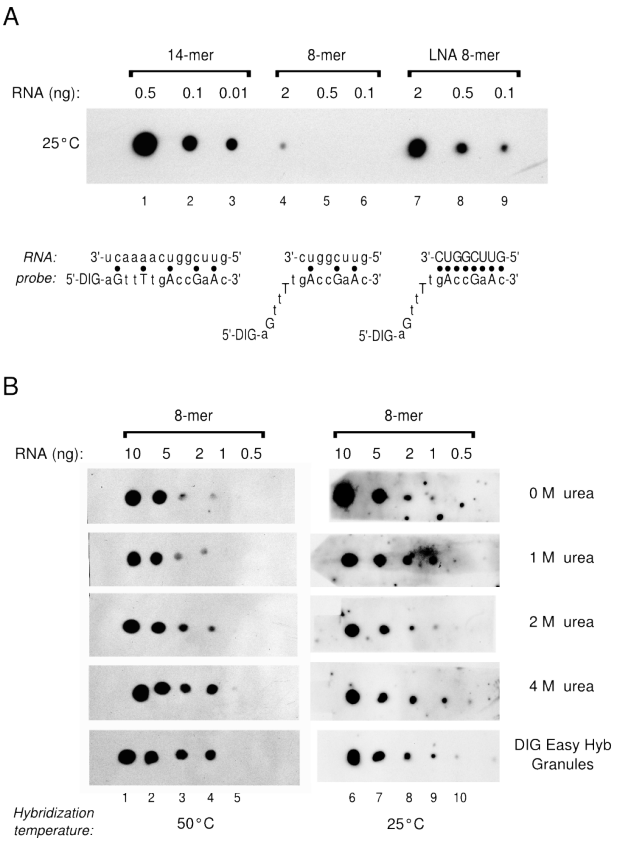

Figure 1.4 Detection sensitivity limitations. (**A**) Dot blot of chemically synthesized 5'-phosphorylated RNA 14- or 8-mers spotted directly onto the nylon membrane before EDC crosslinking; RNA and probe sequences are given at the bottom: the LNA 8-mer carried LNA instead of RNA residues indicated by upper-case letters; for the probes, upper-case letters indicate LNA and lower-case letters DNA residues; filled circles between target RNA (or LNA) and probe indicate base pairs involving stabilizing LNA residues. Detection sensitivity of the RNA 8-mer was estimated to be $\geq$ 40-fold reduced compared to the 14-mer (cf. lanes 1 to 3 versus 4 to 6). The LNA 8-mer improved detection sensitivity relative to the isosequential RNA 8-mer; however, sensitivity for the LNA 8-mer was still ~20-fold lower than for the RNA 14-mer (cf. lane 9 versus 3). (**B**) Influence of hybridization temperature and buffer on detection sensitivity. "DIG Easy Hyb Granules" (bottom panels) describes the hybridization buffer provided by Roche, for which the composition is undisclosed, but said to correspond to 50% formamide in terms of nucleic acid denaturation efficacy. The other buffers contained 50 mM Na_2HPO_4/NaH_2PO_4 pH 7.0, 0.02% (w/v) SDS, and indicated concentrations of urea. At the lower hybridization temperature of 25°C, background speckles increased relative to 50°C, particularly at 1 and 0 M urea (cf. lanes 1 to 5 versus 6 to 10). Reduction of the urea concentration below 4 M tended to impair detection sensitivity. Sensitivity appeared best for the simple phosphate-based buffer containing 4 M urea combined with a hybridization temperature of 25°C.

1.2
Northern hybridization protocols

Protocol: RNA extraction from cells using hot phenol

- Extraction buffer: 10 mM NaOAc, 150 mM sucrose, adjust to pH 4.8 with acetic acid; pass solution through a sterile filter.
- Acid phenol: Use 1 x TBE-saturated phenol and discard upper aqueous phase. Add 1/10 volume of 300 mM NaOAc pH 4.9, vortex, centrifuge for 10 min at 3,000 x g, and discard upper aqueous phase. Repeat three times.

1) Resuspend 100 mg tissue or cell pellet (e.g. 50 ml *E. coli* cells at OD_{600} 1.0 or up to 10^6 HeLa cells) in 3 ml of pre-cooled (4°C) extraction buffer by vigorous vortexing.
2) (optional) If Gram-positive bacteria are used, add 100 µl lysozyme (20 mg/ml in 1 x TBE) and incubate at room temperature (RT) for 10 min.
3) Add 333 µl 10% SDS to a final concentration of 1% SDS.
4) Add 3 ml of pre-heated (65°C) acid phenol, vortex.
5) Incubate at 65°C for 5 min.
6) Incubate on ice for 5 min.
7) Centrifuge for 20 min at 11,000 x g and keep upper aqueous phase.
8) Perform phenol and chloroform extractions: add 1 volume of acid phenol, vortex and centrifuge for 5 min at 11,000 x g; keep upper aqueous phase and repeat with 1 volume of chloroform.
9) Precipitate RNA by adding 0.1 volume of 3 M NaOAc pH 4.9 and 2.5 volumes of ethanol. Cool solution at -20°C for 20 min and centrifuge for 30 min at 11,000 x g and 4°C, discard supernatant.
10) (optional) Wash pellet with 70% ethanol, centrifuge for 10 min at 11,000 x g and 4°C, discard supernatant.
11) Air-dry the pellet for 5 min before redissolving the RNA in 20 µl of RNase-free double-distilled H_2O (ddH_2O) or 1 x TBE.

Protocol: RNA extraction by the "single step method"

- Denaturation solution: 4 M guanidinium isothiocyanate, 25 mM sodium citrate, 0.5% (w/v) N-lauroylsarcosyl, 0.1 M β-mercaptoethanol, pH 7.0.
- Acid phenol: Use 1 x TBE-saturated phenol and discard upper aqueous phase. Add 1/10 volume of 300 mM NaOAc pH 4.9, vortex, centrifuge for 10 min at 3,000 x g, and discard upper aqueous phase. Repeat three times.

1) Resuspend 100 mg tissue or cell pellet (e.g. 50 ml *E. coli* cells at OD_{600} 1.0 or up to 10^6 HeLa cells) in 1 ml denaturation solution, vortex.
2) (optional) If Gram-positive bacteria are used, add 100 µl lysozyme (20 mg/ml in 1 x TBE) and incubate at RT for 10 min.
3) Add 100 µl 2 M NaOAc pH 4.0, vortex.
4) Add 1 ml acid phenol and 200 µl chloroform, vortex.

5) Incubate on ice for 15 min.
6) Centrifuge for 20 min at 11,000 x g and keep upper aqueous phase.
7) Precipitate by adding 1 volume isopropanol, incubate at -20°C for 20 min, centrifuge for 30 min at 11,000 x g and 4°C and discard supernatant.
8) Dissolve pellet in 300 µl denaturation solution.
9) Precipitate again with isopropanol.
10) Wash pellet with 70% ethanol, centrifuge for 10 min at 11,000 x g and 4°C, discard supernatant.
11) Redissolve RNA in 20 µl RNase-free ddH_2O or 1 x TBE.

Protocol: Northern hybridization of small RNA

PAGE and transfer of RNA

- 5 x TBE: 445 mM Tris, 445 mM borate, 10 mM EDTA.
- Native polyacrylamide gel: 1 x TBE, acrylamide/bisacrylamide (24:1), 10% APS (ammonium persulfate), TEMED (N,N,N',N'-tetramethylethylenediamine).
- Denaturing polyacrylamide gel: 1 x TBE, 8 M urea, acrylamide/bisacrylamide (24:1), 10% APS (ammonium persulfate), TEMED.
- 6 x native loading buffer: 0.25% (w/v) bromophenol blue, 0.25% (w/v) xylene cyanol blue, 30% (v/v) glycerol.
- 2 x denaturing loading buffer: 0.02% (w/v) bromophenol blue, 0.02% (w/v) xylene cyanol blue, 2.6 M urea, 66% (v/v) formamide, 2 x TBE.
- Whatman paper (> 1 mm thickness).
- Nylon membranes, positively charged (Roche, No. 11209299001); microporous nylon 66 membrane on a polyester support, carrying positively quaternary ammonium groups; surface properties: 0.45-µm pore size.
- Semi-dry blotter (C.B.S. Scientific Co., model EBU-4000).

1) Redissolve 10 µg of ethanol-precipitated total RNA in 1 volume of 2 x denaturing loading buffer or 0.2 volumes of native loading buffer, respectively.
2) Incubate mixture at 95°C for 3 min and put on ice immediately.
3) Load gel pockets and run the gel using 1 x TBE as buffer (15 mA for a 15 x 20 cm sized gel with 1 mm thickness).
4) After the run, wash gel in 0.5 x TBE for 5 min at RT.
5) Transfer RNA to a positively charged nylon membrane using a semi-dry blotting apparatus (see Fig. 1.5): Place 1 piece of Whatman paper (gel size) soaked with 0.5 x TBE on the anode plate. Layer on top in the following order: membrane (soaked with 0.5 x TBE, gel size), the gel to be transferred, and a piece of Whatman paper (soaked with 0.5 x TBE, gel size). Put the cathode plate on top and run transfer overnight at 0.27 mA/cm^2. Take care to avoid any air bubbles between membrane and gel.

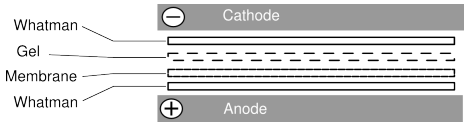

Figure 1.5 Northern blot assembly

Fixation of small RNAs by EDC crosslinking

- EDC solution: 130 mM 1-methylimidazole, 160 mM 1-ethyl-3-(3-dimethylaminopropyl) carbodiimide, pH 8.0

1) Soak a Whatman paper with EDC solution and place the membrane on it (membrane side with blotted RNA should not get in direct contact with the EDC solution to avoid detachment of RNA).
2) Wrap in kitchen wrapping film and incubate for 2 h at 60°C.
3) Wash membrane carefully with ddH_2O, wrap in kitchen wrapping film and store at 4°C until use.

Probe generation by T7 transcription

- 5 x T7 transcription buffer: 200 mM Tris-HCl , 30 mM $MgCl_2$, 50 mM DTT, 50 mM NaCl, 10 mM spermidine, pH 7.9.
- 10 x DIG labeling mix (Roche).
- T7 polymerase, e.g. purchased from Fermentas[8)].

1) Mix T7 transcription reaction and incubate for 2 h at 37°C.

Table 1.1 T7 transcription reaction

PCR template (200 ng/µl)	5 µl
5 x T7 transcription buffer	4 µl
10 x DIG labeling mix	2 µl
T7 polymerase (10 U/µl)	2 µl
ddH_2O	7 µl

2) Stop transcription reaction by adding 2 µl 10 mM EDTA and store at -20°C.

Hybridization Hybridization temperature depends on the probe's properties (length, G/C content, LNA-modification, etc.) and on the hybridization solution. With the hybridization buffers described here, we usually perform the first hybridization experiment at 68°C in the case of probes transcribed by T7 RNA polymerase in the presence of DIG-11-UTP (see above), or at 50°C in the case of 12 to 16-nt LNA/DNA mixmer probes. The example protocol is given for 50°C.

- Hybridization solution: DIG Easy Hyb Granules (Roche) or
- 50 mM Na_2HPO_4/NaH_2PO_4 pH 7.0, 0.02% (w/v) SDS, 4 M urea

1) Pre-heat 7 ml of hybridization solution to 50°C.
2) Place the membrane in a hybridization tube (or a 50 ml Falcon tube for small membranes). Make sure that the "RNA side" does not touch the glass wall but is directed inward.

8) http://www.fermentas.com

3) Add hybridization solution and perform pre-hybridization at 50°C for 2 h with slow rotation in a hybridization oven.
4) Denature the probe (10 µl T7 transcript or 300 pmol DIG-LNA/DNA mixmer) for 3 min at 95°C, put on ice immediately.
5) Add the probe to 7 ml pre-heated (50°C) hybridization solution, discard the pre-hybridization solution and add solution containing the probe to the membrane.
6) Perform hybridization overnight (or at least for 6 h) at 50°C with slow rotation in a hybridization oven.

Detection of DIG-labeled probes

- 20 x SSC: 3 M NaCl, 0.3 M Na-citrate, pH 7.0.
- Stringent wash buffer 1: 2 x SSC, 0.1% (w/v) SDS.
- Stringent wash buffer 2: 0.1 x SSC, 0.1% (w/v) SDS.
- Maleic acid buffer: 0.1 M maleic acid, 0.15 M NaCl, pH 7.5.
- Blocking solution: 10 x Blocking solution (Roche) diluted 1:10 in maleic acid buffer.
- Antibody solution: Blocking solution with 1:10,000 diluted Anti-Digoxygenin-AP Fab Fragments (Roche).
- Wash buffer: 0.1 M maleic acid, 0.15 M NaCl, 0.3% (v/v) Tween 20, pH 7.5.
- Detection buffer: 0.1 M Tris-HCl, 0.1 M NaCl, pH 9.5.
- CDP-Star (Roche).
- Autoradiography film: Kodak BioMax Light Film.

For detection, all steps should be carried out using clean glass/plastic ware. Take care that membranes are covered with buffer and that shaking takes place at low speed.

1) Wash membrane twice in stringent wash buffer 1 for 5 min at RT.
2) Wash membrane twice in stringent wash buffer 2 for 15 min at RT.
3) Wash membrane for 2 min in ddH_2O.
4) Incubate in blocking solution for 30 min at RT.
5) Incubate in antibody solution for 30 min at RT.
6) Wash twice in wash buffer for 15 min at RT.
7) Incubate in detection buffer for 5 min at RT.
8) Place membrane on a kitchen wrapping film, add some drops of CDP-Star until the membrane is covered with the solution, wrap it up completely in the kitchen wrapping film and incubate for 10 min at RT to allow development of a robust chemical signal. Avoid any air bubbles.
9) Place an autoradiography film of identical size on the gel and expose it for 5 min to 1 h.
10) Develop the film according to the manufacturer's instructions.
11) Take care that the membrane does not run dry after detection if subsequent stripping is intended!

Stripping of membranes

- Stripping buffer: 50% formamide, 50 mM Tris-HCl pH 7.5, 5% (w/v) SDS, always freshly prepared.
- 2 x SSC: 300 mM NaCl, 30 mM Na citrate pH 7.0.

1) Wash membrane with ddH_2O.
2) Incubate twice in stripping buffer for 60 min at 80°C while shaking gently.
3) Wash twice in 2 x SSC for 5 min at RT.
4) Start with pre-hybridization and prepare for hybridization with new probe (see above).

References

1 Waters, L.S. and Storz, G. (2009) Regulatory RNAs in bacteria. *Cell*, **136**, 615–628.

2 Ghildiyal, M. and Zamore, P.D. (2009) Small silencing RNAs: an expanding universe. *Nat Rev Genet*, **10**, 94–108.

3 Chen, C., Ridzon, D.A., Broomer, A.J., Zhou, Z., Lee, D.H., Nguyen, J.T., Barbisin, M., Xu, N.L., Mahuvakar, V.R., Andersen, M.R., Lao, K.Q., Livak, K.J., and Guegler, K.J. (2005) Real-time quantification of microRNAs by stem-loop RT-PCR. *Nucleic Acids Res*, **33**, e179.

4 Pall, G.S., Codony-Servat, C., Byrne, J., Ritchie, L., and Hamilton, A. (2007) Carbodiimide-mediated cross-linking of RNA to nylon membranes improves the detection of siRNA, miRNA and piRNA by northern blot. *Nucleic Acids Res*, **35**, e60.

5 Pall, G.S. and Hamilton, A.J. (2008) Improved northern blot method for enhanced detection of small RNA. *Nat Protoc*, **3**, 1077–1084.

6 Beckmann, B.M., Grünweller, A., Weber, M.H., and Hartmann, R.K. (2010) Northern blot detection of endogenous small RNAs (approximately 14 nt) in bacterial total RNA extracts. *Nucleic Acids Res*, **38**, e147.

7 Mraz, M., Malinova, K., Mayer, J., and Pospisilova, S. (2009) MicroRNA isolation and stability in stored RNA samples. *Biochem Biophys Res Commun*, **390**, 1–4.

8 Chomczynski, P. and Sacchi, N. (1987) Single-step method of RNA isolation by acid guanidinium thiocyanate-phenol-chloroform extraction. *Anal Biochem*, **162**, 156–159.

9 Chomczynski, P. and Sacchi, N. (2006) The single-step method of RNA isolation by acid guanidinium thiocyanate-phenol-chloroform extraction: twenty-something years on. *Nat Protoc*, **1**, 581–585.

10 Mattatall, N.R. and Sanderson, K.E. (1996) *Salmonella typhimurium* LT2 possesses three distinct 23S rRNA intervening sequences. *J Bacteriol*, **178**, 2272–2278.

11 Sambrook, J. and Russel, D.W. (2001) *Molecular Cloning*, Cold Spring Harbor Laboratory Press. 3rd edn., Chapter 7.

12 Kim, S.W., Li, Z., Moore, P.S., Monaghan, A.P., Chang, Y., Nichols, M., and John, B. (2010) A sensitive non-radioactive northern blot method to detect small RNAs. *Nucleic Acids Res*, **38**, e98.

13 Várallyay, E., Burgyán, J., and Havelda, Z. (2008) MicroRNA detection by northern blotting using locked nucleic acid probes. *Nat Protoc*, **3**, 190–196.

14 Válóczi, A., Hornyik, C., Varga, N., Burgyán, J., Kauppinen, S., and Havelda, Z. (2004) Sensitive and specific detection of microRNAs by northern blot analysis using LNA-modified oligonucleotide probes. *Nucleic Acids Res*, **32**, e157.

15 Vester, B. and Wengel, J. (2004) LNA (locked nucleic acid): high-affinity targeting of complementary RNA and DNA. *Biochemistry*, **43**, 13 233–13 241.

16 Grünweller, A. and Hartmann, R.K. (2007) Locked nucleic acid oligonucleotides: the next generation of antisense agents?

BioDrugs, **21**, 235–243.

17 Zuker, M. (2003) Mfold web server for nucleic acid folding and hybridization prediction. *Nucleic Acids Res*, **31**, 3406–3415.

18 Hofacker, I.L. and Stadler, P.F. (2006) Memory efficient folding algorithms for circular RNA secondary structures. *Bioinformatics*, **22**, 1172–1176.

19 Bernhart, S.H., Tafer, H., Mückstein, U., Flamm, C., Stadler, P.F., and Hofacker, I.L. (2006) Partition function and base pairing probabilities of RNA heterodimers. *Algorithms Mol Biol*, **1**, 3.

20 Mosig, A., Sameith, K., and Stadler, P. (2006) Fragrep: an efficient search tool for fragmented patterns in genomic sequences. *Genomics Proteomics Bioinformatics*, **4**, 56–60.

21 Grünweller, A., Purschke, W.G., Kügler, S., Kruse, C., and Müller, P.K. (1997) Chicken vigilin gene: a distinctive pattern of hypersensitive sites is characteristic for its transcriptional activity. *Biochem J*, **326 (Pt 2)**, 601–607.

22 Wassarman, K.M. and Saecker, R.M. (2006) Synthesis-mediated release of a small RNA inhibitor of RNA polymerase. *Science*, **314**, 1601–1603.

23 Simard, C., Lemieux, R., and Côté, S. (2001) Urea substitutes toxic formamide as destabilizing agent in nucleic acid hybridizations with RNA probes. *Electrophoresis*, **22**, 2679–2683.

D

PUBLICATION III

In vivo and in vitro analysis of 6S RNA-templated short transcripts in Bacillus subtilis.

In revision: 2010RNABIOL0153

Author contributions:
Research design: 60%
Experimental work: 85%
Data analysis and evaluation: 60%
Manuscript writing: 50%

In vivo and *in vitro* analysis of 6S RNA-templated short transcripts in *Bacillus subtilis*

Benedikt M. Beckmann[1], Olga Y. Burenina[2], Philipp G. Hoch[1], Elena A. Kubareva[2], Cynthia M. Sharma[3] and Roland K. Hartmann[1] *

[1]Institut für Pharmazeutische Chemie, Philipps-Universität Marburg, Marbacher Weg 6, 35037 Marburg, Germany

[2]Chemistry Department and A.N. Belozersky Institute of Physico-Chemical Biology, M.V. Lomonosov Moscow State University, Leninskie Gory 1, 199991, Russia.

[3] Institut für Molekulare Infektionsbiologie, Zentrum für Infektionsforschung, Julius-Maximilians-Universität Würzburg, Josef Schneider-Str. 2 / D15, 97080 Würzburg, Germany

*Corresponding author

E-mail: roland.hartmann@staff.uni-marburg.de

Running title: 6S RNA-derived pRNA transcripts in *B. subtilis*

Keywords: 6S-1 RNA, *bsrA*, 6S-2 RNA, *bsrB*, pRNA transcripts, dRNA-seq

Abstract

By differential high-throughput RNA sequencing (dRNA-seq) we have identified “product RNAs” (pRNAs) as short as 8-12 nucleotides that are synthesized by *Bacillus subtilis* RNA polymerase (RNAP) *in vivo* using the regulatory 6S-1 RNA as template. The dRNA-seq data were confirmed by *in vitro* transcription experiments and Northern blotting. In our libraries, we were unable to detect statistically meaningful numbers of reads potentially representing pRNAs derived from 6S-2 RNA. However, pRNAs could be synthesized *in vitro* from 6S-2 RNA as template by the *B. subtilis* σ^A RNAP. 6S-1 pRNA levels are low during exponential, increase in stationary, and burst during outgrowth from stationary phase, demonstrating that pRNA synthesis is a conserved regulatory mechanism, but a more dynamic and fine-tuning process than previously thought. Most pRNAs have a length of 8-15 nt, very few up to 24 nt. The average length of pRNAs tended to increase from stationary to outgrowth conditions. Synthesis of pRNA is initiated at C40 of 6S-1 RNA and U41 of 6S-2 RNA, yielding pRNAs with a 5’-terminal G or A residue, respectively. A *B. subtilis* 6S-1 RNA mutant strain encoding a pRNA with a 5’-terminal A residue showed the same relative distribution of ~ 14-nt pRNAs between the different growth states, but generally displayed lower pRNA levels than the reference strain encoding wild-type 6S-1 RNA. We infer that 6S-1 pRNA synthesis, although evolutionarily optimized for initiation with a +1G residue, is not primarily regulated at the transcription initiation level via growth phase-dependent variations in the cellular GTP pool.

3

INTRODUCTION

Small bacterial non-coding RNAs have emerged as important players in the regulation of cellular transcription and translation processes (reviewed e.g. in Wassarman, 2002, Storz et al., 2005, Waters and Storz, 2009). 6S RNA was one of the first small bacterial RNAs to be discovered (Hindley, 1967; Brownlee, 1971) and is one of the most abundant cellular RNAs. Yet strikingly, it has escaped functional analysis for decades, and was only lately discovered to be ubiquitous in bacteria (Barrick et al., 2005; Trotochaud and Wassarman, 2005; Willkomm et al., 2005).

In *E. coli*, 6S RNA accumulates during stationary phase and acts as a competitor for σ^{70} -dependent promoters by complex formation with the σ^{70} RNA polymerase (RNAP) holoenzyme (Wassarman, 2007; Wassarman and Storz, 2000). 6S RNA is primarily double-stranded, with a large internal loop in the center (Willkomm and Hartmann, 2005). This highly conserved secondary structure is essential for the ability of 6S RNA to form stable complexes with σ^{70} RNAP and serves as a template for the transcription of short "product RNAs" (pRNAs, 14 to 24 nucleotides) under conditions of nutrient resupply during outgrowth from stationary phase (Wassarman and Saecker, 2006; Gildehaus et al., 2007). Synthesis of these short transcripts leads to dissociation of 6S RNA/RNAP complexes and 6S RNA degradation (Wurm et al., 2010). In contrast to *E. coli* which harbors only a single 6S RNA gene, the *B. subtilis* genome encodes at least two 6S RNA homologs, termed 6S-1 (*bsrA*) and 6S-2 (*bsrB*) (Ando et al., 2002; Suzuma et al., 2002). Both RNAs are co-immunoprecipitated with the σ^{A} housekeeping RNAP holoenzyme using antibodies against σ^{A} or the α–subunit (Trotochaud and Wassarman, 2005). So far, it has been unclear whether these 6S RNAs have functions identical or similar to that of *E. coli* 6S RNA. Similar expression profiles of *B. subtilis* 6S-1 RNA and *E. coli* 6S RNA suggested that they may have homologous functions in the two organisms (Barrick et al., 2005)

Here we describe the identification of pRNA transcripts derived from 6S-1 RNA in RNA extracts from *B. subtilis* using 454 deep sequencing (dRNA-Seq, Sharma et al., 2010). In contrast, pRNAs derived from 6S-2 RNA were essentially not identifiable in *B. subtilis* cells at different stages of growth in rich medium. However, we were able to demonstrate pRNA synthesis from 6S-2 RNA *in vitro*. We conclude that *B. subtilis* 6S-1 RNA is the genuine ortholog of the prototypic 6S RNA from *E. coli*, whereas 6S-2 RNA function in *B. subtilis* remains enigmatic at present.

RESULTS

Expression and maturation of 6S RNAs in *B. subtilis*

As a first step, we analyzed expression levels of the two 6S RNAs in our model strain *B. subtilis* 168 at different stages of growth in rich (LB) medium (Fig. 1 A). Total RNA isolated at different growth stages was separated on denaturing PAA gels and subjected to Northern blot analysis using probes antisense to 6S-1 and 6S-2 RNA, respectively. Intracellular 6S-1 RNA levels were found to peak at the transition from late exponential to stationary phase, whereas 6S-2 RNA was most abundant during early exponential phase and barely detectable in extended stationary phase (Fig. 1 B), in line with previous observations (Barrick et al., 2005; Ando et al., 2002). 6S-1 RNA gives two signals in Northern blots (Fig. 1 B), consistent with the presence of a 201-nt precursor form (p6S-1) and a 190-nt mature RNA (m6S-1) as reported previously (Suzuma et al., 2002). During stationary phase (Fig. 1 B, timepoints f and g), intracellular levels of p6S-1 decrease relative to m6S-1 during stationary phase, suggesting that *de novo* synthesis of p6S-1 ceases in stationary phase while existing p6S-1 is converted to m6S-1. In contrast to 6S-1 RNA, 6S-2 RNA gives rise to a single signal in Northern blots (Fig. 1 B).

For 6S-1 RNA, we reproducibly detected a faster migrating band under conditions of extended stationary growth (Fig. 1 B, lane 9, “cleavage product”), indicative of site-specific endonucleolytic processing. To further characterize this putative degradation product, we fractionated total RNA from late stationary phase cells (timepoint g in Fig. 1 A) by denaturing PAGE and excised and eluted RNAs running faster than m6S-1 (190 nt). Using the eluted material as template for 5'- and 3'-RACE experiments, we identified a "hot spot" of cleavage: the majority of mapped 5'- or 3'- ends were located in or very close to the apical loop region, splitting the RNA roughly into two halves (Fig. S1, region I). We infer that the prominent signal of increased mobility seen in Northern blots (Fig. 1 B, lane 9) includes 6S-1 RNA 5’- and 3’-fragments of roughly equal length that arose from endonucleolytic cleavage in the apical loop region. 5’- and 3’-RACE of unfractionated total cellular RNA from late stationary phase further identified 6S-1 RNA fragments with 3’-ends in and close to the lower part of the central bulge (Fig. S1, region II) as well as in the 5’-portion of 6S-1 RNA. This included the 5’-proximal processing site (Fig. S1), thus confirming the maturation site at position 11 of p6S-1, consistent with results from primer extension analysis (Suzuma et al., 2002).

Secondary structure analysis of 6S-2 RNA

So far, structure probing has been reported for *B. subtilis* 6S-1 RNA (Barrick et al., 2005), but not yet for 6S-2 RNA. The *in silico* predicted secondary structure of 6S-2 RNA (Trotochaud and Wassarman, 2005; Barrick et al., 2005) displays the key identity elements of 6S RNAs, which is a large internal loop flanked by imperfect helical arms on both sides. Yet, the stability of the 6S-2 RNA secondary structure is predicted to be 9.3 kcal/mol lower than that of 6S-1 RNA (Fig. 1 C, D). Generally, continuous helical segments are rather short in 6S-2 RNA, including only a limited number of G-C base pairs. We scrutinized the proposed 6S-2 RNA structure by probing with the guanosine-specific RNase T1 and Pb^{2+}-

ions under non-denaturing conditions where both hydrolyze phosphodiester bonds in single-stranded flexible regions. Comparison of RNase T1 cleavage patterns under denaturing versus native conditions did not reveal substantial protections from T1 cleavage under native conditions, except for G53-55 (Fig, 1 D and S2). A more differentiated picture was obtained by Pb^{2+}-induced cleavage. The Pb^{2+}-hydrolysis pattern (Fig. S2) was consistent with the 6S-2 RNA secondary structure illustrated in Fig. 1 D.

We further analyzed for 6S-1 and 6S-2 RNA if variation in Mg^{2+} concentration may affect the Pb^{2+}-induced cleavage pattern. However, no significant Mg^{2+}-dependent changes were observed (Fig. S2; data for 6S-1 RNA not shown). For 6S-2 RNA, we oberserved a prominent Pb^{2+}-cleavage product (Fig. S2, asterisk). The fact that this cleavage remained prominent at increasing Mg^{2+} concentration argues against the possibility that this Pb^{2+} cleavage site reflects a natural high affinity Mg^{2+}-binding site (Fig. S2).

dRNA-seq analysis

We have addressed the question whether *B. subtilis* 6S-1 and 6S-2 RNAs serve as templates for the synthesis of short pRNA transcripts, which have previously been identified in *E. coli* and *Helicobacter pylori* (Wassarman and Saecker, 2006; Gildehaus et al., 2007, Sharma et al, 2010). Since initial attempts to detect pRNA transcripts in total RNA extracts from *B. subtilis* by standard Northern blotting techniques failed, we pursued a dRNA-seq approach as recently described for the characterization of the *H. pylori* primary transcriptome (Sharma et al., 2010). For this purpose, total RNA was harvested from *B. subtilis* 168 cells in exponential, stationary or outgrowth (3 min after 1:5 dilution of stationary cells in fresh LB medium) phase, followed by preparation of dRNA-seq libraries as previously described (Sharma et al., 2010), but including a size-fractionation step (isolation of RNAs smaller than ~ 50 nt by denaturing PAGE). As the hallmark of the

dRNA-Seq approach, the three RNA preparations were each split into two halves, of which one subfraction was further treated with Terminator™ 5'-Phosphate-Dependent Exonuclease (5'-P-exonuclease). This enzyme degrades RNA species carrying a 5'-monophosphate derived from cellular processing events, whereas primary transcripts are protected by their 5'-triphosphates. As a result of this treatment, 5'-monophosphorylated RNAs are depleted, thus enriching for 5'-triphosphorylated primary transcripts (for details, see Materials and Methods). The total number of cDNA reads obtained by 454 sequencing was 165,000 for all six libraries (~ 20,000-35,000 reads per individual library; see Table 1). The abundance of read length variants in the range of 1 to 60 nt is shown in Fig. S3.

Our libraries also contained sequence reads representing fragments derived from 6S-1 or 6S-2 RNA encoded by the genes *bsrA* and *bsrB*, respectively (Fig. 1 C-E). The highest numbers of 6S-1 fragment reads were observed in stationary phase and during outgrowth (Fig. 1 E, left panel). This is in line with the observation that cellular 6S-1 RNA levels are high in stationary phase (Fig. 1 B). The detection of high 6S-1 levels during outgrowth is also plausible, since outgrowth was defined as the state of cells immediately (3 min) after release from stationary phase. The increase in the relative abundance of reads representing a 5'-extended version of 6S-1 RNA in stationary and outgrowth fractions treated with 5'-P-exonuclease [marked by (+), Fig. 1 E] indicated that the 5'-extended version is the primary transcript carrying a 5'-triphosphate protecting the RNA from 5'-exonucleolytic degradation. These findings are consistent with 6S-1 RNA being transcribed as a 201 nt long 5'-precursor that is processed to its mature form (190 nt) (Suzuma et al., 2002), in line with the appearance of two bands in the Northern blot (Fig. 1 B).

The highest numbers of 6S-2 RNA fragment reads were detected in cells harvested during exponential and stationary phase. (Fig. 1 E, right panel). This was somewhat surprising, as Northern blot analyses have indicated that 6S-2 RNA peaks in early

exponential phase (timepoints a and b, Fig. 1 B), whereas levels drop severalfold from early exponential to stationary phase (timepoint f, Fig. 1 B). An explanation for this discrepancy is that cellular levels of full-length 6S-2 RNA dropped from early exponential to stationary phase, but stable degradation fragments of 6S-2 RNA accumulated and were picked up and enriched in our libraries including predominantly RNAs < 50 nt. Indeed, it was inferred from *lacZ* promoter fusion analyses that the *bsrB* (6S-2) promoter is active during stationary phase, suggesting that the disappearance of full-length 6S-2 RNA in this growth phase is due to an increase in the degradation rate (Ando et al., 2002).

In contrast to 6S-1 RNA (Fig. 1 E, left panel), we did not find reads in our libraries that would correspond to a 5'-precursor form of 6S-2 RNA (Fig. 1 E, right panel). This indicates that 6S-2 transcription starts at the mature 5'-end (G+1, Fig. 1 D, which is in line with the Northern blot results (Fig. 1 B) and a previous primer extension analysis (Ando et al., 2002) Furthermore, 6S-2 RNA 5'-segments were enriched in the libraries treated with 5'-P-exonuclease, indicating that transcription indeed starts at the mature 5'-G residue (Fig. 1 D) and a substantial fraction of 6S-2 molecules keep the 5'-triphosphate. In general, our libraries contained less reads representing 6S-2 RNA relative to 6S-1 RNA (Fig. 1 E). Although our libraries were biased as they contained only 6S RNA fragments and excluded full-length 6S RNAs, this observation is consistent with previous findings. Based on ethidium bromide staining of gels, Barrick et al. (2005) estimated 6S-1 RNA levels to still exceed those of 6S-2 RNA roughly twofold at the point where 6S-2 RNA levels peak during exponential phase.

dRNA-Seq identifies pRNAs exclusively from 6S-1 RNA

To perform an unbiased screen for potential pRNA transcripts, we searched all libraries for sequence reads with full complementarity to sliding 8-nt windows (in 1-nt displacement steps) along the 6S-1 and 6S-2 RNA sequences using scripts written in *Perl* and *awk*. This

revealed potential pRNAs derived from 6S-1 RNA, which were further examined according to the following criteria: (i) If the reads are initiated in the 5'-proximal central bulge region of 6S RNA as in *E. coli* (Wassarman and Saecker, 2006; Gildehaus et al., 2007) ? (ii) Reads, should be present in high number; (iii) have the same 5'-nucleotide, and (iv), as primary transcripts, should be overrepresented in (+) libraries. By these criteria, we identified the 6S-1 RNA-encoded pRNA sequence 5'-GUU CGG UC-3' as the most abundant candidate (Table 1). This octamer (i) was encoded in the 5'-portion of the central bulge of 6S-1 RNA (Fig. 1 C), (ii) was present in uniquely high copy number, (iii) had the same 5'-terminal G residue in the vast majority of reads, and (iv) was increased ~ 3- and 17-fold in stationary (+) and outgrowth (+) libraries, respectively, relative to the corresponding (-) libraries (Table. 1), demonstrating that the octamer represents primary transcripts carrying a 5'-triphosphate. Since cDNA library construction involved poly(A)-tailing of RNA 3'-ends, we were unable to differentiate for RNAs potentially ending with A residues if the latter were part of the original RNA or added by poly(A) polymerase. Since 6S-1 RNA encodes a stretch of four A residues after the initial eight pRNA nucleotides (5'-GUU CGG UCA AAA; Fig. 1 C), extended variants of the 5'-GUU CGG UC octamer would be masked by poly(A) tailing. Thus, the 5'-GUU CGG UC reads potentially included variants either terminating at C8 or at A9, A10, A11 or A12. This type of read has therefore been classified as "8-12 nt" in Table 1. The same holds for some of the longer 6S-1 pRNA reads potentially originating from pRNA transcripts with 3'-terminal A residues: those were categorized as 14-15 nt, 20-21 nt and 22-24 nt (Table 1).

Growth-dependent 6S-1 pRNA length distribution

Comparison of the six libraries revealed a "boost" of 6S-1 RNA-templated pRNA synthesis 3 min after induction of outgrowth, but pRNA synthesis at a lower but substantial level was also evident during stationary phase and even occurred, at a very low level, during

exponential phase (Table 1). As expected, the abundance of pRNA reads was linked to enrichment for primary transcripts (see stationary and outgrowth columns, "+" versus "-", Table 1), supporting the notion that a major fraction of, if not all, pRNAs retain their 5'-triphosphate after transcription.

The 8-12 nt reads represented the major fraction of pRNAs, the 14-15 nt reads were the second most abundant species, followed by the 13-mer and very few pRNA reads ranging from 16 to 24 nt (Table 1). In the outgrowth (+) library, pRNA reads made up 47% of all reads and 76% of reads in the range of 8 to 20 nt (Table 1). Comparing the relative levels of 8-12 nt and 14-15 nt long pRNA reads, we noticed that the latter represented 7.2% and 5.5% of pRNA reads in the outgrowth (+) and (-) libraries, relative to 1.2% and 1.4% in the stationary (+) and (-) libraries, respectively (Table 1).

***In vitro* transcription using 6S-1 RNA as template**

To further explore the length distribution of pRNAs derived from 6S-1 RNA, we conducted *in vitro* transcription experiments with the *B. subtilis* housekeeping σ^A RNAP using 6S-1 RNA as template. In the presence α-^{32}P-UTP or γ-^{32}P-GTP for transcript labeling, we observed a major transcript of ~ 14 nt in length and prominent signals corresponding to ~ 8-mers (Fig. 2 A, lanes 2 and 4). In contrast, no radioactive product was seen in the presence of γ-^{32}P-ATP (lane 3), indicating that *in vitro* transcripts are initiated with a G residue. These findings are in perfect agreement with our dRNA-Seq data (Table 1).

Northern blot detection of pRNAs

To further verify our dRNA-seq results, we applied a recently developed Northern blot procedure (Beckmann et al., 2010) for the detection of small RNAs. We compared total extracts from cells grown to stationary phase and during outgrowth using a LNA/DNA mixmer probe complementary to the 6S-1 pRNA 14-mer (Fig. 2 B and S4). As previously reported (Beckmann et al., 2010), pRNA from 6S-1 RNA is mainly detectable as a 14-mer,

while reads representing 8-12-mers dominated our dRNA-seq libraries. Therefore, we evaluated the hybridization properties of our probe to bind to a chemically synthesized 14-mer pRNA (5'-pGUU CGG UCA AAA CU), 8-mer pRNA (5'-pGUU CGG UC) or an 8-meric all-LNA of identical sequence (Fig. S4). While the RNA 14-mer was detected with high sensitivity, the RNA 8-mer could only be detected at a sensitivity reduced by ~ two orders of magnitude, attributable to a high off-rate of RNA 8-mer/probe hybrids. The corresponding LNA 8-mer LNA was detectable with at least 20-fold higher sensitivity, but still with ~ tenfold lower sensitivity than the RNA 14-mer (Fig. S4). We therefore conclude that the failure to detect pRNAs < 14 nt by Northern blotting reflects a technical limitation of the method.

The putative role of the starting nucleotide of 6S-1 pRNA

In *B. subtilis*, the cellular GTP pool plays a central role in regulating transcription and was shown to drop in stationary phase (Lopez et al., 1979). During nutrient limitation (e.g. in stationary phase), rRNA promoters and others encoding a G at +1 are downregulated due to decreased GTP levels, while many transcripts initiated with an A residue are upregulated (Krásny et al., 2004 and 2008). Since transcription of 6S-1-derived pRNA is inititated with a G residue, we considered the possibility that cellular GTP levels may also be a key regulator of pRNA synthesis. To explore the importance of the initiating G nucleotide for 6S-1 pRNA synthesis *in vivo*, we constructed a mutant strain (Fig. 3 A) expressing a 6S-1 RNA with a C40U point mutation (see Fig. 1 C) encoding a pRNA with a 5'-terminal A instead of a G residue. Endogenous pRNAs were synthesized in the mutant strain, but to reduced levels at all analyzed physiological states (early stationary, stationary and outgrowth phase; Fig. 3 B). We also tested by Northern blot analysis if this mutation might alter the cellular 6S-1 RNA levels. However, no significant differences in 6S-1 RNA levels were observed for the mutant and control strain (Fig. 3 C). We conclude that 6S-1

pRNA synthesis has been evolutionarily optimized for initiation with a +1G residue. However, synthesis of wt +1G and mutant +1A pRNA showed the same correlation between cellular pRNA (≥ 14 nt) levels and growth state, i.e. low levels during early stationary growth, increased levels in stationary phase and highest levels during outgrowth.

pRNAs derived from 6S-2 RNA?

The best candidate for a potential pRNA transcribed from 6S-2 RNA we could identify in our dRNA-seq libraries was the sequence 5'-AAA GGU U (complementary to nucleotides 39-45 of 6S-2 RNA, Fig. 1 B), which occurred 8-times in our stationary (+) library (see Suppl. Material, Section IV) and which may include up to four addional A residues at the 3'-end (Fig. 1 B) potentially masked due to poly(A) tailing. To scrutinize whether pRNA transcription using 6S-2 RNA as the template is in principal feasible, we pursued *in vitro* transcription experiments similar to those conducted with 6S-1 RNA (Fig. 2 A). As shown in Fig. 4 A, radiolabeled pRNAs derived from 6S-2 RNA could be detected in the presence of γ-^{32}P-ATP, but not with γ-^{32}P-GTP (cf. lanes 2 and 3). Furthermore, in the presence of α-^{32}P-GTP, α-^{32}P-CTP or α-^{32}P-UTP, radioactive transcripts appeared in transcripts ≥ 4, 12 or 6 nucleotides, respectively (Fig. 4 A, lanes 4 to 6), thus perfectly matching a 6S-2 pRNA sequence of 5'-AAA GGU UAA AAC UUA whose transcription is initiated in the 5'-portion of the central bulge analogous to 6S-1 RNA (Fig. 1 C, D). To validate this finding, we performed *in vitro* transcriptions with the *B. subtilis* σ^A RNAP either using 6S-1 or 6S-2 RNA as template, followed by Northern hybridization either using a probe complementary to 6S-1 pRNA (Fig. 4 B, upper panel) or to the putative 6S-2 pRNA (5'-AAA GGU UAA AAC UUA; Fig. 4 B, lower panel). The probe complementary to the putative 6S-2 pRNA gave a specific signal only when 6S-2 RNA was used as the template for transcription (Fig. 4 B,

lower panel). These results confirmed that the *B. subtilis* σ^A RNAP is able to utilize 6S-2 RNA as a template to synthesize pRNAs initiating opposite to U41 of 6S-2 RNA (Fig. 1 D).

DISCUSSION

pRNA synthesis – a dynamic process

According to mechanistic models proposed for the *E. coli* system, pRNA synthesis selectively occurs during outgrowth from stationary phase when nutrients are resupplied and cellular NTP levels rise (Wassarman 2007) to promote dissociation of 6S RNA-RNAP complexes. In view of this model, the substantial amount of pRNA reads obtained from late stationary *B. subtilis* cells (Table 1) and the detection of pRNA ~ 14-mers in late stationary phase by Northern blotting (Fig. 2 B and 3 B) is surprising. This indicates that pRNA synthesis is a more dynamic and fine-tuning process rather than an all-or-nothing mechanism, at least in *B. subtilis*, not to mention the possibility that pRNA synthesis and decay rates may differ at different physiological states. The synthesis of pRNAs during stationary phase (Table 1, Fig. 2 B and 3 B) suggests that some dissociation of 6S-1 RNA/RNAP complexes also takes place in stationary phase, assuming that the same mechanism as during outgrowth is operative. Alternatively, the different NTP pools or other factors in stationary versus outgrowth phase may affect the kinetics of pRNA synthesis and the average length of pRNA transcripts such that dissociation of 6S-1 RNA/RNAP complexes is preferably triggered during outgrowth and less under stationary conditions. Some evidence in support of this possibility may be inferred from the observation that the fraction of ~ 14-nt pRNAs increase from stationary to outgrowth conditions (Table 1). The shorter pRNA transcripts may not necessarily lead to dissociation of 6S-1 RNA/RNAP complexes. As a consequence, fewer complexes would decompose in stationary versus outgrowth phase. We are currently investigating this hypothesis.

Relation to other studies

6S-1 pRNAs have also been recognized in a very recent global deep sequencing study of *B. subtilis* stationary cells grown in a modified glucose minimial medium (Irnov et al., 2010). The pRNA transcription start was mapped to A38 which is not supported by our data, escpecially as we have shown that pRNA from 6S-1 RNA is initiated by a G residue (Fig. 3 A, Table 1), mapping to the complementary C40 in 6S-1 RNA (Fig. 1 C). Also, in contrast to this previous study (Irnov et al., 2010), we have not identified pRNAs transcribed up to position 14 of 6S-1 RNA, corresponding to a 27-mer. However, we can not exclude the possibility that these discrepancies are attributed to differences in growth media or the experimental setup.

Authenticity of short pRNA reads

While sequences corresponding to longer pRNA transcripts including the 13-mer (5'-GUU CGG UCA AAA C; Table 1) are unique in the genome of *B. subtilis* 168 (NC_000964.2), the 5'-GUU CGG UC octamer is potentially encoded at 63 loci. However, we are convinced that the vast majority of the octamer reads counted in Table 1 represent authentic pRNA transcripts because: (i) hundreds to thousands of reads of this octamer were found in our libraries (see Table 1) which all start at the same 5'-terminal G residue; for fragments derived from, e.g., mRNAs or rRNAs, more variation in the 5'- boundary would have been expected; indeed, 23S rRNA-derived reads including this octamer sequence were present in our libraries, but here the reads had pRNA-unrelated and varying 5'- and 3'-extensions of the 5'-GUU CGG UC core sequence (Supplementary section III); (ii) in the case of 5'-GUU CGG UC octamer sequences derived from other transcribed genome regions, no substantial enrichment due to 5'-P-exonuclease treatment would be expected, as the likelihood that they originate from the 5'-end of primary transcripts is extremely low. Indeed, for the aforementioned 23S rRNA fragments, we saw a depletion of reads upon 5'-

P-exonuclease treatment (Supplementary Section III), which is the opposite of the pRNA enrichment effect. In summary, we are confident that the number of 5'-GUU CGG UC reads considered in Table 1 which might not represent pRNA transcripts is negligible.

pRNA synthesis in other organisms

For *E. coli* σ^{70} RNAP and *E. coli* 6S RNA as template pRNA transcripts of 14 to 24 nt have been described (Wassarman and Saecker, 2006; Gildehaus et al., 2007). Recently, predominantly transcripts of 10-11 nt and 15-20 nt were shown to be transcribed in *E. coli* cells immediately after initiation of outgrowth (Wurm et al., 2010). This correlates with our findings for *B. subtilis*, indicating that 8- to 9-mers and 14- to 15-mers represent the major pRNA transcripts derived from 6S-1 RNA (Fig. 3 A, Table 1). A 12-13 nt long pRNA was recently identified by dRNA-seq as the major 6S RNA-templated transcript in *H. pylori* (Sharma et al., 2010). These observations indicate that pRNA lengths are comparable in different bacteria, consistent with the basic mechanism being similar among bacteria. For *H. pylori*, another 6S RNA-derived transcript (pRNA*) initiated approx. 70 nt downstream of the canonical pRNA initiation site was found (Sharma et al., 2010). Such a second pRNA transcript complementary to 6S-1 RNA was not detected by dRNA-seq in *B. subtilis*. It will be interesting to explore if such secondary 6S RNA-derived transcripts may point to another regulatory facet of 6S RNA in at least some bacteria.

Importance of cellular GTP pool and initiator nucleotide for 6S-1 pRNA synthesis

In exponentially growing *B. subtilis* cells, the ATP concentration exceeds that of the three other NTPs by 3 to 4-fold (Lopez et al., 1979). Upon entry into stationary phase, the GTP level decreases by roughly 70%, while UTP levels decrease more slowly and to a lesser extent; dependent on the specific conditions, ATP levels develop as for UTP or even increase and CTP levels strongly increase (2- to 4-fold) upon entry into stationary phase (Lopez et al., 1979). In *B. subtilis*, the cellular GTP pool, a central handle to regulate

transcription in this organism, is further connected to the stringent response, which results in (p)ppGpp synthesis: in *B. subtilis*, the alarmone (p)ppGpp has no direct effect on RNAP, as in *E. coli*, but indirectly affects the synthesis of transcripts intitiating with guanosine, such as rRNA, namely through GTP consumption during (p)ppGpp biosynthesis and inhibition of GTP production by (p)ppGpp inhibiting the enzyme inosine monophosphate dehydrogenase that catalyzes an early step in GTP biosynthesis. We considered the possibility that the cellular GTP pool may also exert a strong regulatory effect on the transcription of 6S-1 pRNAs initiated with a G residue in contrast to *E. coli* where pRNAs start with an A residue (Wassarman and Saecker, 2006; Gildehaus et al., 2007). Accordingly, replenishment of the GTP pool upon outgrowth from stationary phase could explain the burst of +1 G pRNA transcription. Low levels of pRNA synthesis during exponential phase despite elevated GTP levels can be attributed to low levels of the 6S-1 RNA template (Barrick et al., 2005).

We were able to detect 6S-1 pRNAs in our mutant strain encoding pRNA variants with a 5'-terminal A residue, but mutant pRNA steady-state levels were reduced in all analyzed physiological states (early stationary, stationary and outgrowth phase; Fig. 3 B). We conclude that 6S-1 pRNA synthesis has been evolutionarily optimized for initiation with a +1G residue. However, synthesis of wt +1G and mutant +1A pRNA showed the same correlation between cellular pRNA levels and growth state, i.e. low levels during early stationary growth, increased levels in extended stationary phase and highest levels during outgrowth. This result and the fact that substantial amounts of native pRNAs (starting with a G residue) are produced during stationary phase (Table 1) when the cellular GTP pool is low suggests that 6S-1 pRNA synthesis is not primarily regulated at the transcription initiation level via growth phase-dependent variations in the cellular GTP pool. This would be in line with results of a recent *in vitro* study in the *E. coli* system (Shephard et al., 2010),

which led the authors to question the key role of NTP concentration for 6S RNA:pRNA release from RNA polymerase in *E. coli*. This was based on the finding that the rate of release, for which pRNA synthesis is a prerequisite, was relatively insensitive to NTP concentration, but very sensitive to the level of free magnesium. However, more mechanistic and kinetic experiments are required to define rate-limiting steps along the 6S RNA functional cycle as well as their relevance to different physiological conditions.

pRNA synthesis from 6S-2 RNA

A statistically meaningful number of potential 6S-2 RNA-derived pRNAs has neither been identified in our dRNA-Seq approach nor in a recent transcriptome analysis of *B. subtilis* (Irnov et al., 2010). Nevertheless, we have demonstrated here that the σ^A RNAP holoenzyme is capable of utilizing 6S-2 RNA as a template for pRNA synthesis (Fig. 4). Specific initiation of transcription (opposite to U41, Fig. 1 D) occurs at a position in the 5'-proximal central bulge part that is typical for 6S RNAs in general. Possible explanations to reconcile the *in vitro* versus *in vivo* discrepancy include a rapid degradation of 6S-2 pRNAs *in vivo*, or specific 6S-2 pRNA synthesis during defined adaptations to environmental or stress conditions.

MATERIALS AND METHODS

Cell culture and sample prepration

Bacillus subtilis 168 cells were grown in LB medium at 37°C. For growth curve determination and total cellular extract preparations, 100 ml cultures were inoculated to an OD_{600} of 0.05 using an overnight culture and shaken at 220 rpm at 37°C. Aliquots were withdrawn at different timepoints and cells were pelleted by centrifugation and snap-frozen in liquid nitrogen. To induce outgrowth, cells in extended stationary phase were diluted 1:5 in fresh, prewarmed LB medium and shaken for another 3 min before pelleting and

freezing. Total cellular RNA was prepared using the hot-phenol method (Mattatall and Sanderson, 1996).

Strain construction

To construct strains BB*bsrAC40T* and BB*bsrA*, naturally competent *B. subtilis* 168 cells were transformed with linear PCR fragments comprising a kanamycin cassette, the *bsrA* wild-type gene for the BB*bsrA* strain or the mutated gene *bsrA:*C40T for the BB*bsrAC40T* strain, respectively, and two flanking regions of 500 bp each, identical to the up- and downstream regions of the chromosomal *bsrA* locus, for efficient homologous recombination. For details, see Supplementary Material.

454 Sequencing and data evaluation

cDNA library generation and 454 pyrosequencing was performed as described (Sittka et al., 2008; Sharma et al., 2010). For the library preparation, total RNA of *B. subtilis* 168 from either exponential growth phase, late stationary phase or 3 min after induction of outgrowth was split into two fractions each; one fraction was treated with Terminator™ 5'-Phosphate-Dependent Exonuclease (Epicentre, Cat. No.TER51020) to deplete processed RNAs carrying a 5'-monophosphate, and both fractions were subsequently treated with TAP (tobacco acid pyrophosphatase, Epicentre, Cat. No. T19100) to convert 5'-triphosphates into 5'-monophosphates for linker ligation. For size selection of RNAs < 50 nt, the six library samples were separated on denaturing 15% PAA gels and stained with SYBRgreen II. Small RNAs migrating just above the bromophenol blue dye were eluted from gels by electro-elution, followed by ethanol precipitation. After ligation of specific 5'-linkers to the RNA and poly(A)-tailing, the RNA was converted into cDNA. Library generation was done at vertis Biotechnologie AG. The cDNA libraries were then sequenced on a Roche FLX sequencer. For each library, graphs representing the number of mapped reads per nucleotide were calculated and visualized using the Integrated

Genome Browser software (Affymetrix). Transcriptional start sites were detected by higher cDNA coverage at the 5'-end of a given RNA in the library constructed from RNA treated with Terminator™ 5'-Phosphate-Dependent Exonuclease. For raw library data and data processing, see Supplementary Material, sections II – IV.

Gel electrophoresis and Northern blotting

6S and 5S RNAs were separated by denaturing (8 M urea) PAGE using 1 x TBE as running buffer. For loading onto denaturing gels, 1 volume of denaturing gel loading buffer (0.02 % (w/v) bromophenol blue, 0.02% (w/v) xylene cyanol blue, 2.6 M urea, 66 % (v/v) formamide, 2 x TBE) was added to RNA samples. Before gel loading, samples were heated to 95 °C for 3 min, followed by immediate cooling on ice. For 6S RNA detection, 3 µg (Fig. 1 B) or 2.5 µg (Fig. 3 C) of total RNA prepared from cells withdrawn at different timepoints were separated by 10% denaturing PAGE, followed by Northern blotting. For this purpose, RNA was blotted on positively charged nylon membranes (Roche Diagnostics, Cat. No. 11209299001) overnight using a semi-dry blotter with 3.75 mA/cm2 and 0.5 TBE as transfer buffer. After transfer, the wet membrane was incubated at 80°C for 30 min (RNA immobilization) and stored at 4°C before use. Hybridization was performed at 68°C as described (Beckmann et al., 2010). As hybridization probes, antisense transcripts covering the respective full-length 6S or 5S RNA, internally labeled with digoxigenin-UTP, were synthesized from PCR templates by T7 RNA polymerase (according to the DIG RNA Labeling Mix protocol provided by Roche Diagnostics).

For pRNA detection, 6 µg total cellular RNA was analyzed on a 10% or 20% native polyacrylamide gel. Here, samples were adjusted to 1 x native loading buffer by mixing with 6 x native loading buffer [0.25% (w/v) bromophenol blue, 0.25% (w/v) xylene cyanol blue, 30% (v/v) glycerol], followed heating to 95 °C for 3 min and immediate cooling on ice. Gels were blotted to nylon membranes as described above, however RNAs were fixed to

the membrane using EDC (1-ethyl-3-(3-dimethylaminopropyl)-carbodiimide; Sigma Aldrich, Cat. No. 03450) EDC crosslinking. As controls, chemically synthesized RNA (IDT Technologies) oligomers comprising the pRNA sequences derived from 6S-1 RNA or 6S-2 RNA (6S-1 pRNA: 5'- GUUCGGUCAAAACU; 6S-2 pRNA: 5'- AAAGGUUAAAAC) were used; an all-LNA octamer (5'-GTT[m^{5}C]GGT[m^{5}C]; RiboTask) was further used in Fig. S4. For hybridization, 5'-digoxigenin-labeled DNA/LNA probes complementary to the two pRNAs (6S-1p: 5'-DIG-aGttTtgAccGaAc-3'; 6S-2p: 5'-DIG-gTttTaaCctTt-3'; upper case letters depict LNA and lower case letters DNA; Exiqon) were used and Northern signals were detected using the DIG Northern Starter Kit (Roche, Cat. No. 12039672910), according to our Northern hybridization protocol for small RNAs (hybridization at 50°C; Beckmann et al., 2010).

Preparation of *B. subtilis* RNAP and *in vitro* transcription

B. subtilis RNAP was prepared from the *B. subtilis* strain MH5636 as described (Anthony et al., 2000), except that Ni-NTA chromatography was the only chromatographic step performed. Sigma factor A (σA) was prepared separately as described in Yang and Lewis (2008). For *in vitro* transcription, 0.5 µl of σA (0.86 µg\µl, > 95% purity) was added to 1 µl of RNAP (1.4 µg\µl, ~ 80% purity), corresponding to a 3 to 4-fold molar excess of σA to over RNAP in order to saturate RNAP with σA. The mixture of σA to RNAP was kept on ice for 10 min, followed by addition of 2 µl 6S RNA (3 pmol in double-distilled water), 2 µl 5 x transcription buffer (200 mM Tris-HCl pH 8.0, 25 mM $MgCl_2$; 800 mM KCl, 5 mM DTT), 0.5 µl RiboLock RNAse Inhibitor (40 U\ µl, Fermentas) and incubation for 10 min at 37°C. Then, 1 µl of heparin (1µg\µl) was added to suppress non-specific RNA binding by RNAP, followed by incubation for 10 min at 37°C. Finally, 2 µl of 5 x NTP mix (1 mM each) and 1 µl α-^{32}P-BTP (B = C, G or U) or γ-^{32}P-RTP (R = A or G) (0.5 µCi; 3000 Ci/mmol) were added (final volume: 10 µl) and reactions were incubated for another 30 min at 37°C.

Thereafter, 1 volume of denaturing sample loading buffer (see above) was added, followed by 25% denaturing PAGE. Radioactive RNAs were visualized using a Bio-Imaging Analyzer FLA 3000-2R (FUJIFILM) and the analysis software PCBAS/AIDA (Raytest).

REFERENCES

1. Wassarman, K. M. Small RNAs in bacteria: diverse regulators of gene expression in response to environmental changes. Cell 2002; 109:141-44.

2. Storz, G., Altuvia, S., Wassarman, K. M. An abundance of RNA regulators. Annu Rev Biochem. 2005; 74:199-217.

3. Waters, L. S., Storz, G. Regulatory RNAs in bacteria. Cell 2009; 136:615-28.

4. Hindley, J. J. Fractionation of ^{32}P-labelled ribonucleic acids on polyacrylamide gels and their characterization by fingerprinting. J. Mol. Biol. 1967; 30:125-36.

5. Brownlee, G. G. Sequence of 6S RNA of *E. coli*. Nat. New. Biol. 1971; 229:147–49.

6. Barrick, J. E., Sudarsan, N., Weinberg, Z., Ruzzo, W. L., Breaker, R. R. 6S RNA is a widespread regulator of eubacterial RNA polymerase that resembles an open promoter. RNA 2005; 11:774–84.

7. Trotochaud, A. E., Wassarman, K. M. A highly conserved 6S RNA structure is required for regulation of transcription. Nat. Struct. Mol. Biol. 2005; 12:313–19.

8. Willkomm, D. K., Minnerup, J., Hüttenhofer, A., Hartmann, R. K. Experimental RNomics

in *Aquifex aeolicus*: identification of small non-coding RNAs and the putative 6S RNA homolog. Nucleic Acids Res. 2005; 33:1949–60.

9. Wassarman, K. M. 6S RNA: a small RNA regulator of transcription. Curr. Opin. Microbiol. 2007; 10:164-68.

10. Wassarman, K. M., Storz, G. 6S RNA regulates *E. coli* RNA polymerase activity. Cell 2000; 101:613-23.

11. Willkomm, D. K., Hartmann, R. K. 6S RNA – an ancient regulator of bacterial RNA polymerase rediscovered. Biol. Chem. 2005; 386:1273–77.

12. Wassarman, K. M., Saecker, R.M. Synthesis-mediated release of a small RNA inhibitor of RNA polymerase. Science 2006; 314:1601–03.

13. Gildehaus, N., Neusser, T., Wurm, R., Wagner, R. Studies on the function of the riboregulator 6S RNA from *E. coli*: RNA polymerase binding, inhibition of *in vitro* transcription and synthesis of RNA-directed *de novo* transcripts. Nucleic Acids Res. 2007; 35:1885–96.

14. Wurm, R., Neußer, T., Wagner, R. 6S RNA-dependent inhibition of RNA polymerase is released by RNA-dependent synthesis of small de novo products. Biol. Chem. 2010; 391:187-96.

15. Ando, Y., Asari, S., Suzuma, S., Yamane, K., Nakamura, K. Expression of a small RNA,

BS203 RNA, from the yocI-yocJ intergenic region of *Bacillus subtilis* genome. FEMS Microbiol. Lett. 2002; 207:29–33.

16. Suzuma, S., Asari, S., Bunai, K., Yoshino, K., Ando, Y., Kakeshita, H., Fujita, M., Nakamura, K., Yamane, K. Identification and characterization of novel small RNAs in the aspS-yrvM intergenic region of the *Bacillus subtilis* genome. Microbiology 2002; 148: 2591–25.

17. Sharma, C. M., Hoffmann, S., Darfeuille, F., Reignier, J., Findeiss, S., Sittka, A., Chabas, S., Reiche, K., Hackermüller, J., Reinhardt, R., et al. The primary transcriptome of the major human pathogen *Helicobacter pylori*. Nature 2010; 464:250-55.

18. Beckmann, B. M., Grünweller, A., Weber, M. H., Hartmann, R. K. Northern blot detection of endogenous small RNAs (~ 14 nucleotides) in bacterial total RNA extracts. Nucleic Acids Res. 2010; 38:e147

20. Lopez , J. M., Marks, C. L., Freese, E. The decrease of guanine nucleotides initiates sporulation of *Bacillus subtilis*. Biochim. Biophys. Acta 1979; 587:238-52.

21. Krásny, L., Gourse, R. L. An alternative strategy for bacterial ribosome synthesis: *Bacillus subtilis* rRNA transcription regulation. EMBO J. 2004; 23:4473-83.

22. Krásny, L., Tiserová, H., Jonák, J., Rejman, D., Sanderová, H. The identity of the transcription +1 position is crucial for changes in gene expression in response to amino acid starvation in *Bacillus subtilis*. Mol. Microbiol. 2008; 69:42-54.

23. Irnov, I., Sharma, C. M., Vogel, J., Winkler, W. C. Identification of regulatory RNAs in *Bacillus subtilis*. Nucleic Acids Res. 2010 Jun 4. [Epub ahead of print].

24. Shephard, L., Dobson, N., Unrau, P. J. Binding and release of the 6S transcriptional control RNA. RNA 2010; 16:885-92.

25. Mattatall, N. R., Sanderson, K. E. *Salmonella typhimurium* LT2 possesses three distinct 23S rRNA intervening sequences. J. Bacteriol. 1996; 178:5323-26.

26. Sittka, A., Lucchini, S., Papenfort, K., Sharma, C. M., Rolle, K., Binnewies, T. T., Hinton, J. C., Vogel, J. Deep sequencing analysis of small noncoding RNA and mRNA targets of the global post-transcriptional regulator Hfq. PLoS Genet. 2008; 4:e1000163.

27. Anthony, L. C., Artsimovich, I., Svetlov, V., Landic, R. Burgess, R. R. Rapid purification of His(6)-tagged *Bacillus subtilis* core RNA polymerase. Protein Expression and Purification 2000; 19:350-54.

28. Yang, X. Lewis, P. J. Overproduction and purification of recombinant *Bacillus subtilis* RNA polymerase. Protein Expression and Purification 2008; 59: 86-93.

ACKNOWLEDGEMENTS

This work was supported by the Deutsche Forschungsgemeinschaft (HA 1672/16-1, GK 1384) and the Russian Foundation for Basic Research (08-04-91972, 10-04-01578). We thank Manja Marz for help with awk scripts and Dominik Helmecke for excellent technical

assistance.

FIGURE LEGENDS

Fig. 1: Expression of the two 6S RNAs in *B. subtilis*. (**A**) Representative growth curve of *B. subtilis* 168 in LB medium for 24 h. Filled dots represent growth points at which samples were withdrawn for total RNA preparation (a-g). (**B**) Expression of 6S-1 RNA (top), 6S-2 RNA (middle) and 5S rRNA (bottom) analyzed by Northern hybridization. For each represented timepoint of the growth curve (panel A), 3 µg of total cellular RNA was loaded on a 10% denaturing PAA gel. T7 transcripts were used as controls (lanes 1 - 2) for total RNA preparations from the different growth stages (lanes 3 – 9). 6S-2 RNA levels peak during early exponential growth whereas 6S-1 RNA peaks upon entry into stationary phase. (**C, D**) Proposed secondary structures of 6S-1 RNA (C) and 6S-2 RNA (D). The template regions for pRNA synthesis, starting at C40 in 6S-1 RNA and U41 in 6S-2 RNA, respectively, are indicated by orthogonal arrows and grey lines; the varying line thickness in panel C illustrates that shorter pRNAs from 6S-1 RNA were more abundant than longer ones (for details, see Table 1). The precusor segment of p6S-1 RNA is indicated in grey letters; T7 transcripts of mature 6S-1 RNA carried two additional G residues preceding A+1 for the sake of efficient transcription; likewise, T7 transcripts of 6S-2 RNA (panel D) included an additional 5'-terminal G residue (lower case grey letter). The ΔG values for the two 6S RNAs were calculated by RNAfold (Vienna RNA WebServers) with the constraint to render the central bulge single-stranded. (**E**) Reads representing fragments of 6S-1 and 6S-2 RNA in the different *B. subtilis* total RNA (< 50 nt) libraries as presented by the Integrated Genome Browser software (Affymetrix). At the top, the two 6S RNAs have been arbitrarily split into 3 segments. Below, the number of reads corresponding to these

segments are given as circled numbers for the six individual libraries; thin horizontal lines indicate at least 1 or a few reads, while larger peak areas cover nucleotides that were represented by multiple reads; reads overlapping the boundary between two segments have been arbitrarily assigned to one of the segments. Note that the library contains only smaller fragments of 6S RNAs owing to selection of RNAs < 50 nt by preparative denaturing PAGE. exp., stat.: RNA from cells in exponential or stationary phase, respectively (timepoints b and g in Fig. 1 A); outgr.: cells harvested 3 min after 1:5 dilution of stationary cells in fresh LB medium; (-), (+): RNAs not treated (-) or treated (+) with Terminator™ 5´-Phosphate-Dependent Exonuclease (Epicentre) to enrich for primary transcripts by depletion of processed RNAs carrying a 5'-monophosphate. At the bottom, the genomic context and mapped transcriptional start positions (orthogonal arrows; genomic nucleotide indicated at the bottom) of *bsrA* encoding 6S-1 RNA and *bsrB* encoding 6S-2 RNA are illustrated; the open arrowhead indicates the processing site in the 6S-1 RNA primary transcript, as in panel C.

Fig. 2: (**A**) *In vitro* transcription of pRNAs using 6S-1 RNA as template. Products were analyzed by 20% denaturing PAGE and phosphoimaging. A 5'-endlabeled 6S-1 pRNA 8-mer (5'-GUU CGG UC) served as size marker (lane 1). Internal labeling achieved by α^{32}P-UMP incorporation (lane 2) supports the dRNA-Seq analysis data as it shows pRNAs of 8-9 nt and ~ 14 nt as the major products. Also in line with Table 1, *in vitro* transcription of 6S-1 RNA-derived pRNAs starts with a guanosine (lanes 3 and 4) as only γ^{32}P-GTP but not γ^{32}P-ATP resulted in product labeling. (**B**) Northern blot analyses (10% native PAGE) detecting endogenous pRNAs of ~ 14 nt synthesized from 6S-1 RNA as template in total RNA extracts derived from stationary phase (lane 3) or outgrowth (lane 4) *B. subtilis* cells. A chemically synthesized pRNA 14-mer (5'-GUU CGG UCA AAA CU (Beckmann et al.

2010) and *in vitro* transcribed 6S-1 RNA were loaded as controls in lanes 1 and 2; the type and amount of RNA loaded is indicated above each lane. Note, that shorter pRNA species are not detectable by this method (see Fig. S4).

Fig. 3: (**A**) Construction of a *B. subtilis* 168 derivative strain (BB *bsrA*_C40T) with a C40T *bsrA* mutant gene encoding a 6S-1 pRNA initiating with a +1A residue. The control strain BB *bsrA* was used to directly compare pRNA transcript levels independent of possible effects generated by insertion of the downstream resistance cassette. (**B**) Northern blot analysis (10% native PAGE) analyzing total RNA extracts derived from either early stationary (es; cells harvested at OD_{600} ~ 4.7) phase (lanes 2 and 5; corresponding to timepoint "f" in Fig. 1 A), stationary phase (stat., lanes 3 and 6, corresponding to timepoint "g" in Fig. 1 A; ~ 24 h after inoculation) or outgrowth (outgr., lanes 4 and 7). The chemically synthesized pRNA 14-mer was loaded as control (lane 1). The BB *bsrA*_C40T mutant strain produces pRNA with a 5'-terminal A residue, whereas pRNA synthesis is initiated with a G residue in BB *bsrA* bacteria. At all growth stages, pRNA expression levels were lower in extracts from BB *bsrA*_C40T bacteria. (**C**) Northern blots of 5S rRNA and 6S-1 RNA in both strains (10% denaturing PAGE). Levels of 6S-1 RNA were comparable in the mutant and wild-type strain, indicating that changes in pRNA levels are not attributable to changes in 6S-1 RNA levels owing to the point mutation. The specific 6S-1 RNA cleavage product(s) accumulating in extended stationary phase are indicated (see also Fig. 1 B).

Fig. 4: Detection and sequence identification of pRNAs synthesized by the σ^A RNAP holoenzyme utilizing 6S-2 RNA as template. (**A)** Identification of 6S-2 RNA-templated pRNA sequences by combinatorial use of different radiolabeled NTPs during *in vitro*

transcription. Products were analyzed by 20% denaturing PAGE and phosphoimaging. 6S-2 pRNAs are initiated with an A residue as only γ^{32}P-ATP, but not γ^{32}P-GTP, results in transcript labeling (lanes 2 and 3). The 5'-proximal sequence of 6S-2 pRNAs was inferred from combinatorial insertion of α^{32}P-NTPs. In the presence of α-^{32}P-GTP, α-^{32}P-CTP or α-^{32}P-UTP, radioactive transcripts appeared in transcripts ≥ 4, 12 or 6 nucleotides, respectively (lanes 4 to 6), thus perfectly matching a 6S-2 pRNA sequence of 5'-AAA GGU UAA AAC UUA whose transcription is initiated in the 5'-portion of the central bulge analogous to 6S-1 RNA (see Fig. 1 C, D); *in vitro* pRNA transcripts derived from 6S-1 RNA as template were loaded for comparison in lane 7. (**B**) Northern blot analysis (20% native PAGE) of transcrips synthesized *in vitro* by *B. subtilis* σ^A RNAP using either 6S-1 RNA (lane 5) or 6S-2 RNA (lane 6) as template. Chemically synthesized oligonucleotides mimicking the 6S-1 pRNA 14-mer (5'-GUU CGG UCA AAA CU) or a 6S-2 pRNA 12-mer (5'-AAA GGU UAA AAC) were used as controls (lanes 1 – 4). The same set of samples was loaded on the gels represented by the upper and lower panel; the blots at the top and bottom were hybridized with a probe complementary to 6S-1 pRNA or 6S-2 pRNA, respectively; for more details, see Materials and Methods.

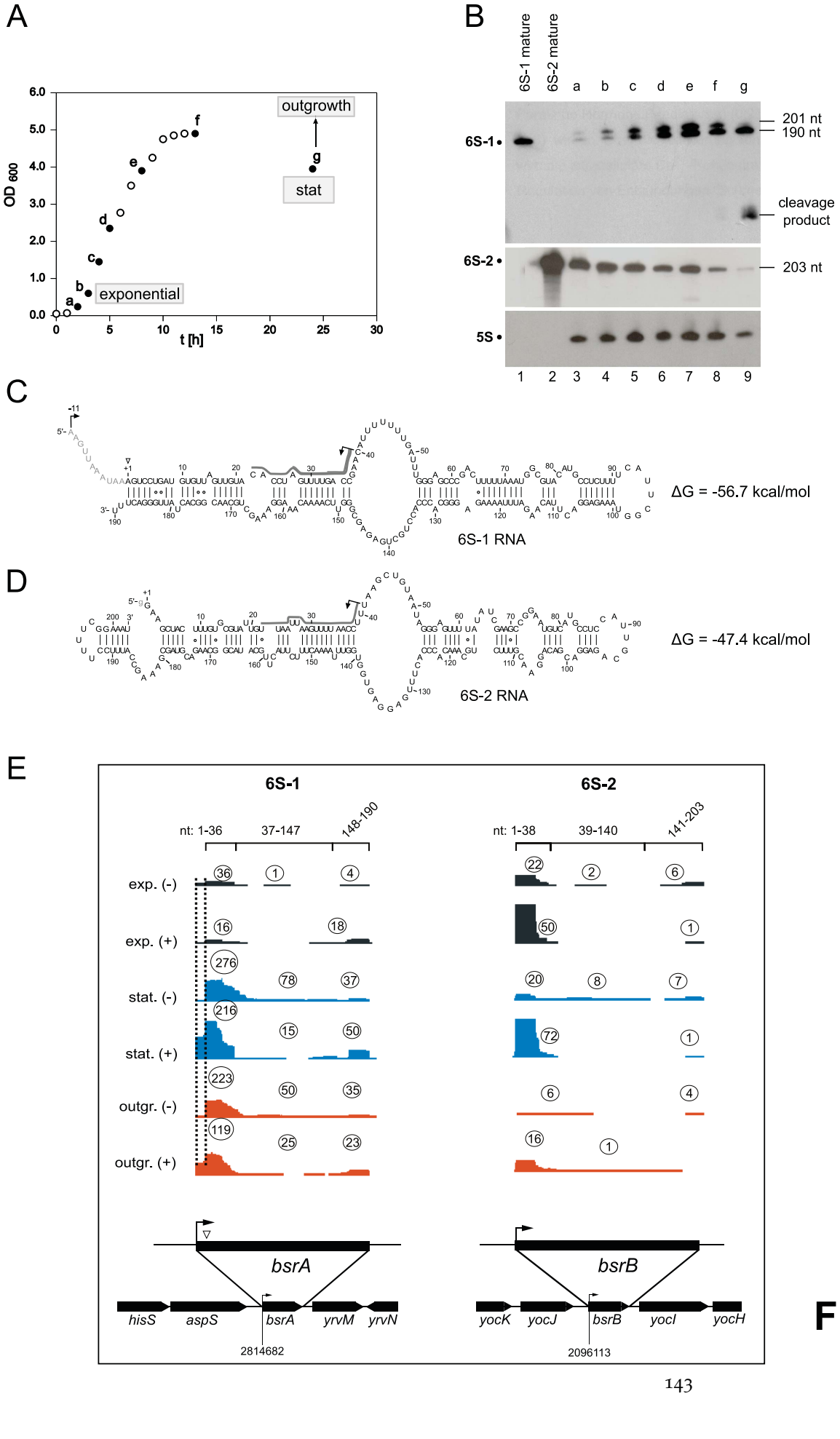
A
OD 600
t [h]
outgrowth
stat
exponential
a
b
c
d
e
f
g
B
6S-1 mature
6S-2 mature
a b c d e f g
6S-1
6S-2
5S
201 nt
190 nt
cleavage product
203 nt
1 2 3 4 5 6 7 8 9
C
ΔG = -56.7 kcal/mol
6S-1 RNA
D
ΔG = -47.4 kcal/mol
6S-2 RNA
E
6S-1
6S-2
nt: 1-36
37-147
148-190
nt: 1-38
39-140
141-203
exp. (-)
exp. (+)
stat. (-)
stat. (+)
outgr. (-)
outgr. (+)
bsrA
bsrB
hisS aspS bsrA yrvM yrvN
yocK yocJ bsrB yocI yocH
2814682
2096113

Fig. 1

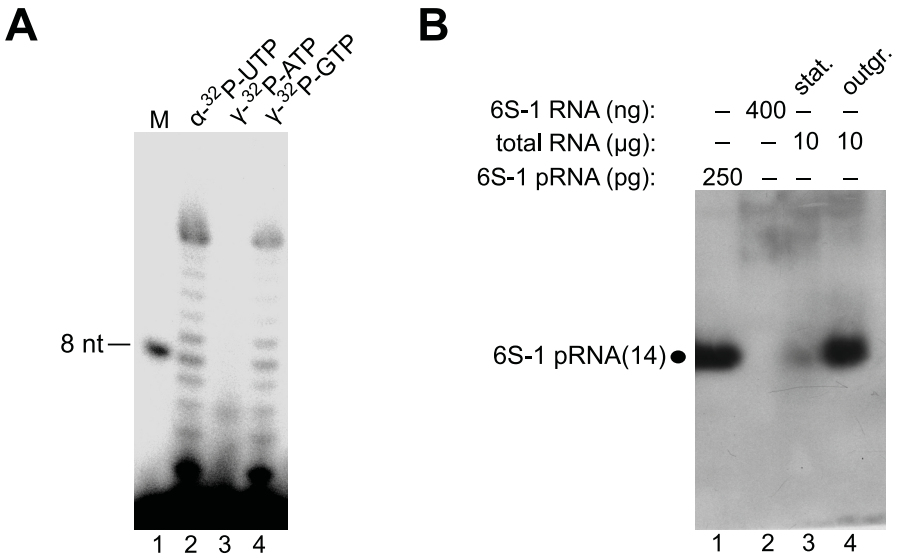
A
M
α-32P-UTP
γ-32P-ATP
γ-32P-GTP
8 nt
1 2 3 4
B
stat.
outgr.
6S-1 RNA (ng): – 400 – –
total RNA (µg): – – 10 10
6S-1 pRNA (pg): 250 – – –
6S-1 pRNA(14)
1 2 3 4

Fig. 2

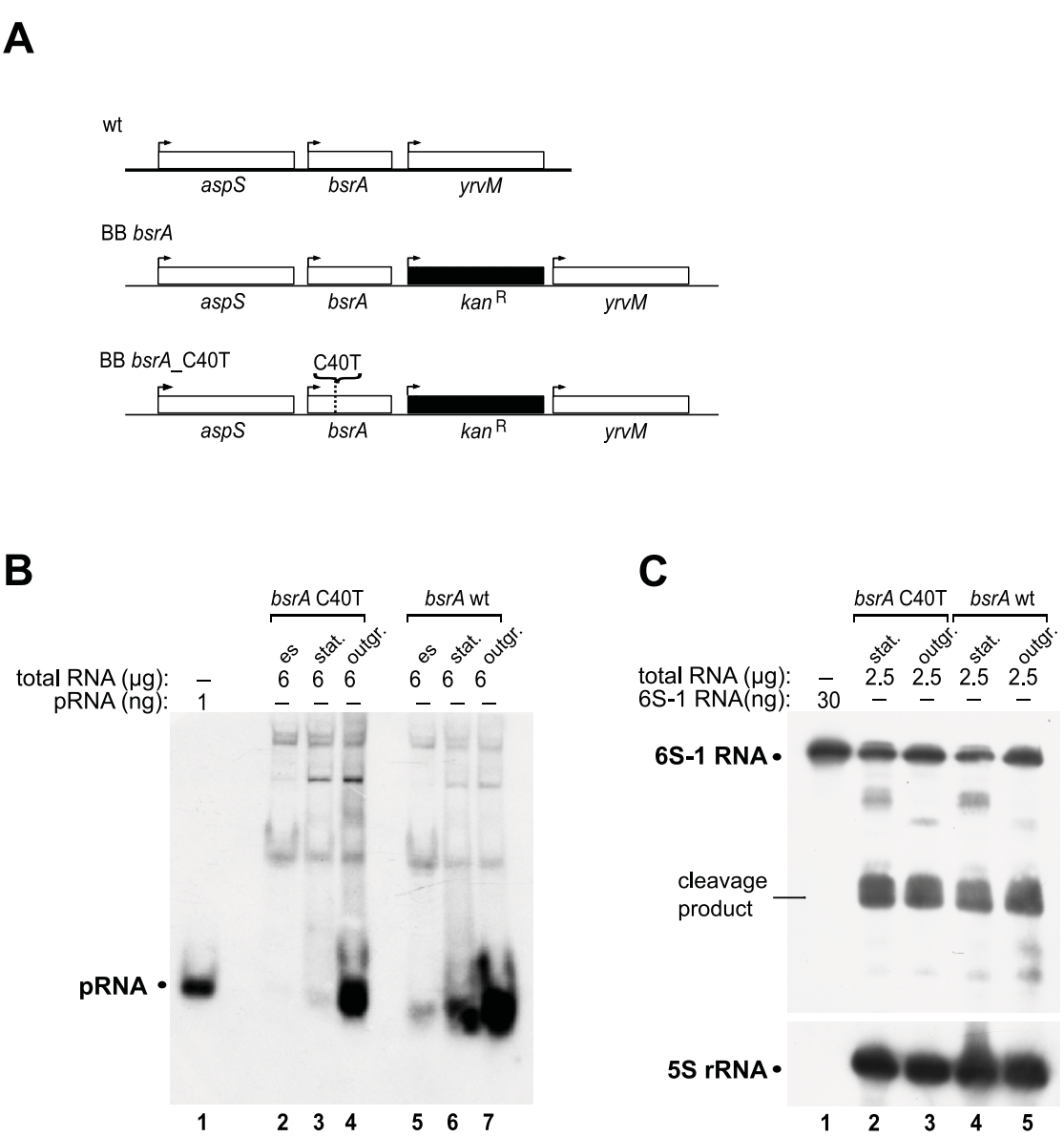
A
wt
aspS
bsrA
yrvM
BB bsrA
aspS
bsrA
kan R
yrvM
BB bsrA_C40T
C40T
aspS
bsrA
kan R
yrvM
B
bsrA C40T
bsrA wt
es
stat.
outgr.
es
stat.
outgr.
total RNA (µg): –
pRNA (ng): 1
6 6 6 6 6 6
pRNA •
1 2 3 4 5 6 7
C
bsrA C40T
bsrA wt
stat.
outgr.
stat.
outgr.
total RNA (µg): –
6S-1 RNA(ng): 30
2.5 2.5 2.5 2.5
6S-1 RNA •
cleavage product
5S rRNA •
1 2 3 4 5

Fig.3

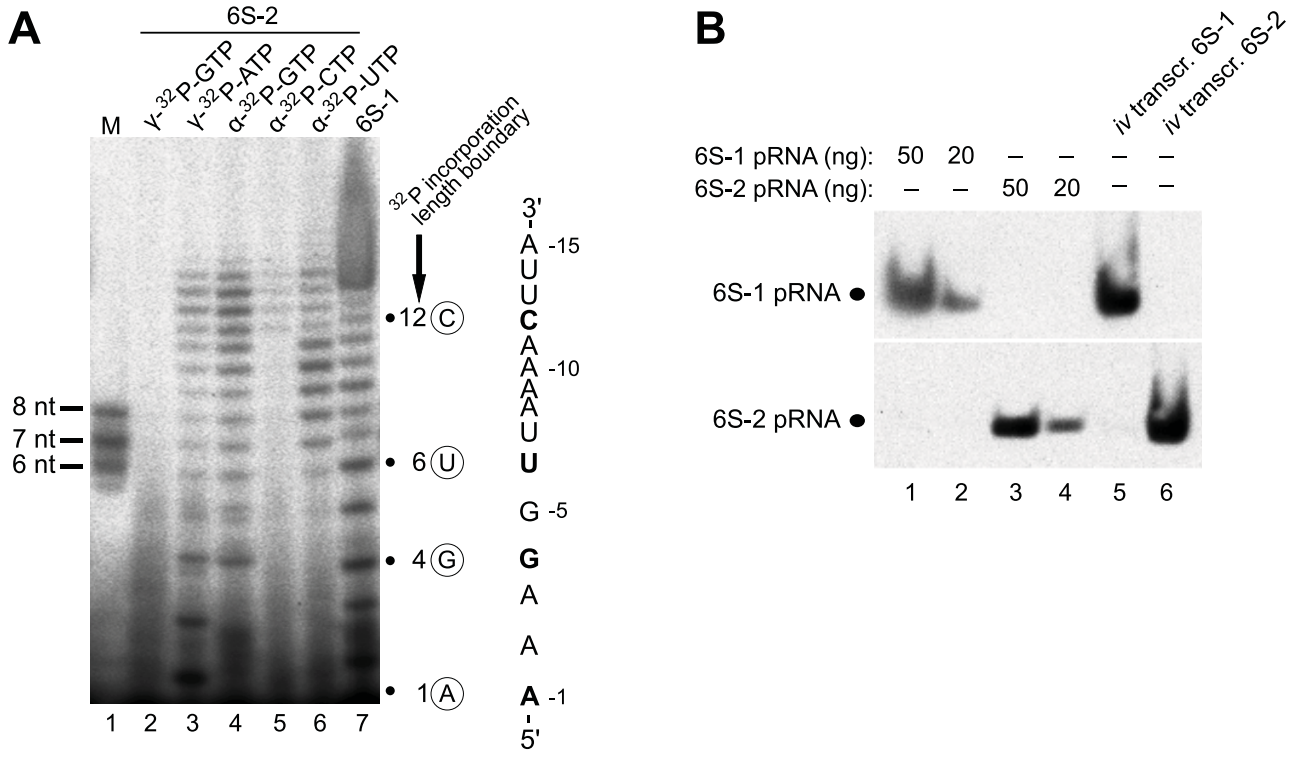
A
6S-2
M
γ-32P-GTP
γ-32P-ATP
α-32P-GTP
α-32P-CTP
α-32P-UTP
6S-1
32P incorporation length boundary
8 nt
7 nt
6 nt
12 C
6 U
4 G
1 A
1 2 3 4 5 6 7
3'
A -15
U
U
C
A
A
A
U -10
U
G -5
G
A
A
A -1
5'
B
iv transcr. 6S-1
iv transcr. 6S-2
6S-1 pRNA (ng): 50 20 – – – –
6S-2 pRNA (ng): – – 50 20 – –
6S-1 pRNA
6S-2 pRNA
1 2 3 4 5 6

Fig. 4

Table 1: Length distribution and number of 6S-1 pRNA reads in the different libraries

		exp.(-)	exp.(+)	stat.(-)	stat.(+)	outgr.(-)	outgr.(+)	nt: 8 14 20
length distribution	22-24 nt	–	–	–	–	–	2	5'-GTTCGGTCAAAACTAGGTGTAC(AA)
	20-21 nt	–	–	–	–	–	6	5'-GTTCGGTCAAAACTAGGTGT(A)
	19 nt	–	–	–	–	–	3	5'-GTTCGGTCAAAACTAGGTG
	18 nt	–	1	–	–	1	8	5'-GTTCGGTCAAAACTAGGT
	17 nt	–	–	1	3	–	2	5'-GTTCGGTCAAAACTAGG
	16 nt	–	–	–	3	–	9	5'-GTTCGGTCAAAACTAG
	14-15 nt	1	1	7	18	51	1174	5'-GTTCGGTCAAAACT(A)
	13 nt	–	–	4	16	5	76	5'-GTTCGGTCAAAAC
	8-12 nt	40	51	484	1413	867	15096	5'-GTTCGGTC(AAAA)
pRNAs reads		41	53	496	1453	924	16376	
% of total reads		0.16	0.26	1.35	7.25	3.14	47.01	
% of 8-20 mers		0.6	0.75	3.79	25.6	21.55	75.58	
% pRNAs 14-15 nt		2.4	1.9	1.4	1.2	5.5	7.2	
reads total		25160	19645	35757	20041	29431	34781	

Table 1

E

PUBLICATION IV

The release mechanism of RNA polymerase from Bacillus subtilis 6S-1 RNA.

Manuscript in preparation

Author contributions:
Research design: 60%
Experimental work: 60%
Data analysis and evaluation: 60%
Manuscript writing: 50%

The release mechanism of RNA polymerase from Bacillus subtilis 6S-1 RNA

Benedikt M Beckmann [*], Philipp G Hoch [*], Manja Marz [*], Margarita Salas [§], and Roland K Hartmann [*]

[*] Institut für Pharmazeutische Chemie, Philipps Universität Marburg, Marbacher Weg 6, 35037 Marburg, Germany, and [§] Centro de Biología Molecular 'Severo Ochoa', Universidad Autónoma de Madrid, Cantoblanco 28049 Madrid, Spain

For *Escherichia coli* it is known that 6S RNA binds to the housekeeping RNA polymerase (σ^{70}-RNAP) to inhibit transcription particularly during stationary growth. Upon outgrowth from stationary phase, σ^{70}-RNAP transcribes short "product" RNAs (pRNAs) from 6S RNA as template, leading to dissociation of 6S RNA:RNAP complexes. We demonstrate for 6S-1 RNA of *B. subtilis* that newly synthesized pRNAs *in cis* induce a structural rearrangement in 6S-1 RNA, which involves formation of an extended hairpin in the 3'-part of the central bulge, as well as base-pairing of its 5'-part with nucleotides that become accessible (termed "central bulge collapse"). The rearrangement largely decreases 6S-1 RNA affinity for RNAP. Among the pRNA length variants synthesized by RNAP (up to $\sim$14 nt), only the longer ones, such as 12 to 14-mers, form a duplex with 6S-1 RNA that is stable enough to induce the rearrangement. We propose a model according to which an interplay of rate constants for polymerization (k_{pol}) particularly at pRNA positions $<$12, for pRNA:6S-1 RNA hybrid duplex dissociation (k_{off}) and for the rearrangement (k_{conf}) determines whether pRNAs dissociate or rearrange 6S-1 structure to trigger 6S-1 RNA release from RNAP. Since the fraction of longer pRNA 14-mers increases in outgrowing versus stationary cells, we predict a more efficient 6S-1 RNA release in outgrowing than stationary cells. We further show that 6S-1 RNA becomes accessible to degradation as a result of pRNA-induced dissociation of 6S-1 RNA:RNAP complexes. A bioinformatic screen suggests that essentially all bacterial 6S RNAs can potentially undergo the pRNA-induced structural rearrangement.

ncRNA | bacterial gene regulation | 6S RNA | pRNA | ncRNA | RNAP

Abbreviations: ncRNA, non-coding RNA; RNAP, RNA polymerase

The discovery and investigation of bacterial small non-coding RNAs (ncRNAs) has become an emerging field in recent years. Beside roles in processing, translation and genome defense, many of these ncRNAs act as regulators, e.g. by masking binding sites or inducing structural changes in their specific target RNA [1].

A unique ncRNA is bacterial 6S RNA [2, 3], which was identified as an abundant RNA species some 40 years ago [4], but whose function remained enigmatic for 30 years [5]. 6S RNA, $\sim$200 nt in length has now been identified in all bacterial branches [6]. In stationary phase *E. coli* cells, 6S RNA competes with DNA promoters for binding to the housekeeping RNA polymerase (σ^{70}-RNAP), resulting in transcriptional repression of a variety σ^{70}-dependent genes [5]. The conserved secondary structure of 6S RNA, thought to resemble an open DNA promoter complex [6, 7], enables stable binding to RNAP. During outgrowth from stationary phase, 6S RNA itself serves as a template for transcription of small "product" RNAs (pRNAs) [8, 9] which results in the dissociation of the 6S RNA:RNAP complex (see Fig. 1 A).

In contrast to most bacteria, *Bacillus subtilis* harbors two 6S RNA homologs, termed 6S-1 and 6S-2, which differ in their expression profiles [6, 7, 10, 11]. In a previous study, we were able to demonstrate that 6S-1 RNA indeed serves as a template for pRNA synthesis, particularly during outgrowth from stationary phase, similar to the prototypic 6S RNA of *E. coli*. Deep sequencing and *in vitro* transcription revealed that pRNA synthesis is always initiated at C40 of 6S-1 RNA, yielding primarily pRNAs with a length of 8/9 or 14 nt in addition to very short ones (5 nt) [12]. As a continuation of our previous work, we analyzed the mechanism of 6S-1 RNA:RNAP release in the present study. We demonstrate that dissociation of 6S-1 RNA:RNAP complexes is the result of a pronounced structural rearrangements of 6S-1 RNA induced by pRNA transcripts that have a minimal length and confer sufficient stability to pRNA:6S-1 RNA hybrid duplexes, such as pRNA 14-mers. Furthermore, *in silico* analysis predicts that pRNA-induced rearrangements in 6S RNA structure occur in all known bacterial 6S RNAs. Our findings provide a basis towards understanding the escape of RNAP from its 6S RNA-mediated activity block. The unique mechanism interdigitates RNA-dependent RNA polymerase activity with a pRNA length-dependent switch in 6S RNA structure that disrupts 6S-1 RNA:RNAP interactions.

Results

Release of RNAP is controlled via stable pRNA binding. The major pRNA species transcribed from 6S-1 RNA as template ([12] Fig. 1 B) are 5, 8/9 or 14 nt in length. We then analyzed by native PAGE whether pRNA 8- and 14-mers (both chemically synthesized) are able to form gel-resolvable complexes with 6S-1 RNA. Since pRNA annealing to 6S-1 RNA is inefficient at ambient temperature (data not shown) because it requires partial disruption of 6S-1 RNA secondary structure, we heated a mixture of the two RNAs to 95°C followed by stepwise cooling to 37°C to allow hybrid formation. The heating procedure itself did not change the structure of 6S-1 RNA as inferred from structure probing (see below) and unaltered mobility in native PAA gels (Fig. 1 C, lanes 1, 2). These experiments revealed that only annealing of unlabeled pRNA 14-mer, but not 8-mer, to 5'-endlabeled 6S-1 RNA caused a shift in 6S-1 RNA mobility (Fig. 1 C, lanes 3 versus 7). In a mirror-like setup, we hybridized 5'-endlabeled pRNA 8- or 14-mer to unlabeled 6S-1 RNA (Fig. 1 C, lanes 4 to 6 versus 8 to 10). Again, formation of a stable hybrid was restricted to the 14-mer.

We then tested if the *B. subtilis* housekeeping RNA polymerase (σ^{A}-RNAP) is able to synthesize pRNA transcripts from 6S-1 RNA pre-annealed to the pRNA 14-mer. As illustrated in Fig. 1 D (lanes 6 and 7), 6S-1 RNA:pRNA 14-mer complexes prevent *de novo* pRNA transcription. Replacement of the pRNA 14-mer with the 8-mer in the pre-annealing step abrogated the inhibitory effect on *in vitro* transcription (Fig. 1 D, lanes 8 to 10), consistent with the 8-mer being unable to stably anneal to 6S-1 RNA. Next, we combined *in vitro* transcription by the σ^{A}-RNAP holoenzyme with native PAGE for the analysis of 6S-1 RNA:RNAP complex formation, utilizing 5'-endlabeled 6S-1 RNA as transcription template. Binding to RNAP

Reserved for Publication Footnotes

and transcription were started at different time points before all samples were concertedly loaded on a native PAA gel. This experiment revealed, in addition to the formation of 6S-1 RNA:RNAP complexes, the appearance of a 6S-1 RNA:pRNA hybrid band of retarded mobility already at the first time point (10 min; Fig. 1 E, lanes 1 to 7). At the latest time point (180 min), very little free 6S-1 RNA remained and the fraction of 6S-1 RNA in complex with RNAP was substantially reduced (lane 7). The idiosyncratic feature of 6S-1 RNA to encode the first A residue at pRNA position 9 opened the perspective to transcribe only shorter pRNAs up to 8-mers through omission of ATP during *in vitro* transcription (Fig. 1 B, lane 2; the fact that we observed also 9-mers despite the absence of ATP might be explained by RNAP adding a non-templated residue to the 3'-end). When ATP or all four NTPs were omitted during the transcription step (Fig. 1 E, lanes 8-21), neither a signal corresponding to the 6S-1 RNA:pRNA hybrid nor a time-dependent reduction in the amount of 6S-1 RNA:RNAP complexes was observed.

We conclude that pRNAs 7 to 9-mers, demonstrated to be synthesized in the absence of ATP (Fig. 1 B, lane 2) under the conditions of the experiment illustrated in Fig. 1 E, are unable to form stable hybrids with 6S- 1 RNA and thus do not affect 6S-1 RNA:RNAP complex formation (Fig. 1 E, lanes 8 to 14 versus 1 to 7).

Deep sequencing had revealed that 6S-1 RNA-derived pRNA 14 to 15-mers represent the second most abundant length variant *in vivo* beyond the shorter 8 to 12-mers, whereas surprisingly few 13-meric pRNA reads were detected [12]. This raised the question of the minimal pRNA length that confers sufficient stability to pRNA:6S-1 RNA hybrids in order to be able to induce the structural rearrangement of 6S-1 RNA. We thus compared chemically synthesized pRNA 12-, 13- and 14-mers for their ability to induce the conformational switch of 6S-1 RNA and to affect 6S-1 RNA:RNAP complex formation. The pRNA oligomers were annealed to 5'-endlabeled 6S-1 RNA and either directly (Fig. 2 A, lanes 6 to 8) loaded onto the native PAA gel or after preincubation with σ^A-RNAP (lanes 2 to 4). This experiment revealed that the 14-mer is required for persistent gel-resolvable binding of pRNA to 6S-1 RNA, as inferred from the prevalence of the shifted 6S-1 RNA conformer (Fig. 2 A, lane 6). The shifted conformer was still detectable with the 13-mer, and to a further reduced extent also with the 12-mer, but the "equilibrium" was shifted towards free 6S-1 RNA in both cases (Fig. 2 A, lanes 7 and 8). In the case of the 13-mer, the free 6S-1 RNA band migrated more diffusely than in the lane representing the 12-mer, suggesting that 13-mer:6S-1 RNA hybrids underwent multiple cycles of dissociation and reassociation during electrophoresis, in line with the intermediate stability relative to 14-mer:6S-1 RNA and 12-mer:6S-1 RNA complexes. When pRNA/6S-1 RNA mixtures were incubated with RNAP after the pRNA pre-annealing step and before gel loading, we observed a reduction in the amount of 6S-1 RNA:RNAP complexes for the 14-, 13-, as well as the 12-mer (Fig. 2 A, lanes 2 to 4). We conclude that pRNA 13- and 12-mer hybrid structures with 6S-1 RNA are sufficiently long-lived to induce the conformational shift in 6S-1 RNA. However, the 6S-1 RNA hybrids containing the 13- or 12-mer have increased dissociation rate constants relative to the 14-mer, leading to the decay of pRNA:6S-1 complexes during native PAGE.

We further addressed the question whether a pRNA 8-mer, if able to form a more stable duplex with 6S-1 RNA, may be capable of inducing the conformational switch of 6S-1 RNA. For this purpose, we pre-annealed an isosequential all-LNA 8-mer (LNA = locked nucleic acid [13, 14]; all-LNA: LNA analogs at every position) to 6S-1 RNA, exploiting the duplex-stabilizing effect of LNA residues. In contrast to the pRNA 8-mer, the pLNA 8-mer was able to form a stable hybrid with 6S-1 RNA and to induce the same conformational switch as the RNA 14-mer (Fig. 2 B, cf. lanes 1 and 2). We conclude that stability of pRNA:6S-1 RNA hybrids is the critical feature here. Likewise, when pre-annealed pLNA 8-mer:6S-1 RNA complexes were incubated with σ^A-RNAP, 6S-1 RNA binding to RNAP was reduced relative to the control sample with the pRNA 8-mer (Fig. 2 B, cf. lanes 3 and 4). This suggests that the decrease in affinitiy for σ^A-RNAP is similar for pLNA 8-mer:6S-1 RNA and pRNA 14-mer:6S-1 RNA complexes relative to free 6S-1 RNA.

To address this affinity decrease from another perspective, we switched to using labeled pRNA as the probe. With 5'-endlabeled pRNA 8-mer as the probe, no radioactive band corresponding to the pRNA:6S-1 RNA complex was detectable, as expected (Fig. 2 B, lanes 5 to 7). In the case of 5'-endlabeled pRNA 14-mer, the pRNA:6S-1 RNA complex was detectable, but only a very faint signal at the position of 6S-1 RNA-RNAP complexes appeared after further incubation of the pre-annealed pRNA:6S-1 RNA hybrid with σ^A-RNAP (Fig. 2 C, lane 6). The faint signal may also stem from direct binding of labeled pRNAs to RNAP, as inferred from a similarly faint signal at identical position in the corresponding pRNA 8-mer lane (Fig. 2 B, lane 6). In summary, our results obtained with labeled pRNAs support the notion that pRNA:6S-1 RNA hybrid structures have a largely reduced affinity for σ^A-RNAP relative to free 6S-1 RNA.

pRNA synthesis induces structural rearrangements of 6S-1 RNA. To understand the conformational switch induced by base pairing of pRNA to 6S-1 RNA, we performed probing experiments with 6S-1 RNA in its free form or in complex with the pRNA 14-mer (Fig. 3 A-D). Using 5'- and 3'-endlabeled mature 6S-1 RNA (190 nt), we were able to identify structural differences particularly in the central bulge region of 6S-1 RNA. Pb^{2+}-induced cleavage, preferentially occurring in single-stranded flexible RNA regions, decreased substantially in the top part of the central bulge (around nt 35-53) upon annealing of the pRNA 14-mer (Fig. 3 A, cf. lanes 4 and 5). Likewise, we observed pRNA-mediated protections from cleavage by RNase T1 (preference for single-stranded G residues) in the lower part of the central bulge at G138 and G145, and an enhanced signal at G143 (Fig. 3 B and C, cf. lanes 5 and 6); protections from Pb^{2+}-induced cleavage were found in the region of nt 135 to 146, except for G141 which showed enhanced accessibility upon pRNA binding (Fig. 3 B, cf. lanes 6 and 7). Since 3'-endlabeled 6S-1 RNA showed a band compression in the region of nt 131 to 137 (Fig. 3 B, lane 2), preventing a clear assignment of signals in this part of 6S-1 RNA, we employed a 5'-endlabeled circularly permuted 6S-1 RNA (with its new 5'-end in the apical loop, Fig. S1) for better resolution, which behaved as the wild-type 6S-1 RNA in terms of the pRNA-induced structural rearrangement (Fig. 3 D) and binding to σ^A-RNAP (Fig. S1). This RNA enabled us to resolve the region of nt 131 to 138, while the region of band compression was now shifted to around nt 147 (Fig. 3 D, lane 2). Partial protections from RNase T1 cleavage were identified at G138 and G145, and enhanced cleavage at G143. In addition, C135 cleaved by RNase T1 for unknown reasons was partially protected in the pRNA:6S-1 RNA hybrid (Fig. 3 D, lanes 4 and 5), and the enhancement of Pb^{2+}-induced hydrolysis at G141 was seen (lanes 8 and 9) as with 3'-endlabeled 6S-1 RNA (Fig. 3 B, lanes 6 and 7). Probing with the double strand-specific RNase V1 mainly revealed enhanced cleavage at nt 137 (Fig. 3 C and D, lanes 6 and 7), suggesting an increased helical character in this part of pRNA:6S-1 RNA hybrid structures. An ambiguity was seen at G141, at which we observed pRNA-mediated partial protection from RNase T1 in panel B (lanes 4 and 5), but partial enhancement of T1 cleavage in panel D (lanes 4 and 5), and generally enhanced Pb^{2+}-induced hydrolysis (panel B, lanes 6 and 7; panel D, lanes 8 and 9). Similar probing results were obtained for hybrid structures composed of 6S-1 RNA and the all-LNA 8-mer instead of the RNA 14-mer (Fig. S2). As expected, the corresponding RNA 8-mer failed to affect 6S-1 RNA structure (data not shown).

It has been recognized before that the lower part of the central bulge has the potential to form a short hairpin with a 3-bp stem [6] (Fig. 3 E, bottom) that is expected to be in equilibrium with an open bulge structure. Our probing results combined with *in sil-*

ico secondary structure predictions are consistent with the pRNA-induced structural rearrangement illustrated in Fig. 3 E (structure on the right). The central feature of the model is the formation of an extended hairpin in the bottom part of the central bulge, whose formation becomes possible when pRNA invasion disrupts the distal part (starting at bp C36:G148) of the closing stem comprising nt 28-36/148-157. As a result nt 148-150 become available for base pairing with nt 134-136 to extend the stem of the hairpin whose formation is only transient in free 6S-1 RNA. Increasing disruption of 6S-1 RNA secondary structure as a result of pRNA invasion then seems to favour base-pairing between nt 42-53 and nt 152-164, resulting in a "collapse" of this usually accessible central bulge region. Thus, the central bulge known to interact with RNAP [5, 9, 15] is subjected to three major alterations in the case of 6S-1 RNA: (i) formation of the pRNA:6S-1 RNA hybrid helix and concomitant disruption of the endogenous closing stem, (ii) formation of the extended hairpin, and (iii) a further collapse of the central bulge structure (Fig. 3 E). An all-LNA 8-mer, disrupting the terminal four base pairs of the closing stem, is sufficient to trigger at least the formation of the extended hairpin (Fig. S2), in line with its capacity to induce the gel mobility shift of 6S-1 RNA and to reduce RNAP affinity when annealed to 6S-1 RNA (Fig. 2 B).

Specific structural changes in 6S RNA are conserved among bacteria. We *in silico* screened all known 6S RNA sequences available from Rfam [16] to investigate whether the conformational rearrangement observed for *B. subtilis* 6S-1 RNA is a general feature of bacterial 6S RNAs. We assumed that pRNA synthesis starts in all bacterial species in the proximal part of the upper central bulge strand (corresponding to C40 in *B. subtilis* 6S-1 RNA, Fig. 3 E). This assumption was reasonable since initiation of pRNA transcription could also been assigned to this region for *E. coli* [8, 9], *Helicobacter pylori* [17] and *Aquifex aeolicus* (unpublished results) 6S RNAs. To evaluate the potential of extended hairpin formation in the lower bulge strand, we executed three operations: (1) *Negative control*: To simulate the ground state (no pRNA present and no structural rearrangement), we analyzed the potential of the bottom part of the central bulge (corresponding to nt 134-147 of *B. subtilis* 6S-1 RNA; Fig. 3 E) to form a helix. For 55 out of 163 6S RNA sequences, a hairpin-like structure was evident (with mostly marginal low energy values: μ = -0.54 kcal/mol, standard deviation = 0.91 kcal/mol). (2) *Positive control*: For a simulation of pRNA:6S RNA hybrids we extended our region of unpaired nucleotides (mimicking pRNA-induced disruption of the closing stem), testing for potential hairpin formation in the region corresponding to nt 134-157 of *B. subtilis* 6S-1 RNA. Surprisingly, 159 out of 163 sequences had the potential to form a persistent hairpin with μ = -7.80 kcal/mol (standard deviation = 4.10 kcal/mol), with the colour code in Fig. 4 indicating the individual hairpin stability. (3) *Collapse of central bulge*: in this third setup, we analyzed if the upper part of the central bulge (nt 41 to 53 in *B. subtilis* 6S-1 RNA) has the potential to base-pair with nucleotides in the 3'-portion of the closing stem (nt 148 to 171 in *B. subtilis* 6S-1 RNA) that become accessible after stem disruption as a result of pRNA invasion (Fig. 3 E). For 160 of the 163 sequences such a bulge collapse was found to be possible, the majority of them being plausible (μ = -5.70 kcal/mol (standard deviation = 3.48 kcal/mol); Fig. 4, squares). This also included *Aquifex aeolicus* [18], for which we identified the pRNA sequence by deep sequencing (data not shown). All input and output files can be obtained at the Supplement web page.

RNAP release and 6S-1 RNA degradation are coupled. As outgrowth from stationary phase has been shown to be the time point of massive pRNA production in *B. subtilis* [12], we conducted Northern blot analyses of total cellular RNA from cells after induction of outgrowth. To analyze the impact of *in vivo* synthesized pRNA on its templating 6S-1 RNA, we induced outgrowth by addition of fresh LB-medium either without (Fig. 5 A, lanes 2 to 9) or supplemented with rifampicin (Fig. 5 A, lanes 10 to 17) to inhibit RNAP activity. Rifampicin treatment blocked pRNA synthesis (Fig. 5 A, bottom panels) as well as *de novo* 6S-1 RNA synthesis (Fig. 5 A, top panel), the latter inferred from the disappearance of the 6S-1 RNA precursor. In addition, we observed a stabilization of mature 6S-1 RNA levels in the presence of rifampicin, whereas 6S-1 RNA levels decreased during outgrowth in the absence of the antibiotic (Fig. 5 A, cf. lanes 2 and 7) to increase again when cells entered a new stationary phase (lanes 8 and 9). We interpret these findings as follows: pRNA synthesis triggers the intracellular 6S-1 RNA release from RNAP; as a consequence, 6S-1 RNA becomes susceptible to degradation. In the presence of rifampicin and thus absence of pRNA synthesis, 6S-1 RNA remains bound to RNAP which protects the RNA from nucleolytic attack. An alternative explanation could be that rifampicin blocks expression of an RNase involved in 6S-1 RNA decay. We thus tested 6S-1 RNA degradation in extracts from outgrowing cells treated with and without rifampicin. No differences in the decay rate were observed (data not shown), arguing against this alternative explanation. We also tested if pre-annealed pRNA:6S-1 RNA hybrids may accelerate 6S-1 RNA decay. Again, no significant differences were found when we compared the decay rates for radiolabeled 6S-1 RNA in its free form or complexed with the pRNA 14-mer (data not shown), making a direct effect of pRNA on 6S-1 RNA degradation unlikely.

Discussion

Using differential high-throughput RNA sequencing (dRNA-seq), we recently identified pRNAs transcribed *in vivo* from *B. subtilis* 6S-1 RNA as template [12]. 6S-1 pRNA levels were found to be low during exponential, to increase in stationary, and to burst during outgrowth from stationary phase. The major identified pRNA species were 8 to 12-mers and 14 to 15-mers. Since sequencing library construction involved poly(A) tailing of RNAs at their 3'-ends and 6S-1 pRNAs carry A residues at positions 9 to 12 and 15, we were unable to further resolve the length distribution between 8 and 12 nt or 14 and 15 nt. *In vitro* transcription then indicated that the major pRNA species are 5, 8, 9 and 14 nt in length ([12] Fig. 1 B). dRNA-seq further revealed an increase in the relative abundance of 14 to 15-mers compared to 8 to 12-mers in outgrowing versus stationary cells, suggesting that the length distribution of pRNAs varies upon the physiological state and may have functional implications [12]. Here we have demonstrated that a pRNA 8-mer is unable to stably associate with 6S-1 RNA and to induce the structural rearrangement of 6S-1 RNA that decreases the affinity for σ^A-RNAP (Fig. 1 C, E). In contrast, an all-LNA 8-mer has this capacity (Fig. 2 B), clearly demonstrating that the high rate constant for dissociation (k_{off}) of an 8-bp RNA/RNA is the problem here, not the duplex length *per se*. We further compared pRNA 12-, 13- and 14-mers (Fig. 2 A), showing that only 6S-1 RNA:pRNA 14-mer complexes have a sufficiently low k_{off} to resist any dissociation during native PAGE (Fig. 2 A, lanes 6 to 8). Of note, native PAGE does not mimic equilibrium conditions, and complexes undergoing repeated dissociation and reassociation cycles in gel "cages" are at risk to dissociate irreversibly when they fall below a certain thermodynamic stability. Nonetheless, pRNA 12- and 13-mers were able to reduce the fraction of 6S-1 RNA bound to RNAP (Fig. 2 A, lanes 1 to 4), suggesting that even the amount of complexes composed of 6S-1 RNA and pRNA 12-mer is substantial under equilibrium conditions. In conclusion, we propose a kinetic model, according to which 6S-1 RNA:pRNA hybrids can either decompose (determined by the k_{off} of 6S-1 RNA:pRNA duplexes) or induce the structural/conformational rearrangement in 6S RNA (described by the rate constant k_{conf}) that reduces the affinity for σ^A-RNAP. Also, the rate constant for nucleotide addition (k_{pol}) will be critical at pRNA positions such as nt 8, where k_{off} is high, but will be clearly uncritical at e.g. position 14 where k_{off} negligible. If the rate

of pRNA polymerization and thus the average pRNA length distribution varies depending on the pyhsiological state, as suggested by our dRNA-seq data [12], then our model predicts more "non-productive" rounds e.g. of pRNA 8-mer synthesis during stationary phase compared to outgrowth conditions (Fig. 5 B).

In the experiment in Fig. 1 E, roughly 50% of 6S-1 RNA molecules were bound to RNAP (lane 1) and it seems that these molecules are rapidly (within 10 min; lane 2) converted to the gel-resolvable shifted conformer, indicating that the latter represent pRNA 14-mer:6S-1 RNA complexes. Under comparable conditions, 6S-1 RNA-templated *in vitro* transcription for 1 h resulted in a transcript pattern, according to which pRNAs migrating as 5-mers represent the most abundant length species (Fig. 1 B, lane 1). If the transcript pattern in Fig. 1 B had resulted from single transcription rounds, then the efficient formation of gel-resolvable pRNA 14-mer:6S-1 RNA in Fig. 1 E (lanes 1 to 7) could not be explained. Thus, a straightforward interpretation of our results is that σ^A-RNAP molecules repeatedly traverse "non-productive" rounds of pRNA 5-mer synthesis before they stochastically succeed in synthesizing a longer pRNA.

The fate of 6S-1 RNA:pRNA hybrids after dissociation from RNAP is unknown so far. As mentioned before, we have evidence that 6S-1 RNA is degraded at the same rate in its free state or if part of complexes with pRNA. RNases involved in degradation of 6S RNA have not yet identified in *B. subtilis* nor in any other bacterium.

We have provided evidence that the pRNA-induced structural rearrangement revealed for *B. subtilis* 6S-1 RNA is likely conserved among all bacteria. This observation is remarkable, taking into account that 6S RNAs are very weakly conserved on the sequence level [6, 7]. Interestingly, a C132A mutant of *E. coli* 6S RNA was recently observed to be decreased in the rate of 6S RNA:pRNA release from RNAP [19]. This mutation would affect the base pair at the base of the extendend hairpin predicted to form in the rearranged structure of *E. coli* 6S RNA (Fig. 4). Future studies will have to explore if the C132A mutation indeed affects the kinetics of the 6S RNA rearrangement via impairing formation of the extended hairpin. It has not escaped our attention that the extended hairpin stability is highest in γ-proteobacterial 6S RNAs, of which *E. coli* is a member (Fig. 4). This points to idiosyncrasies in the mechanism of pRNA-induced 6S RNA:RNAP dissociation in γ-proteobacteria.

The unique mechanism of 6S RNA release from RNAP via pRNA synthesis raises the question if pRNAs, which accumulate to considerable levels in outgrowing cells, might play additional roles in the regulation of gene expression [20]. Although the question still awaits a final answer, our results clearly demonstrate that a central pRNA function is exerted *in cis* through inducing a switch in the structure of 6S RNA. Thus, additional pRNA functions at least do not have to be invoked to explain the biological function of 6S RNA, but, of course, cannot be excluded at present.

Materials and Methods

Northern analysis. Total RNA was isolated from *B. subtilis* 168 cells grown in LB-medium at 37°C using the single step method [21]. 3 μg of total RNA was separated on 8% denaturing (8 M urea) polyacrylamide (PAA) gels. Gels were washed for 5 min in 0.5 x TBE and transferred overnight to a positively charged nylon membrane (Roche) by semi-dry blotting in 0.5 x TBE at 3.75 mA/cm^2. Northern hybridization was performed using the Northern Starter Kit (Roche) following the manufacturer's instructions. Fully complementary DIG-labeled RNA was used as probe for 6S-1 RNA. Detection of pRNA transcripts was performed as described previously [22].

For outgrowth experiments, cells in late stationary phase were diluted 1:5 in fresh prewarmed LB-medium and samples were taken from 2 min to 4 h. Rifampicin was added with the dilution medium to a final concentration of 100 μg/ml.

6S-1 RNA:pRNA annealing, gel shift assays and *in vitro* transcription. *6S-1 RNA:pRNA annealing*: *in vitro* transcribed 190 nt (mature) 6S-1 RNA was incubated with pRNA oligonucleotides (Noxxon; the LNA 8-mer was from RiboTask) and trace amounts of either 5'-γ^{32}P-labeled 6S-1 RNA or pRNA in a volume of 4 to 6 μl 1 x TE buffer for 5 min at 95°C. For concentrations, see figure legends. Annealing of the denatured RNAs was then accomplished by stepwise cooling (5 min 80°C, 5 min 70°C, 5 min 50°C, 5 min 50°C and 5 min 37°C) in a thermocycler (Biometra). Samples were mixed with 5 μl of 2 x native RNA loading buffer [2 mM $MgCl_2$, 0.025% bromophenol blue (w/v), 0.025% xylene cyanol blue (w/v), 10% glycerol] and subsequently separated on a 10% native PAA gel (1 x TBE).

6S-1 RNA:RNAP gel shifts without transcription: to 6 μl pre-annealed 6S-1 RNA (without or with pRNA), 2 μl of 5 x activity buffer (200 mM Tris-HCl pH 8.0, 25 mM $MgCl_2$; 800 mM KCl, 5 mM DTT), 1 μl of heparin solution (400 ng/μl) and 1.06 μl σ^A-RNAP holoenzyme (8 μg/μl; prepared as described [23]) were added and samples were incubated for 30 min at 37°C to promote 6S1 RNA:RNAP (f. c. σ^A-RNAP: 2 μM; f. c. 6S-1 RNA: 1 or 10 μM); samples were mixed with an equal volume of 2 x native RNA loading buffer (see above) and loaded onto a 7.5% native PAA gel (1 x TBE). 6S-1 RNA:RNAP gel shifts with transcription: to 4 μl pre-annealed 6S1 RNA (2.5 μM), 2 μl of 5 x activity buffer, 1 μl of heparin solution (400 ng/μl) and 1.06 μl σ^A-RNAP holoenzyme (8 μg/μl) were added and samples were incubated for 30 min at 37°C. Transcription was then started by adding 2 μl NTP mix A (1 mM each ATP, CTP, GTP and UTP; or an NTP mix lacking ATP; or 2 μl ddH_2O instead); the f. c. of σ^A-RNAP was 2 μM, and that of 6S-1 RNA 1 μM.

Transcription of 32P-labeled pRNAs using 6S-1 RNA as template: 6S-1 RNA (f. c. 2.5 to 3.2 μM) was mixed with 2 μl 5 x activity buffer, 2 μl NTP mix B (1 mM each ATP, CTP, GTP, and 0.25 mM UTP), 0.5 μl α-^{32}P-UTP (20,000 Cerenkov cpm) and 1.06 μl σ^A RNAP holoenzyme (8 μg/μl) in a final volume of 10 μl, followed by incubation for 1 h at 37°C. Samples were mixed with an equal volume of 2 x denaturing RNA loading buffer [0.02% (w/v) bromophenol blue, 0.02% (w/v) xylene cyanol blue, 2.6 M urea, 66% (v/v) deionized formamide, 2 x TBE, pH 8.0] and loaded onto 20% denaturing PAA gels (1 x TBE).

Structure probing. *In vitro* transcribed 6S-1 RNA was 5'-endlabeled using T4 PNK (Fermentas) and (γ^{32}P-ATP) or 3'-endlabeled using T4 RNA ligase (Fermentas) and (5'-^{32}P)pCp. After gel purification, 10 μM unlabeled 6S-1 RNA, trace amounts of radiolabeled 6S-1 RNA (usually 20,000 cpm per reaction) or pre-annealed 6S-1 RNA:pRNA hybrids (see above) were subjected to partial enzymatic digestion using RNase T1, RNase V1 or partial chemical cleavage using $NaHCO_3$ or Pb^{2+}-ions. After separation on thin denaturing PAA gels, cleaved RNA was analyzed on a phosphoimager (Fujifilm). For further details see Supplementary material.

Bioinformatics. To derive a model for the pRNA-induced structural rearrangement in 6S-1 RNA, we compared our structural probing data with different constraints of the `RNAsubopt -C` [24] output.

To explore whether the conformational rearrangement observed for *B. subtilis* 6S-1 RNA may be phylogenetically conserved, we downloaded a secondary structural alignment of all deposited bacterial 6S RNAs from `Rfam v.10.0` [16] (output file **RF00013_seed.stk**). By manually adding *Aquificales* sequences, the alignment increased to 163 sequences. We performed three steps:

(1) *Negative control.* To simulate the case of no pRNA and no structural rearrangement, we tested the 3' internal loop region (alignment positions 184–209, a length of 12–20 nt without gaps) to form a helix with `RNAfold v.1.6` [25].

(2) *Positive control.* For a simulation of pRNA:6S RNA hybrids we extended our region of unpaired nucleotides and tested the alignment positions 184–224 (a length of 20–30 nt) with the same method for stable hairpin formation.

(3) *Collapse of central bulge.* Here we analyzed if the upper part of the central bulge (alignment positions 55–70) has the potential to base-pair with nucleotides in the 3'-portion of the closing stem (alignment positions 210–241) that become accessible after stem disruption as a result of pRNA invasion (two interacting sequences, 12–20 and 17–29 nt in length). All input and output files can be obtained at the Supplement page `http://bioinf.pharmazie.uni-marburg.de/supplements/136`.

Finally, we used `SplitsTree v.4` [26] to create a NJ-Tree and to further evaluate these findings. We color-coded the energy values of predicted extended hairpins ranging from -0.40 kcal/mol (blue) to -9.50 kcal/mol (red). The collapse of the central bulge was marked by squares in case of energy values below -1.30 kcal/mol.

ACKNOWLEDGMENTS. We thank Dagmar K. Willkomm for competent help in the initial phase of the project, D. Helmecke for technical support and A. Grünweller for critically reading of the manuscript.

1. L.S. Waters and G. Storz: Regulatory RNAs in bacteria. *Cell*, 136(4):615-628 (2009).
2. D.K. Willkomm and R.K. Hartmann: 6S RNA - an ancient regulator of bacterial RNA polymerase rediscovered. *Biol Chem*, 386(12):1273-1277 (2005).
3. K.M. Wassarman: 6S RNA: a regulator of transcription. *Mol Microbiol*, 65(6):1425-1431 (2007).
4. G.G. Brownlee: Sequence of 6S RNA of *E. coli*. *Nat New Biol*, 229(5):147-149 (1971).
5. K.M. Wassarman and G. Storz: 6S RNA regulates *E. coli* RNA polymerase activity. *Cell*, 101(6):613-623 (2000).
6. J.E. Barrick, N. Sudarsan, Z. Weinberg, W.L. Ruzzo, and R.R Breaker: 6S RNA is a widespread regulator of eubacterial RNA polymerase that resembles an open promoter. RNA, 11(5):774-784 (2005).
7. A.E. Trotochaud, and K.M. Wassarman: A highly conserved 6S RNA structure is required for regulation of transcription. *Nat Struct Mol Biol*, 12(4):313-319 (2005).
8. K.M. Wassarman and R.M. Saecker: Synthesis-mediated release of a small RNA inhibitor of RNA polymerase. *Science*, 314(5805):1601-1603 (2006).
9. N. Gildehaus, T. Neusser, R. Wurm, and R. Wagner: Studies on the function of the riboregulator 6S RNA from *E. coli*: RNA polymerase binding, inhibition of *in vitro* transcription and synthesis of RNA-directed *de novo* transcripts. *Nucleic Acids Res*, 35(6):1885-1896 (2007).
10. Y. Ando, S. Asari, S. Suzuma, K. Yamane, and K. Nakamura: Expression of a small RNA, BS203 RNA, from the yocI-yocJ intergenic region of *Bacillus subtilis* genome. *FEMS Microbiol Lett*, 207(1):29-33 (2002).
11. S. Suzuma, S. Asari, K. Bunai, K. Yoshino, Y. Ando, H. Kakeshita, M. Fujita, K. Nakamura, and K. Yamane: Identification and characterization of novel small RNAs in the aspS-yrvM intergenic region of the *Bacillus subtilis* genome. *Microbiology*, 148(Pt 8):2591-2598 (2002).
12. B.M. Beckmann, O.Y. Burenina, P.G. Hoch, C.M. Sharma, E.A. Kubareva and R.K. Hartmann: *In vivo* and *in vitro* analysis of 6S RNA-templated short transcripts in *Bacillus subtilis*. *submitted*.
13. B. Vester and J. Wengel: LNA (locked nucleic acid): high-affinity targeting of complementary RNA and DNA. *Biochemistry*, 43(42):13233.13241 (2004).
14. A. Grünweller and R.K. Hartmann: Locked nucleic acid oligonucleotides: the next generation of antisense agents? *BioDrugs*, 21(4):235-243 (2007).
15. A.T Cavanagh, A.D. Klocko, X. Liu and K.M. Wassarman: Promoter specificity for 6S RNA regulation of transcription is determined by core promoter sequences and competition for region 4.2 of sigma70. *Mol Microbiol*, 67(6):1242-1256 (2010).
16. P.P. Gardner, J. Daub, J.G. Tate, E.P. Nawrocki, D.L. Kolbe, S. Lindgreen, A.C. Wilkinson, R.D. Finn, S. Griffiths-Jones, S.R. Eddy, and A. Bateman: Rfam:updates to the RNA families database. *Nucleic Acids Res*, 37:D136-140 (2009).
17. C.M. Sharma, S. Hoffmann, F. Darfeuille, J. Reignier, S. Findeiss, A. Sittka, S. Chabas, K, Reiche, J. Hackermüller, R. Reinhardt, P.F. Stadler, and J. Vogel: The primary transcriptome of the major human pathogen *Helicobacter pylori*. *Nature*, 464(7268):250-255 (2010).
18. D.K. Willkomm, J. Minnerup, A. Hüttenhofer, and R.K. Hartmann: Experimental RNomics in *Aquifex aeolicus*: identification of small non-coding RNAs and the putative 6S RNA homolog. *Nucleic Acids Res*, 33(6):1949-1960 (2005).
19. L. Shephard, N. Dobson, and P.J. Unrau: Binding and release of the 6S transcriptional control RNA *RNA*, 16(5):885-892 (2010).
20. R. Wurm, T. Neusser, and R. Wagner: 6S RNA-dependent inhibition of RNA polymerase is released by RNA-dependent synthesis of small *de novo products*. *Biol Chem*, 391(2-3):187-196 (2010).
21. P. Chomzynski and N. Sacchi: Single-step method of RNA isolation by acid guanidinium thiocyanate-phenol-chloroform extraction. *Anal Biochem*, 162(1):156-159 (1987).
22. B.M. Beckmann, A. Grünweller, M.H.W. Weber, and R.K. Hartmann: Northern blot detection of endogenous small RNAs (~ 14 nt) in bacterial total RNA extracts. *Nucleic Acids Res*, 38(14):e147 (2010).
23. J.M. Sogo, M.R. Inciarte, J. Corral, E. Viñuela, and M. Salas: RNA polymerase binding sites and transcription map of the DNA of *Bacillus subtilis* phage ϕ29. *J Mol Biol*, 127(4):411-436 (1979).
24. S. Wuchty, W. Fontana, I.L. Hofackerm, and P. Schuster: Complete suboptimal folding of RNA and the stability of secondary structures. *Biopolymers*, 49(2):145-165 (1999).
25. I.L. Hofacker: Vienna RNA secondary structure server. *Nucleic Acids Res*, 31(13):3429-3431 (2003).
26. D.H. Hudson and D. Bryant: Application of Phylogenetic Networks in Evolutionary Studies. *Mol Biol Evol*, 23(2):254-267 (2006).

Figure legends

Fig. 1 *B. subtilis* 6S-1 RNA forms stable hybrids with pRNA *in vitro*. (**A**) Current model of 6S RNA function in *E. coli*. The housekeeping RNAP (top panel) is inhibited by 6S RNA during stationary phase (middle panel) and is released during outgrowth via synthesis of pRNA (bottom panel). (**B**) *In vitro* transcription (2 μM RNAP holoenzyme) of pRNA using 3.2 μM 6S-1 RNA as template, either in the presence of all four NTPs (lane 1) or CTP, GTP and UTP only (lane 2). Control lanes: lane 3, as in lane 1 but omission of the 6S-1 RNA template; lanes 4 and 5, chemically synthesized 5'-endlabeled pRNA 8-mer (5'-GUU CGG UC; lane 4) and 14-mer (5'-GUU CGG UCA AAA CU; lane 5) used as size markers. Omission of ATP (lane 2) results in synthesis of short pRNA (8-mers) because 6S-1 RNA encodes four consecutive A residues at pRNA positions 9-12 (see sequence at the bottom); our observation of 9- in addition to 8-mers despite the absence of ATP might be explained by RNAP adding a no-templated residue to the 3'-end. RNA products were separated by 20% denaturing PAGE. (**C**) Annealing of chemically synthesized pRNAs (8- or 14-mers) to 6S-1 RNA. Asterisks denote the radiolabeled RNA species (6S-1 RNA, 14-mer or 8-mer). Lanes 1 and 2: 5'-endlabeled 6S-1 RNA without (lane 1) or after the annealing step (lane 2) at 95°C followed by stepwise cooling (for details, see Materials and Methods); lane 3: 5'-endlabeled 6S-1 RNA (100 nM unlabeled 6S-1 RNA and trace amounts, $<$ 1 nM, of 5'-endlabeled 6S-1 RNA) with pRNA 14-mer (1 μM) pre-annealed as just mentioned; lanes 4 to 6: annealing (95°C) of 100 nM unlabeled 6S-1 RNA, trace amounts ($<$ 1 nM) of 5'-endlabeled pRNA 14-mer, plus 100 nM (lane 4), 200 nM (lane 5) or 500 nM (lane 6) unlabeled 14-mer; lane 7, as lane 3, but using the pRNA 8-mer instead of the 14-mer; lanes 8 to 10: as lanes 4 to 6, but using the pRNA 8-mer. Samples were analyzed by 9% native PAGE. (**D**) *In vitro* transcription of pRNA from 6S-1 RNA (1 μM) as template using 1 μM RNAP holoenzyme. Lanes 1 to 3: as lanes 5, 4 and 1, respectively, in panel B; lane 4: as lane 3, but subjecting 6S-1 RNA to the annealing procedure before transcription; lanes 5 to 10: 2 μM (lane 5), 4 μM (lane 6), 20 μM (lane 7) pRNA 14-mer, or 2 μM (lane 8), 4 μM (lane 9), 20 μM (lane 10) pRNA 8-mer were subjected to the annealing procedure in the presence of 2 μM 6S-1 RNA in a final volume of 5 μl 1 x TE buffer; then, 2 μl of 5 x activity buffer and 0.5 μl RNAP were added and samples were incubated for 30 min at 37°C before addition of nucleotides and transcription for 1 h at 37°C (final volume 10 μl). RNA products were separated by 20% denaturing PAGE. (**E**) Trace amounts ($<$ 1 nM) of 5'-endlabeled 6S-1 RNA and 2.5 μM unlabeled 6S-1 RNA were subjected to the annealing procedure in a volume of 4 μl (see Materials and Methods); then, 1 μl of a heparin solution (400 ng/μl) and 2 μl 5 x activity buffer were added and samples were kept at 37°C; then 1.06 μl RNAP holoenzyme (8 μg/μl) was added and samples were incubated for 30 min at 37°C, followed by addition of 2 μl nucleotide solution (all four NTPs: lanes 2 to 7; only CTP, GTP and UTP: lanes 9 to 14) or ddH_2O (lanes 15-21) (final volume 10 μl;f. c. RNAP: 2 μM; f. c. 6S-1 RNA: 1 μM). After transcription at 37°C for the time period indicated above each lane, samples were analyzed by 7.5% native PAGE.

Fig. 2 Role of pRNA length and pRNA:6S-1 RNA duplex stability (**A**) Trace amounts ($<$ 1 nM) of 5'-endlabeled 6S-1 RNA and 1.7 μM unlabeled 6S-1 RNA, either alone (lane 5) or in the presence of 17 μM pRNA 14-mer (lane 6), 13-mer (5'-GUU CGG UCA AAA C, lane 7) or 12-mer (5'-GUU CGG UCA AAA, lane 8) were subjected to the annealing procedure in a volume of 6 μl 1 x TE buffer; lanes 1–4: as lanes 5–8, but before gel loading 1 μl of a heparin solution (400 ng/μl) and 2 μl 5 x activity buffer were added and samples were kept at 37°C; then 1.06 μl RNAP holoenzyme (8 μg/μl) was added and samples were incubated for 30 min at 37°C followed by gel loading. (**B**) Lanes 1 and 2: as lane 6 in panel A, except that a pRNA 8-mer and an LNA 8-mer instead of the pRNA 14-mer was used; lanes 3 and 4: as lane 2 in panel A, except that a pRNA 8-mer and an LNA 8-mer instead of the pRNA 14-mer was used; lanes 5 and 6: as lanes 1 and 3 except that 1.7 μM 5'-endlabeled pRNA 8-mer and 17 μM unlabeled 6S-1 RNA were subjected to the annealing procedure in a volume of 6 μl 1 x TE buffer; lane 7: 5'-endlabeled pRNA 8-mer loaded as size marker. (**C**) Lanes 1 to 4 correspond to lanes 6, 1, 2, 5, respectively, in panel A; lanes 5 to 7: as lanes 5 to 7 in panel B, but using 5'-endlabeled pRNA 14-mer. 7.5% native PAA gels were used in panels A to C.

Fig. 3 pRNA induces structural changes in 6S-1 RNA. (**A**) Structure probing using 5'-endlabeled 6S-1 RNA. Lane 1: 5'-endlabeled 6S-1 RNA directly loaded onto the gel; lane 2: alkaline hydrolysis ladder of 6S-1 RNA; lane 3: limited RNase T1 digest under denaturing conditions; lanes 4 and 5: free 6S-1 RNA subjected to the annealing procedure (lane 5) or not (lane 4) before lead probing; lane 6: 10 pmol 5'-endlabeled 6S-1 RNA and 100 pmol pRNA 14-mer were subjected to the annealing procedure in 6 μl 1 x TE buffer before lead probing. (**B**) Structure probing using 3'-endlabeled 6S-1 RNA. Lanes 1 to 3, 6 and 7: as lanes 1 to 3, 5 and 6, respectively, in panel A; lanes 4 and 5: as lanes 6 and 7, but RNase T1 cleavage under native conditions. (**C**) Structure probing using 3'-endlabeled 6S-1 RNA. For lanes 1 to 5, see panel B; lanes 6 and 7, but cleavage by RNase V1. (**D**) Structure probing of the 5'-endlabeled circularly permuted 6S-1 RNA variant (Fig. S1). Lanes 1 to 7 correspond to lanes 1 to 7 in panel C; lanes 8 and 9 correspond to lanes 6 and 7 in panel B. For details of probing reactions, see Supplementary Material. Asterisks in panels B to D mark the regions of band compression. (**E**) Structural model for the pRNA (14-mer or LNA 8-mer, see Fig. S2)-induced structural rearrangement of the 6S-1 RNA core region (grey-shaded in the 6S-1 RNA secondary structure at the top). The open central bulge structure (top) is thought to be in equilibrium with a structure in which a weak hairpin is (transiently) formed in the lower bulge region (bottom; [6]).

Fig. 4 *In silico* prediction of pRNA-induced rearrangements in the structural core of bacterial 6S RNAs. The figure shows a phylogenetic tree of 6S RNA sequences (obtained from `Rfam`, ***RF00013 seed.stk*** [16]), using the program SplitsTree [26]. Stabilities of the predicted extended hairpin structures are differentiated by the colour code ranging from -0.40 kcal/mol (dark blue) to -9.50 kcal/mol (red). The potential to undergo the central bulge collapse is indicated by squares in the case of energy values below -1.30 kcal/mol (circled otherwise). Hairpin stabilities are relatively uniform within bacterial branches. γ-proteobacteria have the potential to form the most stable hairpins. Predicted structural rearrangements of 6S RNAs with known pRNA sequences (*B. subtilis* 6S-1 RNA, *E. coli* and *Aquifex aeolicus* 6S RNA) and their position in the tree are indicated. Input and output files can be obtained at the Supplement web page (`http://bioinf.pharmazie.uni-marburg.de/supplements/136`).

Fig. 5 Effect of rifampicin on pRNA synthesis and 6S-1 RNA stability. (**A**) Analysis of 6S-1 RNA steady-state levels following outgrowth from stationary phase by Northern blots of cellular RNA extracted at different time points after induction of outgrowth, either in the absence of rifampicin (lanes 2–9) or in the presence of rifampicin (100 μg/ml; lanes 10–17). Lane 1: RNA extracted from stationary cells immediately before 1:5 dilution in fresh LB medium. An antisense 6S-1 RNA, internally labeled with digoxigenin-UTP (top panel), or a 5'-digoxigenin-labeled LNA/DNA mixmer complementary to the pRNA 14-mer (bottom panel) were used as Northern probes; for details see [22]. (**B**) New model of pRNA length-controlled release of RNAP from 6S-1 RNA. For details, see text.

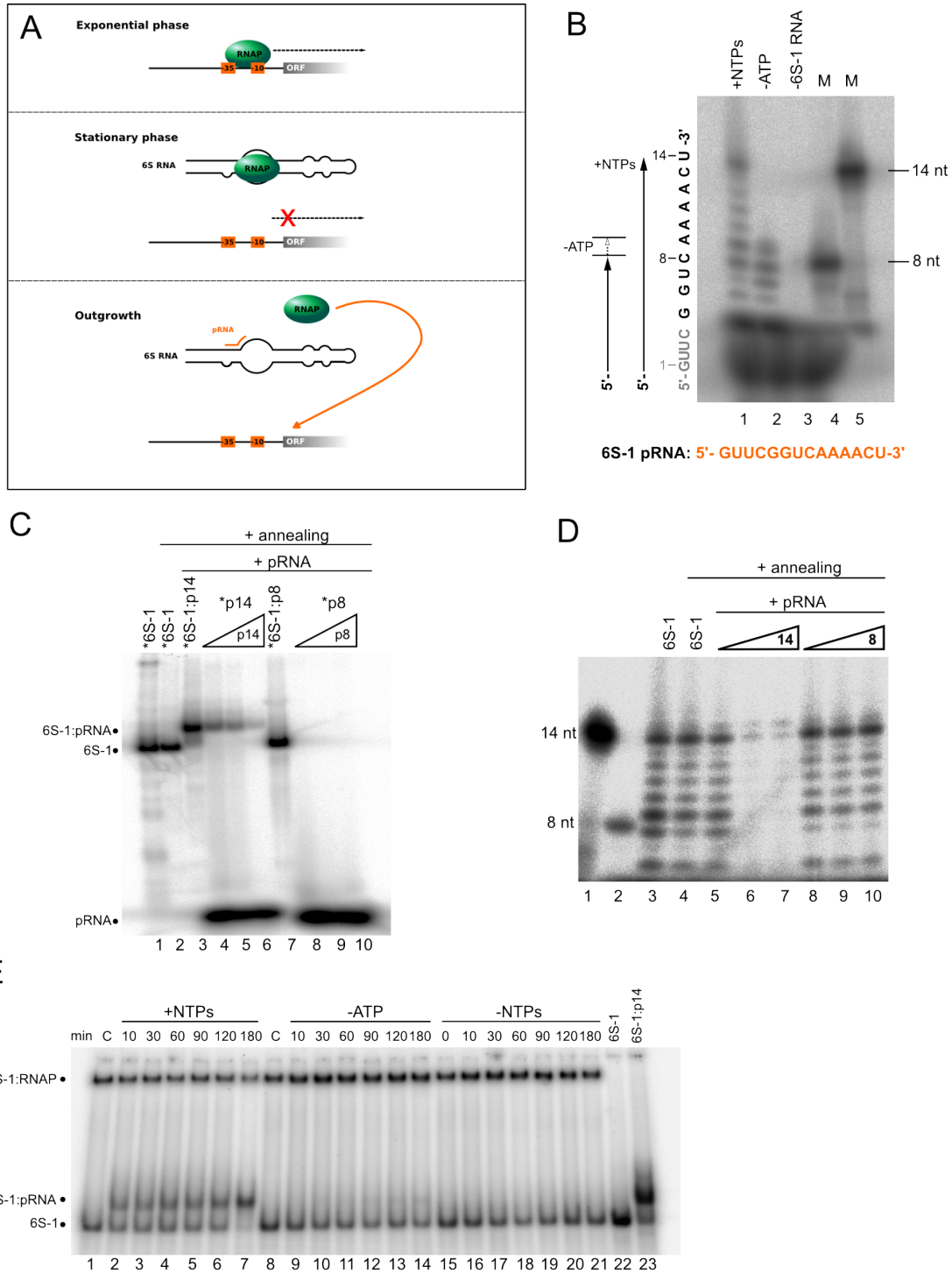
A
Exponential phase
RNAP
-35
-10
ORF
Stationary phase
6S RNA
RNAP
ORF
Outgrowth
RNAP
pRNA
6S RNA
ORF
B
+NTPs
-ATP
-6S-1 RNA
M M
+NTPs
-ATP
14
8
1
5'- G U C A A A A C U -3'
5'- G U U C
5'-
5'-
14 nt
8 nt
1 2 3 4 5
6S-1 pRNA: 5'- GUUCGGUCAAAACU-3'
C
+ annealing
+ pRNA
*6S-1
*6S-1
*6S-1:p14
*p14
p14
*6S-1:p8
*p8
p8
6S-1:pRNA
6S-1
pRNA
1 2 3 4 5 6 7 8 9 10
D
+ annealing
+ pRNA
6S-1
6S-1
14
8
14 nt
8 nt
1 2 3 4 5 6 7 8 9 10
E
+NTPs
-ATP
-NTPs
6S-1
6S-1:p14
min C 10 30 60 90 120 180 C 10 30 60 90 120 180 0 10 30 60 90 120 180
6S-1:RNAP
6S-1:pRNA
6S-1
1 2 3 4 5 6 7 8 9 10 11 12 13 14 15 16 17 18 19 20 21 22 23

Fig. 1

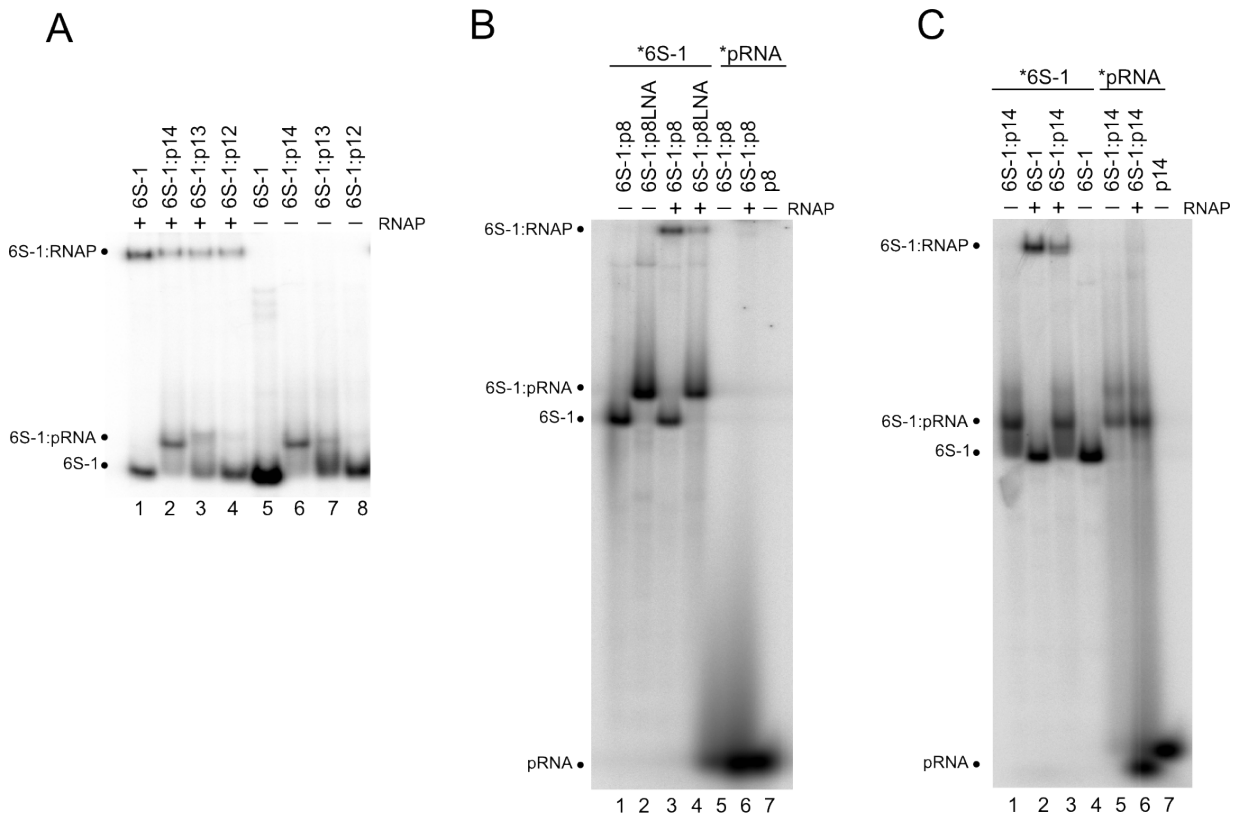
A
+ 6S-1
+ 6S-1:p14
+ 6S-1:p13
+ 6S-1:p12
– 6S-1
– 6S-1:p14
– 6S-1:p13
– 6S-1:p12
RNAP
6S-1:RNAP
6S-1:pRNA
6S-1
1 2 3 4 5 6 7 8
B
*6S-1
*pRNA
– 6S-1:p8
– 6S-1:p8LNA
+ 6S-1:p8
+ 6S-1:p8LNA
– 6S-1:p8
+ 6S-1:p8
– p8
RNAP
6S-1:RNAP
6S-1:pRNA
6S-1
pRNA
1 2 3 4 5 6 7
C
*6S-1
*pRNA
– 6S-1:p14
+ 6S-1
+ 6S-1:p14
– 6S-1
– 6S-1:p14
+ 6S-1:p14
– p14
RNAP
6S-1:RNAP
6S-1:pRNA
6S-1
pRNA
1 2 3 4 5 6 7

Fig. 2

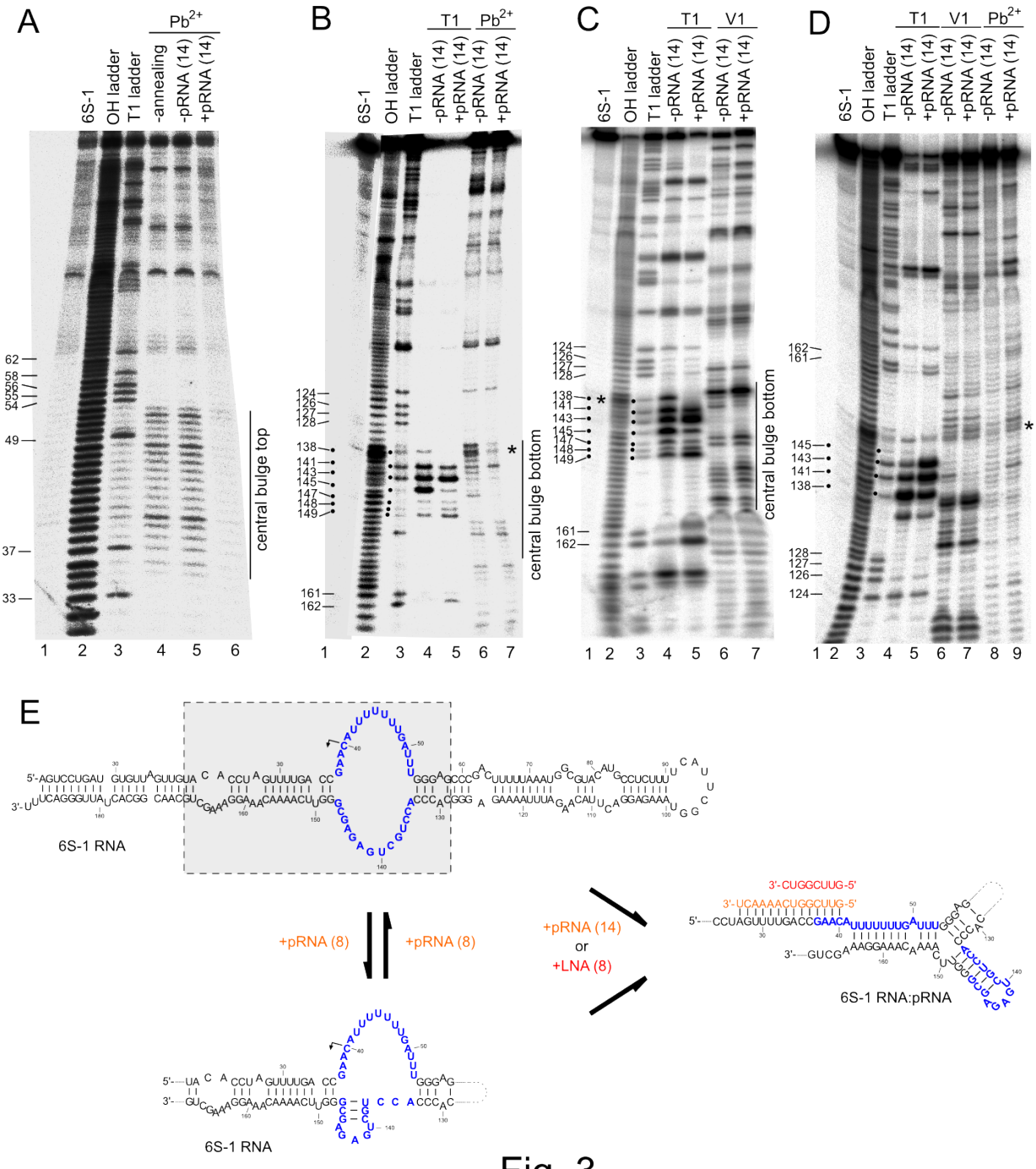
A
B
C
D
E
6S-1
OH ladder
T1 ladder
-annealing
-pRNA (14)
+pRNA (14)
Pb2+
T1
V1
central bulge top
central bulge bottom
6S-1 RNA
+pRNA (8)
+pRNA (14)
or
+LNA (8)
3'-CUGGCUUG-5'
3'-UCAAAACUGGCUUG-5'
6S-1 RNA:pRNA

Fig. 3

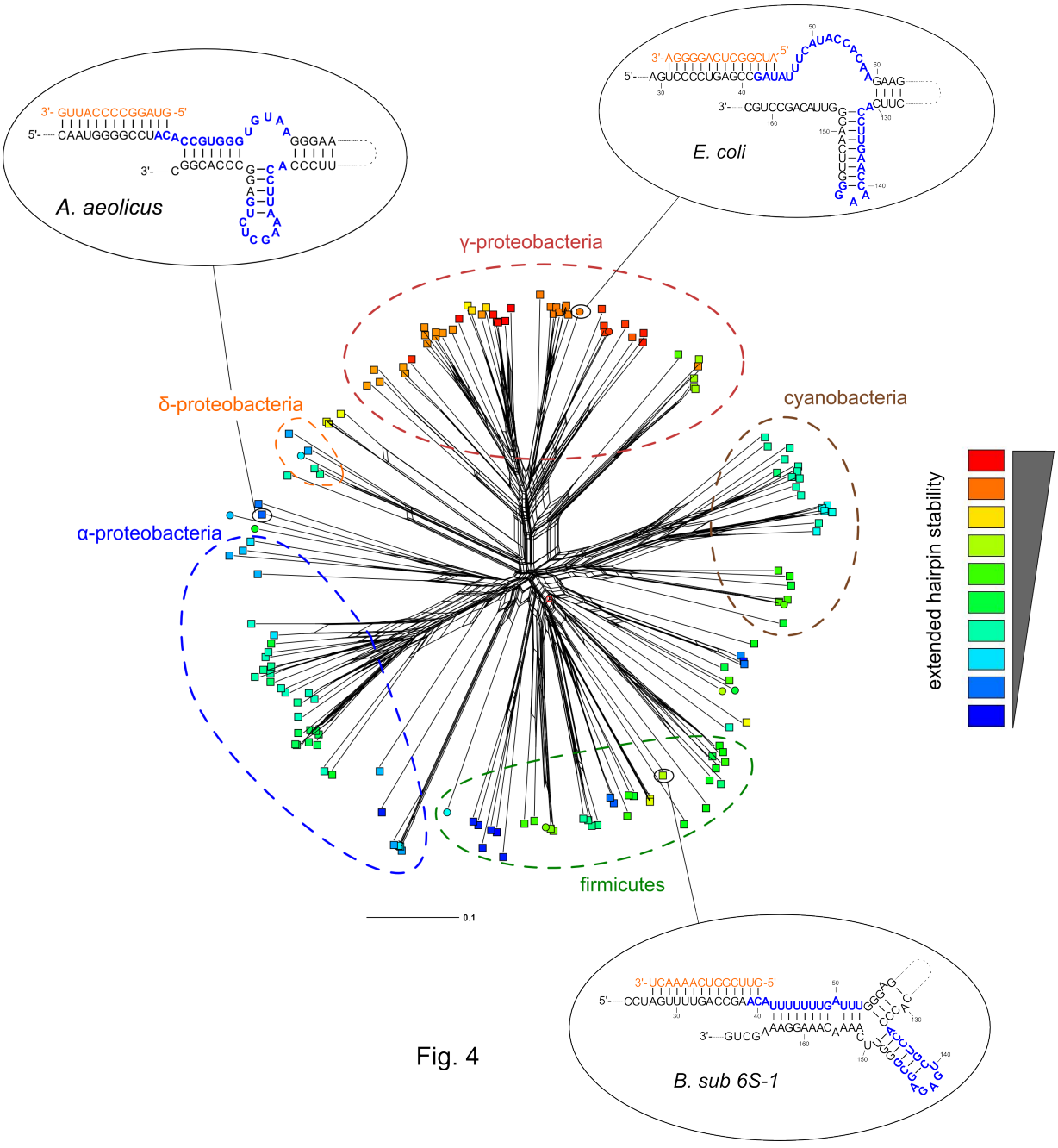
A. aeolicus
E. coli
γ-proteobacteria
δ-proteobacteria
cyanobacteria
α-proteobacteria
firmicutes
extended hairpin stability
0.1
B. sub 6S-1

Fig. 4

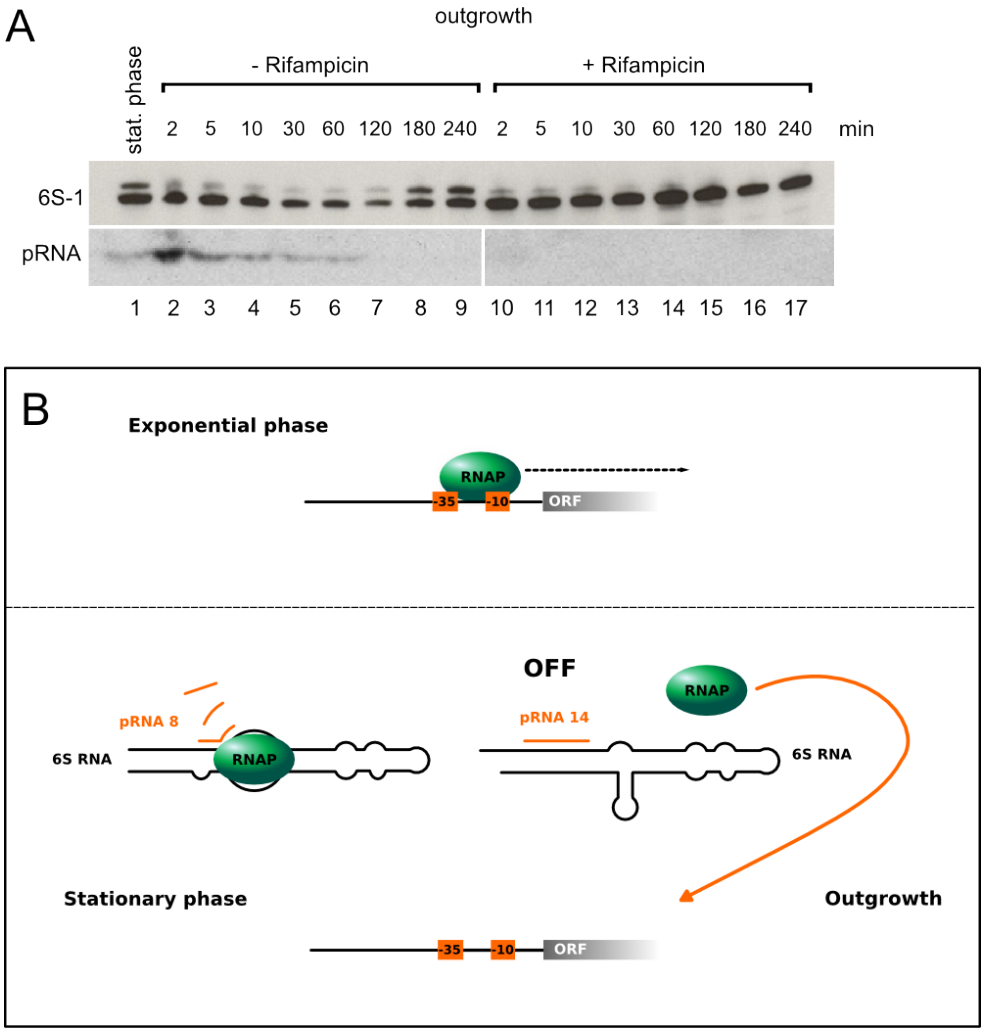
A
outgrowth
stat. phase
- Rifampicin
+ Rifampicin
2 5 10 30 60 120 180 240 2 5 10 30 60 120 180 240 min
6S-1
pRNA
1 2 3 4 5 6 7 8 9 10 11 12 13 14 15 16 17
B
Exponential phase
RNAP
-35
-10
ORF
OFF
pRNA 8
6S RNA
RNAP
pRNA 14
RNAP
6S RNA
Stationary phase
Outgrowth
-35
-10
ORF

Fig. 5

Supplementary material

Structure probing

6S-1 RNA was transcribed *in vitro* using T7 run-off transcription. The DNA template for transcription was generated by PCR from genomic *B. subtilis* 168 DNA (6S-1: primers 5'-TAA TAC GAC TCA CTA TAG GAG TCC TGA TGT GTT AGT TGT ACA CCT AG-3' and 5'-AAA GTC CCA ATA GTG CCG TTG-3'; 6S-2: primers 5'-TAA TAC GAC TCA CTA TAG GAA GCT ACT TTG TGC GTA TTG TTA ATT AAG-3' and 5'-ATT TCC GAA AAG GAA ATG GCT TTC-3'; T7 promoter sequence underlined). Transcription reactions coantained 8 mM guanosine as initiator nucleoside to generate transcripts with 5'-OH ends for direct 5'-endlabeling.For 5'-endlabeling, 60 pmol 6S-1 RNA, 10 U T4 polynucleotidkinase (PNK, Fermentas) and 3 μl of (γ^{32}P)-ATP (3000 Ci/mmol) were incubated in a volume of 15 μl 1 x PNK buffer (Fermentas) for 90 min at 37°C.

RNA was purified by gel extraction overnight in 1 M NaOAc pH 4.9 at 8°C and ethanol precipitation prior to probing. For all probing experiments, 10 pmol of unlabeled RNA together with trace amounts (20,000 Cerenkov cpm) of labeled RNA were used. Probed RNA was separated on thin (0.5 mm) 12% polyacrylamide gels containing 8 M urea and analyzed with a Bio-Imaging Analyzer FLA-3000-2R (Fujifilm). RNase T1 and V1 digestions were performed under native conditions (50 mM HEPES pH 7.9, 4.5 mM $Mg(OAc)_2$, 100 mM NH_4OAc). RNase T1 digestion was further conducted under denaturing conditions (20 mM Na-Citrate pH 5.0, 7 M urea, 1 mM EDTA). After preincubation of the RNA in the respective buffer for 10 min at 37°C, 0.8 U RNase T1 (0.05 U RNase V1) were added and samples were incubated in a final volume of 50 μl at 37°C for 20 min (7 min for RNase V1). Reactions were stopped by addition of 15 μl 0.45 M NH_4OAc and ethanol precipitation.

Lead cleavage was performed in PA buffer (50 mM Tris-HCl pH 7.5, 100 mM NH_4Cl). After preincubation of the RNA in PA buffer for 10 min at 37°C, 250 μM $Pb(OAc)_2$ was added and samples were incubated in a final volume of 100 μl for 3 min at 37°C. Reactions were stopped by addition of 20 μl 2 mM EDTA, followed by ethanol precipitation.

Alkaline hydrolysis of RNA was performed in alkaline buffer (50 mM $NaHCO_3$) in a volume of 13 μl for 8 min at 100°C. Reactions were stopped by adding 13 μl 10 mM EDTA, followed by ethanol precipitation.

For 3'-endlabeling, we employed a 6S-1 RNA carrying an HDV ribozyme at its 3'-end in order to generate homogeneous 3'-ends derived from HDV *cis*-cleavage. For this purpose, the *bsrA* gene was amplified by PCR (5'-AAA GTC CCA ATA GTG CCG TTG-3' and 5'-CAG GAA TTC TAA TAC GAC TCA CTA TAG GAG TCC TGA TGT GTT AGT TGT ACA CCT AG-3'). Next, the HDV coding sequence was amplified (5'-CAA CGG CAC TAT TGG GAC TTT GGC CGG CAT GGT CCC AG-3' and 5'-GGC CAG TGC CAA GCTT GTC CCA TTC GCC ATT ACC GAG-3') and both PCR products were combined for overlap extension PCR resulting in the final T7-bsrA-HDV product which was cloned into the pUC18 vector using EcoRI and HindIII. After T7 transcription, the released 6S-1 RNA was eluted from the gel and 2',3'-cyclic phosphates were removed using 20 U T4 PNK in 100 mM imidazole pH 6.0, 100 μM ATP, 10 mM $MgCl_2$ 0.07% (v/v) 2-mercaptoethanol and 20 ng/μl BSA (final volume 100 μl, 6 h at 37°C). 3'-endlabeling was performed using 10 U T4 RNA ligase (Fermentas) and 3 μl of (5'-^{32}P)pCp (3000 Ci/mmol) in a final volume of 15 μl in 1 x ligation buffer (Fermentas) overnight at 10°C before probing was performed as described above.

Supplementary figure legends

Fig. S1 Structure and function of a circularly permuted 6S-1 RNA. (**A**) Construction strategy: two copies of *bsrA* encoding 6S-1 RNA were inserted into pUC18 via EcoRI/HindIII and HindIII to generate plasmid pBB6. Using pBB6 as template, a PCR product for T7 transcription was generated using primers bsrAcpT7 fw (5'-TAA TAC GAC TCA CTA TAG GTA AAG AGG ACT TAC AAG ATT TAA AA) and bsrAcprev (5'-GAA TGA AAA GAG GCA TGT ACG). (**B**) Secondary structure of wild-type 6S-1 RNA (6S-1wt) and the circularly permuted mutant variant (6S-1cp). Numbering of 6S-1 cp was as for the wild-type 6S-1 RNA. The HindIII site served as a linker to connect the original 5'- and 3'-ends of the wild-type RNA. The triangle depicts the natural maturation site of 6S-1 RNA; black arrows mark the start for pRNA synthesis. (**C**) Capability of 6S-1 cp RNA to bind to the σ^A-RNAP and to form the rearranged structure upon binding of the pRNA 14-mer. Samples in lanes 1 to 4 were prepared as lanes 2, 3, 4 and 1, respectively, of Fig. D.

Fig. S2 The all-LNA 8-mer (5'-GUU CGG UC) is able to induce the structural rearrangement in 6S-1 RNA. Samples loaded in lanes 1 to 5 were prepared as lanes 1 to 5 in Fig. B.

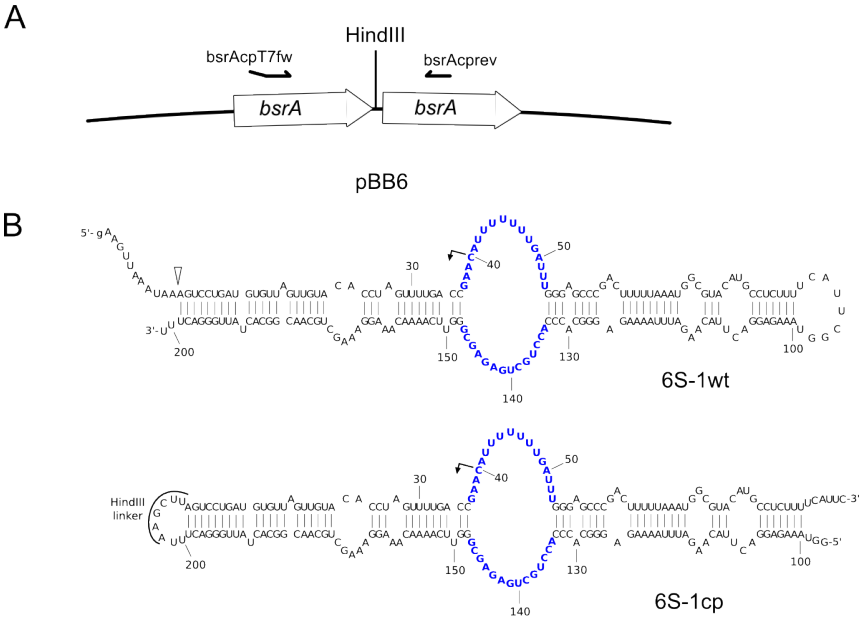
A
HindIII
bsrAcpT7fw
bsrAcprev
bsrA
bsrA
pBB6
B
6S-1wt
HindIII
linker
6S-1cp
C
+RNAP
6S-1cp
6S-1cp:p14
6S-1cp
6S-1cp:p14
6S-1:RNAP
6S-1:pRNA
6S-1
1 2 3 4

Fig. S1

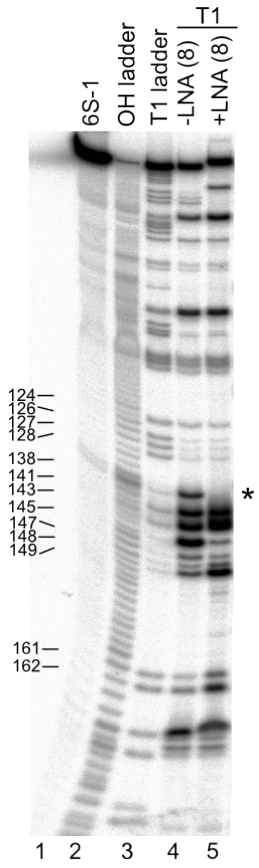
6S-1
OH ladder
T1 ladder
T1
-LNA (8)
+LNA (8)
124
126
127
128
138
141
143
145
147
148
149
161
162
*
1 2 3 4 5

Fig. S2

F

ALIGNMENT OF BACTERIAL 6S RNAS

The known 6S RNA sequences were downloaded from the Rfam database (Griffiths-Jones et al., 2003): RF00013_seed.stk and we added the sequences from the Aquificales manually. The file in Stockholm format was modified with a ruler to give easier access to the alignment.

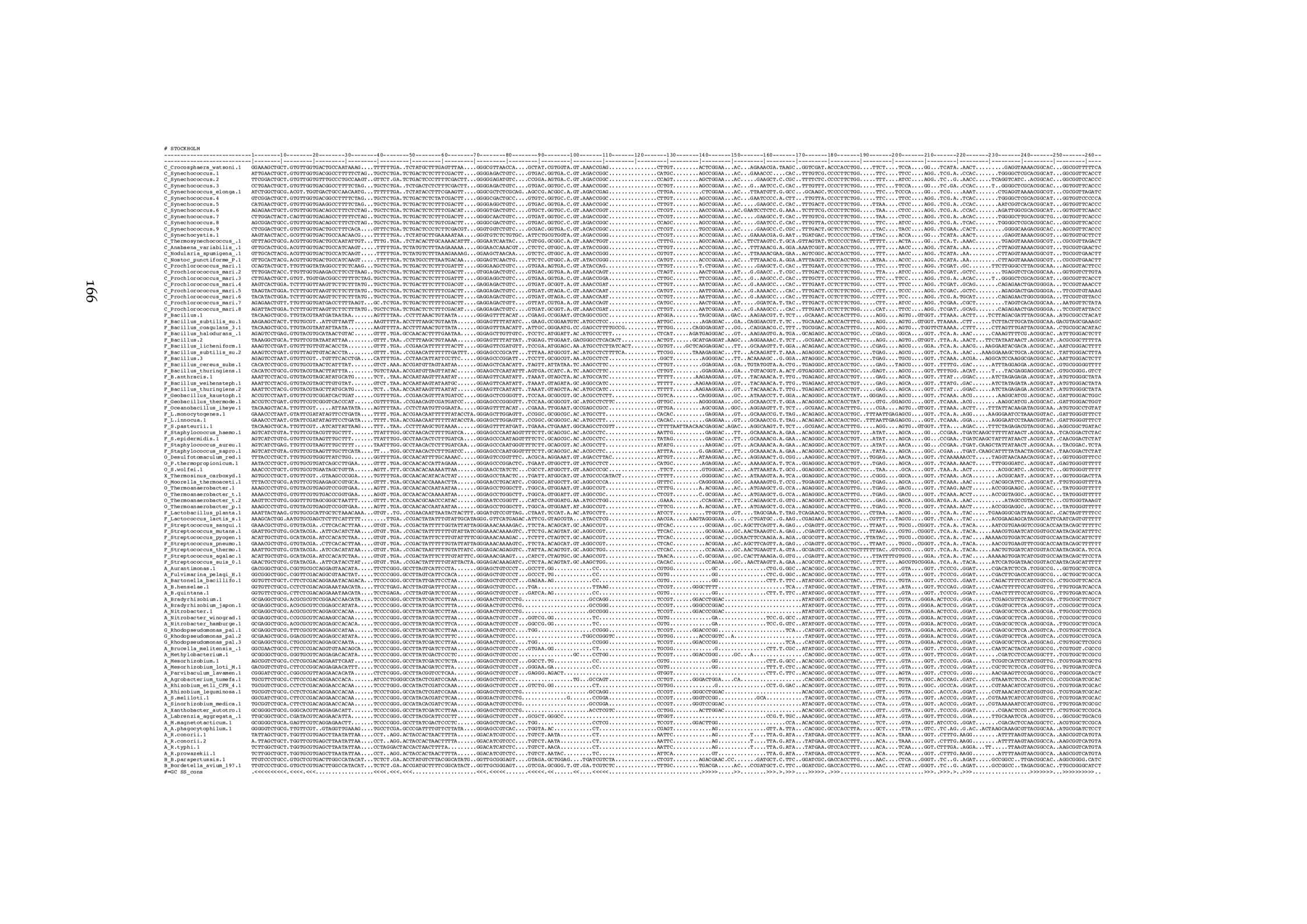
STOCKHOLM
C_Crocosphaera_watsonii.1
C_Synechococcus.1
C_Synechococcus.2
C_Synechococcus.3
C_Synechococcus_elonga.1
C_Synechococcus.4
C_Synechococcus.5
C_Synechococcus.6
C_Synechococcus.7
C_Synechococcus.8
C_Synechococcus.9
C_Synechocystis.1
C_Thermosynechococcus_.1
C_Anabaena_variabilis_.1
C_Nodularia_spumigena_.1
C_Nostoc_punctiforme_P.1
C_Prochlorococcus_mari.1
C_Prochlorococcus_mari.2
C_Prochlorococcus_mari.3
C_Prochlorococcus_mari.4
C_Prochlorococcus_mari.5
C_Prochlorococcus_mari.6
C_Prochlorococcus_mari.7
C_Prochlorococcus_mari.8
F_Bacillus.1
F_Bacillus_subtilis_su.1
F_Bacillus_coagulans_3.1
F_Bacillus_halodurans_.1
F_Bacillus.2
F_Bacillus_licheniform.1
F_Bacillus_subtilis_su.2
F_Bacillus.3
F_Bacillus_cereus_subs.1
F_Bacillus_thuringiens.1
F_B.anthracis.1
F_Bacillus_weihenstleph.1
F_Bacillus_thuringiens.2
F_Geobacillus_kaustoph.1
F_Geobacillus_thermode.1
F_Oceanobacillus_iheye.1
F_L.monocytogenes.1
F_L.innocua.1
F_S.pasteurii.1
F_Staphylococcus_haemo.1
F_S.epidermidis.1
F_Staphylococcus_aureu.1
F_Staphylococcus_sapro.1
O_Desulfotomaculum_red.1
O_P.thermopropionicum.1
O_S.wolfei.1
X_Thermosinus_carboxyd.1
O_Moorella_thermoaceti.1
O_Thermoanaerobacter.1
O_Thermoanaerobacter_t.1
O_Thermoanaerobacter_t.2
O_Thermoanaerobacter_p.1
F_Lactobacillus_planta.1
F_Lactococcus_lactis_s.1
F_Streptococcus_sangui.1
F_Streptococcus_mutans.1
F_Streptococcus_pyogen.1
F_Streptococcus_pneumo.1
F_Streptococcus_thermo.1
F_Streptococcus_agalac.1
F_Streptococcus_suis_0.1
A_Aurantimonas.1
A_Fulvimarina_pelagi_H.1
A_Bartonella_bacillifo.1
A_B.henselae.1
A_B.quintana.1
A_Bradyrhizobium.1
A_Bradyrhizobium_japon.1
A_Nitrobacter.1
A_Nitrobacter_winograd.1
A_Nitrobacter_hamburge.1
G_Rhodopseudomonas_pal.1
G_Rhodopseudomonas_pal.2
G_Rhodopseudomonas_pal.3
A_Brucella_melitensis_.1
A_Methylobacterium.1
A_Mesorhizobium.1
A_Mesorhizobium_loti_M.1
A_Parvibaculum_lavamen.1
A_Agrobacterium_tumefa.1
A_Rhizobium_etli_CFN_4.1
A_Rhizobium_leguminosa.1
A_S.meliloti.1
A_Sinorhizobium_medica.1
A_Xanthobacter_autotro.1
A_Labrenzia_aggregata_.1
A_M.magnetotacticum.1
A_A.phagocytophilum.1
A_R.conorii.1
A_R.conorii.2
A_R.typhi.1
A_R.prowazekii.1
B_B.parapertussis.1
B_Bordetella_avium_197.1
#=GC SS_cons

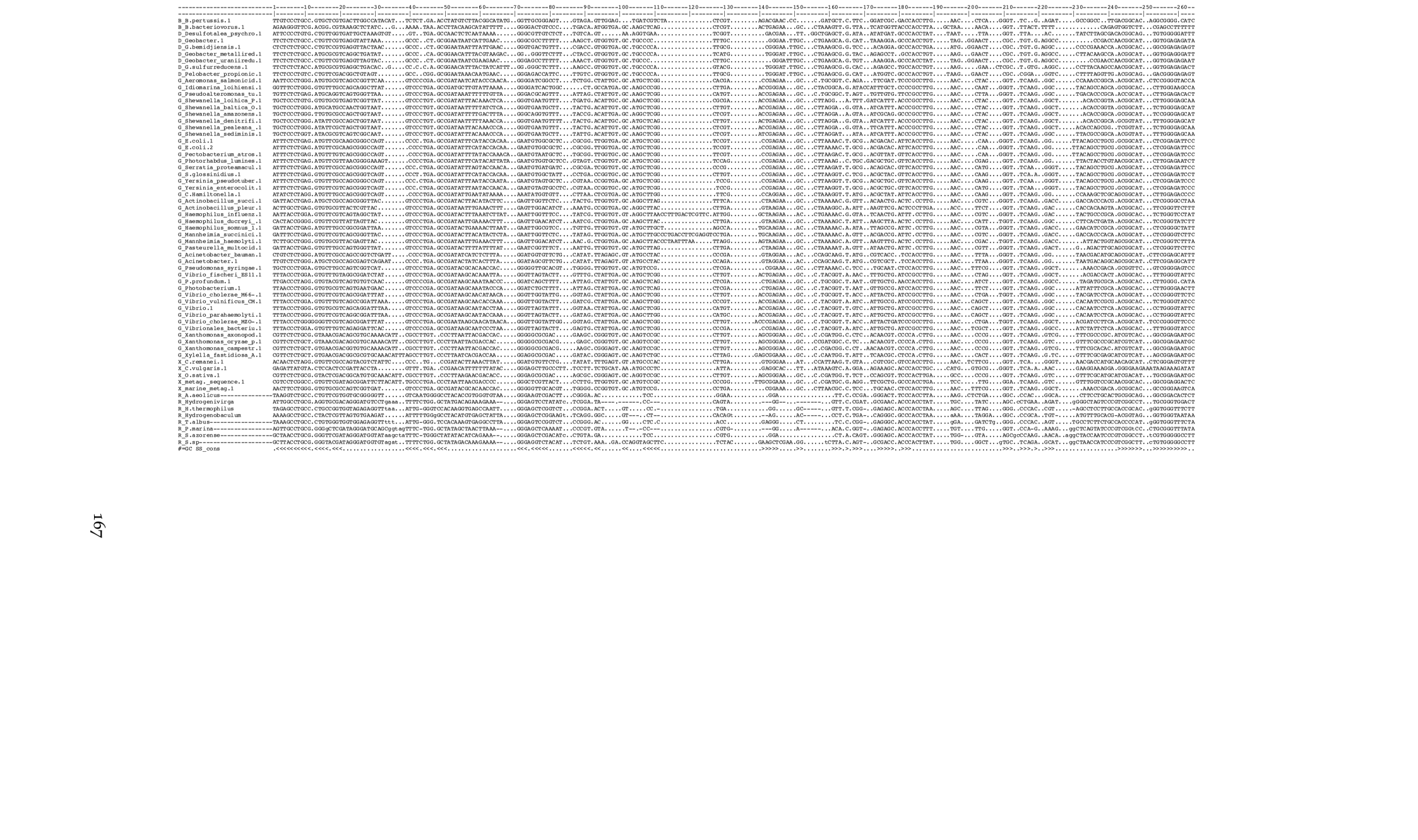

G

SCIENTIFIC CURRICULUM VITAE

curriculum vitae

Personal

Name	Beckmann
First name	Benedikt
Date of Birth	September 15th, 1980
Place of Birth	Ratingen, Germany
Status	married

Education

since October 2006	**Ph.D. studies**, *Institute of Pharmaceutical Chemistry, Philipps University Marburg*.
2002–2006	**Studies in biology (Diploma)**, *Johannes-Gutenberg University Mainz*. Main topics: Genetics, Biophysics, Biochemistry

Diploma thesis

title	*Heterologous expression, purification and biochemical characterization of the eukaryotic endonucleases EGL-1 and DNaseIIα*
supervisors	Prof. Dr. T. Hankeln (Johannes Gutenberg Universität Mainz) and Prof. Dr. A. Pingoud (Justus Liebig Universität Giessen)

Ph.D. thesis

title	*The mechanism of pRNA-mediated release of RNA polymerase from Bacillus subtilis 6S-1 RNA*
supervisor	Prof. Dr. R. K. Hartmann (Philipps Universität Marburg)

Experience

Field of interest	Molecular biology, RNA biochemistry, bioinformatics
Graduate school	Student spokesperson of the International Research Training Group IRTG 1384 "Enzymes and multienzyme-complexes acting on nucleic acids"
Teaching	Supervision of students practical courses and undergraduate students lab courses

Scientific skills and methods

Molecular biology	Work with genetically modified organisms (bacteria and eukaryotic cell lines); standard DNA techniques (preparation/modification); cloning; PCR
RNA methods	*In vitro* transcription; RNA structure probing; tandem affinity purification of tagged RNA; analysis of sRNA-protein binding; detection of very short RNAs (siRNAs and smaller) by Northern blotting and LNAs; siRNA knockdown experiments; ncRNA analysis in bacteria
Protein Methods	Recombinant and native protein expression and purification using FPLC based chromatography, Western blotting, construction of mutant proteins
Bioinformatics	Analysis and data mining of deep sequencing data; Perl/BioPerl and database (MySQL) programming

• ☎ +49-6421-2825844 • ✉ benedikt.beckmann@staff.uni-marburg.de

Scientific achievements

Poster presentations

Conference Jaques-Monod "RNA at the center of gene regulation"; April 2009, Roscoff (France)

5th Meeting of the GBM Study Section "RNA-Biochemistry"; September 2008, Kassel (Germany)

International Symposium "RNA Ligand Interactions" of the SFB 579; September 2007, Frankfurt (Germany)

Oral presentations

EMBO|EMBL Symposium "The non-coding genome"; Oktober 2010, Heidelberg (Germany)

15th Annual meeting of the RNA society; June 2010, Seattle (USA)

9th NordForsk Meeting; Oktober 2009, Reykjavik (Iceland)

International meeting of the DFG priority program SPP 1258 "Regulatory RNA in prokaryotes"; June 2009, Berlin (Germany)

Meeting of the DFG priority program SPP 1258 "Sensory and regulatory RNAs in prokaryotes"; September 2008, Kassel (Germany)

Workshop "Protein-nucleic acids interactions" of the IRTG 1384; June 2007, Suzdal (Russia)

Publications

Cymerman IA, Chung I, **Beckmann BM**, Bujnicki JM and Meiss G: EXOG, a novel paralog of Endonuclease G in higher eukaryotes. *Nucleic Acids Res., 2008; 36(4):1369-79*

Beckmann BM, Grünweller A, Weber MHW and Hartmann RK: Northern blot detection of endogenous small RNAs (14 nucleotides) in bacterial total RNA extracts. *Nucleic Acids Res., 2010; 38(14):e147*

Beckmann BM, Grünweller A, Hartmann RK. "Northern Blot Detection of Small RNAs". In: Handbook of RNA Biochemistry 2nd Edition (eds. R. K. Hartmann, A. Bindereif, A. Schön, E. Westhof), WILEY-VCH, Weinheim, Germany; year of publication: 2011

Merkel OM, Beyerle A, **Beckmann BM**, Hartmann RK, Stöger T and Kissel T: Off-target effects in non-viral siRNA delivery - A study on the effect of polymer genomics on *in vitro* cell culture models. (*Submitted*)

Beckmann BM, Burenina, OY, Hoch PG, Sharma CM, Kubareva EA and Hartmann RK: *In vivo* and *in vitro* analysis of 6S RNA-templated short transcripts in *Bacillus subtilis*. (*In revision: 2010RNABIOL0153*)

Languages

German	**Native**	
English	**Very good**	*Ongoing experience in reading english literature, giving talks and writing proposals.*
French	**Good**	*School education for four years.*

Benedikt Beckmann, Marburg, November 10th 2010

BIBLIOGRAPHY

H Aiba. Mechanism of RNA silencing by Hfq-binding small RNAs. *Curr Opin Microbiol*, 10(2):134–139, Apr 2007.

H T Allawi and J SantaLucia. Thermodynamics and NMR of internal G.T mismatches in DNA. *Biochemistry*, 36(34):10581–10594, Aug 1997.

S F Altschul, W Gish, W Miller, E W Myers, and D J Lipman. Basic local alignment search tool. *J Mol Biol*, 215(3):403–410, Oct 1990.

Y Ando, S Asari, S Suzuma, K Yamane, and K Nakamura. Expression of a small RNA, BS203 RNA, from the yocI-yocJ intergenic region of Bacillus subtilis genome. *FEMS Microbiol Lett*, 207(1): 29–33, Jan 2002.

I M Axmann, J Holtzendorff, B Voss, P Kensche, and W R Hess. Two distinct types of 6S RNA in Prochlorococcus. *Gene*, 406 (1-2):69–78, Dec 2007.

P Babitzke and T Romeo. CsrB sRNA family: sequestration of RNA-binding regulatory proteins. *Curr Opin Microbiol*, 10(2): 156–163, Apr 2007.

J E Barrick, N Sudarsan, Z Weinberg, W L Ruzzo, and R R Breaker. 6S RNA is a widespread regulator of eubacterial RNA polymerase that resembles an open promoter. *RNA*, 11 (5):774–784, May 2005.

H C Birnboim and J Doly. A rapid alkaline extraction procedure for screening recombinant plasmid DNA. *Nucleic Acids Res*, 7 (6):1513–1523, Nov 1979.

M Bouvier, C M Sharma, F Mika, K H Nierhaus, and J Vogel. Small RNA binding to 5' mRNA coding region inhibits translational initiation. *Mol Cell*, 32(6):827–837, Dec 2008.

S Brantl. Regulatory mechanisms employed by cis-encoded antisense RNAs. *Curr Opin Microbiol*, 10(2):102–109, Apr 2007.

G G Brownlee. Sequence of 6S RNA of E. coli. *Nat New Biol*, 229 (5):147–149, Feb 1971.

V Cameron and O C Uhlenbeck. 3'-Phosphatase activity in T4 polynucleotide kinase. *Biochemistry*, 16(23):5120–5126, Nov 1977.

A T Cavanagh, A D Klocko, X Liu, and K M Wassarman. Promoter specificity for 6S RNA regulation of transcription is determined by core promoter sequences and competition for region 4.2 of sigma70. *Mol Microbiol*, 67(6):1242–1256, Mar 2008.

P Chomczynski and N Sacchi. Single-step method of RNA isolation by acid guanidinium thiocyanate-phenol-chloroform extraction. *Anal Biochem*, 162(1):156–159, Apr 1987.

T E England and O C Uhlenbeck. 3'-terminal labelling of RNA with T4 RNA ligase. *Nature*, 275(5680):560–561, Oct 1978.

S P Faucher, G Friedlander, J Livny, H Margalit, and H A Shuman. Legionella pneumophila 6S RNA optimizes intracellular multiplication. *Proc Natl Acad Sci U S A*, 107(16):7533–7538, Apr 2010.

G E Geier and P Modrich. Recognition sequence of the dam methylase of Escherichia coli K12 and mode of cleavage of Dpn I endonuclease. *J Biol Chem*, 254(4):1408–1413, Feb 1979.

K Gerdes and E G Wagner. RNA antitoxins. *Curr Opin Microbiol*, 10(2):117–124, Apr 2007.

N Gildehaus, T Neusser, R Wurm, and R Wagner. Studies on the function of the riboregulator 6S RNA from E. coli: RNA polymerase binding, inhibition of in vitro transcription and synthesis of RNA-directed de novo transcripts. *Nucleic Acids Res*, 35(6):1885–1896, 2007.

B Görke and J Vogel. Noncoding RNA control of the making and breaking of sugars. *Genes Dev*, 22(21):2914–2925, Nov 2008.

S Gottesman. Micros for microbes: non-coding regulatory RNAs in bacteria. *Trends Genet*, 21(7):399–404, Jul 2005.

S Griffiths-Jones, A Bateman, M Marshall, A Khanna, and S R Eddy. Rfam: an RNA family database. *Nucleic Acids Res*, 31(1): 439–441, Jan 2003.

A R Gruber, R Lorenz, S H Bernhart, R Neuböck, and I L Hofacker. The Vienna RNA websuite. *Nucleic Acids Res*, 36(Web Server issue):70–74, Jul 2008.

T M Gruber and C A Gross. Multiple sigma subunits and the partitioning of bacterial transcription space. *Annu Rev Microbiol*, 57:441–466, 2003.

A Grünweller and R K Hartmann. Locked nucleic acid oligonucleotides: the next generation of antisense agents? *BioDrugs*, 21 (4):235–243, 2007.

A M Guérout-Fleury, K Shazand, N Frandsen, and P Stragier. Antibiotic-resistance cassettes for Bacillus subtilis. *Gene*, 167 (1-2):335–336, Dec 1995.

M Guillier, S Gottesman, and G Storz. Modulating the outer membrane with small RNAs. *Genes Dev*, 20(17):2338–2348, Sep 2006.

M S Guyer, R R Reed, J A Steitz, and K B Low. Identification of a sex-factor-affinity site in e. coli as gamma delta. *Cold Spring Harb Symp Quant Biol*, 45 Pt 1:135–140, 1981.

R K Hartmann, A Bindereif, A Schön, and E Westhof. *Handbook of RNA Biochemistry*. WILEY-VCH Verlag GmbH & Co. KGaG, Weinheim, 2005.

J Hindley. Fractionation of 32P-labelled ribonucleic acids on polyacrylamide gels and their characterization by fingerprinting. *J Mol Biol*, 30(1):125–136, Nov 1967.

I L Hofacker. Vienna rna secondary structure server. *Nucleic Acids Res*, 31(13):3429–3431, Jul 2003.

S Hoffmann, C Otto, S Kurtz, C M Sharma, P Khaitovich, J Vogel, P F Stadler, and J Hackermüller. Fast mapping of short sequences with mismatches, insertions and deletions using index structures. *PLoS Comput Biol*, 5(9), Sep 2009.

L M Hsu, J Zagorski, Z Wang, and M J Fournier. Escherichia coli 6S RNA gene is part of a dual-function transcription unit. *J Bacteriol*, 161(3):1162–1170, Mar 1985.

E Huntzinger, S Boisset, C Saveanu, Y Benito, T Geissmann, A Namane, G Lina, J Etienne, B Ehresmann, C Ehresmann, A Jacquier, F Vandenesch, and P Romby. Staphylococcus aureus RNAIII and the endoribonuclease III coordinately regulate spa gene expression. *EMBO J*, 24(4):824–835, Feb 2005.

D H Huson and D Bryant. Application of phylogenetic networks in evolutionary studies. *Mol Biol Evol*, 23(2):254–267, Feb 2006.

I Irnov, C M Sharma, J Vogel, and W C Winkler. Identification of regulatory RNAs in Bacillus subtilis. *Nucleic Acids Res*, Jun 2010.

F V Karginov and G J Hannon. The CRISPR system: small RNA-guided defense in bacteria and archaea. *Mol Cell*, 37(1):7–19, Jan 2010.

S W Kim, Z Li, P S Moore, A P Monaghan, Y Chang, M Nichols, and B John. A sensitive non-radioactive northern blot method to detect small RNAs. *Nucleic Acids Res*, Jan 2010.

A D Klocko and K M Wassarman. 6S RNA binding to Esigma(70) requires a positively charged surface of sigma(70) region 4.2. *Mol Microbiol*, 73(2):152–164, Jul 2009.

L Krásny and R L Gourse. An alternative strategy for bacterial ribosome synthesis: Bacillus subtilis rRNA transcription regulation. *EMBO J*, 23(22):4473–4483, Nov 2004.

L Krásny, H Tiserová, J Jonák, D Rejman, and H Sanderová. The identity of the transcription +1 position is crucial for changes in gene expression in response to amino acid starvation in Bacillus subtilis. *Mol Microbiol*, 69(1):42–54, Jul 2008.

S G Landt, E Abeliuk, P T McGrath, J A Lesley, H H McAdams, and L Shapiro. Small non-coding RNAs in Caulobacter crescentus. *Mol Microbiol*, 68(3):600–614, May 2008.

C A Lee, M J Fournier, and J Beckwith. Escherichia coli 6S RNA is not essential for growth or protein secretion. *J Bacteriol*, 161 (3):1156–1161, Mar 1985.

J Livny and M K Waldor. Identification of small RNAs in diverse bacterial species. *Curr Opin Microbiol*, 10(2):96–101, Apr 2007.

J Livny, H Teonadi, M Livny, and M K Waldor. High-throughput, kingdom-wide prediction and annotation of bacterial noncoding RNAs. *PLoS One*, 3(9), 2008.

J M Lopez, C L Marks, and E Freese. The decrease of guanine nucleotides initiates sporulation of Bacillus subtilis. *Biochim Biophys Acta*, 587(2):238–252, Oct 1979.

M Mandal and R R Breaker. Gene regulation by riboswitches. *Nat Rev Mol Cell Biol*, 5(6):451–463, Jun 2004.

M Margulies, M Egholm, W E Altman, S Attiya, J S Bader, L A Bemben, J Berka, M S Braverman, Y J Chen, Z Chen, S B Dewell, L Du, J M Fierro, X V Gomes, B C Godwin, W He, S Helgesen, C H Ho, C H Ho, G P Irzyk, S C Jando, M L Alenquer, T P Jarvie, K B Jirage, J B Kim, J R Knight, J R Lanza, J H Leamon, S M Lefkowitz, M Lei, J Li, K L Lohman, H Lu, V B Makhijani, K E McDade, M P McKenna, E W Myers, E Nickerson, J R Nobile, R Plant, B P Puc, M T Ronan, G T Roth, G J Sarkis, J F Simons, J W Simpson, M Srinivasan, K R Tartaro, A Tomasz, K A Vogt, G A Volkmer, S H Wang, Y Wang, M P Weiner, P Yu, R F Begley, and J M Rothberg. Genome sequencing in microfabricated high-density picolitre reactors. *Nature*, 437 (7057):376–380, Sep 2005.

M G Marinus and N R Morris. Isolation of deoxyribonucleic acid methylase mutants of Escherichia coli K-12. *J Bacteriol*, 114(3): 1143–1150, Jun 1973.

N R Mattatall and K E Sanderson. Salmonella typhimurium LT2 possesses three distinct 23S rRNA intervening sequences. *J Bacteriol*, 178(8):2272–2278, Apr 1996.

J F Milligan and O C Uhlenbeck. Synthesis of small RNAs using T7 RNA polymerase. *Methods Enzymol*, 180:51–62, 1989.

T Mizuno, M Y Chou, and M Inouye. A unique mechanism regulating gene expression: translational inhibition by a complementary RNA transcript (micRNA). *Proc Natl Acad Sci U S A*, 81(7):1966–1970, Apr 1984.

K B Mullis, F Ferre, and R A Gibbs. *The polymerase chain reaction*. Birkäuser Boston, 1994.

H D Murray, D A Schneider, and R L Gourse. Control of rRNA expression by small molecules is dynamic and nonredundant. *Mol Cell*, 12(1):125–134, Jul 2003.

C Mülhardt. *Der Experimentator: Molekularbiologie/Genomics*. Spektrum Akad. Verlag, 3 edition, 2002.

F Narberhaus, T Waldminghaus, and S Chowdhury. RNA thermometers. *FEMS Microbiol Rev*, 30(1):3–16, Jan 2006.

J W Nicol, G A Helt, S G Blanchard, A Raja, and A E Loraine. The Integrated Genome Browser: free software for distribution and exploration of genome-scale datasets. *Bioinformatics*, 25 (20):2730–2731, Oct 2009.

R P Novick and E Geisinger. Quorum sensing in staphylococci. *Annu Rev Genet*, 42:541–564, 2008.

U D Priyakumar, C Hyeon, D Thirumalai, and A D Mackerell. Urea destabilizes RNA by forming stacking interactions and multiple hydrogen bonds with nucleic acid bases. *J Am Chem Soc*, 131(49):17759–17761, Dec 2009.

F Repoila and F Darfeuille. Small regulatory non-coding RNAs in bacteria: physiology and mechanistic aspects. *Biol Cell*, 101 (2):117–131, Feb 2009.

J Sambrook and D W Russel. *Molecular Cloning*. Cold Spring Harbor Laboratory Press, 3 edition, 2001.

J P Schlüter, J Reinkensmeier, S Daschkey, E Evguenieva-Hackenberg, S Janssen, S Jänicke, J D Becker, R Giegerich, and A Becker. A genome-wide survey of sRNAs in the symbiotic nitrogen-fixing alpha-proteobacterium Sinorhizobium meliloti. *BMC Genomics*, 11:245–245, 2010.

C M Sharma, S Hoffmann, F Darfeuille, J Reignier, S Findeiss, A Sittka, S Chabas, K Reiche, J Hackermüller, R Reinhardt, P F Stadler, and J Vogel. The primary transcriptome of the major human pathogen Helicobacter pylori. *Nature*, 464(7286): 250–255, Mar 2010.

A Sittka, S Lucchini, K Papenfort, C M Sharma, K Rolle, T T Binnewies, J C Hinton, and J Vogel. Deep sequencing analysis of small noncoding RNA and mRNA targets of the global post-transcriptional regulator, Hfq. *PLoS Genet*, 4(8), 2008.

J M Sogo, M R Inciarte, J Corral, E Viñuela, and M Salas. Rna polymerase binding sites and transcription map of the DNA of bacillus subtilis phage phi29. *J Mol Biol*, 127(4):411–436, Feb 1979.

S Suzuma, S Asari, K Bunai, K Yoshino, Y Ando, H Kakeshita, M Fujita, K Nakamura, and K Yamane. Identification and characterization of novel small RNAs in the aspS-yrvM intergenic region of the Bacillus subtilis genome. *Microbiology*, 148(Pt 8): 2591–2598, Aug 2002.

A E Trotochaud and K M Wassarman. A highly conserved 6S RNA structure is required for regulation of transcription. *Nat Struct Mol Biol*, 12(4):313–319, Apr 2005.

B Vester and J Wengel. LNA (locked nucleic acid): high-affinity targeting of complementary RNA and DNA. *Biochemistry*, 43 (42):13233–13241, Oct 2004.

J Vogel and K Papenfort. Small non-coding RNAs and the bacterial outer membrane. *Curr Opin Microbiol*, 9(6):605–611, Dec 2006.

J Vogel and E G Wagner. Target identification of small noncoding RNAs in bacteria. *Curr Opin Microbiol*, 10(3):262–270, Jun 2007.

K M Wassarman. 6S RNA: a regulator of transcription. *Mol Microbiol*, 65(6):1425–1431, Sep 2007.

K M Wassarman and R M Saecker. Synthesis-mediated release of a small RNA inhibitor of RNA polymerase. *Science*, 314(5805): 1601–1603, Dec 2006.

K M Wassarman and G Storz. 6S RNA regulates E. coli RNA polymerase activity. *Cell*, 101(6):613–623, Jun 2000.

K M Wassarman, A Zhang, and G Storz. Small RNAs in Escherichia coli. *Trends Microbiol*, 7(1):37–45, Jan 1999.

T Watanabe, M Sugiura, and M Sugita. A novel small stable RNA, 6Sa RNA, from the cyanobacterium Synechococcus sp. strain PCC6301. *FEBS Lett*, 416(3):302–306, Oct 1997.

L S Waters and G Storz. Regulatory RNAs in bacteria. *Cell*, 136 (4):615–628, Feb 2009.

D K Willkomm and R K Hartmann. 6S RNA - an ancient regulator of bacterial RNA polymerase rediscovered. *Biol Chem*, 386(12): 1273–1277, Dec 2005.

D K Willkomm, J Minnerup, A Hüttenhofer, and R K Hartmann. Experimental RNomics in Aquifex aeolicus: identification of small non-coding RNAs and the putative 6S RNA homolog. *Nucleic Acids Res*, 33(6):1949–1960, 2005.

R Wurm, T Neusser, and R Wagner. 6S RNA-dependent inhibition of RNA polymerase is released by RNA-dependent synthesis of small de novo products. *Biol Chem*, 391(2-3):187–196, Feb-Mar 2010.

C Yanisch-Perron, J Vieira, and J Messing. Improved m13 phage cloning vectors and host strains: nucleotide sequences of the m13mp18 and puc19 vectors. *Gene*, 33(1):103–119, 1985.

DECLARATION

Ich versichere, dass ich meine Dissertation

The mechanism of pRNA-mediated release of RNA polymerase from *Bacillus subtilis* 6S-1 RNA

selbstständig ohne unerlaubte Hilfe angefertigt und mich dabei keiner anderen als der von mir ausdrücklich bezeichneten Quellen bedient habe.

Die Dissertation wurde in der jetzigen oder einer ähnlichen Form noch bei keiner anderen Hochschule eingereicht und hat noch keinen sonstigen Prüfungszwecken gedient.

Marburg, November 2010

Benedikt M Beckmann

COLOPHON

This thesis was typeset with LaTeX 2ε and the great *classicthesis* package from André Miede using Hermann Zapf's *Palatino* and *Euler* type faces (Type 1 PostScript fonts *URW Palladio L* and *FPL* were used). The listings are typeset in *Bera Mono*, originally developed by Bitstream, Inc. as "Bitstream Vera". (Type 1 PostScript fonts were made available by Malte Rosenau and Ulrich Dirr.)

Figures were drawn using *Inkscape* 0.46 and plots were generated with *Rlplot* 1.5 or *Grace* 5.1.22